Investigating the Survival Response of *Staphylococcus aureus* to the Antimicrobial Lipid Sphingosine

Yiyun Chen

Thesis submitted in accordance with the requirements of the University of Liverpool for the degree of Doctor in Philosophy

November 2017

Acknowledgement

I would like to express my deepest thanks to my supervisor Mal Horsburgh for his invaluable assistance, support and guidance, as well as his smile and patience, throughout my PhD studies.

I would like to thank all members in Horsburgh's group for their kindly support and assistance, especially Josephine Moran who trained me a lot with bioinformatics and data analysis.

I would like to thank all members of LabH who created such a great environment for working and studying, with special thanks to lab manager Paul Loughnane who was always around to help.

I would like to thank my family for their unconditional support, encouragement and love in my life.

Abstract

The human skin surface is covered with a lipid film that forms the interface between the viable epidermal layers and outer environment, and influences the colonisation of bacteria. Hydrolysis of the epidermal lipid ceramide via ceramidase yields sphingosine, an antimicrobial lipid that is able to kill staphylococci rapidly. Studies of patients with atopic dermatitis have indicated a correlation between levels of sphingosine and *S. aureus* colonisation of human skin, yet the contribution of sphingosine to the composition of the human skin microbiome and microbiota colonisation is unclear. This study investigates the effect of the host epidermal antimicrobial lipid D-sphingosine on *S. aureus* and *S. epidermidis*, with a focus on discovering components that contribute to survival of the former.

The methods RNA-Seq and qPCR were used to dissect the transcriptional responses of *S. aureus* Newman and *S. epidermidis* Tü3298 after challenge with D-sphingosine. *S. aureus* displayed a large set of differentially expressed genes (1331), which contrasted with a smaller set for *S. epidermidis* (340). There was a clearly defined stimulon that was common between the species that included pathways for energy maintenance, amino acid and ion transport and metabolism, and protein repair. Previously reported transcriptomic responses to multiple cell wall and membrane-targeting antimicrobials shared commonalities with the response to sphingosine that supports its reported mode of action at the cell surface with membrane damage. The VraSR cell wall stress stimulon was upregulated in both species.

Each species displayed pronounced upregulation of a putative phosphate-specific ABC transporter system encoded by the *pstS-pstCAB* operons. Experiments identified a contribution of this transport system to sphingosine survival and phosphate supplementation was shown to markedly increase sphingosine survival.

Previous studies by the Horsburgh group identified experimentally evolved *S. aureus* strains with high levels of D-sphingosine resistance after serial passage with increasing concentrations of the lipid. SNPs associated with increased resistance were determined by genome resequencing and some of these were localised to the *farER* genes encoding a FarR-regulated FarE (mmpL) lipid efflux transporter. An isogenic *farR* SNP mutant of *S. aureus* was generated using molecular genetics approaches and showed a 10-fold higher MIC for D-sphingosine compared with the wild type Newman strain, indicating that the purported FarER fatty acid efflux system may have the capacity to mediate transport of sphingosine. The study findings of a link between sphingosine challenge and phosphate metabolism indicates future research potential to study host spingosine-1-phosphate in staphylococcal lifecycles, during health and disease.

Contents

List of Tables

List of Figures

Abbreviations

AD: atopic dermatitis

ADP: adenosine diphosphate

AdsA: adenosine synthase A

AFAs: antimicrobial fatty acids

AIP: autoinducing peptide

AMP: antimicrobial peptide

ATP: adenosine triphosphate

BHI: Brain Heart Infusion

BWA: Burrows-Wheeler aligner

CAMPs: cathelicidin antimicrobial peptides

CDM: chemical defined medium

CGR: Centre for Genomic Research

CL: cardiolipin

CoNS: coagulase-negative staphylococci

DE: differentially expressed

DEPC: diethypyrocarbonate

Ebh: extracellular matrix-binding protein homologue

FAME: fatty acid modifying enzyme

FarRE: fatty acid resistance regulator and effector

GAS: group A *Streptococcus*

GO: Gene ontology

hBD: human beta defensins

LB: Lysogeny Broth

McrA: myosin-cross reactive antigen

MRSA: methicillin-resistant *S. aureus*

MSCRAMMs: microbial surface components recognising adhesive matrix molecules

NADP+: nicotinamide adenine dinucleotide phosphate, abbreviated

PBP: penicillin binding protein

PBS: phosphate buffered saline

PCR: polymerase chain reaction

PGA: poly-γ-glutamic acid

PIA: polysaccharide intracellular adhesin

PMF: proton motive force

PSMs: phenol-soluble modulins

qPCR: quantitative polymerase chain reaction

RH: relative humidity

RIN: RNA integrity number

ROS: reactive oxygen species

Sae: *S. aureus* exoprotein

SCC*mec*: staphylococcal chromosome cassette *mec* element

SERAMs: secretable expanded repertoire adhesive molecules

SNP: single nucleotide polymorphism

SSLs: skin surface lipids

SssF: *S. saprophyticus* surface protein F

TAE: Tris base, acetic acid and EDTA

TCS: two-component system

TE: Tris base and EDTA

TFA: trifluoroacetic acid

THB: Todd Hewitt broth

WTA: wall teichoic acid

Chapter 1: Introduction

1.1 Staphylococci

Species of the genus *Staphylococcus* are Gram-positive cocci, which are non-flagellate, non-motile, and non-spore forming, facultative anaerobes (Ray, 2004). There are at least 40 recognised species of staphylococci, of which *S. aureus* and *S. intermedius* are coagulase-positive, with the remainder being coagulase-negative (Foster, 1996). Most species of staphylococci are harmless colonisers of the skin and mucosa of human and other mammals and birds (Cogen *et al*., 2008; Costello *et al*., 2009; Taylor *et al*., 2003; Nagase *et al*., 2002). More than one dozen species are frequent colonisers of humans, including the coagulase-negative *S. epidermidis*, *S. capitis*, *S. cohnii*, *S. haemolyticus*, *S. hominis*, *S. saprophyticus*, *S. simulans, S. warneri* and *S. xylosus* (Kloos and Schleifer, 1975; Kloos and Musselwhite, 1975; Coates *et al*., 2014). In contrast, the coagulase-positive *S. aureus* is a transient skin coloniser (Kluytmans and Wertheim, 2005; Moss and Squire, 1948; Cho *et al*., 2010).

1.1.1 *Staphylococcus aureus*

Staphylococci that secrete coagulase to clot blood are associated with disease (Kloos and Musselwhite, 1975) and the coagulase-positive *S. aureus* is an important human pathogen. The species name *aureus* was assigned due to the golden colour it produces when grown on solid media, while the coagulase-negative (CoNS) species such as *S. epidermidis*, *S. capitis*, and *S. hominis*, form translucent, white to pale yellow colonies (Howard and Kloos, 1987).

S. aureus has a protective cell wall ~20-40 nm thick that is relatively amorphous in appearance (Shockman and Barrett, 1983). Peptidoglycan together with teichoic acids makes up 90% of the cell wall mass (Knox and Wicken, 1973, Waldvogel, 1990). Teichoic acids bind to the peptidoglycan covalently or insert in the lipid bacterial membrane and provide a negative charge for the

staphylococcal cell surface, which assists in the acquisition and localization of cations as well as autolytic enzyme activities (Wilkinson, 1997). The remaining 10% cell wall mass is composed of peptidoglycan hydrolases (autolysins), surface proteins and exoproteins, some of which are virulence determinants. This integral tight multi-layered cell wall network contributes to withstanding environmental challenges, such as osmotic pressure (Wilkinson, 1997). Over 90% of clinical strains of *S. aureus* are found to produce polysaccharide (poly-β-1,6-*N*-acetyl-d-glucosamine) that protect bacteria from phagocytosis, in addition to capsular polysaccharide that is more variably produced by strains (Thakker *et al.*, 1998). Adhesins with specificity for a range of host components, including fibrinogen, fibronectin, vitronectin, collagen and laminin are expressed on the *S. aureus* surface (Foster and McDevitt, 1994). These cell wall-associated surface proteins play a key role in *S. aureus* attachment to plasma and extracellular matrix (ECM) proteins.

The most important site of *S. aureus* colonisation is the nose (Williams, 1963), which is considered its primary niche, though it can also be found in the perineum, axillae, pharynx and on the skin (especially on the hands, chest and abdomen where it is considered to be a transient member of the skin flora) (Wertheim *et al.*, 2005). *S. aureus* nasal carriage among the general adult population shows global variation, with the carrier percentage varying from 9.1% in Indonesia to 41.7% in French Guiana (Sollid *et al.*, 2013).

S. aureus can cause local infections of the skin, nose, gastrointestinal tract, urethra and vagina (Shulman and Nahmias, 1972). The most frequent pathology of *S. aureus* is an abscess lesion when it enters the underlying tissue of the human body (Elek, 1956), which will cause septicaemia if it reaches the blood or lymphatic channels (Waldvogel, 1990). A range of extracellular toxins such as enterotoxin A-E, exfoliative toxins A and B, and toxic shock syndrome toxin-1 (TSST-1) can be produced by *S. aureus* (Projan and Novick, 1997). TSST-1 is responsible for the toxic shock syndrome (TSS) that is commonly associated with menstruating women. The exfoliative toxins can cause staphylococcal scalded skin syndrome (SSSS) and will damage the epidermal layer of the skin.

When enterotoxin is produced in contaminated food its subsequent ingestion may cause food poisoning (Howard and Kloos, 1987).

1.1.2 *Staphylococcus epidermidis*

Those coagulase-negative staphylococcus species that are normal commensals colonise the skin, anterior nares, and ear canals of human. *S. epidermidis* is the best characterised and most frequently isolated *Staphylococcus* species on skin and is isolated from up to 100 % of healthy tested individuals (Foster, 2009; Roth and James, 1988). Healthy individuals can possess up to 24 strains of *S. epidermidis*. Approximately 65-90% of all staphylococci isolated from human aerobic flora were found to be *S. epidermidis*, and can survive under desiccation stress for long periods. (Nilsson *et al*. 1998).

Whilst being a very common skin commensal, *S. epidermidis* can also be invasive and cause hospital-acquired infections. But it is a true opportunistic pathogen, as it requires a major breach in the host's innate defences, which typically occurs by colonising in-dwelling medical devices, e.g. catheters or heart valves (Uckay *et al.*, 2009). Once attached, the organism produces an exopolysaccharide matrix that assists adherence to plastic and cells, and contributes to defence against phagocytosis by the host immune system, and antibiotics. The biofilm of *S. epidermidis* consists of cells embedded in this extracellular polymer that can be up to 160 μm thick. These disease-causing strains of *S. epidermidi*s are now leading pathogens of nosocomial infections (Villari *et al.,* 2000). Diagnosis can be difficult since these infections are often indolent and chronic with few obvious symptoms, due to the smaller array of virulence factors and toxins compared with those produced by *S. aureus* (Foster, 1996).

1.2 Human skin

Skin is a vital barrier, resisting penetration by microorganisms and potential toxins while retaining moisture and nutrients inside the body (Proksch *et al*., 2008; Elias, 2007; Segre, 2006). Resident bacteria of the skin microbiome can survive and thrive within this hostile and demanding environment. The microbiota, including certain species of staphylococci, bestows a barrier function to the host epidermis by competing with overt skin pathogens such as *S. aureus* and inhibiting their colonisation (Cogen *et al*., 2008).

1.2.1 Structure of human epidermis

Sebaceous units comprise human epidermis and enable thermoregulation and protection activities of the skin. Each unit contains a hair follicle (HF), sebaceous gland, and interfollicular epidermis (IFE). Forming the epidermis, the skin layers can be classified into four categories in order of least to most differentiated as: basal (stratum basale); spinous (stratum spinosum); granular (stratum granulosum); and stratified (stratum corneum) (Figure 1.1) (Candi *et al*., 2005; Proksch *et al*., 2008). The skin is a continuously self-renewing organ. Cell numbers of the skin are maintained due to stem cells that progressively differentiate and migrate towards the outermost layer (Segre, 2006). Suprabasal cell division occurs during formation of the epidermis. These progeny cells differentiate into suprabasal spinous keratinocytes, then granular cells and finally corneocytes to complete development of the stratified skin structure (Blanpain and Fuchs, 2009).

Migration of keratinocytes is accompanied by a series of morphological changes, such as the round shape changed into flattened or polygonal and the plasma membrane becomes permeable (Coates *et al*., 2014). The majority of changes with terminally differentiated keratinocytes occur between the granular layer and the stratum corneum (Candi *et al*., 2005). Development ends with enucleation and maturation of a cornified envelope (Rice and Green, 1977). The

cornified envelope is a protein layer cross-linked by isopeptide bonds and is extremely resistant to common proteolytic enzymes (Proksch *et al.*, 2008).

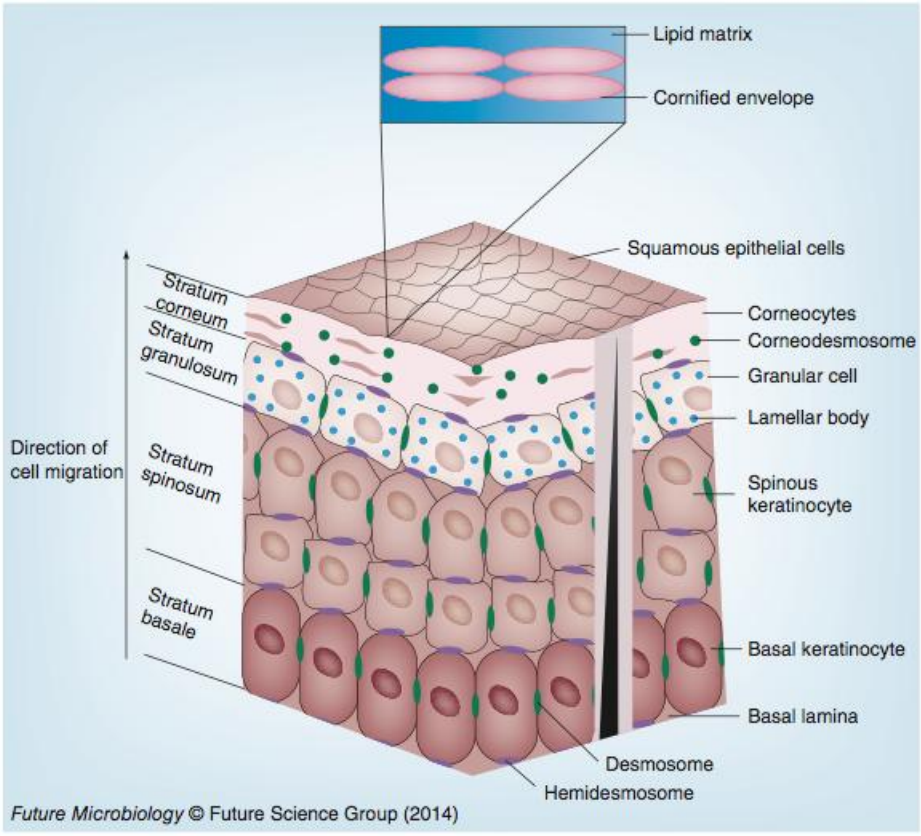

Figure 1.1 Structure of human skin. (Coates *et al.*, 2014)

Ceramides and free fatty acids are produced by hydrolysis of phospholipids and glucosylceramides released from the lamellar granules (Madison, 2003; Drake *et al.*, 2008). These granules are extruded during the transition between the granular layer and the stratum corneum. Keratin is bound into tight bundles by fillagrin and results in flattening of the keratinocytes (Candi *et al.*, 2005). The plasma membrane disintegrates and the cell's organelles are degraded under apoptosis (Candi *et al.*, 2005).

The terminally differentiated cells are known as cornified cells or corneocytes (Candi *et al*., 2005; Proksch *et al*., 2008). Cornified envelope, which is a protein layer self-associated by isopeptide bonds, forms beneath the plasma membrane. The bonds are so tight as to make this layer resistant to common proteolytic enzymes (Proksch *et al*., 2008). In addition, this cornified envelope is also linked to a lipid envelope, which contains ω-hydroxyceramides, via covalent bonds (Proksch *et al*., 2008; Candi *et al*., 2005; Madison, 2003). The lipid matrix that surrounds corneocytes consists of ceramides (45-50 %), cholesterol (25 %), free fatty acids (10-15 %) and other lipids (< 5 %) (Madison, 2003), and is maintained by non-covalent interaction with intercellular lamellae. This lipid matrix forms both gel phase domains, which are highly ordered and relatively impermeable, and liquid crystalline phase domains, which are more fluid and provide flexibility (Madison, 2003). Corneodesmosomes differ from desmosomes that are found in lower layers of the epidermis and bind corneocytes together. Proteolytic degradation of corneodesmosome proteins results in shedding of the stratum corneum, which is known as desquamation (Jonca *et al.*, 2011). The keratinocye cells in the basal layer proliferate at a rate matched by the rate of desquamation and a complete turnover occurs every 14 days (Candi *et al*., 2005; Roth and James, 1988).

The stratum corneum extracellular matrix (ECM) comprises mostly skin lipids with ceramides, cholesterol and free fatty acids at a ratio of 1:1:1 in a stacked bilayer organization (Iwai *et al.,* 2012). This matrix plays an important role in tissue organisation, wound healing and ageing (Watt and Fujiwara, 2011).

1.2.2 Human skin microbiome

As the largest organ of the human body, skin is an ecosystem composed of 1.8 m^2 of diverse habitats, where approximately 10^2-10^7 microorganisms can be found in every cm^2 of human skin (Schroder and Harder, 2006). The skin, being an interface with the outside environment, has abundant folds, invaginations and specialised niches that support a wide range of microorganisms, including bacteria, fungi and viruses (Chiller *et al.*, 2001; Fredricks, 2001; Cogen *et al.*,

2008). Most of these microorganisms are harmless or even benefit their host by providing vital functions that cannot be expressed by the human genome. Symbiotic microorganisms occupy a wide range of skin niches; they can prime and educate the skin T cells to respond to similar pathogenic factors and they may also assist in protection against invasion of pathogenic or harmful organisms through nutrient competition (Grice and Segre, 2011).

The microenvironment and the variability of skin microbial flora can be influenced by host factors such as age (Leyden *et al.,* 1975; Somerville, 1969), gender (Marples, 1982; Fierer *et al.,* 2008; Giacomoni *et al.*, 2009), genotype, immune system variation (including previous exposures and inflammation), pathobiological conditions, such as diabetes, as well as environmental factors such as lifestyle, climate and usage of antibiotics.

Most skin bacteria can be classified into four phyla: Actinobacteria, Firmicutes, Bacteroidetes and Proteobacteria, according to metagenomic sequencing of 16S ribosomal RNA genes. Actinobacteria represent the dominant colonisers of skin, while Firmicutes and Bacteroidetes are more abundant in the gastrointestinal tract (Grice and Segre, 2011).

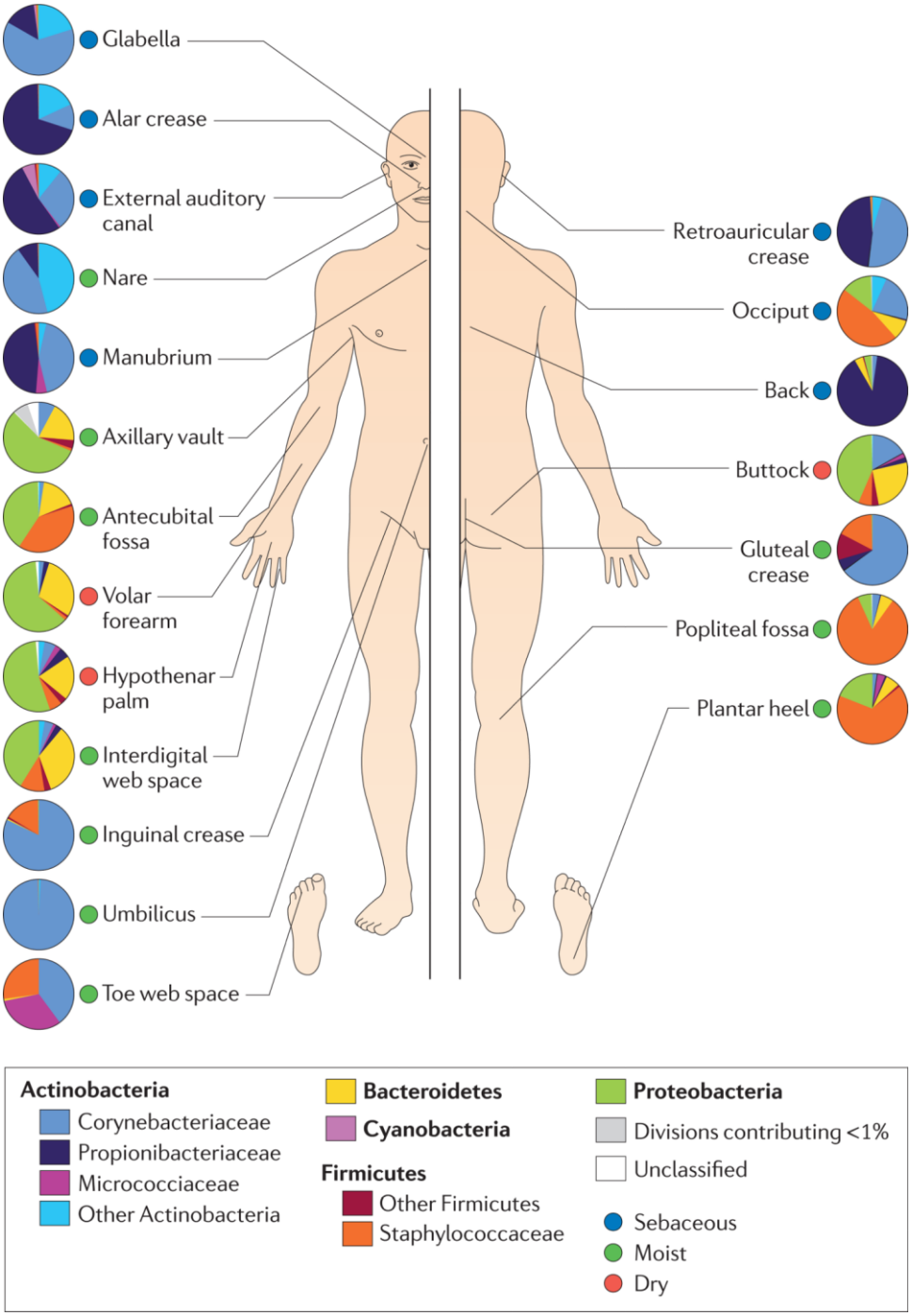

Figure 1.2 Topographical distribution of bacteria on skin. (Figure from Grice and Segre, 2011, data from Grice *et al.*, 2009)

Molecular analysis has indicated that colonisation of bacteria is dependent on the physiology of the skin site (Figure 1.2), with taxa being associated with moist, dry and sebaceous microenvironments. Temporal variation is also dependent on the skin site and the most consistent populations are at sites that

are partially occluded, including the external auditory canal (inside the ear), the nares (inside the nostril) and the inguinal crease (Grice *et al.*, 2009). The skin microbial variation is more dependent on the site than on the individual, since intrapersonal variation in microbial community membership and structure between symmetric skin sites is less than the interpersonal variation, as determined by 16S rRNA gene-based metagenomic sequencing (Gao *et al.*, 2007; Grice *et al.*, 2009; Costello *et al.*, 2009).

1.3 Staphylococcal skin survival

The acidic pH, high salt and low moisture conditions of the skin limit bacterial colonisation (Roth and James, 1988; Coates *et al.*, 2014). Microbes must firstly adhere to the skin to colonise, and must be able to evade components such as antimicrobial peptides and antimicrobial lipids of the innate immune system to persist on the skin (Coates *et al.*, 2014). Moreover, for microbes to outcompete other skin bacteria they have to survive their antimicrobial peptides and target them through various mechanisms (Cogen *et al.*, 2008; Cogen *et al.*, 2010a; Cogen *et al.*, 2010b). *S. epidermidis* has a better adaptation to these challenges than *S. aureus* (McEwan *et al.*, 2006; Cho *et al.*, 2001; Melnik, 2006; Ong *et al.*, 2002; Arikawa *et al.*, 2002; Takigawa *et al.*, 2005; Ishikawa *et al.*, 2010), but insufficient information is known about what determinants lead to the differences in skin colonisation observed between *S. epidermidis* and *S. aureus*.

1.3.1 Colonisation and persistence

A primary requirement for skin colonisation is to adhere to the flattened, cornified keratinocytes, then being able to attach to the new layers before cells are shed through desquamation. Adhesins mediate strong attachment to specific receptors on the skin and minimise loss (Brooker and Fuller, 1984; Zeeuwen *et al.*, 2012; Grice *et al.*, 2009).

There are three groups of staphylococcal adhesins: non-proteinaceous adhesin, microbial surface components recognising adhesive matrix molecules (MSCRAMMs), and secretable expanded repertoire adhesive molecules (SERAMs) (Heilmann, 2011). Non-proteinaceous adhesins that are usually embedded in the membrane lipids act through non-covalent bonds; MSCRAMMs covalently bind the staphylococcal cell wall and adhere to one or more host factor; SERAMs non-covalently bind to the staphylococcal surface and provide both adhesive and enzymatic functions adhesion (Heilmann *et al*., 2003; Bowden *et al*., 2002).

Different adhesins facilitate *S. aureus* nasal colonisation at distinct stages. The non-proteinaceous adhesin, wall teichoic acid (WTA) is found to be important in the initial stages of nasal colonisation (Burian *et al.*, 2010a; Burian *et al*., 2010b; Weidenmaier *et al*., 2004) since WTA mutants with disruption of WTA biosynthesis are unable to colonise (Weidenmaier *et al.*, 2008). The MSCRAMMs IsdA and ClfB are important in long-term colonisation of the nose (Burian *et al.*, 2010a; Burian *et al*., 2010b).

Table 1.1 Staphylococcal adhesins with known receptors for skin. (Coates *et al*., 2014)

Host receptor	Adhesin	Adhesin (abbreviations)	Species	Reference
Collagen type I	Collagen adhesin	Cna	*S.aureus*	(Snodgrass *et al*., 1999)
	Extracellular adhesive protein/Major histocompatability complex type II analog protein	Eap/Map	*S.aureus*	(Hansen *et al*., 2006)
	Extracellular matrix protein-binding protein	Emp	*S.aureus*	(Hussain *et al.*, 2001)
	Glycerol ester hydrolase D	GehD	*S.epidermidis*	(Bowden *et al*., 2002)
	Serine aspartate repeat family protein F	SdrF	*S.epidermidis*	(Arrecubiete *et al*., 2007)
	Serine aspartate repeat family protein I	SdrI	*S.saprophyticus*	(Sakinc *et al*., 2006)
Cytokeratin-10	Clumping factor B	ClfB	*S.aureus*	(O' Brien *et al*., 2002)
	Iron-regulated surface determinant protein A	IsdA	*S.aureus*	(Clarke *et al.*, 2009)

Table 1.1 Continued

Host receptor	Adhesin	Adhesin (abbreviations)	Species	Reference
Fibrinogen	Autolysin/Adhesin of *S. aureus*	Aaa	*S.aureus*	(Heilmann *et al*., 2005)
	Autolysin	Atl	*S.aureus*	(Hirschhausen *et al*., 2010)
	Clumping factor A	ClfA	*S.aureus*	(McDevitt *et al*., 1994)
	Clumping factor B	ClfB	*S.aureus*	(Ni Eidhin *et al*., 1998)
	Extracellular adhesive protein/Major histocompatability complex type II analog protein	Eap/Map	*S.aureus*	(Hussain *et al*., 2001)
	Extracellular matrix protein-binding protein	Emp	*S.aureus*	(Hussain *et al*., 2001)
	Fibrinogen binding protein of *S. epidermidis*/serine aspartate repeat family protein G	Fbe/SdrG	*S.epidermidis*	(Hartford *et al*., 2001)
	Fibrinogen binding protein of *S. lugdunensis*	Fbl	*S.lugdunensis*	(Nilsson *et al*., 2004)

Table 1.1 continued

Host receptor	Adhesin	Adhesin (abbreviations)	Species	Reference
Fibrinogen	Fibronectin binding protein A	FnbpA/FnbA	*S.aureus*	(Wann *et al*., 2000)
	Fibronectin binding protein B	FnbpB/FnbB	*S.aureus*	(Burke et al., 2011)
	Iron-regulated surface determinant protein A	IsdA	*S.aureus*	(Clarke *et al.*, 2004)
	Uro-adherence factor	UafB	*S.saprophyticus*	(King *et al.*, 2011)
Fibronectin	Autolysin/Adhesin of *S. aureus*	Aaa	*S.aureus*	(Heilmann *et al.*, 2005)
	Autolysin/adhesin of *S. epidermidis*	Aae	*S.epidermidis*	(Heilmann *et al.*, 2003)
	Autolysin/adhesin of *S. saprophyticus*	Aas	*S.saprophyticus*	(Hell *et al.*, 1998)
	Autolysin	Atl	*S.aureus*	(Hirschhausen *et al.*, 2010)

Table 1.1 Continued

Host receptor	Adhesin	Adhesin (abbreviations)	Species	Reference
Fibronectin	Autolysin of *S. caprae*	AtlC	*S.caprae*	(Allignet *et al.*, 2002)
	Extracellular adhesive protein/Major histocompatability complex type II analog protein	Eap/Map	*S.aureus*	(Hussain *et al.*, 2001)
	Extracellular matrix binding protein	Embp	*S.epidermidis*	(Williams *et al.*, 2002)
	Extracellular matrix protein-binding protein	Emp	*S.aureus*	(Hussain *et al.*, 2001)
	Fibrinogen binding protein of *S. epidermidis*/serine aspartate repeat family protein G	Fbe/SdrG	*S.epidermidis*	(Nilsson *et al.*, 1998)
	Fibronectin binding protein A	FnbpA/FnbA	*S.aureus*	(Flock *et al.*, 1987)
	Fibronectin binding protein B	FnbpB/FnbB	*S.aureus*	(Jonsson *et al.*, 1991)
	Iron-regulated surface determinant protein A	IsdA	*S.aureus*	(Clarke *et al.*, 2004)

Table 1.1 continued

Host receptor	Adhesin	Adhesin (abbreviations)	Species	Reference
Fibronectin	Serine aspartate repeat family protein I	SdrI	*S.saprophyticus*	(Sakinc *et al.*, 200)
	Uro-adherence factor	UafB	*S.saprophyticus*	(King *et al.*, 2011)
Involucrin	Iron-regulated surface determinant protein A	IsdA	*S.aureus*	(Clarke *et al.*, 2009)
Keratinocyte lipids/glycolipis	Plasmin sensitive protein	Pls	*S.aureus*	(Huesca *et al.*, 2002)
Loricrin	Clumping factor B	ClfB	*S.aureus*	(Mulcahy *et al.*, 2012)
	Iron-regulated surface determinant protein A	IsdA	*S.aureus*	(Clarke *et al.*, 2009)
Undetermined receptor on desquamated epithelial cell	Accumulation associated protein	Aap	*S.epidermidis*	(Macintosh *et al*., 2009)
Undetermined receptor on desquamated nasal cells	Clumping factor B	ClfB	*S.aureus*	(Corrigan *et al*., 2009)
	Iron-regulated surface determinant protein A	IsdA	*S.aureus*	(Corrigan *et al*., 2009)

Table 1.1 continued

Host receptor	Adhesin	Adhesin(abbreviations)	Species	Reference
Undetermined receptor on keratinocyte cell line	Serine aspartate repeat family protein C	SdrC	*S.aureus*	(Corrigan *et al*., 2009)
	Serine aspartate repeat family protein D	SdrD	*S.aureus*	(Corrigan *et al*., 2009)
	Serine aspartate repeat family protein G	SasG	*S.aureus*	(Corrigan *et al*., 2007)
	Coagulase		*S.aureus*	(Mempel *et al*., 1998)
	Clumping factor A	ClfA	*S.aureus*	(Mempel *et al*., 1998)
	Fibronectin binding protein A	FnbpA/FnbA	*S.aureus*	(Mempel *et al*., 1998)
	Fibronectin binding protein B	FnbpB/FnbB	*S.aureus*	(Mempel *et al*., 1998)
	Staphylococcal protein A	Spa	*S.aureus*	(Mempel *et al*., 1998)

Known staphylococcal adhesins to the human epidermis and their receptors are displayed in table 1.1. The *S. epidermidis* Rp62a genome encodes 12 MSCRAMMs, whereas *S. aureus* strains expresses up to 20 MSCRAMMs (Heilmann, 2011).

Binding to different layers of the stratum corneum due to receptor variation between skin layers could affect long-term colonisation and survival. Studies of *S. epidermidis* identified three patterns of adhesion to layers of the stratum corneum: binding to superficial, fully differentiated corneocytes and hairs; binding to deeper, less differentiated epithelia at cell-cell junctions; and universal binding to all layers across the entire surface of the cell (Brooker and Fuller, 1984).

Variation in repertoire may result in colonisation differences between *S. aureus* and *S. epidermidis* (Ben *et al.*, 2008). For example, Aap of *S. epidermidis* binds buccal epithelial cells and desquamated corneocytes, while the Aap homologue SasG, expressed by *S. aureus,* binds desquamated nasal cells, but not buccal epithelial or keratinocyte cells (Roche *et al.*, 2003; Macintosh *et al.*, 2009). It is suggested that the receptor for Aap and SasG is the same, but Aap binds the receptor better than SasG, since recombinant Aap could block SasG adhesion (Roche *et al.*, 2003).

1.3.2 Osmotic stress and resistance

Osmotic stress that affects bacterial colonisation of the skin environment can be divided into three classes: low relative humidity (RH), matric water stress (desiccation) and ionic stress (salts or ions) (Potts, 1994). On skin, the relative humidity is low while the ionic stress is often high (Grice and Segre, 2011). Skin bacteria also face the additional stress of a sudden increase in water availability caused by sweating or washing. Although *Staphylococcus* species are one of the most abundant organisms colonising moist areas (Grice *et al.*, 2009; Costello *et al.*, 2009), their transmission and survival are still threatened when the relative humidity (RH) is below the threshold for growth.

It was shown that *S. aureus* can grow at 87% RH and *S. epidermidis* was tolerant of 81-84% RH, while *Escherichia coli, Bacillus subtilis* and *Pseudomonas fluorescens* required 92-94.5% RH for growth (de Goffau *et al.*, 2009). The lower RH that *S. epidermidis* can tolerate compared with *S. aureus* may be a reason for its enhanced survival on the skin. This hypothesis was supported by the finding that *S. epidermidis* was inhibited by *Pseudomonas fluorescens* at high RH, but gains competitive advantage at lower RH (de Goffau *et al.*, 2009).

To tolerate desiccation conditions, *S. aureus* and *S. epidermidis* undergo morphology changes that are probably controlled by autolysin activity (de Goffau *et al*., 2011). As a result, the cells become larger in size, forming thicker walls and cuboidal packs of eight cells, instead of their typical grape-like clusters (de Goffau *et al*, 2009; de Goffau *et al*., 2011). Through these morphology changes, the bacteria reduce their surface area to volume ratio to prevent water loss and maintain turgor pressure (de Goffau *et al.*, 2011). Further work has indicated that staphylococci grown at low RH also become more hydrophilic to increase water acquisition (de Goffau *et al*., 2011).

The ability of staphylococci to produce the polysaccharide intercellular adhesin (PIA) might contribute to desiccation resistance through buffering activity, similar to exopolysaccharide (EPS) that protects *Pseudomonas* spp. (Roberson and Firestone, 1992). *S. epidermidis* strain Rp62a is a PIA producer (McKenney *et al.*, 1998) that was found to be the most low RH tolerant *S. epidermidis* strain tested by de Goffau *et al* (2009). Potentially, this tolerance of Rp62a to low RH could result from its ability to form biofilms, which would further reduce the ratio of surface area to volume (de Goffau *et al*., 2009).

Poly-γ-glutamic acid (PGA) forms a capsule around *S. epidermidis* ubiquitously and was reported to assist in protection from high NaCl concentration (2M) (Kocianova *et al.*, 2005). Genomes of *S. epidermidis* and some other coagulase-negative staphylococci, including *S. capitis*, *S. caprae*, *S. haemolyticus*, *S. warneri* and *S. hominis*, encode the PGA biosynthesis genes *pgsBCAD/capBCAD* while *S. aureus* do not (Kocianova *et al.*, 2005).

Membrane zwitterionic phospholipids decrease in conditions of increasing salinity, and cardiolipin (CL) is known to play a role in osmotic stress responses in various bacteria. CL can stiffen membrane to reduce its permeability and prevent loss/gain of small solutes (Nagamachi *et al*., 1992). CL also interacts and regulates expression of the mechanosensitive channel MscL and the osmosensory transporter ProP (Romantsov *et al*., 2009). *S. aureus* encodes two CL synthase genes, one responsive to stress and the other is a housekeeping gene maintaining biosynthesis. Mutation of both genes leads to a decrease in long-term survival in high salinity media (Tsai *et al.,* 2011).

Other gene products that were identified to be important in osmotic stress resistance include proteases, ClpX and YjbH that assist in ionic and matric stress resistance, and extracellular matrix binding protein homologue (Ebh) that increases survival in high salt conditions (Kuroda *et al.*, 2008). Ebh (extracellular matrix-binding protein homologue) which is only found in *S. aureus* and *S. epidermidis* and absent from *S. haemolyticus* and *S. saprophyticus* is a cell wall and membrane-associated protein. Invaginated vacuoles along their septum were observed within 30 min when *ebh* mutants were exposed to high salt conditions, suggesting that this protein contributes to initial ionic stress resistance (Kuroda *et al*., 2008), however a specific role for Ebh during the cell cycle of *S. aureus* remains unknown.

1.3.3 Acid stress and resistance

Acid stress contributes to innate defence against microbial colonisation on the surface of skin. Across the skin layers there is an acidic gradient, increasing throughout the stratum corneum from pH 7.4 in the stratum granulosum to pH 4-5 at the skin surface (Rippke *et al.*, 2002, Matousek and Campbell, 2002, Schmid-Wendtner and Korting, 2006). This acidic gradient is established by several components, including lactic acid and free amino acids from sweat, free fatty acids from sebum, the filaggrin degradation products urocanic acid and pyrrolidone carboxylic acid, and cholesterol sulphate (Rippke *et al*., 2002, Matousek and Campbell, 2002).

The acid gradient is important in the maintenance of the cohesion and integrity of the stratum corneum, as well as permeability homeostasis of the outer layers of the skin (Hachem *et al*., 2003). The acid gradient also facilitates regulation of skin enzymes such as β-glucocerebrosidase and serine proteases, dependent on their location within the stratum corneum to ensure timely differentiation and desquamation of keratinocytes. Change of pH is considered as a causal factor for skin diseases, such as atopic dermatitis and ichthyosis (Rippke *et al*., 2002; Matousek and Campbell, 2002; Schmid-Wendtner and Korting, 2006).

The more acidic pH of the human skin surface relative to most other mammals may contribute to the difference between the flora of each (Matousek and Campbell, 2002). Low pH can cause direct damage to bacterial proteins and DNA by denaturation and, additionally, acidic conditions increases activity of cationic antimicrobial peptides (CAMPs) and antimicrobial fatty acids (AFAs) (Walkenhorst *et al*., 2013; Cartron *et al*., 2014).

Gram-positive bacteria respond to acid stress by increasing resistance mechanisms that raise pH inside the cell, change architecture of the cell surface, and repair protein and DNA damage (Cotter and Hill, 2003). The most direct approach to keep the internal pH at an acceptable level is the use of proton pumps, which move protons out of the cell. Acidification of the cytoplasm is counteracted by increasing the concentration of alkaline compounds within the cell (Cotter and Hill, 2003). Genes encoding urease subunits A, B and C (*ureA, ureB* and *ureC*), as well as *ureF* encoding the urease accessory protein UreF, are all strongly upregulated in *S. aureus* by acid shock (Matforsk *et al.*, 2007). In comparison, urease is expressed at a very high level in *Helicobacter pylori*, and this organism has adapted itself to colonise the strongly acidic environment of the human stomach. Urease activity is the major acid-resistance mechanism of *H. pylori*, and the enzyme neutralises acid by producing NH_3 and CO_2 (Valenzuela *et al.*, 2003).

In addition to its membrane lipid synthesis role mentioned above, CL synthase contributes to acid shock resistance by changing membrane structure. CL

production under normal conditions synthesised by Cls2, is changed to Cls1 under acute acid stress (Ohniwa *et al.,* 2013).

1.3.4 Antimicrobial fatty acids and resistance

Antimicrobial fatty acids (AFAs) are abundant on healthy mammalian skin. The majority of skin fatty acids originate from the sebum and the lamellar granules, and some can be released from the hydrolysis of triglycerides and biglycerides (Kohler *et al*., 2009; Madison, 2003; Drake *et al*., 2008). Fatty acids facilitate the maintenance of skin homeostasis by reducing inflammation and promoting wound healing (Brogden *et al*., 2012; Huang *et al*., 2014; Lai *et al*., 2009), and they contribute to the acid mantle of the skin together with lactic acid and amino acids in sweat (Fluhr *et al*., 2001). The free fatty acids on skin that are antimicrobial include sapienic acid, linoleic acid and oleic acid (Drake *et al*., 2008).

AFAs are proposed to limit staphylococcal colonisation (Costello *et al*., 2009; Lampe et al., 1983). While *S. aureus* is isolated from less than 5% of individuals with healthy skin, it is routinely isolated from atopic dermatitis patients who have lower AFA levels (Noble *et al*., 1967; Leyden *et al*., 1974; Breuer *et al*., 2002). There is also an inverse relationship between sebaceous (and thus AFA rich) regions and frequency of staphylococcal isolation from skin (Grice and Segre, 2011; Grice *et al.*, 2009) (Figure 1.2). These correlations support AFAs as potentially important contributing factors in differential survival of *S. epidermidis* and *S. aureus* on human skin.

AFAs are able to disrupt bacterial membranes. The insertion of AFA molecules increases membrane fluidity and permeability that results in leakage of low molecular weight (<20 kDa) compounds, such as ATP and amino acids from the cell, as well as alteration of pH within the cell (Greenway and Dyke, 1979; Cartron *et al*., 2014; Parsons *et al*., 2012). Whilst there is evidence to support membrane insertion by AFAs, membrane insertion was not essential to inhibit growth (Greenway and Dyke, 1979; Cartron *et al*., 2014). AFAs are able to

uncouple oxidative phosphorylation as protonophores and lead to inhibition of respiration, disruption of the electron transport chain and collapse of the proton gradient (Cartron *et al*., 2014; Parsons *et al*., 2012; Jezek *et al*., 1998).

S. aureus possesses several mechanisms for AFA defence. Wall teichoic acids (WTA) and MSCRAMM IsdA reduce hydrophobicity of the bacterial surface to limit AFA interaction (Parsons *et al*., 2012; Kohler *et al*., 2009; Clarke *et al*., 2007). Transcription of capsule and peptidoglycan genes increases after AFA challenge (Kenny *et al*., 2009) and might contribute to the reduced hydrophobicity in response to AFAs. Moreover, *S. aureus* synthesises carotenoid staphyloxanthin to maintain membrane integrity (Chamberlain *et al*., 1991). Staphyloxanthin also contributes to antioxidant defences and counteracts AMP-mediated membrane fluidity (Clauditz *et al*., 2006; Mishra *et al*., 2011).

Staphylococci produce enzymes to detoxify AFAs. Myosin-cross reactive antigen (McrA) protein of *S. pyogenes* is a fatty acid hydratase and a homolog is encoded by *S. aureus* (Volkov *et al*., 2010; Moran *et al*., 2017). The McrA family of cell wall-anchored proteins includes the *S. aureus* surface protein F (SasF) (Kenny et al., 2009) and the *S. saprophyticus* surface protein F (SssF), and homologues of these proteins were found in all sequenced staphylococci by King *et al.* (2012).

Both *S. aureu*s and *S. epidermidi*s secrete the exoenzyme fatty acid modifying enzyme (FAME) that esterifies lipids with cholesterol or primary alcohols to reduce their cellular toxicity (Chamberlain and Brueggemann, 1997; Kapral *et al*., 1992). The gene for this enzyme remains to be identified. Most skin isolates of staphylococci encode lipases that hydrolyse triglycerides and diglycerides releasing free fatty acids as substrates for FAME (Kapral *et al*., 1992).

The arginine catabolic mobile element (ACME) encoding arginine deiminase (AD) activity improves survival of *S. aureus* on the skin in community acquired MRSA isolates (Diep *et al*., 2006). Genes encoding deiminase pathway enzymes such as those in the oligopeptidepermease operon (*opp*) and the *arcABDC* operon are upregulated by challenge of AFAs. An *arcA* mutant is more susceptible to AFAs than wild type strain (Kenny *et al.,* 2009). Induced arginine deiminase activity is proposed to counteract acidity from lactic acid in sweat

(Thurlow *et al.*, 2013) and may similarly contribute to AFA defense (Kenny *et al.*, 2009; Moran *et al.*, 2017).

FarRE (fatty acid resistance regulator and effector), which belongs to the multidrug pumps superfamily was identified as an exporter pump that facilitates resistance to linoleic acid and arachidonic acid (Kenny *et al.*, 2009; Alnaseri *et al.*, 2015). Linoleic and arachidonic acids strongly induce expression of *farE* in an *farR*-dependent manner, and inactivation of *farE* resulted in significant increased susceptibility of *S. aureus* to linoleic and arachidonic acid (Alnaseri *et al.*, 2015).

1.3.5 Antimicrobial peptides and resistance

Antimicrobial peptides (AMPs) are part of the innate immune system on human skin. A variety of AMPs are effective against a wide range of pathogens like fungi, bacteria and viruses (Giuliani *et al.*, 2008). They are synthesized as pre-forms and need to be activated to mature peptides, when needed. Most AMPs are positively charged and amphipathic with common structural motifs. The cationic AMPs bind to the commonly anionic bacterial surface and form channels or pores in the cytoplasmic membrane (Otto, 2010). Many cell types of the human immune system are able to produce CAMPs, including mast cells, T cells, and neutrophils where the antimicrobial peptides are secreted within phagosomes that kill ingested microorganisms (Faurschou and Borregaard, 2003). Keratinocytes are the most important source of AMPs on the skin, while sebocytes and hair bulb cells also contribute to AMP production.

Human skin produces dermcidin, adrenomedullin, lysozyme, RNase7 and skin-derived antileukoproteinase as common AMPs. Dermcidin is secreted from sweat glands (Schittek *et al.*, 2001; Rieg *et al.*, 2004) and it inhibits synthesis of staphylococcal RNA and protein (Senyurek *et al.*, 2009) via formation of ion channels in the bacterial membrane (Paulmann *et al.*, 2012; Song *et al.*, 2013). Adrenomedullin is a 52 amino acid peptide and functions in hormone regulation, vasodilatation and neutransmission (Richards *et al.*, 1996). Although it is

effective against many bacteria, particularly *Propionibacterium acnes* (Allaker and Kapas, 2003), its effect on *S. aureus* and *S. epidermidis* is moderate (Allaker *et al.*, 1999). The enzyme lysozyme is active against both Gram-positive and Gram-negative organisms (Neu *et al.*, 1968) and can be found in many body fluids, such as tears and mucosal secretions. It cleaves the β-1,4 glycosidic bond in bacterial peptidoglycan between the *N*-acetylmuramic acid (MurNAc) and *N*-acetylglucosamine (GlcNAc) residues (Chipman and Sharon, 1969). Pathogenic species of staphylococci, including *S. epidermidis* and *S. aureus*, are resistant to lysozyme due to activity of a transferase that *O*-acetylates MurNAc in peptidoglycan (Bera *et al.*, 2006). The cationic RNase7 acts upon a wide range of bacteria, including *S. aureus* (Zhang *et al.*, 2003), and is expressed in many tissue types such as keratinocytes on the skin. Keratinocytes also produce skin-derived antileukoproteinase that controls inflammation by inhibiting neutrophil elastase; it is not bactericidal but inhibits growth of bacteria, including *S. aureus* (Williams *et al.*, 2006).

The skin-colonising and pathogenic bacteria have evolved resistance mechanisms for CAMPs, with an important approach being to modify the cell surface with positive charge that repels CAMPs. *S. epidermidis* encodes a two-component sensor-regulator ApsSR that is activated by CAMPs (Li *et al*., 2007; Matsuo *et al*., 2011). Sensor protein ApsS has a negatively charged extracellular loop domain that binds the CAMPs, and gene deletion *apsS* mutants have reduced survival to hBD3 (Li *et al*., 2007). The *dlt* operon that is regulated by ApsSR plays an important role in staphylococcal resistance to CAMPs, cathelicidins and defensins via encoding enzymes for covalent attachment of D-alanine to wall teichoic acids (Herbert *et al*., 2007; Peschel *et al.,* 1999). In addition, expression of the MprF flippase that modulates cell surface charge by addition of lysine to membrane lipid via lysyl-phosphatidylglycerol synthetase activity is similarly regulated by ApsSR (Ernst and Peschel, 2011; Peschel *et al*., 2001).

S. aureus has a homologue of the Aps system, GraRS (Yang *et al*., 2012). Mutation of the genes for GraRS increased sensitivity to CAMPs and reduced *S. aureus* virulence in a mouse infection model (Kraus *et al*., 2008; Herbert *et al*.,

2007; Yang *et al*., 2012). The GraRS system requires the contribution of GraX and the VraFG ABC transporter for sensing and resistance to CAMPs (Herbert *et al*., 2007; Meehl *et al*., 2007; Falord *et al*., 2012; Yang *et al*., 2012). GraS has a substitution of a serine for a proline residue in the extracellular loop, compared with the *S. epidermidis* ApsS sensor, accounting for altered expression of *dlt* and *mprF*, which might contribute to the different responses to AMPs by *S. aureus* and *S. epidermidis* (Li *et al*., 2007).

Production of proteases is another key defence for AMPs in staphylococci. The extracellular neutral metalloprotease SepA of *S. epidermidis* contributes to dermcidin resistance by degradation (Lai *et al*., 2007). Metalloprotease aureolysin produced by *S. aureus* disables the human cathelicidin LL-37 and assists in skin persistence and contributes to disease by limiting phagocytosis via complement inhibition (Kubica *et al*., 2008; Garzoni and Kelley, 2009; Laarman *et al*., 2011).

1.3.6 Competitive exclusion

Microbe interactions on the skin include bacterium-bacterium, virus-bacterium, and fungus-bacterium interactions. Correlated species distributions relative to staphylococcal colonisation were observed with skin and the nasal cavity. Infrequent co-isolation of *S. epidermidis* and *S. aureus* was shown in several studies (Frank *et al.*, 2010), with *S. epidermidis* considered to associate with competitive exclusion of *S. aureus* from the nasal epithelium (Iwase *et al.*, 2010). Other competing species from the nasal cavity correlated with absence of *S. aureus* include, *S. haemolyticus*, *S. hominis, Finegoldia magna*, *Corynebacterium accolens*, and *Micrococcus* spp. (Libberton *et al*., 2014; Wos Oxley *et al*., 2010; Iwase *et al*., 2010). Several *Corynebacterium spp*. were found to inhibit staphylococcal colonisation of the nasal cavity, presumably by competition for nutrients or adhesin receptors (Uehara *et al.*, 2000).

There are several mechanisms to circumvent colonisation inhibition by other species: interference via adhering to a range of receptors; resistance to

competitor antimicrobials similar to AMP resistance described in section 1.3.5, and production of inhibitory compounds targetting competitors.

The skin commensal *S. epidermidis* is proposed to also protect the skin from pathogens by producing AMPs, such as phenol-soluble modulins (PSMs) (Schommer and Gallo, 2013). The phenol-soluble modulins (PSMs) δ and γ of *S. epidermidis* are amphipathic, α-helical staphylococcal proteins that, interact with lipid membrane, similarly to mammalian AMPs. These PSMs show antimicrobial activity against *S. aureus,* Group A *Streptococcus* (GAS), and *Escherichia coli*, via their insertion into membranes that leads to lipid vesicle leakage (Periasamy *et al*., 2012; Cogen *et al*., 2010b). *S. epidermidis* produces the serine protease Esp that was proposed to inhibit biofilm formation and nasal colonisation of *S. aureus* (Iwase et al., 2010). Esp-secreting *S. epidermidis* cleared *S. aureus* colonisation when applied intranasally (Iwase *et al.*, 2010; Park *et al.*, 2011). Esp stimulated production of the AMPs, human beta defensins 2 and 3 (hBD2 and hBD3) act upon *S. aureus,* but not *S. epidermidis* (Lai *et al*., 2010; Iwase *et al*., 2010). Separately, the frequency of *S. epidermidis* consistently increases, together with *S. aureus,* during the dysbiosis of atopic dermatitis (AD) when no treatment is applied, suggesting that *S. epidermidis* may not only benefit its eukaryotic host, but could also share a mutualistic or commensal relationship between staphylococci (Kong *et al*., 2012).

Bacteriophages are potential competitors of staphylococci on the skin and staphylococcal phages were isolated from mammalian skin (Slanetz and Jawetz, 1941). Phages capable of infecting *S. epidermidis* were also found in the anterior nares at low levels (Aswani *et al*., 2011).

Clustered Regularly Interspaced Palindromic Repeats (CRISPRs) and their associated Cas proteins that provide phage resistance have been described in some staphylococci (van der Oost *et al*., 2009; Vale and Little, 2010; Marraffini and Sontheimer, 2008; Ramia *et al*., 2014). The Cas proteins process phage derived-DNA and store them as short repeat regions within CRISPR regions in the genome. These repeat regions in association with Cas proteins then lead to sequence-specific interference and degradation of phage genetic material in

subsequent infections with a similar phage or reactivation of a prophage within the cell (Vale and Little, 2010).

1.3.7 Two-component systems

Bacteria rely on sensory elements within their cell envelope to trigger adaptive responses to wide-ranging environmental conditions. The large family of signal transducers called two-component systems (TCS), consist of a membrane-bound sensor kinase that responds to environmental signals and then activates a cognate response regulator to induce or repress specific sets of target genes. (McCallum *et al.,* 2010; Stock *et al.*, 2000). Phosphorylation of the response regulator (RR) by the sensor histidine kinase (HK) regulates differential expression of the regulon (Mascher *et al.*, 2006). The CAMP defence TCS, ApsSR and GraSR were described above. VraSR, SaeRS and LytSR are three further well-studied TCS of *S. aureus* that have cell surface and survival roles (Belcheva and Golemi-Kotra, 2008; Liu *et al.*, 2016; Patel and Golemi-Kotra, 2015).

S. aureus VraSR (vancomycin resistance associated sensor/regulator) was shown to mediate resistance to cell wall synthesis inhibitors, such as vancomycin and β-lactams (Bae and Schineewind, 2006; Belcheva and Golemi-Kotra, 2008). VraSR TCS is activated following exposure to a variety of cell wall-targeting antibiotics, or the depletion of essential cell wall synthesis enzymes, and regulates expression of a cell wall stress stimulon (CWSS) (Gardete *et al.*, 2006; Kuroda *et al.,* 2003; Sobral *et al.,* 2007; Utaida *et al.*, 2003). Induction of the VraSR-dependent CWSS protects *S. aureus* against cell envelope damage through upregulation of cell wall peptidoglycan biosynthesis genes, including *pbpB* (bifunctional staphylococcal penicillin binding protein PBP (Pinho *et al.*, 2001)), *fmtA* (an accessory PBP with low affinity for β-lactams (Fan *et al.*, 2007)), *murZ* (a redundant MurA isozyme (Blake *et al.*, 2009)), and *sgtB* (a soluble transglycosylase (Wang *et al.*, 2001)) (Kuroda *et al.,* 2003; McAleese et al., 2006; Utaida *et al.*, 2003). Inactivation of VraSR results in decreased resistance of *S. aureus* to most VraSR inducing cell wall antibiotics (McCallum *et al.,* 2010).

SaeRS (*S. aureus* exoprotein expression regulator/sensor) is an important virulence regulator, demonstrated using various animal models of *S. aureus* infection (Goerke *et al*., 2005; Liang *et al*., 2006; Voyich *et al*., 2009; Montgomery *et al*., 2010; Cho *et al*., 2015; Zhao *et al*., 2015). SaeRS regulates transcription and expression of an innate immune evasion regulon of genes, including *hla, hlb, hlgABC, lukED* and *coa* (Giraudo *et al*., 1999; Liang *et al*., 2006; Rogasch *et al*., 2006; Nygaard *et al*., 2010). Inactivation of SaeRS leads to impaired cytotoxicity and ability of *S. aureus* to adhere to and invade epithelial and endothelial cells (Liang *et al*., 2006; Steinhuber *et al.,* 2003).

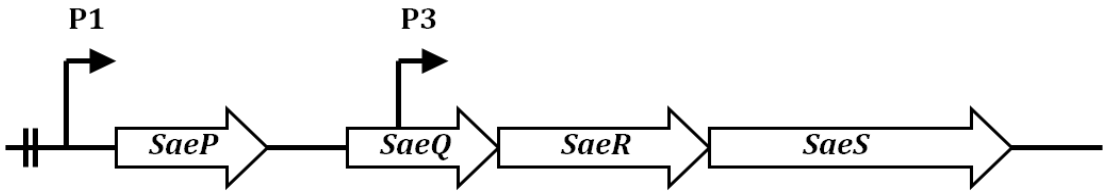

Figure 1.3 Organisation of the *sae* operon. Two angled arrows represent the P1 and P3 promoters, respectively. Two vertical lines in the P1 promoter region indicate the SaeR binding sequences.

The *sae* operon consists of four genes (*saeP, saeQ, saeR* and *saeS*) transcribed from two promoters, P1 and P3 (Figure 1.3) (Novick and Jiang, 2003; Jeong *et al*., 2011; Steinhuber *et al*., 2003). P1 upstream of the first gene *saeP* is a strong promoter, due to two SaeR binding sequences, that direct transcription of all four genes (Novick and Jiang, 2003; Steinhuber *et al*., 2003). The P3 promoter within *saeQ* that only directs transcription of *saeR* and *saeS* (Novick and Jiang, 2003; Jeong *et al*., 2011) is weaker than P1, yet transcription of *saeRS* from P3 is sufficient for activation of the *sae* regulon (Jeong *et al*., 2011).

There are three well-described *S. aureus* SaeS polymorphisms: $SaeS^{P}$, $SaeS^{SK}$, and $SaeS^{SKT}$ (Liu *et al*., 2016). The $SaeS^{P}$ variant was originally identified in the strain Newman, with a L18P substitution mutation (T53C) in the first

transmembrane helix (Steinhuber *et al*., 2003; Adhikari and Novick, 2008). Kinase activity of SaeS^{P} is highly increased due to the substitution mutation (Sun *et al*., 2010). An altered signal response was determined for SaeS^{P} with 0.006% SDS (sodium dodeceyl sulfate) treatment, where for SaeS^{P} the response was increased while wild type SaeS was inhibited (Schafer *et al*., 2009). SaeS^{P} is unstable in the absence of SaeQ, which indicates that SaeS^{P} is subject to proteolytic degradation in the membrane, from which SaeQ protects SaeS^{P} (Jeong *et al*., 2011). SaeS^{SK} has two substitution mutations (N227S and E268K) and is found in the strains MW2, Mu50 and USA600 (Olson *et al*., 2013). SaeS^{SKT} is a SaeS^{SK} variant with one more amino acid substitution at the last position (S351T) and is found in ST30 and ST36 lineages of *S. aureus* (Ramundo *et al*., 2016). SaeS^{SK} does not show altered enzymatic activity of SaeS (Olson *et al*., 2013) while SaeS^{SKT} shows highest activity in the exponential growth phase and reduced activity in the stationary phase (Ramundo *et al*., 2016), while the wild type Sae reaches maximal activity at the post-exponential growth phase (Novick and Jiang, 2003; Steinhuber *et al*., 2003). Thus, SaeS appears to be under genetic selection, potentially reflecting its role in immune evasion.

LytSR TCS is associated with signal transduction of cell membrane electrical potential perturbation and is involved in the adaptation of *S. aureus* to cationic antimicrobial peptides (CAMPs) (Patton *et al*., 2006; Sharma-Kuinkel *et al*., 2009; Yang *et al*., 2013). LytSR can participate in two signal transduction pathways through two phosphorylation processes: phosphorylation of LytR by LytS; and phosphorylation of LytR by acetyl phosphate (Patel and Golei-Kotra., 2015). LytR regulates the expression of *lrgAB* and *cidABC* operons to control programmed cell death and lysis during biofilm formation (Rice *et al*., 2007; Bayles, 2007; Rice and Bayles, 2008). Upregulation of *cidABC* operon contributes to increased activity of murein hydrolysis and antibiotic tolerance (Rice *et al*., 2003), while *lrgAB* inhibits these processes (Groicher *et al*., 2000). Both *lrgAB* and *cidABC* operons were also found to be induced by excess of glucose metabolism (Patton *et al*., 2006). Phosphorylation of LytR by acetyl phosphate was found to be associated with regulation of *lrgAB* operon under high levels of glucose *in vivo* (Lehman *et al*., 2015).

1.4 Sphingosine and staphylococci

The epidermal lipids in the stratum corneum comprise a 1:1:1 ratio of ceramide, fatty acids and cholesterol. The hydrolysis of ceramide yields fatty acids and sphingosine (Pruett *et al.*, 2008; Shirakura *et al*., 2012). A sphingosine concentration of approximately 270 μM of is observed on healthy skin, whilst only 140-160 μM is present on atopic skin that becomes typically heavily colonised by *S. aureus* (Arikawa *et al.*, 2002). Sphingosine is able to kill *S. aureus* rapidly with a similar action mode to AFAs (Parsons *et al.,* 2012), however resistance mechanisms and transcriptional responses of staphylococci have not been characterised.

1.4.1 Atopic dermatitis: sphingosine defence against *S. aureus* colonisation

Atopic dermatitis (AD) is a chronic, inflammatory skin disease characterised by dry, flaky skin lesions (Bieber, 2008). The skin stratum corneum of AD patients has increased bacterial colonisation, and is particularly susceptible to infections with *S. aureus,* and viruses such as herpes and vaccinia (Leung, 2013; Kim *et al*., 2013). The frequency of bacterial colonisation in non-lesional skin of patients with AD is significantly higher than that of other types of dermatitis (Akiyama *et al.*, 1996). Around 80% of AD skin of patients can be colonised by *S. aureus*, and high levels of *S. aureus* colonisation were also observed on their non-lesional skin (Roth and James, 1988; Takigawa *et al*., 2005; Kong *et al*., 2012; Higaki *et al*., 1999).

The constitutive barrier disruption of the stratum corneum seen with AD patients, including decreased levels of sphingolipid metabolites such as ceramide, was considered to be associated with the increased susceptibility to *S. aureus* colonisation (Arikawa *et al.*, 2002; Imkawa *et al.*, 1991). Studies that compared the stratum corneum of AD patients with age-matched normal controls detected no significant difference in the activities of major ceramide-generating and degrading enzymes: sphingomyelinase (SMase); β-glucocerebrosidase (GlCDase); and alkaline ceramidase (CDase) (Hara *et al*,

2000; Jin *et al*, 1994). Further work identified a sphingomyelin (SM) deacylase, which degrades SM at its acyl site to produce sphingosylphosphorylcholine instead of ceramides (Murata *et al.*, 1996). SM deacylase is overexpressed in the epidermidis of AD patients, being at least three to five times higher than in the epidermis of healthy controls (Hara *et al*., 2000). These studies supported the hypothesis that overexpression of SM deacylase competes with SMase for their common substrate SM and may account for the ceramide deficiency in the epidermidis of AD patients (Murata *et al.*, 1996; Hara *et al*., 2000).

Altered sphingolipid metabolism in AD patients suggests that ceramide or its metabolite sphingosine may be involved in defence from *S. aureus* colonisation (Bibel *et al.,* 1992; Bibel *et al.*, 1993). The amount of sphingosine is reduced by approximately 2-fold in the upper three layers of the stratum corneum of AD patients compared with healthy controls, and this decreased level of sphingosine results in an approximately 200-fold increase of *S. aureus* colonisation (Arikawa *et al.*, 2002). Other factors associated with AD and *S. aureus* skin colonisation include reduction of AFAs and AMPs in the epidermis of AD patients (Cho *et al*., 2010; Schafer and Kragballe,1991).

1.4.2 Sphingoid bases and antimicrobial activities

Sphingoid bases, including free sphingosine and dihydrosphingosine derived from epithelial sphingolipids via hydrolysis, are present in the stratum corneum and are proposed to contribute to the permeability and innate immunologic barriers of the skin (Brogden *et al.*, 2012; Jungersted *et al.*, 2008).

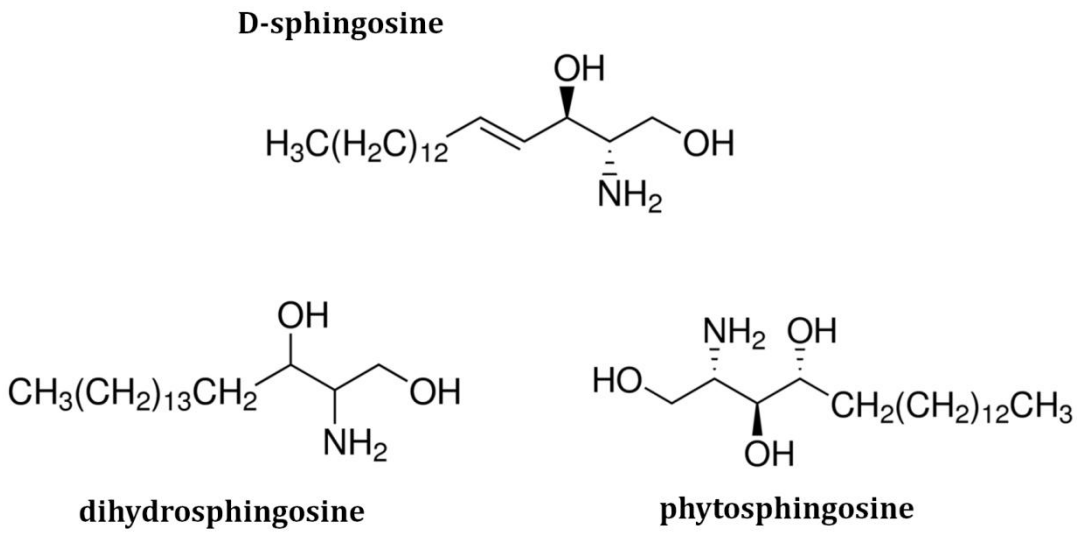

Figure 1.4 Structure of sphingosine, dihydrosphingosine and phytosphingosine (Sigma-Aldrich).

D-sphingosine, dihydrosphingosine and phytosphingosine are all similar in structure (Figure 1.4). D- Sphingosine is the natural isomer of sphingosine (2-amino-4-octadecene-1,3-diol), which is an 18-carbon chain unsaturated amino alcohol with a single trans double bond between C4 and C5, two hydroxyl groups on C1 and C3, and an amino group on C2 (Fischer *et al.*, 2013). Dihydrosphingosine is the saturated analog of sphingosine, and phytosphingosine is structurally similar to dihydrosphingosine with the exception of a hydroxyl group at C4. Both sphingosine and dihydrosphingosine

inhibit protein kinase C (PKC) that can modulate many biochemical actions (Darges, 1997) and play a role in a variety of cellular processes (Bu *et al*., 2006; Shi *et al*., 2007; Saba and Hla, 2004; Spiegel and Milstien, 2003; Spiegel and Milstien, 2011). Phytosphingosine is abundant in plants and fungi and present in animals. Phytosphingosine has anti-inflammatory and anti-proliferative properties (Kim *et al*., 2006; Pavicic *et al*., 2007).

Sphingoid bases: D-sphingosine, dihydrosphingosine, and phytosphingosine all show antimicrobial activity against a variety of Gram-positive and Gram-negative bacteria, including *E. coli, S. aureus, Corynebacterium bovis, C. striatum, C. jeikium, Streptococcus sanguinis, Strep. mitis*, and *Fusobacterium nucleatum* (Drake *et al*., 2008; Bibel *et al*., 1992a; Klee *et al*., 2007; Bibel *et al*., 1992b; Bibel *et al*., 1993; Fischer *et al*., 2011). Kinetic assays showed that sphingosine and phytosphingosine were capable of killing *S. aureus, Strep. sanguinis, Strep. mitis, and C. striatum* within 0.5 to 6 h (Fischer *et al*., 2011).

Electron microscopy revealed cell wall lesions, membrane disruption and leakage of cellular content for sphingoid base-treated *S. aureus*, supporting that the activity site of sphingoid bases is the cell wall (Bibel *et al*., 1993). In a study by Bratt *et al* (2010), fragments of the lysed cell wall were found after sphingoid base treatment of *S. aureus*. Obvious disruption with loss of cell wall and membrane by sphingoid bases in *S. aureus* was also by observed by Fischer *et al.* (2013), who showed sphingoid bases induced ultrastructural damage of *E. coli* and *S. aureus* treated with 10 times MIC concentration of D-sphingosine, dihydrosphingosine or phytosphingosine. These three sphingoid bases induce intracellular inclusions and they accumulate in both *E. coli* and *S. aureus* cells, suggesting both extracellular and intracellular damage (Fischer *et al*., 2013). It was predicted that concentrations lower than MIC are tolerated and metabolised by the bacteria, but concentrations above the MIC are not (Fischer *et al*., 2013).

Although the detailed antimicrobial mechanisms of sphingosine on bacteria at the molecular level are not fully established, several similar possibilities are proposed: sphingosine may act on *S. aureus* by penetrating and disrupting the

cell wall or altering changes in cytoplasmic membrane; or it may penetrate the cell walls and the cytoplasmic membranes of bacteria, then enter and disrupt the cytoplasm, similar to a mechanism described by Bergsson *et al.* (2001).

1.5 Thesis aims

The contribution of sphingosine to the composition of the human skin microbiome and colonisation of microbiota is poorly understood. The basis for differential survival and persistence across the staphylococcal species that colonise human skin is not clear and in particular their skin lipid resistance mechanisms and transcriptional responses remain to be resolved. This study investigates the effect of the host epidermal antimicrobial lipid D-sphingosine on *S. aureus* and *S. epidermidis*, with a focus on discovering components that contribute to resistance in the former.

The initial aims of this study were to characterise and compare the transcriptional response of *S. aureus* and *S. epidermidis* to D-sphingosine. RNA-Seq and qPCR would be used to dissect the transcriptional responses of *S. aureus* Newman and *S. epidermidis* Tü3298 after challenge with D-sphingosine. A parallel approach was designed to dissect the individual contributions of genes and SNPs that increase *S. aureus* survival to sphingosine, by combining data and approaches from previous work that used experimental evolution and selection for survival with increasing concentrations of D-sphingosine (Moran, 2015). These two genetic approaches would then be used to identify candidate genes for further study, thereby constructing gene mutants and SNP variants as a combined approach to enable study of the physiology of cellular resistance. Overall, these approaches were designed to increase understanding of lipid responses and survival in staphylococci that colonise human skin.

Chapter 2: Methods and Materials

2.1 Bacterial strains and culture

The strains used in this study are displayed in Table 2.1. *S. aureus* strain Newman and *S. epidermidis* strain Tü3298 were used for RNA-Seq analysis. *S. aureus* strains Newman, SH1000, RN4220 and *E. coli* Top10 were used in DNA cloning work and strain construction. Further strains were used in qPCR and survival tests as indicated.

Todd Hewitt broth (THB) was used to culture bacteria for RNA purifcation and survival tests. Phosphate-deficient chemically defined media was used for measurement of cell growth with different phosphate concentrations. Remaining experiments were all conducted in BHI media. Solid medium was made by adding agar (12 g L^{-1}) to broth. Plates were grown statically at 37 °C for 12-18 h unless otherwise stated. Overnight cultures were grown for 18 h at 37 °C with shaking. Optical density (600 nm) was measured during growth using a 1 cm path length. D-sphingosine (Sigma-Aldrich) stock solution was prepared at concentration of 5 mg ml^{-1} in 100% (v/v) ethanol. Antibiotics used for *S. aureus* and their concentrations for selection were as follows: tetracycline 5 µg ml^{-1}, erythromycin 5 µg ml^{-1}, lincomycin 25 µg ml^{-1}; For *E. coli* the selective concentration of ampicillin was 100 µg ml^{-1}.

Table 2.1 Bacterial strains used in this study

Species	Strains	Description	References
S. epidermidis	Tü3298	Epidermin producer, used for RNA-seq,survival tests and cloning experiments	(Allgaier *et al.*, 1986)
S. aureus	Newman	Osteomyelitis isolate,common lab strain, used for RNA-seq,survival tests, pigment assay and cloning experiments	(Duthie and Lorenz, 1952)
	SH1000	Lab strain (*rsbU* repaired 8325-4 derivative),dark golden color,used for survival tests, pigment assay and cloning experiments	(Horsburgh *et al.,* 2002)
	SF8300	CA-MRSA, used for qPCR as random selected *S. aureus* strain repeats	(Diep *et al.*, 2008)
	MRSA252	Fatal bacteraemia isolate, MRSA, used for qPCR as random selected *S. aureus* strain repeats	(Holden *et al.*, 2004)
	SH1000 *farE::tet*	*farE* depletion mutant, selected for survival tests	Horsburgh group, Liverpool
	SH1000 *farR::tet*	*farR* depletion mutant, selected for survival tests	Horsburgh group, Liverpool
	SH1000 *vraR::tet*	*vraR* depletion mutant, selected for survival tests	Horsburgh group, Liverpool
	SH1000 *vraS::tet*	*vraS* depletion mutant, selected for survival tests	Horsburgh group, Liverpool
	RN4220	cloning intermediate	(Nair *et al.*, 2011)
E. coli	Top10	cloning intermediate	Thermo Scientific

Table 2.2 Plasmids used in this study.

Plasmids	Description	Reference
pMUTIN4	High copy number cloning vector, used for creation of SNP bearing variants and gene depletion mutants	(Vagner *et al.*, 1998)
pSK5632	low copy number *S. aureus* shuttle vector, high copy number in *E. coli,* used for creation of completed mutants	(Grkovic *et al.*, 2003)
pDG1514	tetracycline cassette vector	(Guérout-Fleury *et al.*, 1995)

2.2 Survival tests

2.2.1 Growth curves

Overnight cultures were diluted with THB medium to OD_{600}=0.5 and 2 ml of this dilution was added into 250 ml flasks containing 50 ml THB broth. The flasks were incubated at 37°C with shaking at 250 rpm. The optical density A600 was measured hourly from 0 to 8 h. Samples were ten-fold diluted with THB broth before recording the OD_{600}.

For the sphingosine challenge titration experiments, D-sphingosine was added at the appropriate concentration to the experimental groups when the OD_{600} value reached 0.5. Ethanol (100 % v/v) was used as a solvent, since D-sphingosine is insoluble in water, and therefore an ethanol control group was included in addition to a blank control group with no addition.

2.2.2 Growth in phosphate deficient media

Chemically-defined media (CDM) was prepared by adding Na_2HPO_4 (7 g), KH_2PO_4 (300 mg), adenine sulfate (20 mg), guanine-HCl (20 mg), L-glutamic acid (2.22 g), L-aspartic acid (2.22 g), L-proline (2.22 g), glycine (2.22 g), L-threonine (2.22 g), L-serine (2.22 g), L-alanine (2.22 g), L-lysine-HCl (560 mg), L-isoleucine (560 mg), L-leucine (560 mg), L-histidine (440 mg), L-valine (440 mg), L-arginine (330 mg), L-cysteine (220 mg), L-phenylalanine (190 mg), L-tyrosine (170 mg), L-methionine (170 mg), L-tryptophan (60 mg), pyridoxal (0.8 mg), pyridoxamine-2HCl (0.8 mg), D-pantothenic acid (0.4 mg), riboflavin (0.4 mg), nicotinic acid (0.4 mg), thiamine-2HCl (0.4 mg), and biotin (0.02 mg) into one litre water. For use, sterile glucose and $MgSO_4$ was added to obtain the final concentration of 10 g L^{-1} and 0.5 g L^{-1}, respectively. Phosphate concentration was controlled by adding different amounts of molar Na_2HPO_4 and KH_2PO_4 solutions.

Cell growth in CDM without or with added phosphate was performed and measured using a 96-well plate using a Fluostar Omega (BMG Labtech) plate

reader. Overnight culture was diluted to OD_{600} 0.02 then 200 µl was aliquoted into 96 well plates. Cells were challenged with D-sphingosine at various concentrations from 1.65-165 µM. Four concentrations of phosphate (0 mM, 12 mM, 30 mM, 60 mM) were tested. Cell density was determined by measurement of OD_{600}.

2.2.3 Minimum inhibitory concentration (MIC) assay

96 well plates were used for MIC determination. A range of different concentrations of D-sphingosine were prepared using ethanol as solvent and 100 µl of prepared solution was added to each well. Tested strains were grown for 24 h and diluted to OD_{600}=0.2 with BHI broth. Next, 100 µl of diluted culture was added to each well and incubated at 37°C for 24 h.

2.2.4 Peroxide survival assay

S. aureus Newman and *S. epidermidis* Tü3298 were grown in BHI with 5 µM sphingosine with 0.02% v/v ethanol, or with solvent alone for 24 h. The cultures were centrifuged and cell pellets were collected and washed twice with PBS. Cells were resuspended in the same buffer and diluted to OD_{600}=0.1 (~1.5×10^8 CFU ml^{-1}). Hydrogen peroxide (Sigma) was added to the diluted cells with a final concentration of 7.5 mM for *S. aureus* and 3.2 mM for *S. epidermidis*. Cell suspensions were incubated at 37 ˚C statically. Samples were collected at time points 0, 15, 30, 60, 90, 120 min into a 96-well plate, for the hydrogen peroxide treated cells, 10 mg ml^{-1} catalase was added immediately to the samples to neutralise the peroxide. Serial dilution and viable counts were performed to measure the survival rate.

2.2.5 Sphingosine survival assay

Overnight cultures of *S. aureus* SH1000, SH1000 *farE::tet*, SH1000 *farR::tet* were diluted with THB medium to OD_{600}=0.5 and 2 ml of this dilution was added to 250 ml flasks containing 50 ml THB broth. The flasks were incubated at 37°C with linear shaking at 125 rpm. Next, 5 µM D-sphingosine (total volume of 15 µl) was added to the sphingosine-treated groups at mid-exponential phase (OD_{600}=0.5), while 15 µl 100% (v/v) ethanol was added to the control groups as solvent control. The bacteria were incubated with the antibiotics at 37°C with shaking at 250 rpm for 24 h before harvesting. The cultures were centrifuged and cell pellets were collected and washed twice with PBS. Cells were resuspended and diluted to OD_{600}=0.1 (~1.5×10^8 CFU ml^{-1}). A series of concentrations (5-20 µM) of D-sphingosine was added to the diluted cells. Cell suspensions were incubated at 37 ˚C statically. Samples were collected at time points 0, 15, 30, 60, 90 min into a 96-well plate. Serial dilution and viable counts were performed to measure the survival rate.

2.3 Construction of allelic replacement variants

2.3.1 Extraction of plasmid DNA

A plasmid extraction kit (Bioline) was used to purify plasmid DNA using 3-10 ml of a stationary-phase culture, according to the manufacturer's instructions. Plasmid DNA concentration was determined using a NanoDrop-2000 spectrophotometer (Thermo Scientific).

2.3.2 PCR

PCR primers were obtained from Eurofins. DNA amplifications using PCR were carried out with BioMix (Bioline) following the instructions provided. The PCR cycle template is shown below: For the reaction, initial denaturation was performed at 98 ˚C for 30s. Next, temperature cycles were: denaturation at 98 ˚C for 10s; annealing at 56 ˚C for 20s; and extension at 72 ˚C for 30 s-3 min. The cycle was repeated 30-35 times. Final extension was performed at 72 ˚C for 5 min to complete DNA fully and then the sample was held at 4 ˚C until taken out.

2.3.3 Restriction digests and ligation

Digestions were performed in a waterbath following the instructions provided with the enzyme (New England BioLabs). For double digests, buffer compatibility was checked using NEB enzyme checker. Digestions were purified using the Bioline PCR clean-up kit, according to the manufacturer's instructions.

DNA ligations were carried out for 4 h at room temperature. One unit of T4 DNA ligase was used with the provided buffer as per the manufacturer's instructions (Thermo Scientific). DNA was ligated at a ratio of 1:3 vector to insert, with the ligated DNA used directly in subsequent transformations.

2.3.4 Transformation of chemically competent *E. coli*

Competent cells were defrosted on ice and DNA was added (approximately 100 ng in a volume of 5 µl or less) or sterile water as a control. The cells were incubated on ice for 30 min to enable DNA uptake and then heat-shocked in a waterbath (42 ˚C for 90s) to increase uptake efficiency. Cells were transferred to ice for 2 min and 900 µl of LB was added. The transformation mixture of bacteria was incubated for one hour at 37 ˚C allowing recovery of cells and to give the bacteria time to switch on antibiotic resistance genes supplied by the plasmid. Bacteria were then plated (100 µl) onto antibiotic-containing plates. Plates were incubated for up to 24 h to select for transformants.

Plasmids were extracted from the colonies and PCR was conducted on them to confirm the colonies contained the correct plasmid.

2.3.5 Preparation of electrocompetent *S. aureus*

A stationary phase culture of *S. aureus* RN4220 was diluted 1:100 into a flask and cells were grown to an OD_{600} of 0.5. Cells were pelleted by centrifugation (4000 g, 10 min, 4 ˚C). The cells were washed three times using sterile water, followed by a further three washes using 10 % (v/v) glycerol. These cells were aliquoted into 100 µl aliquots and frozen at -80 ˚C.

2.3.6 Electroporation of *S. aureus*

Plasmid DNA for electroporation was concentrated to a high concentration, above 800 ng μl^{-1}. First, 10 µl plasmid was added to an aliquot of defrosted electrocompetent cells. Cells were transformed by electroporation in cuvettes with settings of: 100 Ω, 2.5 kv, 25 µF producing a time constant ~2s. Immediately after electroporation, 900 µl of B2 medium with 0.5 M glucose was added to the cells before incubation for 1 h at 37 ˚C with 250 rpm shaking. Cells were plated onto selective antibiotic plates. Agar plates were incubated for up to 72 h.

2.3.7 Phage transduction

The donor bacteria containing the locus for selection, marked with erythromycin resistance, were grown overnight in BHI with Erm (5 μg ml^{-1}). Next, exponential phase (OD_{600}=0.5) bacteria were mixed with 5 ml phage buffer and 100 μl of ϕ11 was then added into the mixture. The mixture was incubated stationary at 30 ˚C until complete lysis was observed.

Recipient cells were grown overnight in 20 ml LK broth (1 % [w/v] tryptone, 0.5 % [w/v], yeast extract, 0.7 % [w/v] potassium chloride). The culture was centrifuged (4000 g, 10 min), and the supernatant was removed; the bacterial pellet was resuspended in 1 ml LK broth. To 500 μl LK broth containing 10 mM $CaCl_2$, 250 μl of cells was added, plus 250 μl of phage lysate. The mixture was incubated at 37 ˚C statically for 25 min and then incubated with shaking (250 rpm) for 15 min. Next, 500 μl of ice-cold 0.02 M Na citrate was added and the samples were centrifuged (4000 g, 10 min). The pellets were resuspended in 500 μl 0.02 M Na citrate and kept on ice for 2 h. Finally, 100 μl of the samples was plated onto LK plates containing 0.05% (v/v) citrate and covered with 5 ml of top agar containing erythromycin until dry. The plates were grown for 48 h until colonies appeared. The collected colonies were grown in BHI without any antibiotics for 72 h. The genome DNA was extracted after growth and PCR was conducted to verify that the plasmid had been deleted.

2.3.8 Nebraska transposon library mutants

An available resource, the Nebraska Transposon Mutant Library was used to obtain gene mutants. The library was generated from the well-characterised community-associated methicillin-resistant *S. aureus* (MRSA) strain *S. aureus* USA300 LAC, isolated from a Los Angeles County jail inmate (Kennedy et al., 2008). Gene insertions were generated for the library using *bursa aurealis*, a mariner-based transposon, in the USA300 LAC-derived strain JE2, following the procedures essentially as described by Bae *et al.* (2008). To examine interesting genes in Newman, the *S. aureus* USA300 JE2 variants with *bursa aurealis* Tn

insertions at described gene locations were selected from the library and transduced into *S. aureus* Newman; 5 µg ml-1 erythromycin (Erm) was used for selection. To verify the location of the transposon insertions and confirm successful transduction, primers were designed specific to the *bursa aurealis* transposon and were used together with primers of the target genes using PCR amplification as confirmation of correct gene insertion. Primers were designed according to Tn orientation within the gene: the 'plus' orientation used the 'Upstream' primer of the transposon; the 'minus' orientation used the 'Buster' primer in combination with the gene-specific primer. The primers used in this thesis and expected/confirmed product size are indicated in table 2.3.

Table 2.3 Primers for confirmation of transposon library mutants.

Tn Primer	Sequence (5'-3')	Tn Orientation	Distance
Upstream	CTCGATTCTATTAACAAGGG	Plus	464bp
Buster	CTAAATGTTTTTTAAGTAAATCAAGTAC	Minus	128bp
Gene Primer	Sequence (5'-3')	Tn Orientation	Product size
phoU	GCAGCGACAAATGGATCGTTA	Minus	166bp
phoR	GATGAAGTTTCACCACCGCTT	Minus	285bp
hrtB	CAAGGGCTTGGTAGGGAGAA	Minus	241bp
pstS	TCTCTGGTGCTGCTACATATCC	Minus	397bp

2.4 Agarose gel electrophoresis

1% (w/v) agarose gels were made with TAE buffer. Melted agarose was stored at 50 °C until required. Midori green (Nippon Genetics) was mixed into molten agarose gel at a ratio of 2 µl per 100 ml. A loading dye was added to samples when necessary and samples were run in 1x TAE buffer at 110 V for 45-60 min.

2.5 RNA sequencing

Benches and pipettes were cleaned and wiped with RNase Zap. For all work done with RNA, RNase-free filter tips and plasticware were used.

2.5.1 Bacteria growth and challenge condition

For RNA extraction, cells grown in BHI were harvested 20 min after the absence or presence of challenge with D-sphingosine to a final concentration of 5 µM. A volume of 500 µl of each culture was sampled and then centrifuged at 4,000 RCF and 4°C for 5 min. Supernatants were removed and the pellets were resuspended in 500 µl RNAlater (RNA stabilization reagent) and incubated overnight at 4°C.

2.5.2 Cell lysis

The cells were pelleted at 4,000 RCF for 10 min at 4°C and resuspended with 1 µl 100 X TE buffer, 21 µl lysostaphin (6 mg ml^{-1}) and 33 µl mutanolysin (2 kU ml^{-1}). Bacteria were incubated for 15 min at 37°C for cell lysis, mixing every 5 min, before 25 µl proteinase K (1.25 µg ml-1) was added and incubation was continued for a further 30 min.

2.5.3 RNA extraction

RNA was extracted following the Qiagen RNeasy protocol with slight alterations. Briefly, 350 µl RLT buffer containing 1% v/v beta-mercaptoethanol was added to the lysed cells, followed by 250 µl of 100% (v/v) ethanol, and mixed well with pipetting. The mixture was centrifuged through an RNeasy column for 15 s at 14,000 RCF. Then the column was washed twice with 700 µl RW1 buffer and three times with 500 µl RPE buffer. The column was centrifuged into a clean collection tube for 1 min and air dried for 5 min. RNA was eluted twice with 30

µl DEPC-treated water pre-warmed to 45°C. DNase treatment was performed in the column.

2.5.4 DNase treatment

DNase was removed using the Qiagen RNeasy MinElute clean up kit. RNA was eluted with 20 µl DEPC-treated water. The extracted RNA samples were tested with Qubit for quantification. Nanodrop and 2100 Bioanalyzer were used for Quality control. 3 µg of qualified RNA samples were submitted for RNA sequencing by the CGR facility at Liverpool and the remainder of the RNA was converted to cDNA for later qPCR assays.

2.5.5 RNA quality control

Quality control analysis was conducted using a Qubit (Invitrogen) for quantification, 2100 Bioanalyser (Agilent technologies) to assess degradation levels and Nanodrop (Thermo Scientific) to assess protein or solvent contamination. Tests were carried out according to manufacturer's instructions for bacterial RNA. Samples were determined to be suitable for sequencing as follows: a paired control and test condition sample were determined to have Qubit read indicating $\geq$ 3 µg RNA, Bioanalyser RIN $\geq$ 7.0, Bioanalyser trace indicating good integrity, Nanodrop 260/280 and 260/230 $\geq$ 1.8.

2.5.6 RNA library preparation

DNA sequencing libraries preparation was performed by the Centre for Genome Research, University of Liverpool. Total RNA samples were rRNA depleted using the Ribo-Zero magnetic kit for Gram-positive bacteria (Epicentre); this cleanup was repeated for samples with poor initial rRNA removal. Libraries were then prepared using strand-specific ScriptSeq kits (epicentre). Samples were sequenced using paired-end sequencing on the HiSeq platform (Illumina).

2.5.7 RNA sequencing differential expression analysis

Bowtie (Langmead *et al*., 2009) and Edge R (Robinson *et al*., 2010; Robinson and Oshlack, 2010) were used to map reads and determine the differentially expressed (DE) genes, respectively. Genes with mapped transcripts that had a false discovery rate > 0.05, as determined by Benjamin and Hochberg analysis, and $\log_2$ fold change not ≥ ±1 were filtered out of the data set. The remaining gene set was considered differentially expressed between control and test conditions. This analysis was produced by the Centre for Genomic Research (CGR), Liverpool.

Changes in gene expression in biosynthetic pathways were assessed using DE gene sets with KEGG mapper-search and colour (Kanehisa *et al*., 2012; Kanehisa and Goto, 2000). Gene ontology (GO) terms were attached to DE genes using Uniprot (UniProt, 2014).

2.5.8 COG analysis

The sequences of all genes within the genomes of *S. aureus* Newman and *S. epidermidis* Tü3298 were extracted into a fasta file using the Galaxy tool "Extract genomic DNA" (Goecks *et al*., 2010; Giardine *et al*., 2005). A bespoke perl script was then used to convert these gene sequences into protein sequences. These protein sequences were then submitted to WebMGA function annotation (COG) (Wu *et al*., 2011), which assigns a COG ID to each gene. Another bespoke Perl script was used to convert the names that had been assigned to the genes by the Galaxy extract genomic DNA tool back to their true gene names. The gene lists of DE genes were then labelled with their assigned COGs using a bespoke Perl script (Appendix II). The numbers of genes in each COG class and the percentage of the genome accounted for by each COG class was then calculated using a further bespoke Perl script.

2.6 qPCR

2.6.1 First-strand cDNA synthesis

Purified RNA was used to synthesise cDNA using the Tetro Reverse Transcriptase kit. For each sample, 1 ng total RNA was mixed with random hexamer primers. The priming premix were prepared on ice in RNase-free reaction tubes and mixed gently by pipetting. Samples were incubated at 25°C for 10 min, followed by 45°C for 30 min. The reaction was terminated by incubation at 85°C for 5 min. Samples were chilled on ice and stored at -20°C for further use.

2.6.2 Primer design

Primers for DNA amplification in PCR and qPCR were taken from the literature, where possible, or designed using primer-BLAST (Ye *et al*., 2012). Primers with a length between 15 and 25 bp, predicted to have only one product, a Tm of 60 ±2 C, low level of single base repeats and a GC clamp towards the 3' end were selected where possible (Table 2.3).

Table 2.4 Primers for qPCR

Gene	Primer sequences (5' to 3')	References
NWMN_0542 (Newman)	F-TCAGTATCACTAAATGAATCGTCAC R-TCAGTATCACTAAATGAATCGTCAC	This study
phoU (Newman)	F-CGATAGAGGCTTTGCACGAC R-GCAAATCACTCGCAATGGGC	This study
pstB (Newman)	F-ATCATTACGTGGCGCTGC R-TGCTGATGTCGGTTCATCC	This study
saeR (Newman)	F-TGGTCACGAAGTCCCTATGC R-TGGACATTCACGGTATTAGCATC	This study
norB (Newman)	F-GCTACACCATCAACAGATACAGC R-CGCCAAATGCTCCACCTAATG	This study
pstA (Tü3298)	F-CCAGGTAATGCTGCGGGTAA R-TTATTTGTTGGCGCAGCAGG	This study
copA (Tü3298)	F-GAACAGCTCAAACCATCGCC R-GATGTGCCTTTTCTTCGGGC	This study

Primers were confirmed to amplify a product of the predicted length without any secondary products using standard PCR and genomic DNA as a template. The PCR mix was made using BioMix Red (Bioline) and ACCUZYME DNA polymerase (Bioline) according to the manufacturer's instructions.

Primer efficiency was confirmed to be within 90-100 % using a dilution curve with genome DNA, as described previously (Nolan *et al.*, 2006). Efficiency testing was done using the same conditions as for qPCR reactions (described below). The reaction mix in a total volume of 20 µl was set up with 0.5 µM of each primer, 10 µl SensiFAST and a dilution range of gDNA between $1x10^{0}$-$1x10^{4}$, with a starting concentration of 10 million copies. Negative controls without template were also implemented. Efficiency values were generated by the qPCR machine software (ABI StepOnePlus), and an average of at least three resulting efficiency values was taken.

2.6.3 qPCR conditions

All qPCR reactions were performed using the SensiFAST SYBR HiMROX kit (Bioline) with the ABI StepOnePlus (Life Technologies). The reaction mix contained 10 µl SensiFAST, 0.4 µM of each primer, 1 ng cDNA and DEPC-treated water up to a total reaction size of 20 µl. The run cycle was 95 C for 5 min, then 40 cycles of 95 C for 10 s and 62 C for 30 s. Data analysis was performed using the ABI StepOnePlus software. At least two technical replicates and three biological replicates were used to determine fold change in gene expression between samples.

2.7 Staphyloxanthin expression and extraction

Staphyloxanthin was extracted from *S. aureus* membrane using methanol and an absorbance spectrum was determined using a Fluostar Omega (BMG Labtech) plate reader. Bacteria were grown in the absence or presence of challenge growth conditions and harvested after 24 h incubation at 37˚C. The cultures were adjusted to OD_{600}=5, and 10 ml of each sampe was harvested by centrifugation. Pelleted cells were resuspended in 1 ml methanol and incubated for 15 min at 37 °C with shaking.

Pigment was extracted by adding 1 ml of methanol to the cell pellet, with mixing and incubation for 15 min at 37 ˚C. Finally, the methanol extract was centrifuged again and 96-well polystyrene microtitre plates were loaded with 250 µl of extract in triplicate, prior to absorbance measurement.

Chapter 3: Comparative transcriptomics of the staphylococcal survival response to the epidermal lipid sphingosine

3.1 Introduction

3.1.1 Transcriptomics technologies

Transcriptomics is the study of an organism's sum of all the RNA transcripts found within a collection of cells (transcriptome). Sampling and measuring the expression of genes in different conditions can provide insight into how cells react to a given stimulus. Microarray and RNA-Seq are the dominant contemporary transcriptomics technologies, with the former developed in 1995 (McGettigan, 2013) and the latter in 2008 (Mantione *et al.*, 2014). Microarray is based on the use of a chip as a matrix, which is printed with an ordered grid that is structured with clusters of short fragments of DNA. Each cluster contains picomoles (10^{-12} moles) of a specific DNA sequence, which are alternately named as probes, reporters or oligos. Fluorescently labelled cDNA fragments from the test sample are hybridised with the corresponding probes on the microarray chips, and the fluorescence intensity detected from the hybridisation provides a relative abundance of each arrayed transcript in the sample.

Microarray technology enables assay of 1000s of transcripts simultaneously at a relatively low cost (Heller, 2002) and is high throughput (Wang *et al.,* 2009). It is able to detect splice variants and produces different results according to the probe used or due to cross-hybridisation. Sensitivity and dynamic range is limited as cross-hybridisation creates a lot of background noise, which leads to the loss of low-level transcripts (Wang *et al.*, 2009). Approximately 1 μg mRNA is required for microarray input, and prior design and preparation of reference transcripts for probes is needed (Mantione *et al.*, 2014). The quantitation accuracy can reach to 90% or higher, limited by the accuracy of fluorescence

detection. The dynamic range of bound fragments is 10^3-10^4, limited by the fluorescence saturation (Black *et al.*, 2014).

The more recent and emergent RNA-Seq technology takes advantage of advances in high-throughput sequencing combined with use of computational algorithms to detect and quantify transcripts in RNA samples (Wang *et al.,* 2009). cDNAs produced from a test RNA sample are sequenced and result in multiple reads for each transcript, which can be further aligned to a reference genome. This method has many advantages: firstly, it gives high throughput with a much lower amount of input RNA (~1 ng total RNA) (Hashimshony *et al.,* 2012) compared with microarray; secondly, it does not prior require sequencing and annotation of the genome (Mantione *et al.*, 2014), although a genome sequence is useful for data analysis; thirdly, the background noise is very low (with 100bp background signals in non-repetitive regions) (Wang *et al.,* 2009), and has a large dynamic range (10^5) without limitation of fluorescence saturation (Black *et al.*, 2014).

3.1.2 Analysis tools

The Clusters of Orthologous Groups (COGs) refers to a protein database generated by comparing predicted and known protein sequences in all completely sequenced microbial genomes. Both prokaryotic clusters (COGs) and eukaryotic clusters (KOGs) databases have been built to date (Tatusov *et al.*, 1997).

The COGs and KOGs are sorted into 25 classes, indicated as A (RNA processing and modification), B (Chromatin structure and dynamics), C (Energy production and conversion), D (Cell cycle control, cell division, chromosome partitioning), E (Amino acid transport and metabolism), F (Nucleotide transport and metabolism), G (Carbohydrate transport and metabolism), H (Coenzyme transport and metabolism), I (Lipid transport and metabolism), J (Translation, ribosomal structure and biogenesis), K (Transcription), L (Replication, recombination and repair), M (Cell wall/membrane/envelope biogenesis), N

(Cell motility), O (Posttranslational modification, protein turnover, chaperones), P (Inorganic ion transport and metabolism), Q (Secondary metabolites biosynthesis, transport and catabolism), R (General function prediction only), S (Function unknown), T (Signal transduction mechanisms), U (Intracellular trafficking, secretion, and vesicular transport), V (Defence mechanisms), W (Extracellular structures), Y (Nuclear structure), Z (Cytoskeleton). Ultimately, these COGs they can be further grouped into four classes: Cellular processes and signalling (D, M, N, O, T, U, V, W, Y, Z), Information storage and processing (A, B, J, K, L), Metabolism (C, E, F, G, H, I, P, Q) and poorly characterised (R, S).

Each COG consists of either a group of proteins found to be orthologous or they are orthologous sets of paralogs across at least three lineages that likely correspond to an ancient conserved domain. This classification allows transfer of functional information from one member to an entire group, and enables predictions of protein function for poorly characterised genes (Tatusov *et al.*, 1997).

KEGG (Kyoto Encyclopedia of Genes and Genomes) is a collection of databases, including genomes, orthologs, biological pathway, chemical compounds, diseases and drugs (Kanehisa and Goto, 2000). The KEGG pathway maps are composed of pathways across several categories, with a network of all pathways included, indicating molecular interactions and reactions. The pathways are designed to link to the genes involved, with information of gene names, sequences, functions, products and so on. The KEGG pathway-mapping tool enables comparison of datasets with the KEGG PATHWAY wiring diagram database, to search for those pathways associated with the provided gene list, which aids analysis of cellular and organismal functions (Kanehisa, 1997; Kanehisa *et al.*, 2006; Kanehisa *et al.*, 2014).

SAMMD (*Staphylococcus aureus* Microarray Meta-Database) is an online database that includes transcriptional data from all the published work on the species, and curates all the genes found to be differentially expressed at a locus of a mutant strain or as a response to change environmental change e.g. growth conditions. The database enables simple search by ORF (open reading frame) ID,

gene name or gene product name. The output displays differentially expressed gene data, along with the metadata, including experimental growth conditions that associate with the query (Nagarajan and Elasri, 2007).

3.2 Chapter aims

Sphingosines are epidermal skin lipids, derived from ceramide, that are able to kill *S. aureus* rapidly at micromolar concentrations (Parsons *et al.,* 2012). The transcriptional responses of staphylococci and their resistance mechanisms to sphingosine have not been characterised. The main aim of this chapter is to identify differentially expressed genes of *S. aureus* and *S. epidermidis* in response to challenge with D-sphingosine (a representative, easily available sphingosine) and compare their transcriptional profiles. It was expected that this approach would find differences in responses and possible resistance determinants by bacteria, relative to the proposed mode of action for D-sphingosine. These data might indicate the potential of sphingosine to influence the colonisation and persistence of staphylococci on human skin (Arikawa *et al.*, 2002).

3.3 Results

3.3.1 D-Sphingosine challenge titration

Sphingosine was proposed to have a role in suppressing *S. aureus* growth on skin (Arikawa *et al.*, 2002). Whilst it is known that D-sphingosine has an antimicrobial effect on *S. aureus*, experiments determined that a narrow range of the amino alcohol decreased growth rate after challenge during exponential phase (Parsons *et al.,* 2012). In this study, experiments tested a range of sphingosine concentrations to determine a defined micromolar range to enable further studies.

To establish a suitable challenge concentration of the antimicrobial lipid D-sphingosine for subsequent transcriptomics, *S. aureus* Newman and *S. epidermidis* Tü3298 were cultured in 50 ml of THB broth in 250 ml flasks to mid-exponential growth phase, prior to addition of sphingosine. A range of D-sphingosine concentrations with 100% (v/v) ethanol as solvent within a consistent volume of 30 µl were prepared and added to separate growing cultures, making final D-sphingosine concentrations of 5 µM, 6 µM and 7 µM. A solvent control consisted of 30 µl 100 % (v/v) ethanol.

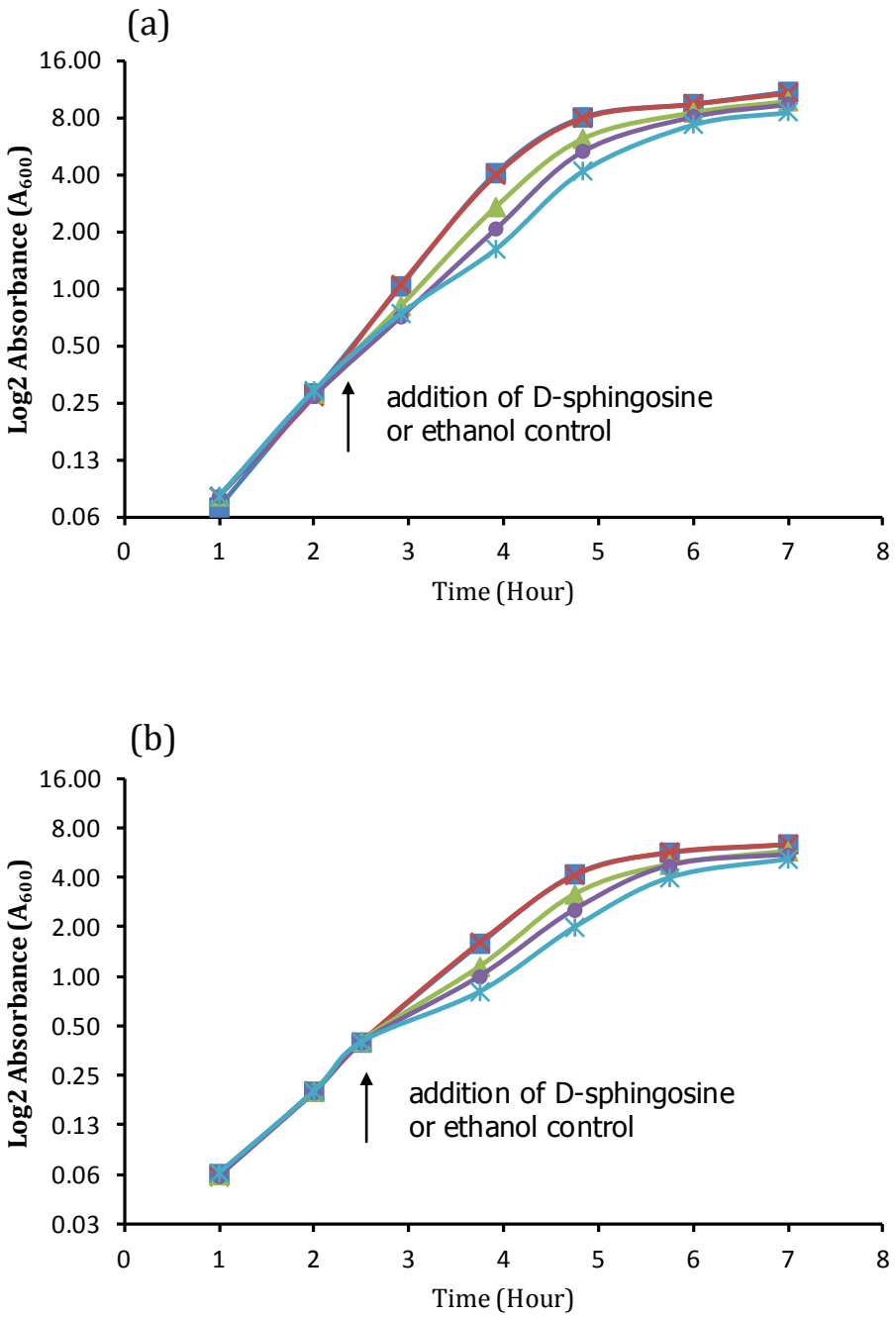

Figure 3.1 Growth curves of staphylococci challenged with a range of D-sphingosine concentrations. *S. aureus* Newman (a) and *S. epidermidis* Tü3298 (b) were cultured in THB to OD_{600}=0.5, whereupon sphingosine was added at different concentrations: 5 µM D-sphingosine (green triangle); 6 µM D-sphingosine (purple closed circle); 7 µM D-sphingosine (light blue star); no solvent broth control (red cross); ethanol (0.3 mM) solvent control (dark blue square).

In separate experiments the growth rates of the broth and solvent control cultures of *S. aureus* and *S. epidermidis* were indistinguishable, indicating that the addition of 30 µl ethanol (0.06% v/v) had no significant effect on cell growth (Figure 3.1). Within one hour after challenge with D-sphingosine, the growth rates decreased for both species with increasing concentration of D-sphingosine. For D-sphingosine treated *S. aureus*, doubling times for 5 µM (49 min), 6 µM (55 min), and 7 µM (75 min) increased relative to both the no solvent (40 min) and ethanol controls (41 min). For D-sphingosine treated *S. epidermidis*, doubling times for 5 µM 49 min, 6 µM (56 min), and 7 µM (74 min) increased relative to both the no solvent (38 min) and ethanol solvent controls (37 min). These data identify a concentration-dependent decrease of growth in the experimental groups caused by addition of D-sphingosine, and for both species treatment with 5 µM D-sphingosine was found to be a sub-lethal concentration that showed a consistent, observable difference from the controls. This concentration was chosen for subsequent RNA-Seq transcriptomic experiments.

3.3.2 RNA quality control

The transcriptional response of *S. aureus* Newman and *S. epidermidis* Tü3298 to D-sphingosine was determined. THB cultures were challenged with 5 µM D-sphingosine, using a 5 mg ml^{-1} stock prepared with ethanol, during the mid-logarithmic phase of growth when OD_{600}=0.5. Control samples were challenged with 0.03% v/v ethanol, an equivalent amount of solvent. RNA was purified from cells harvested after 20 min of incubation with D-sphingosine or ethanol control. RNA was stabilised by adding RNAlater (Qiagen) with incubation overnight at 4 C. Total RNA was then purified from cells the next day using the method described in chapter 2 (section 2.5.3).

Prior to submission for sequencing, purified RNA samples were examined to ensure that they were of sufficient standard using several quality tests (Table 3.1). The ratio of absorbance at 260 nm and 280 nm was used to assess the purity of RNA. Nanodrop 260/280 and 260/230 ratios >1.8 indicated low protein, salt and solvent contamination. All samples of RNA were then determined to be of sufficient concentration (≥30 ng $µl^{-1}$) and yield (≥3 µg) by Qubit assay reads. Finally, RNA integrity number (RIN) scores were determined using the Agilent bioanalyser that indicated levels of RNA degradation, and samples with RIN values > 7.0 were qualified for RNA sequencing.

Table 3.1 Quality control of RNA-Seq samples. Concentration was measured by Qubit, sample purity was assessed using Agilent NanoDrop, and sample integrity was determined using Agilent bioanalyser. Abbreviations: C=control condition, S= sphingosine challenged condition.

Species	Sample	NanoDrop 260/280	NanoDrop 260/230	Concentration (ng µl^{-1})	Sample volume (µl)	RIN
S. aureus	C1	2.17	2.39	694	6	7.1
	C2	2.06	1.8	368	9	8.0
	C3	2.12	2.26	726	6	7.8
	S1	2.06	1.88	426	10	7.1
	S2	1.92	1.88	356	10	8.3
	S3	2.03	2.35	399	10	7.2
S. epidermidis	C1	2.16	2.32	1080	3	8.3
	C2	2.15	2.41	≥1200	3	8.4
	C3	2.16	2.5	≥1200	3	8.5
	S1	2.15	2.03	696	5	8.7
	S2	2.18	2.45	1040	3	8.6
	S3	2.16	1.8	820	4	7.3

Agilent bioanalyser visual output (Figure 3.2) showed the expected RNA integrity and relative levels of particular sizes of RNA; using the Prokaryote Total RNA assay kit, the 16S and 23S prokaryotic RNA fragments were detected. Thus, for the staphylococcal RNA purifications, two large peaks corresponding to 16S and 23S RNA were expected (from left to right). The RNA LabChip kit has a marker solution, which contains a 25 nt DNA fragment that was used as a lower marker to align all samples. The marker is displayed on the left as the first small peak in the electropherogram, and as the green band in the gel-like image on the right. The presence of less pronounced peaks for 23S and 16S RNA or other small peaks indicate degradation and lower quality of the purified samples.

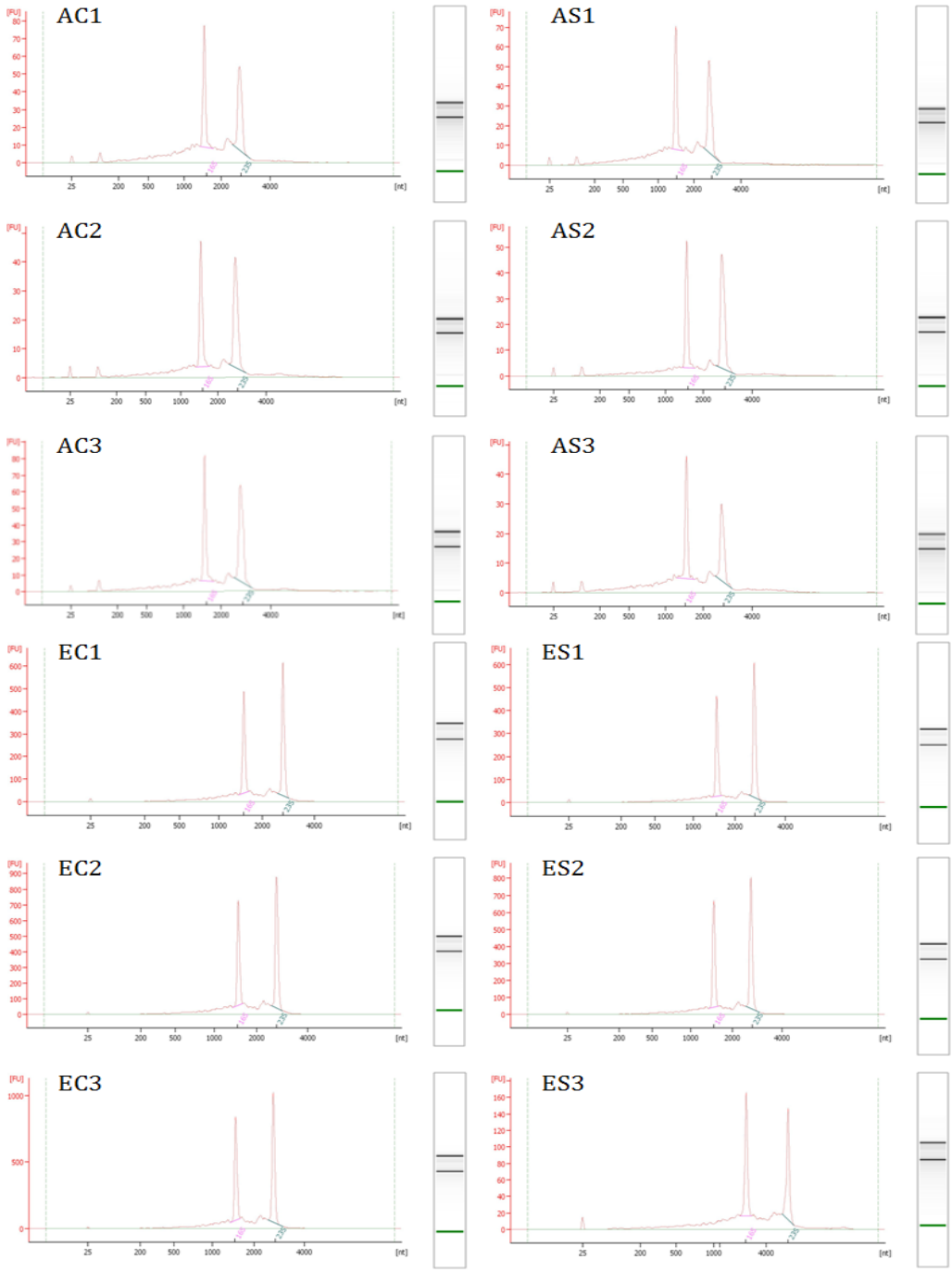

Figure 3.2 Bioanalyser QC of RNA-Seq samples. Samples are : *S. aureus* Newman control 1, 2 and 3 (AC1, AC2 and AC3 respectively), *S. aureus* Newman sphingosine treated 1, 2 and 3 (AS1, AS2 and AS3 respectively), *S. epidermidis* Tü3298 control 1, 2 and 3 (EC1, EC2 and EC3 respectively), and *S. epidermidis* Tü3298 sphingosine treated 1, 2 and 3 (ES1, ES2 and ES3 respectively). The visual output for the determined RNA integrity using the Agilent bioanalyser showed the characteristic profiles for purified, intact RNA with expected levels of particular sizes of RNA. The pronounced two large peaks indicate the presence of 23S and 16S RNA and other small peaks suggest their degradation. The three bands in the gel image on the right show the presence of 23S RNA, 16S RNA and the assay marker.

3.3.3 Comparison of *S. aureus* Newman and *S. epidermidis* Tü3298 transcriptional responses to D-sphingosine challenge

Analysis of RNA sequence reads was performed by the Centre for Genome Research (CGR), Liverpool, which reported genes that were differentially expressed (DE) between the ethanol control and D-sphingosine-challenged samples for *S. aureus* Newman and *S. epidermidis* Tü3298. Following this, curated data for *S. aureus* Newman revealed 1331 DE genes (Appendix III) in response to D-sphingosine challenge, of which 665 were upregulated and 666 genes were downregulated. In contrast, a smaller DE gene set was observed as the response of *S. epidermidis* Tü3298, which exhibited 340 DE genes, of which 211 were upregulated and 129 were downregulated.

Among the *S. epidermidis* Tü3298 DE genes, 260 genes had a homolog in *S. aureus* Newman. Of these, 142 DE genes were present in the *S. aureus* DE gene dataset, with 72 genes sharing upregulation and 42 genes sharing downregulation, while 28 genes were oppositely regulated. A heatmap was generated of up- and downregulated DE genes of D-sphingosine challenged *S. aureus* Newman to compare with those of *S. epidermidis* Tü3298 (Figure 3.3).

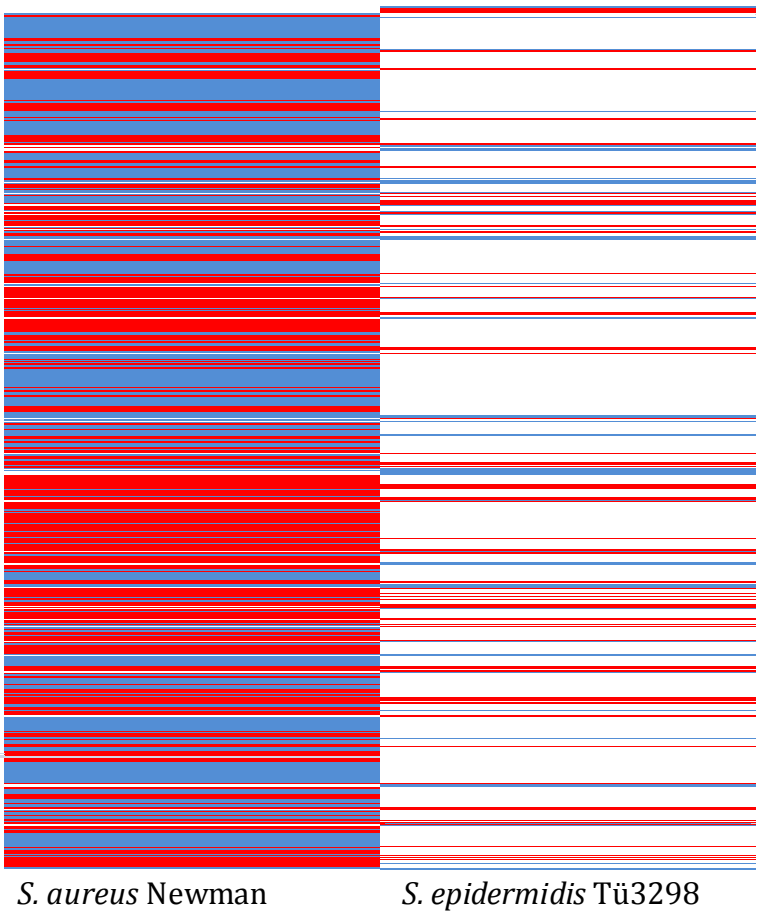

Figure 3.3 Heatmap of differential homologous gene expression for *S. aureus* Newman and *S. epidermidis* Tü3298 after challenge with D-sphingosine. The genes are ordered from top to bottom based on *S. aureus* genome position: upregulated genes (red); downregulated genes (blue). White indicates genes that are not differentially expressed in the corresponding species.

3.3.4 Comparison of DE gene COGs

Classification of DE genes using Clusters of Orthologous Groups (GOG) analysis was used to assess the most affected cellular pathways in *S. aureus* and *S. epidermidis* following D-sphingosine challenge. DE genes found in the transcriptome data were sorted into 20 categories, which were further grouped into four higher functions: cellular processing and signalling, information storage and processing, metabolism and poorly characterised (indicated by "X") genes with hypothesised or unknown function. On the basis that DE genes will be evenly distributed across the genome, the number of DE genes in each COG

class should be proportional to the number of genes encoded by the genome in that class. Thus, COGs analysis will reveal whether the numbers of DE genes in these orthologous classes are higher or lower than would be expected and so reflect the cell response at the pathway level.

Table 3.2 COG classes and upper categories.

Categories	Classes	Description
Cellular processes and signalling	D	Cell cycle control, cell division, chromosome partitioning
	M	Cell wall/membrane/envelope biogenesis
	N	Cell motility
	O	Posttranslational modification, protein turnover, chaperones
	T	Signal transduction mechanisms
	U	Intracellular trafficking, secretion, and vesicular transport
	V	Defence mechanisms
	W	Extracellular structures
	Y	Nuclear structure
	Z	Cytoskeleton
Information storage and processing	A	RNA processing and modification
	B	Chromatin structure and dynamics
	J	Translation, ribosomal structure and biogenesis
	K	Transcription
	L	Replication, recombination and repair
Metabolism	C	Energy production and conversion
	E	Amino acid transport and metabolism
	F	Nucleotide transport and metabolism
	G	Carbohydrate transport and metabolism
	H	Coenzyme transport and metabolism
	I	Lipid transport and metabolism
	P	Inorganic ion transport and metabolism
	Q	Secondary metabolites biosynthesis, transport and catabolism
and poorly characterised	R	General function prediction only
	S	Function unknown

D-sphingosine treatment of *S. aureus* Newman resulted in more up-regulated genes (Figure 3.4) than would be expected in the following COG classes: M, O, C , E, G, H, I, P, Q, R, S. A greater number of downregulated genes than expected were observed in the following COG classes: J, C, F and G.

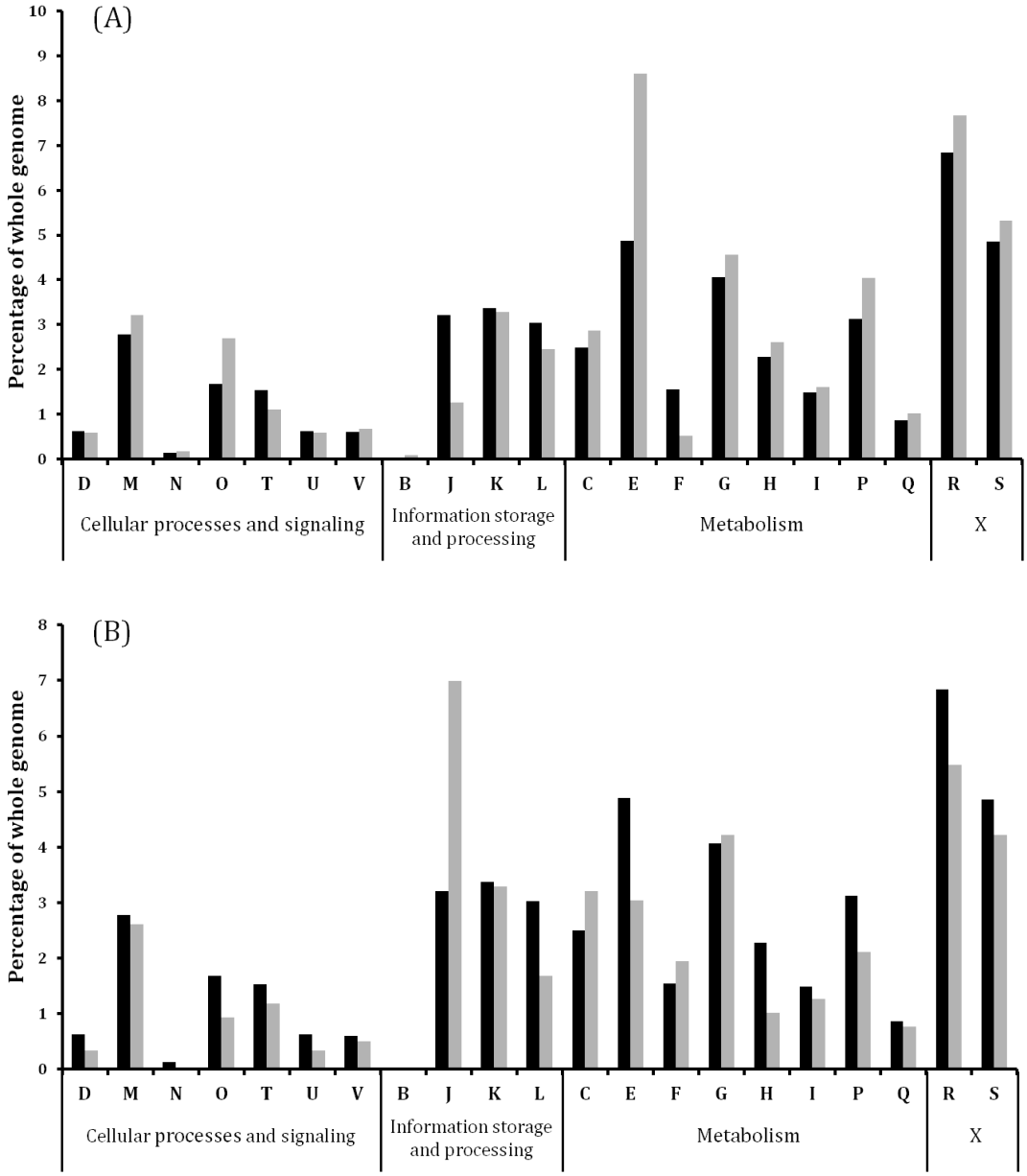

Figure 3.4 Relative percentage of *S. aureus* Newman DE genes in each COG class.

Data of the expected percentage (black bars) versus the observed percentage (grey bars) of genes in each COG class, assuming even expression across the genome, for up regulated DE genes (A) and downregulated DE genes (B). Genes were assigned to COG classes using WebMGA. Categories see table 3.2.

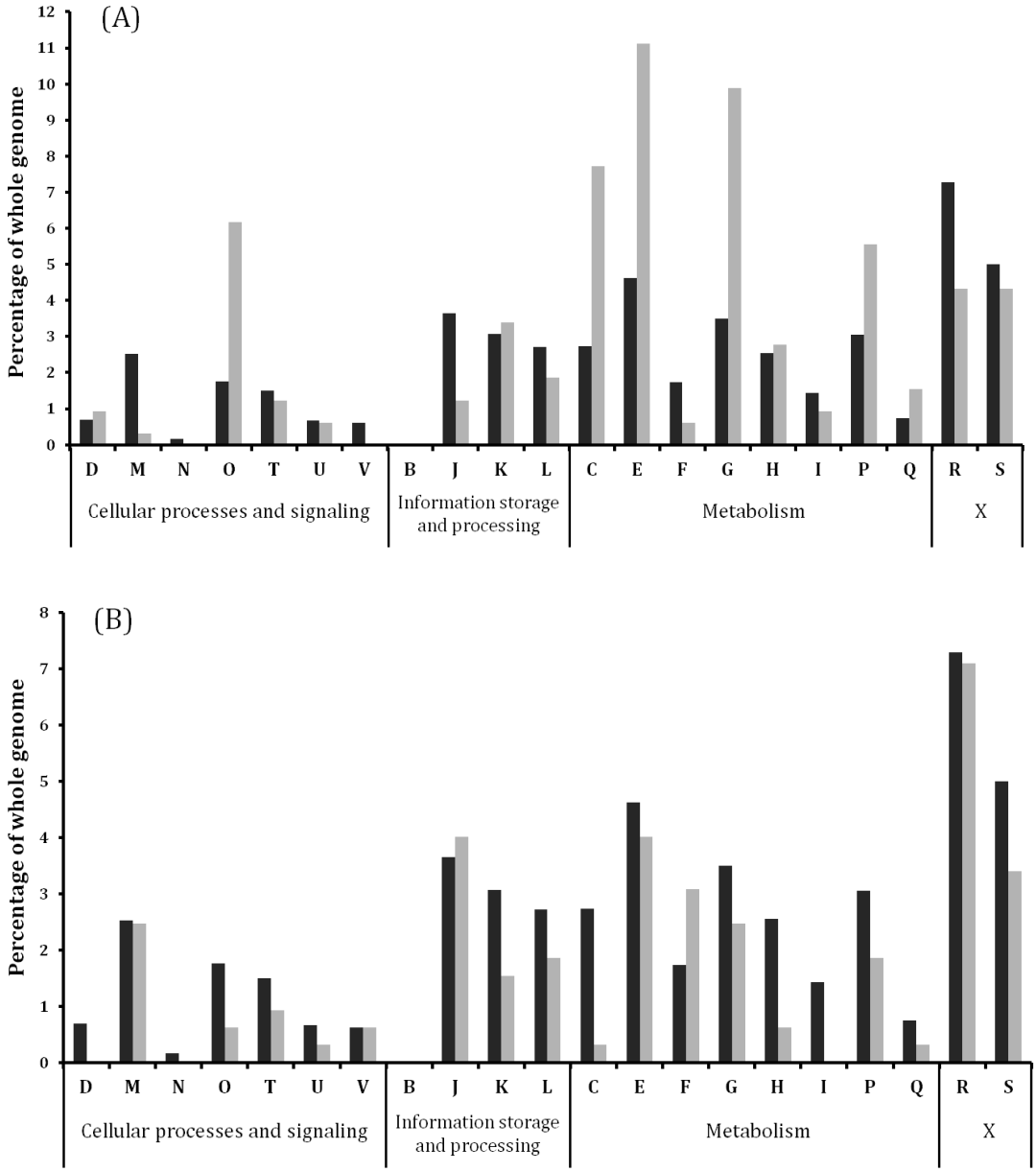

Figure 3.5 Relative percentage of *S. epidermidis* Tü3298 DE genes in each COG class.

Data of the expected percentage (black bars) versus the observed percentage (grey bars) of genes in each COG class assuming even expression across the genome, for up regulated DE genes (A) and downregulated DE genes (B). Genes were assigned to COG classes using WebMGA. Categories are see table 3.2.

Analysis of *S. epidermidis* DE genes using COG classification (Figure 3.5) showed more up-regulated genes than would be expected in classes D, O, K, C, E, G, H, P, and Q.

In comparison, both *S. aureus* and *S. epidermidis* show similar upregulation of genes involved in post translational modification, protein turnover and chaperones, which might reflect a requirement to repair and recycle the proteome. Both species exhibit greater than predicted downregulation in translation, ribosomal structure and biogenesis, as well as nucleotide transport and metabolism, indicative of a reduction in growth and *de novo* biosynthesis.

Both species exhibit greater than predicted upregulation of most metabolism pathways (e.g. energy production and conversion, amino acid, carbohydrate and inorganic ion transport and metabolism). The species differ in their regulation, however, with *S. epidermidis* showing a greater expression of energy related pathways than *S. aureus*, which could indicate that *S. epidermidis* has a faster and/or better adaptive response to D-sphingosine than *S. aureus*.

3.3.5 Comparison of DE metabolic pathways

The metabolic pathways corresponding with the DE genes were displayed by using the KEGG mapper 'search and colour pathway' program (version 2.1) using the DE gene lists produced by the Centre for Genome Research (CGR), University of Liverpool. To achieve this, the *S. epidermidis* Tü3298 gene names were converted to *S. epidermidis* Rp62a homologous gene names using bespoke perl scripts prior to their use in KEGG mapper, because the *S. epidermidis* Tü3298 genome is not an available reference genome for the KEGG database. Fifty nine *S. epidermidis* Tü3298 DE genes had no homolog in strain *S. epidermidis* Rp62a, therefore these genes were removed from the analysis. The differentially expressed genes were highlighted in the KEGG pathway maps, using colours to show the range of up- or downregulated Log_2FC (log2 fold change) values. These pathways enabled detection of metabolic processes corresponding with DE genes to propose an overview of the effects of D-sphingosine on cell metabolism.

Table 3.3 DEenes involved in energy production pathways of D-sphingosine-treated *S. aureus* Newman and *S. epidermidis* Tü3298.

Display of DE genes associated with energy production that were upregulated with Log_2FC >0.5 or downregulated Log_2FC <-0.5 after D-sphingosine treatment in *S. aureus* Newman and *S. epidermidis* Tü3298. The fold level changes are indicated by different colour blocks in the colour key. Dark grey colour blocks indicate genes absent in one species, and a white colour block represents genes that were not differentially expressed in the RNA-Seq data. KEGG mapper output pathways relevant to this table are: glycolysis/gluconeogenesis; pentose phosphate pathway; phosphotransferase system (PTS); citrate cycle (TCA cycle); fructose and mannose metabolism; galactose metabolism; amino sugar and nucleotide sugar metabolism; pyruvate metabolism; propanoate metabolism; butanoate metabolism; and glutathione metabolism.

3.0 to 3.9
2.0 to 2.9
1.0 to 1.9
0.5 to 0.9
-0.9 to -0.5
-1.9 to -1.0
-2.9 to -2.0

S. aureus		***S. epidermidis***	**Enzyme EC**
Log_2FC	Gene name	Log_2FC	**number**
Sugar uptake			
-1.7	*glcA*		2.7.1.199
+1.0	*NWMN_0177*		
+1.7	*NWMN_1333*		
-1.5	*ptsG*		
-0.9	*mtlF*		2.7.1.197
-1.0	*mtlA*		
	NWMN_1619 *SETU_01288*	+1.3	2.7.1.193
-0.7	*NWMN_0136*		2.7.1.211
-1.1	*NWMN_2279*		
+2.0	*NWMN_0199*		2.7.1.-

Table 3.3 continued

S. aureus		*S. epidermidis*	Enzyme EC number
Log_2FC	Gene name	Log_2FC	
Sugar uptake			
+0.7	*NWMN_0182*		2.7.1.200
-0.9	*mtlF*		2.7.1.197
-1.1	*mtlA*		
-1.4	*fruB* *fruK*	+2.6	2.7.1.56
-1.2	*fruA*	+2.6	2.7.1.202
	NWMN_2540 *SETU_02093*	+1.9	
+0.5	*lacE*	+2.3	2.7.1.207
	lacF	+2.2	
	NWMN_0621 *SETU_02169*	+1.2	2.7.1.195
Glycolysis			
+0.5	*glk*		2.7.1.2
+0.7	*pgi*		5.3.1.9
+0.5	*fbp*		3.1.3.11
+0.6	*gapB*		1.2.1.12
-0.5	*gpmA*		5.4.2.11
+0.5	*pckA*	+1.8	4.1.1.49
+0.9	*NWMN_1858* *SETU_01602*		1.2.1.3
+0.9	*NWMN_0534*		5.3.1.27
-0.6	*gntK*	+1.6	2.7.1.12
+0.9	*NWMN_0533*		4.1.2.43
+0.5	*tkt*		2.2.1.1
+1.0	*NWMN_1672*		2.2.1.2
+0.6	*NWMN_0183*		1.1.1.14
-1.0	*manA1*		5.3.1.8
-1.0	*mtlD*		1.1.1.17
-0.6	*gtaB*		2.7.7.9
-0.8	*capE*		5.1.3.2
-0.4	*capN*		

Table 3.3 continued

S. aureus		*S. epidermidis*	Enzyme EC number
Log_2FC	Gene name	Log_2FC	
Glycolysis			
-0.9	*capP*		5.1.3.14
-0.6	*capG*		
	lacA	+2.2	5.3.1.26
	lacB	+2.4	
	lacC	+2.6	2.7.1.144
	lacD	+2.7	4.1.2.40
+0.6	*lacG*	+2.0	3.2.1.85
	malA	+1.5	3.2.1.20
+1.1	*NWMN_0532*		3.5.99.6
+1.1	*nagA*		3.5.1.25
-0.5	*NWMN_2504*		1.1.5.4
-0.5	*sdhC*		1.3.5.1
-0.7	*sdhA*		
-0.7	*sdhB*		
Pyruvate metabolism			
-1.0	*ldh1*		1.1.1.27
+0.4	*ldh*		
+0.6	*NWMN_2422*		1.1.1.28
+1.0	*NWMN_2459*		
-0.6	*ackA*		2.7.2.1
+1.1	*NWMN_1315* *SETU_00980*	+1.0	3.6.1.7
+0.7	*NWMN_2506*		6.2.1.1
-0.5	*pdhA*		1.2.4.1
-0.4	*pdhB*		
-0.4	*pdhC* *SETU_02150*	+2.5	2.3.1.12
-0.5	*pdhD*		1.8.1.4
	lpdA *SETU_02153*	+3.3	
-2.2	*pflB*	+3.7	2.3.1.54
+1.0	*NWMN_1263*		4.2.1.3

Table 3.3 continued

S. aureus		*S. epidermidis*	**Enzyme EC number**
Log_2FC	Gene name	Log_2FC	
Pyruvate metabolism			
+0.9	*citZ* *gltA*	+1.0	2.3.3.1
	sucA	+1.6	1.2.4.2
	sucB	+1.6	2.3.1.61
+1.0	*ilvB*	+1.5	2.2.1.6
	SETU_01538	+2.1	
+1.7	*alsD*		4.1.1.5
	budA *SETU_02007*	+0.7	
	NWMN_0071 *SETU_02090*	+2.0	1.1.1.76
+0.5	*pckA*	+1.8	4.1.1.49
NADH recycling			
-1.0	*ldh1*		1.1.1.27
+0.4	*ldh*		
+0.9	*citC*		1.1.1.42
+1.0	*zwf*		1.1.1.49

Following D-sphingosine challenge, genes associated with sugar uptake, glycolysis and pyruvate metabolism of *S. epidermidis* Tü3298 were notably upregulated, suggesting an overall increase in energy production (Table 3.3). In contrast, *S. aureus* Newman showed mainly upregulated pyruvate metabolism and NADH recycling, but downregulated sugar uptake pathways. Hence, there is no consistent identifiable trend in upregulation or downregulation of general energy production and substrate transport across *S. aureus*.

Table 3.4 DE genes involved in ammonia production pathways of D-sphingosine-treated *S. aureus* Newman and *S. epidermidis* Tü3298.

DE genes associated with ammonia production that were upregulated with Log_2FC >0.5 or downregulated Log_2FC <-0.5 with D-sphingosine treatment in *S. aureus* Newman and *S. epidermidis* Tü3298 are displayed respectively. The levels of fold changes are indicated with different colour blocks in the colour key. A white colour block represents genes that were not differentially expressed in the RNA-Seq data. KEGG mapper output pathways relevant to this table were: purine metabolism; arginine and proline metabolism; nitrogen metabolism; and two-component systems.

1.0 to 1.9
0.5 to 0.9
-0.9 to -0.5
-1.9 to -1.0

S. aureus		***S. epidermidis***	**Enzyme EC number**
Log_2FC	Gene name	Log_2FC	
+1.2	*ureA*		3.5.1.5
+1.3	*ureB*		
conti+1.1	*ureC*		
	arc *arcA*	+1.1	2.7.2.2
-0.5	*NWMN_1852* *SETU_01471*		1.14.14.47
-0.6	*narJ*		NarJ
-0.8	*narH*		1.7.5.1
-2.0	*narG*		
-1.0	*nirD*		1.7.1.15
-1.4	*nirB*		

Similarly, no consistent trend across both species was observed in ammonia production after sphingosine challenge (Table 3.4). Upregulation of the *ureABC* operon was observed in *S. aureus,* where UreA, UreB and UreC are the urease subunits that catalyse the hydrolysis of urea to form ammonia and carbamate. Urease (urea amidohydrolase) is a nickel-binding enzyme, and each subunit

binds two nickel ions via four histidines, an aspartate and a carbamated-lysine (Jabri *et al.*, 1995). Consistent with ammonia production, there was down regulation of nitric-oxide synthase oxygenase (*NWMN_1852*) that would preserve ammonia. However, downregulation of genes that encode for nitrate reductase (*narG, narH, narJ*) and nitrite reductase (*nirB, nirD*) would reduce ammonia generation from these alternative pathways. In *S. epidermidis,* the only pathway change was upregulated *arcA* that encodes arginine deiminase, which catalyses the conversion of arginine to produce ammonia.

Table 3.5 DE genes involved in amino acid production pathways of D-sphingosine-treated *S. aureus* Newman and *S. epidermidis* Tü3298.

DE genes associated with amino acid production that were upregulated with Log_2FC >0.5 or downregulated Log_2FC <-0.5 after D-sphingosine treatment in *S. aureus* Newman and *S. epidermidis* Tü3298 are displayed respectively. The fold level changes are indicated by different colours in the colour key. A white colour block represents genes that were not differentially expressed in the RNA-Seq data. KEGG mapper output pathways relevant to this table are: Histidine metabolism; Glycine, serine and threonine metabolism; Cysteine and methionine metabolism; Lysine biosynthesis; Valine, leucine and isoleucine biosynthesis; and Alanine, aspartate and glutamate metabolism.

2.0 to 2.9
1.0 to 1.9
0.5 to 0.9
-0.9 to -0.5
-1.9 to -1.0
-2.9 to -2.0
-3.9 to -3.0
< -4.0

S. aureus		***S. epidermidis***	**Enzyme EC number**
Log_2FC	Gene name	Log_2FC	
+1.2	*hisD* *SETU_02135*	+0.9	1.1.1.23
	hisG	+2.0	2.4.2.17
+1.1	*NWMN_2577*		2.4.2.17
+1.4	*hisA*		5.3.1.16
+1.2	*hisF*		4.1.3.-
+1.5	*hisH*		2.4.2.-
+1.4	*hisB*		4.2.1.19
+1.5	*hisC*		2.6.1.9
+0.9	*NWMN_1858*		1.2.1.3
-0.8	*hutG*		3.5.3.8
+1.7	*NWMN_2331* *garK*	+1.1	2.7.1.165
+0.5	*NWMN_0711*		

Table 3.5 continued

S. aureus			*S. epidermidis*	Enzyme EC number
Log_2FC	Gene name		Log_2FC	
-4.9	*NWMN_1348*	*ilvA*	+1.6	4.3.1.19
+1.1	*NWMN_1967*			
+0.9	*NWMN_2509*	*betA*	+1.7	1.1.99.1
+1.2	*NWMN_2510*	*betB*	+1.6	1.2.1.8
+2.4	*thrC*		+1.9	4.2.3.1
+2.6	*thrB*		+1.6	2.7.1.39
+2.5	*metL*	*hom*	+1.1	1.1.1.3
+1.5	*serA*			1.1.1.95
+0.7	*trpB*			4.2.1.20
+0.7	*trpA*			
+1.0	*NWMN_1228*			4.1.2.48
+1.3	*asd*			1.2.1.11
+2.6	*thrA*			2.7.2.4
+1.3	*lysC*			
+0.7	*NWMN_0350*			4.4.1.8
+0.4	*NWMN_0011*	*SETU_02277*	+1.0	2.3.1.31
+1.4	*metH*			2.1.1.10
+1.3	*metE*			2.1.1.14
+1.1	*NWMN_1612*			1.8.4.14
+1.6	*dapA*			4.3.3.7
+1.6	*dapB*			1.17.1.8
+1.7	*dapD*			2.3.1.89
+0.7	*NWMN_0919*			2.6.1.-
+1.0	*NWMN_1644*			3.5.1.18
+1.4	*lysA*			4.1.1.20
+0.5	*murF*			6.3.2.10
+1.2	*leuC*			4.2.1.33/4.2.1.35
+1.1	*leuD*		+2.1	
+1.1	*leuB*	*SETU_01541*	+2.1	1.1.1.85
+1.2	*leuA*	*SETU_01540*	+2.2	2.3.3.13
+0.9	*ilvB*	*SETU_01537*	+1.5	2.2.1.6
+1.8	*alsS*			
	SETU_01538		+2.1	

Table 3.5 continued

S. aureus	*S. epidermidis*			Enzyme EC number
Log_2FC	Gene name		Log_2FC	
+1.1	*ilvC*	*SETU_01539*	+2.3	1.1.1.86
+0.7	*ilvD*	*SETU_01536*	+1.1	4.2.1.9
+0.9	*ilvE*			2.6.1.42
-1.9	*pyrB*		-1.5	2.1.3.2
+1.1	*argG*		+1.6	6.3.4.5
+1.8	*argH*	*SETU_00508*	+1.6	4.3.2.1
+0.5	*ansA*			3.5.1.1
-5.1	*ald*			1.4.1.1
	NWMN_2454	*SETU_01983*	+2.7	1.2.1.88
	gltD		+0.8	1.4.1.13/1.4.1.14
-1.4	*pyrAA*	*SETU_00773*	-0.7	6.3.5.5
-1.3	*pyrAB*			

Overall, gene expression concerned with amino acid production was upregulated for both *S. aureus* Newman and *S. epidermidis* Tü3298 (Table 3.5), which is consistent with upregulation of protein turnover and recycling and changes in nitrogen pathways. However, consistent with the greater number of DE genes observed in the *S. aureus* response there was a similar relative increase in these pathways compared with *S. epidermidis*. Consistent with this, the upregulation of pyruvate metabolism detailed in table 3.3 will increase metabolites for amino acid production.

Table 3.6 DE genes involved in peptidoglycan biosynthesis pathways of D-sphingosine-treated *S. aureus* Newman and *S. epidermidis* Tü3298.

Display of DE genes associated with energy production that were upregulated with Log_2FC >0.5 or downregulated Log_2FC <-0.5 after D-sphingosine treatment in *S. aureus* Newman and *S. epidermidis* Tü3298. The fold level changes are indicated as different colours in the colour key shown. A white colour block represents genes that were not differentially expressed in the RNA-Seq data. KEGG mapper output pathway relevant to this table is: Peptidoglycan biosynthesis.

	1.0 to 1.9
	0.5 to 0.9
	-0.9 to -0.5

S. aureus		***S. epidermidis***	**Enzyme EC number**
Log_2FC	Gene name	Log_2FC	
-0.6	*murA*		2.5.1.7
+1.1	*murZ*		
+0.5	*murF*		6.3.2.10
+0.5	*mraY*		2.7.8.13
+0.8	*uppP (bacA)*		3.6.1.27
+1.8	*NWMN_1766* *SETU_01431*		2.4.1.129
+0.8	*pbpB*		3.4.16.4

Gene expression pertaining to peptidoglycan biosynthesis was mostly upregulated in *S. aureus* Newman, but was unaffected in *S. epidermidis* Tü3298 (Table 3.6). This overall trend of increased peptidoglycan biosynthesis indicates a difference in the effect that D-sphingosine is having on the cell wall of *S. aureus*. One interpretation is that *S. aureus* repair and recycling pathways are activated that would help with turnover and/or growth of the cell wall as a protective mechanism. A thicker cell wall can act as a defence from certain antimicrobials due to the peptidoglycan interactions limiting disruption of the cell membrane, an effect well-described for vancomycin (Pechous *et al.*, 2004; Utaida *et al.*, 2003). Alternatively, D-sphingosine activates the cell wall stress stimulon.

Genes *murA* and *murZ* encode the bacterial enzyme UDP-N-acetylglucosamine (UDP-GlcNAc) enolpyruvyltransferase (MurA). This enzyme adds enolpyruvyl to UDP-N-acetylglucosamine to form UDP-N-acetylmuramic acid (UDPMurNAc), which is the first step of bacterial cell wall biosynthesis (Eschenburg *et al.*, 2003). MurF catalyses the synthesis of UDP-N-acetylmuramoyl-pentapeptide, the cytoplasmic precursor (the precursor of murein) of the bacterial cell wall peptidoglycan (Longenecker *et al.*, 2005). MraY is an integral membrane protein responsible for the formation of the first lipid intermediate of the cell wall peptidoglycan synthesis (Bouhss *et al.*, 1999).

UppP is a small, highly hydrophobic protein that involved with bacitracin resistance in *Escherichia coli* (Cain *et al.*, 1993). The protein was originally proposed to be an undecaprenol kinase (BacA) (El Ghachi *et al.*, 2004), but was renamed UppP when it was found to be an undecaprenyl pyrophosphate phosphatase (Bernard *et al.*, 2005; El Ghachi *et al.*, 2005).

VraSR regulates transcription of penicillin-binding protein 2 (PBP2) in *S. aureus* (Kuroda *et al.*, 2003). PBP2 functions in staphylococcal cell wall biosynthesis and susceptibility to antimicrobial agents (Kishida *et al.*, 2006). It is an essential protein in methicillin and vancomycin resistance in *S. aureus* (Boyle-Vavra *et al.*, 2003; Severom *et al.*, 2004), and was reported to be inducible by both vancomycin and oxacillin (Yin et al., 2006). Induction of *pbpB* and by β-lactam and related compounds was found to be dependent on *vraS* (Yin *et al.*, 2006). Gene *pbpB* that encode PBP2 in *S. aureus* was found upregulated by 1.74 fold change in D-sphingosine treated *S. aureus* Newman RNA-Seq data. Moreover, cell wall biosynthesis gene *murZ* of vraSR regulon was also upregulated. Altogether, these changes in gene expression support that expression of the *vraSR* operon is inducible by D-sphingosine treatment.

Table 3.7 DE genes involved in membrane lipid biosynthesis pathways of D-sphingosine - treated *S. aureus* Newman and *S. epidermidis* Tü3298.

Display of DE genes associated with membrane lipid biosynthesis that were upregulated with Log_2FC >0.5 or downregulated Log_2FC <-0.5 after D-sphingosine treatment of *S. aureus* Newman and *S. epidermidis* Tü3298. The fold level changes are indicated as different colour blocks in the colour key shown. A grey colour block represents a gene absent in one species, and a white colour block represents a gene that was not differentially expressed in the RNA-Seq data. KEGG mapper output pathways relevant to this table are: Glycerolipid metabolism; Glycerophospholipid metabolism; Fatty acid degradation; Fatty acid biosynthesis; and Carotenoid biosynthesis.

	1.0 to 1.9
	0.5 to 0.9
	-0.9 to -0.5
	-1.9 to -1.0
	-2.9 to -2.0

S. aureus			***S. epidermidis***	**Enzyme EC number**
LogFC	Gene name		LogFC	
Glycerolipid biosynthesis				
-0.6	*plsK*			2.3.1.15
-0.6	*plsX*			
+0.9	*glpK*			2.7.1.30
-2.6	*geh*	*SETU_02128*	+1.9	3.1.1.3
-1.8	*lip*			
Glycerol, glycerolipid, glycerophospholipid metabolism				
+0.9	*NWMN_1858*	*SETU_01602*		1.2.1.3
-0.6	*plsK*			2.3.1.15
-0.6	*plsX*			
+1.3	*glpQ*			3.1.4.46
+0.8	*NWMN_0984*			
+1.0	*NWMN_1614*			

Table 3.7 continued

S. aureus			*S. epidermidis*	Enzyme EC number
Log_2FC	Gene name		Log_2FC	
Glycerol, glycerolipid, glycerophospholipid metabolism				
+1.7	*NWMN_2331*	*SETU_01869*	+1.0	2.7.1.165
+0.5	*NWMN_0711*			
+0.7	*NWMN_0619*	*SETU_02171*	+1.0	2.7.1.-
+0.6	*NWMN_0620*	*SETU_02170*	+1.3	
+1.6	*glpD*			1.1.5.3
+0.5	*NWMN_1230*			2.7.8.-
-0.6	*NWMN_1926*			3.1.4.3
Fatty acid degradation				
+0.9	*NWMN_1858*	*SETU_01602*		1.2.1.3
+1.0	*fadE*			6.2.1.3
+0.8	*NWMN_0346*	*SETU_00013*		2.3.1.9
-0.7	*adhE*			1.1.1.1
-2.3	*adh1*	*SETU_00229*	+1.6	
+0.9	*NWMN_2091*	*SETU_01662*	-0.8	
+0.6	*fadA*			2.3.1.16
+0.6	*fadB*			1.1.1.35
+0.9	*accC*			6.4.1.2
+0.8	*accB*			
-0.5	*fadD*			2.3.1.39
-1.0	*NWMN_0853*			2.3.1.180
-0.8	*NWMN_0854*			2.3.1.179
-0.5	*fabG*			1.1.1.100
Carotenoid biosynthesis				
-1.3	*crtM*			2.5.1.96
-1.2	*crtN*			1.3.8.2
-1.7	*crtI*			1.14.99.44
-1.6	*NWMN_2463*			2.4.1.-
-1.5	*NWMN_2465*			2.3.1.-

There was a stark difference in membrane lipid biosynthesis gene expression between both species of staphylococci. Fatty acid biosynthesis and degradation pathways were mainly upregulated in *S. aureus,* while glycerophospholipid biosynthesis was downregulated (Table 3.7). This may indicate that D-sphingosine treated *S. aureus* utilise fatty acids as a source of membrane lipid rather than undergoing glycerophospholipid biosynthesis. In contrast, D-sphingosine causes little change to lipid pathway gene expression in *S. epidermidis*, indicative of an absence of changes to gene expression being required due to the presence of sphingosine. These data support that sphingosines are metabolised differently in *S. aureus* and *S. epidermidis*, and more toxic in *S. aureus* than *S. epidermidis*.

The operon *crtMNOPQ* encodes enzymes for catalysis of staphyloxanthin biosynthesis and these genes were downregulated in *S. aureus*. Staphyloxanthin is a yellowish-orange carotenoid pigment that gives this species its descriptive golden colour, and was described as an important antioxidant virulence factor (Liu and Nizet, 2009). Staphyloxanthin contributes to integrity of the *S. aureus* cell membrane (Mishra et al., 2011) and facilitates bacterial survival under oxidative stress and during infections (Giachino *et al.*, 2001; Kahlon *et al.*, 2010; Clauditz *et al.*, 2006). Downregulation of staphyloxanthin production will decrease ROS resistance and alter membrane composition although these changes as a response to the antimicrobial activity of sphingosine are unclear.

Table 3.8 DE virulence factor genes of D-sphingosine treated *S. aureus* Newman and *S. epidermidis* Tü3298.

Display of DE virulence factor genes that were upregulated with Log_2FC >0.5 or downregulated Log_2FC <-0.5 after D-sphingosine treatment of *S. aureus* Newman and *S. epidermidis* Tü3298. The levels of fold changes are indicated as different colour blocks and the colour key is shown. A grey coloured block represents absent genes, and a white colour block represents genes that were not differentially expressed in the RNA-Seq data. The KEGG mapper output pathway relevant to this table was: *Staphylococcus aureus* infection.

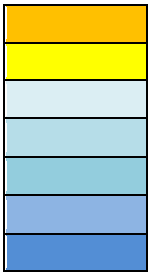

1.0 to 1.9
0.5 to 0.9
-0.9 to -0.5
-1.9 to -1.0
-2.9 to -2.0
-3.9 to -3.0
< -4.0

S. aureus		***S. epidermidis***	**Enzyme EC number**
Log_2FC	Gene name	Log_2FC	
-0.5	*clfA*		ClfA
-1.6	*clfB*		ClfB
-0.5	*sdrE*		SdrC/D
-4.1	*NWMN_1069*		Efb/Ecb
-1.9	*NWMN_0165*		SCIN
-4.2	*NWMN_1070*		
-4.3	*scn*		
-0.9	*spa*		Spa
-3.8	*sbi*		Sbi
-4.2	*NWMN_1067*		FLIPr
-5.4	*chp*		CHIPS
-3.0	*map*		Map
-1.1	*ssl5nm*		SSL5
-4.8	*ssl7nm*		SSL7
-4.6	*ssl11nm*		SSL11

Table 3.8 continued

S. aureus		***S. epidermidis***	**Enzyme Name**
Log_2FC	Gene name	Log_2FC	
-0.5	*dltA*		Dlt
-0.4	*dltB*		
-0.6	*dltC*		
-0.5	*dltD*		
-0.5	*lukE*		Luc
-3.0	*lukF*		
-3.2	*lukS*		
-2.2	*hlgA*		Hlg
-1.8	*hlgC*		
-1.6	*hlgB*		
+1.1	*NWMN_1503*		Enterotoxin
-0.5	*sea*		
-0.9	*eta*		Eta

There was a pronounced downregulation of virulence factor genes in *S. aureus* (Table 3.8) most of which are restricted to this species. This includes genes related to tissue adhesion: *clfA* (Clumping factor A), *clfB* (Clumping factor B), *sdrE* (Serine-aspartate repeat-containing protein E), *NWMN_1069* (Fibrinogen-binding protein); innate immune evasion genes: *scn* (Staphylococcal complement inhibitor), *spa* (Immunoglobulin G binding protein A), *sbi* (Immunoglobulin-binding protein sbi) , *NWMN_1067* (Formyl peptide receptor-like 1 inhibitory protein), *chp* (Chemotaxis inhibitory protein of *S. aureus*), SSLs (*ssl5nm, ssl7nm and ssl11nm*), *map* (MHC class II analog protein Map); and secreted toxins: leukocidin (*lukE, lukF, lukS*), gamma-hemolysin (*hlgA, hlgB, hlgC*), exterotoxins (*NWMN_1503* and *sea*) and exfoliative toxin (*eta*).

The *dltABCD* operon encodes enzymes that esterify lipoteichoic acid (LTA) with D-alanine, which plays an important role in controlling the net anionic charge of LTA. Increased expression of the *dlt* operon in the presence of cationic antimicrobial peptides (CAMPs) limits binding of cationic antimicrobial

peptides since addition of d-alanine to the cell wall results in a net positive charge on the bacterial cell surface, and as a consequence, reduces interaction with CAMPs (Peschel *et al.*, 1999). Expression of the *dlt* operon is also cation-induced in *S. aureus*; *dlt* mRNA was demonstrated to be induced within 15 min by high concentrations of Na^{+} and moderate concentrations of Mg^{2+} and Ca^{2+} (Koprivnjak *et al.*, 2006). Downregulation of the *dlt* operon by D-sphingosine may indicate that interaction with sphingosines is not perceived as being similar to interaction with CAMPs, despite some overlap with the temporin and ovispitin transcriptional responses (Figure 3.8) according to comparison with the SAMMD datasets.

3.3.6 Comparison of sphingosine transcriptome to other *S. aureus* transcriptome data sets

The online bioinformatics web server SAMMD (*S. aureus* Microarray Meta-Database) was used to search for overlaps in gene regulation between the D-sphingosine challenge datasets and published *S. aureus* transcriptomics datasets. Both sphingosine-challenged *S. aureus* Newman and *S. epidermidis* Tü3298 transcriptomes were compared with all datasets in SAMMD (Appendix I).

The gene names were converted to their homologs in strain *S. aureus* N315 to enable the data to be used to search in SAMMD. Genes with a Blast hit to the *S. aureus* N315 genome with an E-value lower than 0.0001 were considered homologous. This resulted in 1239 of 1331 *S. aureus* Newman DE genes and 261 of 340 *S. epidermidis* Tü3298 DE genes being converted to their best match in *S. aureus* N315. Overlaps between *S. epidermidis* Tü3298 and the compared datasets were limited compared with *S. aureus* Newman due to the numbers and matches for DE genes in the *S. epidermidis* data.

Where multiple datasets for the same antimicrobial were available, the dataset using the most similar experimental conditions to that used in the D-sphingosine study was selected. The growth conditions and references of the selected datasets are listed in Appendix.

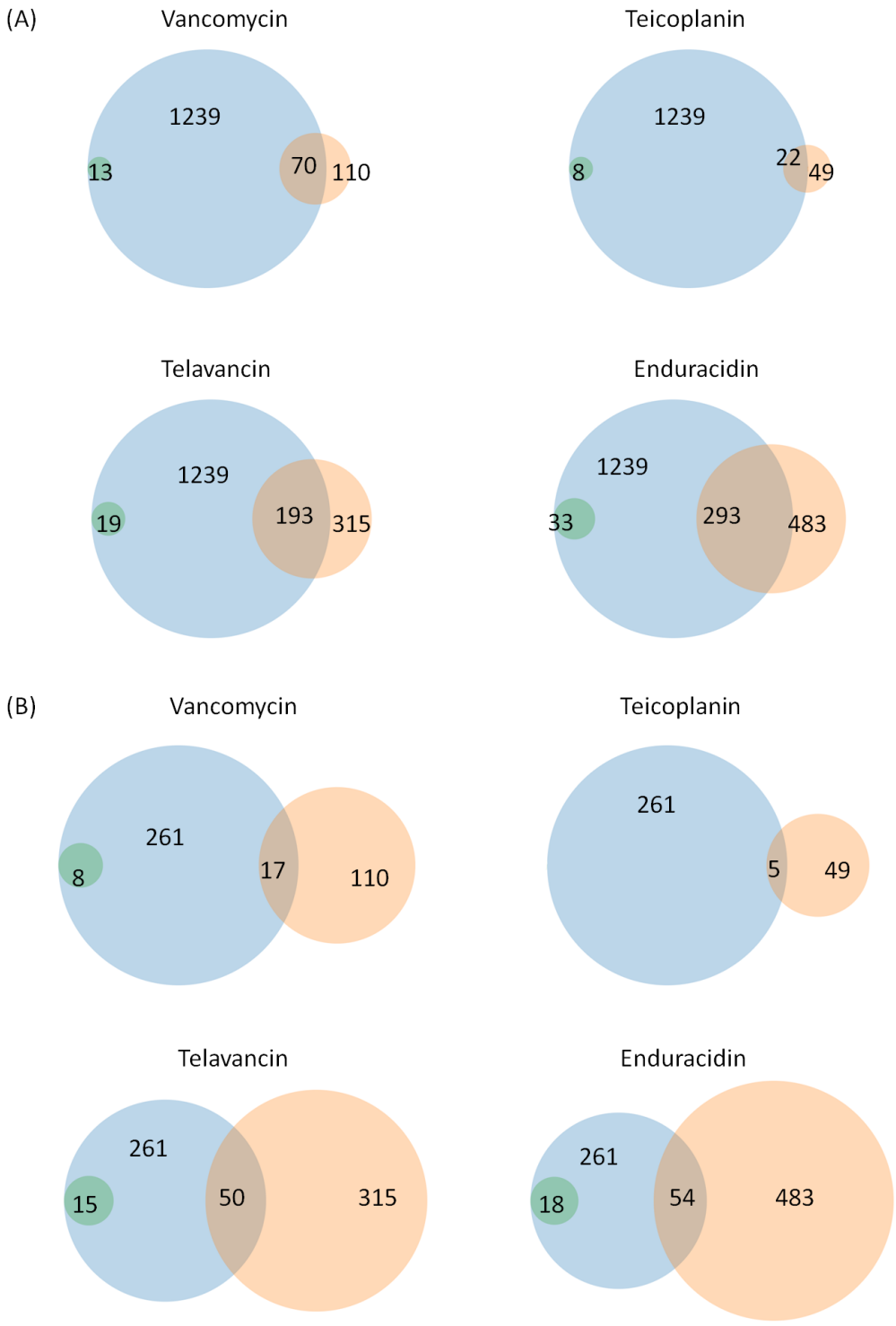

Figure 3.6 SAMMD comparison of D-sphingosine transcriptomes with *S. aureus* vancomycin, teicoplanin, telavancin and enduracidin challenge transcriptomes. Genes in D-sphingosine transcriptome datasets are represented by blue circles and the comparison transcriptome datasets are represented by orange circles, where green circles indicate inversely regulated genes between the datasets. Comparisons between (A) *S. aureus* Newman (B) *S. epidermidis* Tü3298. References and selected experiment conditions of comparison datasets see appendix I.

Although it cannot be argued that the chosen antimicrobials for comparison have similar modes of action, they were nevertheless used to provide insight of potential overlap of cell responses to determine the effects of sphingosine on transcription. In this regard, when considering the high numbers of differentially expressed genes in the *S. aureus* sphingosine dataset there was greatest overlap of regulation (proportion of similarly upregulated or downregulated in the antibiotic challenge comparison dataset) with the vancomycin (64%), teicoplanin (45%), telavancin (61%) and enduracidin (61%) datasets (as a proportion of the comparator datasets) (Figure 3.6).

Of these antimicrobials, vancomycin is a widely-used cell-wall targetting antibiotic in bacterial infection, including methicillin-resistant *S. aureus* (MRSA). Teicoplanin is a semisynthetic glycopeptide with a similar spectrum of activity to vancomycin in the treatment of infections caused by Gram-positive bacteria. Telavancin is a semisynthetic antimicrobial lipoglycopeptide derivative of vancomycin, for use against MRSA and other Gram-positive bacteria that inhibits peptidoglycan biosynthesis (Higgins *et al.*, 2005), and disrupts membrane barrier function by increased cell permeability and depolarisation (Leadbetter *et al.*, 2004). Enduracidin (also named enramycin) is an antimicrobial peptide that induces a similar transcriptome response of *S. aureus* to telavancin (Song *et al.,* 2012).

The overlap between the D-sphingosine challenge response and these transcriptomics datasets of cell-wall targeted and cell membrane targeted antimicrobials supports both cell wall and membrane stress caused by sphingosine. The overlapped gene regulation in these datasets includes cell envelope-related genes *lytM, murF, murZ, pbpB* (named *pbp2* in strain N315), *bacA* and *vraRS*, encoding the cell wall stress TCS.

In addition to the shared cell wall stimulon response, various protease and chaperone protein genes *groES, groEL, dnaJ, dnaK, clpP* and *prsA* shared upregulation in the overlapped datasets, likely indicating accumulation of protein damage. The *clpC* repressor gene *ctsR,* which is part of the protein

quality control system in Gram-positive bacteria, was downregulated in both datasets.

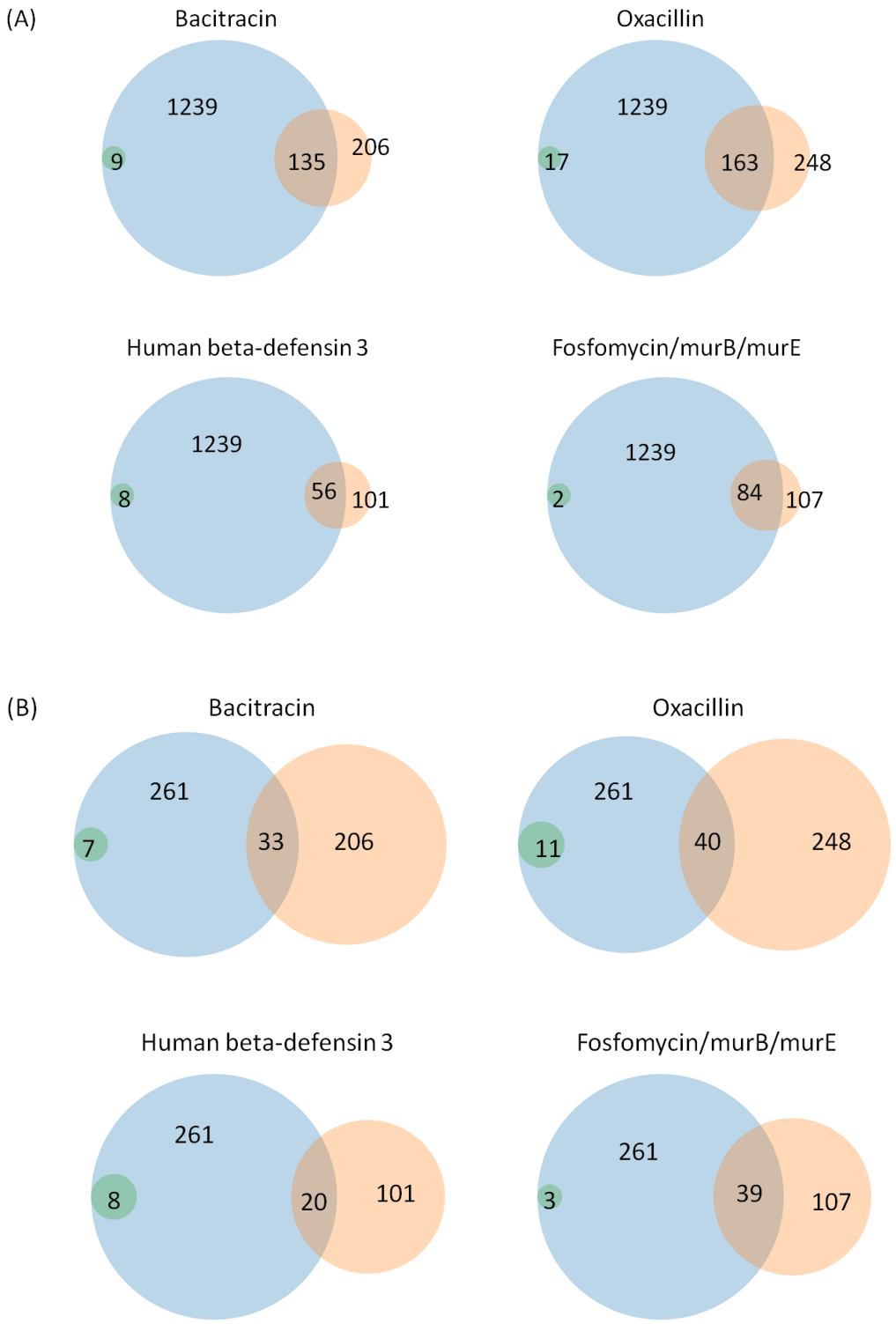

Figure 3.7 SAMMD comparison of D-sphingosine transcriptomes with *S. aureus* cell wall biosynthesis inhibitor transcriptomes.

Genes in D-sphingosine datasets are represented by blue circles, the comparison datasets are represented by orange circles, and green circles indicate inversely regulated genes between the datasets. (A) *S. aureus* Newman. (B) *S. epidermidis* Tü3298. References and selected experiment conditions of comparison datasets see appendix I.

Given the output from the comparative analysis above, where an overlap with the sphingosine and cell wall antibiotic responses was observed, further cell wall active antimicrobials, including AMPs were included in additional comparisons (Figure 3.7): bacitracin is a mixture of cyclic peptides; oxacillin is a beta-lactam similar to methicillin; fosfomycin is a phosphoenolpyruvate analogue; and human beta defensin3 is a cationic antimicrobial peptide (CAMP). Fosfomycin was an inhibitor of *murA* and *murZ* and show similar transcriptomic responses as that in *murB* or *murE* depletion mutants (O'Neill *et al.*, 2009). Each of these listed compounds are reported as cell wall active antibiotics (O'Neill *et al.*, 2009; Utaida *et al.*, 2003; Sass *et al.*, 2008) despite their different molecular structures.

Overlapping regulation (proportion of similarly upregulated or downregulated in the listed antimicrobial comparison dataset) was observed between the *S. aureus* D-sphingosine transcriptome and those of the bacitracin (66%), oxacillin (66%), fosfomycin/*murE/B* mutant (79%) and human beta defensin3 (55%) transcriptomes (as a proportion of the comparator datasets); low overlap numbers were seen for oppositely regulated genes. While a high proportion of these transcriptomes' differentially-regulated genes was determined to resemble the sphingosine transcriptome, a lesser extent of overlapped data was seen with the daptomycin transcriptome (23% similar regulation and 22% opposite regulation; Venn diagram not shown).

The transcriptomic overlaps between the responses to D-sphingosine and these cell wall biosynthesis inhibitors supports an interpretation that part of the response to D-sphingosine is inhibition of cell wall biosynthesis. This could be through direct inhibition of biosynthesis pathways, or via downregulation of genes involved in cell wall biosynthesis both of which could be hierarchically coordinated by VraSR and other described regulators of transcription. Because KEGG pathway analysis (Table 3.6) indicates an overall upregulation in peptidoglycan synthesis, it is equally likely that D-sphingosine simultaneously affects cell wall biosynthesis by direct interactions.

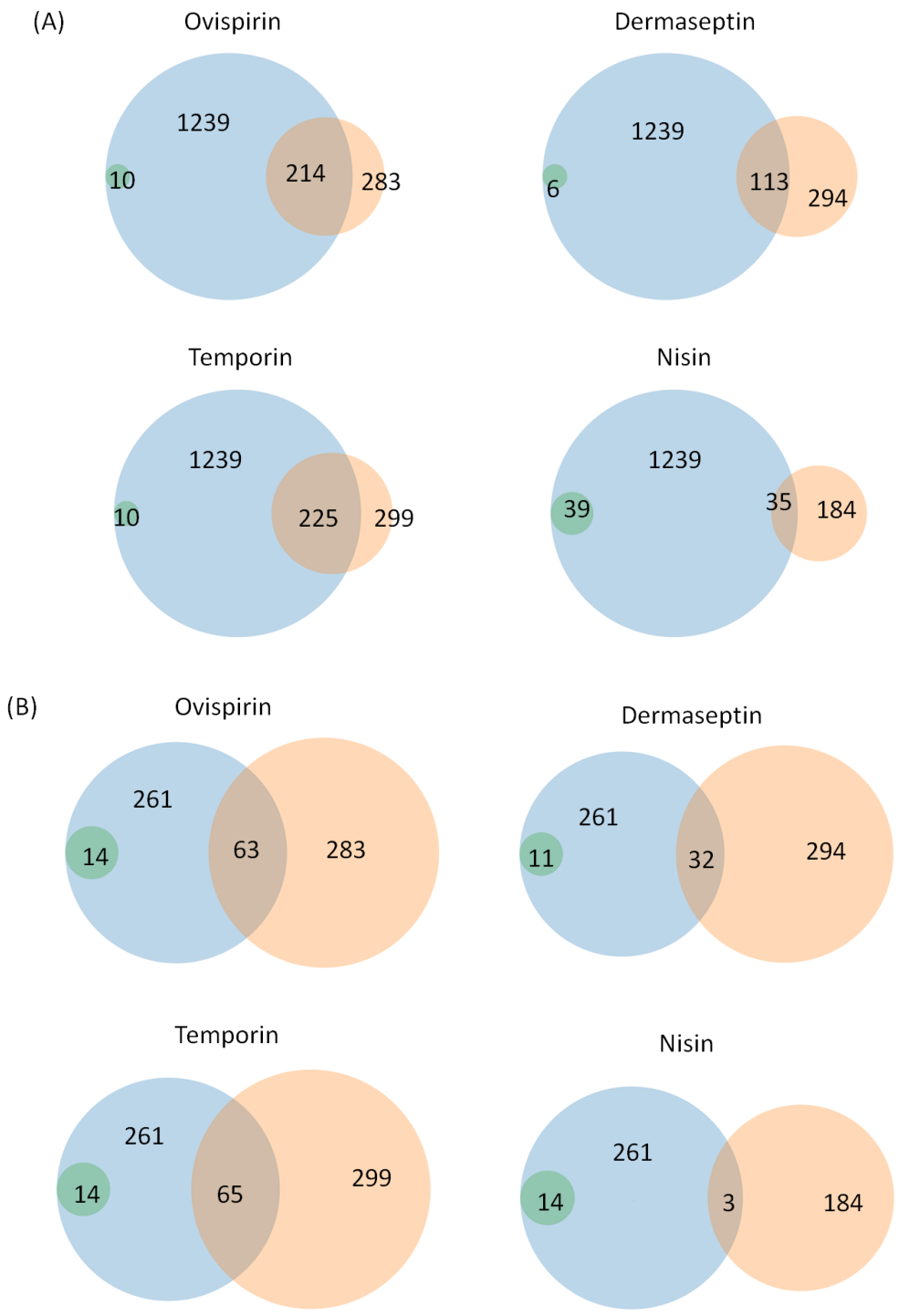

Figure 3.8 SAMMD comparison of D-sphingosine transcriptomes with *S. aureus* membrane disrupting antimicrobials transcriptomes. Genes in D-sphingosine datasets are represented by blue circles and comparison datasets are represented by orange circles, with green circles indicating inversely regulated genes between the datasets. (A) *S. aureus* Newman (B) *S. epidermidis* Tü3298. References and selected experiment conditions of comparison datasets see appendix I.

The transcriptomes of the *S. aureus* responses to AMPs that are reported to cause membrane disruption were also compared with the sphingosine transcriptome (Figure 3.8). The responses of *S. aureus* to D-sphingosine exhibited partial overlap with that of the AMPs- ovispirin (76%) and temporin (75%) responses (as a proportion of the temporin and ovispirin datasets). Whilst a lesser overlap was revealed with dermaseptin (38%) and nisin (19% similar and 21% opposite).

Comparative analysis revealed that the transcriptomes of *S. aureus* responses to ovispirin, temporin and dermaseptin all bear a signature downregulation in nitrate respiration (*nar* operon) and virulence factor genes (*sbi, hlgA, ssl11, clfA, clfB* and *spa*), which were coincident with the D-sphingosine challenge transcriptome. Since the virulence factor genes are all members of the SaeRS regulon this potentially identifies a common response to membrane perturbation via these antimicrobials is a reduction in secreted virulence factors, most of which are concerned with innate immune evasion from complement, antibodies and phagocytes.

Few overlaps were identified between the *S. epidermidis* transcriptomic data and the various cell wall or AMP-related datasets, except upregulation of general stress response genes including the *ctsR-clpC* operon, *groELS* and *dnaJK*, as well as *vraSR*, encoding the two-component system that controls the cell well biosynthesis regulon.

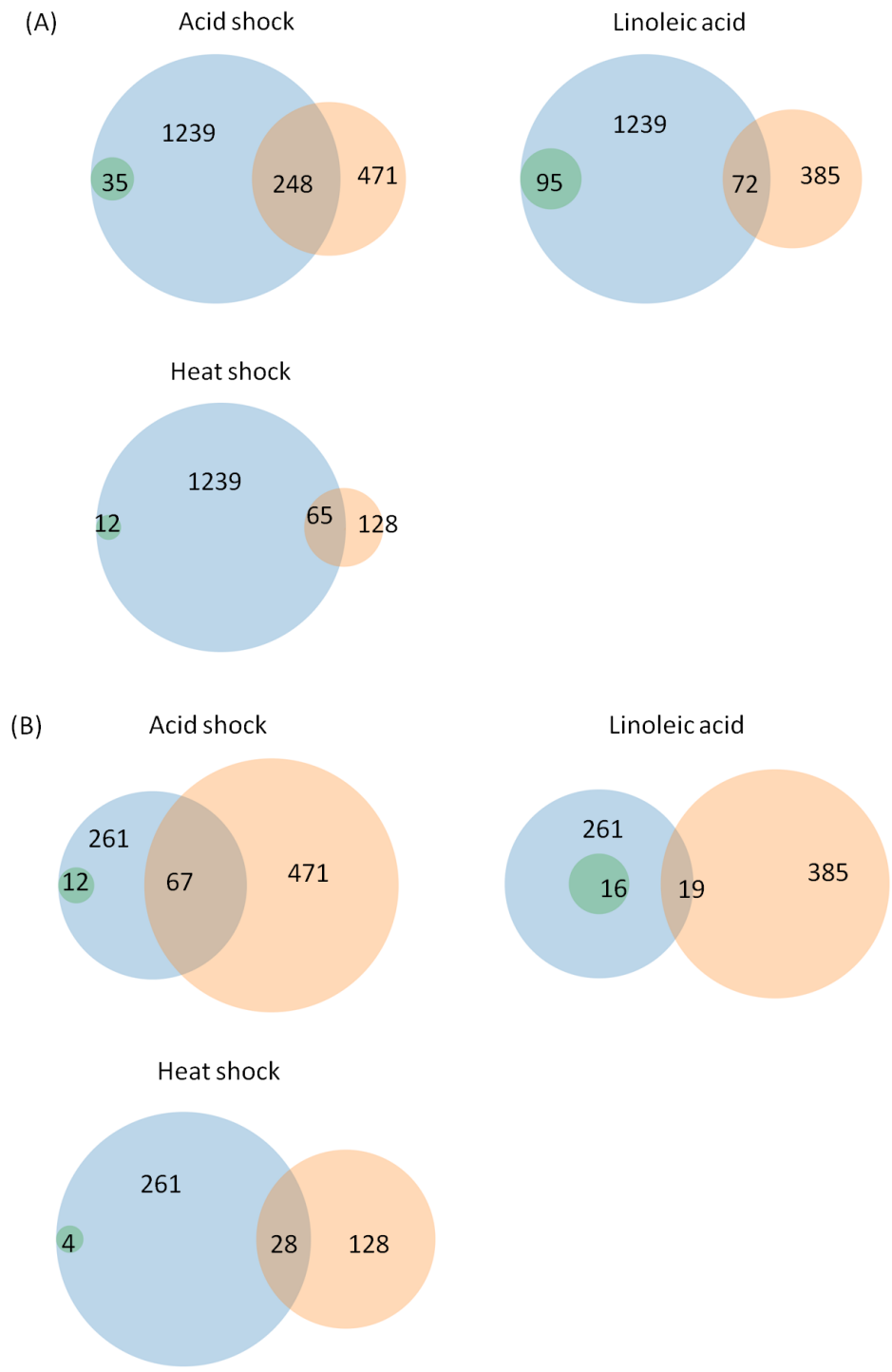

Figure 3.9 SAMMD comparison of D-sphingosine transcriptomes with *S. aureus* acid shock, linoleic acid and heat shock transcriptomes.

Genes in D-sphingosine datasets are represented by blue circles and comparison datasets are represented by orange circles, with green circles indicating inversely regulated genes between the datasets. (A) *S. aureus* Newman (B) *S. epidermidis* Tü3298. References and selected experiment conditions of comparison datasets see appendix I.

As a further comparative exercise, the *S. aureus* D-sphingosine transcriptome was aligned with transcriptomes of acid and heat shock and linoleic acid, another antimicrobial lipid (Figure 3.9). The *S. aureus* data comparison showed a relatively high overlap with the heat shock dataset (51% similar and 9% opposite) (as a proportion of the comparator datasets) including a large number of amino acid metabolism and some general stress response genes. The linoleic acid data was compared because previous work suggested similar transport pathways (*farER* described in chapter 5) for exporting linoleic acid and D-sphingosine, but these datasets were poorly matched (19% similar and 25% opposite)(as a proportion of the comparator datasets).

In contrast, the *S. aureus* D-sphingosine transcriptome overlaps the acid shock dataset to a greater extent, with a high similar proportion (53%) and low opposite proportion (7%) of DE genes (Figure 3.9). Again, this overlap included: upregulation of the urease genes (*ureA, ureB, ureC, ureF*) that encode production of neutralising ammonia as a direct defence to acid shock; genes related to NADH recycling (*zwf, tkt, pgi, gnd*) that assist in reducing energy generation; copper-transporting ATPase *copA* (*SA2344, NWMN_2457*) that pump excess Cu^{2+} to lower metal ion toxicity and oxidative damage caused by excess metal ions; and DNA repair system (*dinP, polA, rexA, rexB*). Additionally, pyrimidine ribonucleotide biosynthesis, ribosomal protein genes and ribosome recycling factor Frr were downregulated in both datasets.

The overlap between the *S. epidermidis* Tü3298 D-sphingosine transcriptome and that of the *S. aureus* acid shock dataset was evident, however, most overlapping regulated genes encode ribosomal proteins. Only two genes were upregulated in both datasets, specifically ammonia production (*arcC*) and *copA* (*SETU_01986*) metal transport.

3.3.7 Comparative transcriptomic responses shared between *S. aureus* and *S. epidermidis*

To build a broader view of the effects that D-sphingosine challenge has on cells of both *S. aureus* and *S. epidermidis,* a catalogue of common DE gene expression was created. Table 3.9 exhibits all common DE homologous genes in response to D-sphingosine challenge of *S. aureus* Newman and *S. epidermidis* Tü3298. These genes can be considered a D-sphingosine stimulon. The changes in gene expression appear to be coordinated by a suite of transcriptional regulators: both species upregulated global regulator *vraSR*, whilst downregulating *saeRS* and together they control most changes in gene expression encoding secreted proteins. In addition, there appears a role for LytR in regulation of autolytic activities. Further hierarchical regulators include: CtsR, HrcA and PhoU. The *pstS* and *pstCABphoU* operon was of specific interest since all members of this operon were strongly upregulated, with Log_2FC value greater than 3 (i.e. >8 fold increase). This operon encodes and regulates expression of the Pst (phosphate-specific transport) system, which is a high-affinity, low-velocity, free-Pi transport system that is structurally similar to an ABC transporter (Ames, 1986). Further investigation of this operon is described in chapter 4.

Upregulated genes associated with transport and metabolism of carbohydrates, amino acids, coenzymes and inorganic ions, identifies an increased need for energy production and conversion. Both species decreased gene expression of nucleotide metabolism and ribosomal biosynthesis, while both species increased expression of genes associated with transcription, post-translational modification, protein turnover and chaperones production. Altogether, this indicates protein damage due to sphingosine challenge and this pattern of gene expression is a general stress response common to various environmental stimuli, including heat and acid stress, and various antimicrobials targeting the cell wall and membrane.

Differences in the responses of both species of *Staphylococcus* include decreased expression of genes for protection against oxidative stress in *S. aureus* contrasting with increased expression in *S. epidermidis* (Table 3.10). The

reduction in expression of staphyloxanthin biosynthesis genes (*crtM,N, P, Q, O*) (Table 3.7) is known to increase susceptibility to oxidative stress in *S. aureus* (Clauditz *et al.*, 2006)

Table 3.9 The D-sphingosine stimulon of *S. aureus* and *S. epidermidis*. Common DE homologous genes with the same trend of regulation in response to D-sphingosine challenge of *S. aureus* Newman and *S. epidermidis* Tü3298. DE genes with greater than two-fold change are listed.

***S. aureus* Newman**		**Description**	***S. epidermidis* Tü3298**	
Gene	Log_2FC		Log_2FC	Gene
Posttranslational modification, protein turnover, chaperones				
clpC	2.3	Clp protease subunit ClpC	2.5	*clpC*
NWMN_0845	2.1	Clp protease subunit ClpB	3.1	*SETU_00522*
dnaJ	1.3	chaperone protein DnaJ	1.1	*SETU_01152*
dnaK	1.5	chaperone protein DnaK	1.5	*dnaK*
grpE	1.4	heat shock protein GrpE	1.7	*SETU_01154*
NWMN_1615	1.5	osmotic stress-related protein	1.1	*SETU_01284*
NWMN_1621	2.4	heat-shock protein htrA	3.0	*SETU_01290*
prsA	2.2	peptidyl-prolyl cis/trans-isomerase	1.9	*SETU_01367*
clpP	2.1	Clp protease proteolytic subunit	1.6	*clpP*
NWMN_0653	1.0	ABC transporter, MsbA family protein	1.4	*SETU_00305*
NWMN_0654	1.1	ABC transporter, MsbA family protein	1.4	*SETU_00306*
Signal transduction mechanisms				
saeS	-3.0	sensor histidine kinase SaeS	-2.3	*SETU_00325*
saeR	-3.0	DNA-binding response regulator SaeR	-2.4	*SETU_00326*
vraS	2.3	sensor histidine kinase VraS	2.7	*SETU_01442*
vraR	2.3	DNA-binding response regulator VraR	2.7	*vraR*
Translation, ribosomal structure and biogenesis				
NWMN_1481	1.1	ribosomal protein L11 methylase	1.0	*prmA*
rplT	-1.2	50S ribosomal protein L20	-1.0	*rplT*
rpmI	-1.2	50S ribosomal protein L35	-1.1	*rpmI*
infC	-1.0	translation initiation factor IF-3	-1.2	*infC*
rpsD	-1.0	30S ribosomal protein S4	-1.1	*rpsD*
rpsI	-1.1	30S ribosomal protein S9	-0.9	*rpsI*

Table 3.9 continued

S. aureus Newman		Description	*S. epidermidis* Tü3298	
Gene	Log_2FC		Log_2FC	Gene
Transcription				
ctsR	2.1	transcriptional regulator CtsR	2.6	*SETU_00140*
hrcA	1.5	heat-inducible transcription repressor	1.8	*SETU_01155*
NWMN_2211	1.2	lyt expression attenuator LytR	1.0	*SETU_01766*
NWMN_2213	1.0	DeoR family transcriptional regulator	1.3	*SETU_01768*
Replication, recombination and repair				
dinP	0.9	DNA polymerase IV	0.9	*SETU_01453*
NWMN_1985	-1.0	RNA helicase	-1.0	*SETU_01562*
Energy production and conversion				
NWMN_1315	1.1	acylphosphatase	1.0	*SETU_00980*
citZ	0.9	citrate synthase	1.0	*SETU_01259*
NWMN_2510	1.2	dehydrogenase gbsA	1.6	*SETU_02028*
NWMN_0653	1.0	ABC transporter, MsbA family protein	1.4	*SETU_00305*
NWMN_0654	1.1	ABC transporter, MsbA family protein	1.4	*SETU_00306*
ndhF	1.1	NADH dehydrogenase subunit 5	2.2	*SETU_00056*
Amino acid transport and metabolism				
leuB	1.1	3-isopropylmalate dehydrogenase	2.1	*SETU_01541*
NWMN_0486	2.3	Arginine kinase	2.6	*SETU_00142*
NWMN_0547	-1.5	cationic amino acid transporter	-1.1	*SETU_00208*
argH	1.8	argininosuccinate lyase	1.6	*SETU_00508*
argG	1.1	argininosuccinate synthase	1.6	*argG*
metL	2.5	homoserine dehydrogenase	1.0	*SETU_00905*
thrC	2.4	threonine synthase	1.9	*SETU_00906*
thrB	2.6	homoserine kinase	1.6	*SETU_00907*
NWMN_1602	1.5	proline dipeptidase	0.9	*SETU_01271*
leuA	1.2	2-isopropylmalate synthase	2.2	*SETU_01540*
leuD	1.1	isopropylmalate isomerase subunit	2.1	*leuD*
ilvA	1.1	threonine dehydratase	1.6	*SETU_01544*
NWMN_2509	0.9	choline dehydrogenase	1.7	*SETU_02027*
hisD	1.2	histidinol dehydrogenase HisD	0.9	*SETU_02135*
hisG	1.1	ATP phosphoribosyltransferase	2.0	*hisG*
ilvB	0.9	acetolactate synthase large subunit	1.5	*SETU_01537*
ilvC	1.1	ketol-acid reductoisomerase	2.3	*SETU_01539*

Table 3.9 continued

S. aureus Newman		Description	*S. epidermidis* Tü3298	
Gene	Log_2FC		Log_2FC	Gene
Nucleotide transport and metabolism				
pyrP	-1.1	uracil permease	-2.5	*SETU_00770*
pyrB	-1.8	aspartate carbamoyltransferase	-1.5	*pyrB*
Carbohydrate transport and metabolism				
NWMN_2331	1.7	glycerate kinase	1.0	*SETU_01869*
NWMN_2048	-1.0	oxidoreductase ylbE	-0.9	*SETU_01623*
Coenzyme transport and metabolism				
ilvB	0.9	acetolactate synthase large subunit	1.5	*SETU_01537*
ilvC	1.1	ketol-acid reductoisomerase	2.3	*SETU_01539*
serA	1.5	D-3-phosphoglycerate dehydrogenase	0.9	*SETU_01286*
Inorganic ion transport and metabolism				
phoU	2.7	Pst regulatory protein PhoU	1.2	*SETU_00960*
pstB	3.1	phosphate ABC transporter	1.7	*SETU_00961*
NWMN_1298	3.5	phosphate ABC transporter	1.6	*SETU_00962*
NWMN_1299	3.8	phosphate ABC transporter	1.5	*SETU_00963*
pstS	4.1	phosphate ABC transporter, PstS	1.5	*SETU_00964*
NWMN_1317	0.9	tellurite resistance protein	1.3	*SETU_00982*
NWMN_2457	1.3	copper-transporting ATPase copA	3.7	*SETU_01986*
Predicted or unknown function				
oppF	1.0	oligopeptide ABC transporter	1.2	*SETU_00530*
NWMN_1316	0.9	phosphate hydrolysis protein XpaC	1.2	*SETU_00981*
oatA	-1.1	secretory antigen precursor SsaA	-1.9	*SETU_01990*
NWMN_0157	-3.3	S-isoprenylcysteine methyltransferase	-2.1	*SETU_02228*
NWMN_0366	-1.6	Transglycosylase associated protein	-1.1	*SETU_00029*
NWMN_0419	1.1	transmembrane protein	2.2	*SETU_00057*
NWMN_0485	2.2	UvrB/UvrC domain-containing protein	2.6	*SETU_00141*
NWMN_1824	2.1	transporter associated with VraSR	2.7	*SETU_01443*
NWMN_2490	-1.0	hypothetical protein	-1.1	*SETU_02000*
NWMN_0542	6.1	hypothetical protein	5.6	*SETU_00201*

Table 3.9 continued

S. aureus Newman		Description	*S. epidermidis* Tü3298	
Gene	Log_2FC		Log_2FC	Gene
Predicted or unknown function				
NWMN_0605	2.5	hypothetical protein	1.3	*SETU_00260*
NWMN_0676	-3.6	DoxX family protein	-2.6	*SETU_00327*
NWMN_0677	-3.2	lipoprotein	-2.7	*SETU_00328*
NWMN_1294	1.2	hypothetical protein	1.4	*SETU_00958*
NWMN_1552	2.6	hypothetical protein	1.1	*SETU_01217*
NWMN_1553	2.9	hypothetical protein	3.8	*SETU_01218*
NWMN_1825	1.7	hypothetical protein	2.4	*SETU_01444*
NWMN_2223	1.8	hypothetical protein	1.4	*SETU_01779*
NWMN_2332	2.0	hypothetical protein	1.4	*SETU_01870*

Table 3.10 Opposite DE homologous genes with the same trend of regulation in response to D-sphingosine challenge of *S. aureus* Newman and *S. epidermidis* Tü3298. DE genes with more than two fold changes were listed.

S. aureus Newman		Description	*S. epidermidis* Tü3298	
Gene	Log_2FC		Log_2FC	Gene
Sugar uptake and energy production				
NWMN_0008	-1.0	homoserine-o-acetyltransferase	1.0	*SETU_02277*
pflB	-2.2	formate acetyltransferase	3.7	*pfl*
NWMN_0163	-2.1	pyruvate formatelyase	4.6	*pflA*
NWMN_0667	-1.2	fructose operon repressor	2.3	*SETU_00318*
fruB	-1.4	fructose 1-phosphate kinase	2.6	*SETU_00319*
fruA	-1.2	PTS fructose-specific transporter	2.6	*SETU_00320*
Protection against oxidative stress				
ahpF	-0.9	alkyl hydrogen peroxide reductase	1.2	*SETU_00034*
ahpC	-1.0	alkyl hydrogen peroxide reductase	1.2	*SETU_00035*
Predicted or unknown function				
NWMN_0511	0.9	amino acid amidohydrolase	-0.9	*SETU_00167*
adh1	-2.3	alcohol dehydrogenase	1.6	*SETU_00229*
NWMN_2585	-1.0	hypothetical protein	1.2	*SETU_02143*

3.3.8 Quantitative PCR validation

Validation of the RNA-Seq data was performed by quantification of selected DE genes in the sphingosine challenge RNA-Seq dataset using qPCR. Method and primers were described in chapter 2 (section 2.6). The fold changes between ethanol control and sphingosine-treated samples were determined for each examined gene. RNA integrity was assessed prior to conversion to cDNA using Bioanalyser, and samples with RIN≥6.5 were considered qualified for subsequent experiments. At least three biological and three technical qPCR replicates were used for each gene.

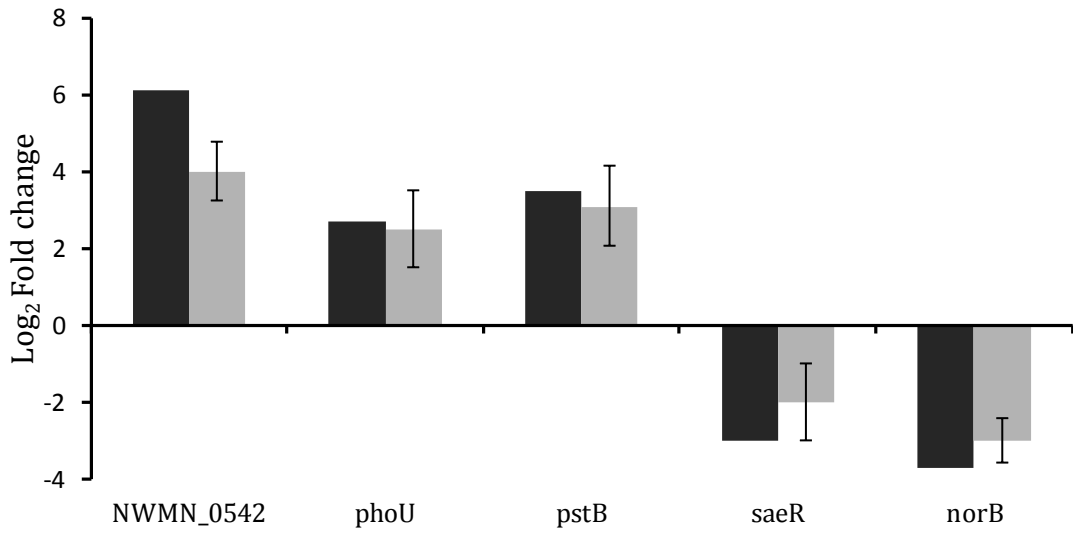

Figure 3.10 Differential expression of *NWMN_0542, phoU, pstB, saeR* and *norB* in *S. aureus* after challenge with D-sphingosine. Black bars indicate the fold change from RNA-Seq data, grey bars indicate fold change from qPCR validation. Error bars refer to standard deviation of fold changes of all replicates.

The log2 fold changes determined by qPCR were consistently lower than the fold changes from RNA-Seq data (Figure 3.10), but all tested genes showed regulation in the same direction and were mostly proportional to the RNA-Seq fold change values. This discrepancy between quantification may be due to underestimation of gene expression by qPCR, or overestimation of gene expression by RNA-Seq or a combination of both. Overall, the qPCR results indicate that regulation direction and general fold changes of RNA-Seq data were consistent.

3.4 Discussion

The transcriptomic dataset of *S. epidermidis* Tü3298 D-sphingosine challenge has much fewer DE genes (340 genes) than the dataset of *S. aureus* Newman (1331 genes). Within those homologous genes shared across the species, 142 genes were differentially expressed in both datasets, which accounts for 42% of all DE genes in *S. epidermidis* Tü3298. Moreover, 80.3% of these DE genes covered in both datasets were regulated in the same direction (50.7% both upregulated and 29.6% both downregulated). Only 19.7% were inversely regulated, indicating a high overlap rate between the transcriptomics response of the two species to D-sphingosine.

Unsurprisinlgy, COG and KEGG pathway analysis also exhibited a strong overlap in transcriptional data of both species, given the gene overlaps. The reasons for the enlarged transcriptional response to sphingosine in *S. aureus* is unclear. This difference could arise for several reasons including: there are more responsive transcriptional regulation regulators; more surface associated damage is caused relative to *S. epidermidis*; sphingosines are not as readily metabolised in *S. aureus* causing widespread changes to occur. The latter explanation might be expected to lead to a reduced MIC for sphingosine. The different primary niches of each species could also have selected for distinct responses to stimuli encountered in their life-cycle and the discrete responses might be indicative of separate evolutionary trajectories.

3.4.1 Virulence factors

Both species of staphylococci showed marked downregulation in the expression of the global regulator *saeRS* operon (8-fold decrease of *saeR* and *saeS* in *S. aureus*; 5.3 and 5 fold decrease of *saeR* and *saeS* in *S. epidermidis* respectively). SaeRS is a two-component regulatory system that controls a regulon of staphylococcal virulence factors, mostly immune evasion proteins such as coagulase (Liu *et al.*, 2016) that directs localised clotting and to protect bacteria from phagocytic and immune defences (Guo *et al.*, 2017).

The majority of the *S. aureus* downregulated virulence factors (Table 3.10) are members of the SaeRS, regulon, including Hla, Hlb, HlgABC, LukED, FnbA, Efb, Ecb, SCIN, Sbi, FLIPr, CHIPS, Map, SSL5, SSL7 and SSL11 (Giraudo *et al.*, 1999, Liang *et al.*, 2006; Rogasch *et al.*, 2006; Nygaard *et al.*, 2010; Steinhuber *et al.*, 2003). These virulence factors promote infection by increasing bacterial survival from the host and the transcriptional changes indicates a specific adjustment of the bacteria to sphingosine, that is also described for other stimuli. Disruption in the SaeRS signalling pathway (loss of function) resulted in cytotoxicity to epithelial and endothelial cells and an increased ability of *S. aureus* to adhere to and invade (Liang *et al.*, 2006; Steinhuber *et al.*, 2003).

In contrast to the findings for *S. aureus*, in which the large majority of the genes regulated by SaeR code for extracellular toxins and cellular adherence factors (Liang *et al*., 2006; Rogasch *et al.*, 2006), genes affected by the loss of SaeR in *S. epidermidis* have multiple functions, including pyruvate metabolism genes *pflA*, *pflB*, *ackA* and *butA* that are positively regulated by SaeR; amino acid synthesis and metabolism genes *hisG*, *hisD, hisH, argC, argJ* and *argG* that are negatively regulated by SaeR; and redox regulation genes *trxA* and *trxB* that are negatively regulated by SaeR in *S. epidermidis* strain 1457 (Handke *et al.*, 2007). Consistent with downregulation of SaeRS by D-sphingosine in *S. epidermidis* Tü3298, *hisG, hisD* and *argG* were upregulated by 4, 1.9 and 3.1 fold, respectively. However, expression of *pflA* and *pflB* were also increased by 24 and 13 fold although they were predicted to be decreased by downregulation of SaeRS. Differential expression of *pflA* and *pflB* might be altered by other regulators changed by D-sphingosine treatment.

A key response to D-sphingosine observed with *S. aureus* is a reduction in virulence gene expression, while no determined virulence factors of *S. epidermidis* (such as *cap* operon) were differentially expressed. This suggests that sphingosines on the skin may act against colonisation of *S. aureus* via altering adhesion and virulence of the bacteria.

3.4.2 Cell wall stress

KEGG pathway analysis indicated upregulation of peptidoglycan biosynthesis in D-sphingosine challenged *S. aureus*. In addition, the SAMMD analysis revealed D-sphingosine transcriptome overlap with transcriptome datasets of several cell-wall-targetting antibiotics, such as vancomycin, bacitracin, fosfomycin and oxacillin. This shared aspect of the responses supports a role for D-sphingosine where it exerts activity towards the cell wall either from direct damage or inhibition of its biosynthesis.

Both species showed marked upregulation in expression of the genes encoding the cell wall biosynthesis controlling TCS VraSR (~5 fold increase for both *vraS* and *vraR* in *S. aureus* and ~6.5 fold increase for both in *S. epidermidis*). Inhibition of cell wall biosynthesis induces expression of the cell wall stress stimulon (Campbell *et al*., 2012; Muthaiyan *et al*., 2008; Sass *et al*., 2008; Utaida, 2003), which enhances resistance to cell wall biosynthesis inhibitors and is primarily regulated by the two-component regulator VraSR (Gardete *et al*., 2006; Boyle-Vavra *et al.*, 2006). Cell wall targetting agents such as the glycopeptide vancomycin and β-lactam oxacillin are potent inducers (Pechous *et al.*, 2004; Utaida *et al.*, 2003).

Upregulation of the cell wall biosynthesis genes *murZ* (~2 fold change) and *pbpB* (~1.74 fold change) that belong to *vraSR* regulon and expression of other genes commonly found upregulated by cell wall inhibitor treatment were also increased in the D-sphingosine challenge transcriptome of *S. aureus*, including genes involved in intermediary metabolism such as *thrB* (~6 fold change), *thrC* (~5.2 fold change), *dapA* (~3 fold change) and *serA* (~2.8 fold change); and genes encoding chaperones, heat shock proteins, and osmoprotectant transporters such as *prsA* (~4.7 fold change), *opuD* (~1.5 fold change) and *NWMN_1621* (5.2 fold change) (Kuroda *et al.*, 2003; McAleese *et al*., 2006; Utaida *et al.*, 2003). In addition, and comparatively, *thrB* (~3 fold change), *thrC* (~3.7 fold change), *prsA* homolog gene *SETU_01367* (~3.8 fold change), *NWMN_1621* homolog gene *SETU_01290* (~8 fold change) showed strong upregulation by D-sphingosine treatment in *S. epidermidis* RNA-Seq data.

In addition to expression of the cell wall stress stimulon, there was altered regulation after D-sphingosine challenge of the autolysis regulatory genes *fmt* and *lytR,* matching observations in a previous study of responses to cell wall stress (Utaida *et al.*, 2003). This supports a hypothesis that the cells coordinately regulate autolysis in response to cell wall active antimicrobials that interfere with wall biosynthesis. Although *fmt* transcription was expected to be upregulated consistent with upregulation of VraSR (Utaida *et al.*, 2003), *fmt* was downregulated in the D-sphingosine challenge transcriptome data. The two-component regulator LytSR, which suppresses autolysis in *S. aureus* and *S. epidermidis* by positively regulating murein hydrolase activity and which is upregulated in response to cell wall stress (Zhu *et al.*, 2010; Groicher *et al.*, 2000), was downregulated ~2 fold in D-sphingosine challenged *S. aureus*. In contrast, neither the *fmt* or *lytSR* genes were DE in D-sphingosine treated *S. epidermidis* transcriptional data.

3.4.3 Membrane disruption

The induction of a cell wall stress-like response by D-sphingosine suggests that it may lead to cell wall biosynthesis inhibition or membrane destabilisation, or both. Membrane destabilisation is supported in part from the observation that there was pronounced overlap between the transcriptomes of the membrane-targetting antimicrobials temporin (75.3%) and ovispirin (75.6%) and the D-sphingosine dataset (as a proportion of the temporin and ovispirin datasets). The *S. aureus* transcriptional response to D-sphingosine had most DE genes overlapping with both of these CAMPs that disrupt the cell membrane electrical potential through membrane perturbation (Yang *et al.,* 2013). In contrast, there was limited similarity between *S. aureus* D-sphingosine transcriptomic data and the dermaseptin or nisin transcriptomes, which are also membrane-targetting antimicrobials. Both dermaseptin and ovispirin permeate and disintegrate the membrane by disrupting the bilayer curvature (Pietiäinen *et al.*, 2009). Temporin and nisin are pore forming, while nisin is reported to be active on

both formation of membrane pores and inhibition of cell wall biosynthesis (Wiedemann *et al.,* 2001; Breukink *et al.,* 1997).

CAMPs can disrupt the cell membrane electrical potential through membrane perturbation and induce upregulated expression of the LytSR regulon (Yang *et al.,* 2013). LytSR is reported to sense alterations of the membrane potential due to perturbations (Sharma-Kuinkel *et al*., 2009; Yang *et al.,* 2013) in addition to regulating genes that control cell apoptosis, autolysis, and biofilm formation (Groicher *et al.,* 2000; Rice *et al.,* 2003). However, while *lytSR* is upregulated in response to membrane potential disruption (Patton *et al.*, 2006), it was downregulated in D-sphingosine treated S. aureus.

Consistent with this LytSR-dependent downregulation, the *lrgAB* operon was downregulated (5 fold, 3.7 fold, respectively) and gene *cidA* of the *cidABC* operon suppressed by *lrgAB* operon was upregulated (4 fold). IrgAB inhibits murein hydrolysis activity and cell lysis (Groicher *et al.,* 2000; Rice *et al.*, 2005), while the *cidABC* gene products enhance murein hydrolysis activity and antibiotic tolerance (Rice *et al.,* 2003). IrgAB and CidABC were proposed to control the programmed cell death and lysis during biofilm formation (Rice *et al.*, 2007; Bayles, 2007; Rice and Bayles, 2008).

The expression of *lytSR, lrgAB* and *cidABC* operons were unchanged in the *S. epidermidis* D-sphingosine challenge transcriptome. This might indicate that the concentration of D-sphingosine used for challenge experiments was insufficient to cause a similar disruption effect on *S. epidermidis* cell membrane or that a discrete response is used to counteract the effects of sphingosine.

Whilst few DE genes related to membrane lipid biosynthesis were determined in *S. epidermidis*, KEGG pathway analysis showed an overall increase in fatty acid degradation and decrease in glycerolipid biosynthesis, which may indicate that D-sphingosine challenged *S. aureus* preferentially use fatty acid as a source of membrane lipid rather than undergoing glycerophospholipid biosynthesis. Although sphingosines are not fatty acids, they share similar carbon backbone structures, and was suggested to act similarly with antimicrobial fatty acids on staphylococci (Parsons *et al.*, 2012). Sphingosine at relatively low

concentrations (below MIC) was predicted as a potential resource for uptake and metabolism by *S. aureus* (Fischer *et al*., 2013). Interaction of D-sphingosine may alter the metabolism pathways to use fatty acids in priority in *S. aureus*.

3.4.4 Capsule biosynthesis

Capsule protects bacteria from antimicrobials by limiting access to and penetration of the membrane. The *cap* operon that encodes the *S. aureus* Newman type 5 capsule biosynthesis proteins (Herbert *et al.*, 2001; O'Riordan and Lee, 2004) was downregulated after D-sphingosine challenge. According to Meier *et al* (2007), capsule biosynthesis is dependent on *yabJ-spoVG* and the latter gene was also downregulated (2.4 fold decrease) showing coordination of expression.

S. epidermidis does not possess a similar *cap* operon for polysaccharide capsule production. Instead, *S. epidermidis* produces poly-γ-glutamic acid (PGA) (McKenney *et al*., 1998; Kocianova *et al*., 2005). The genes involved in PGA biosynthesis (*pgsABCD*) were not DE in D-sphingosine challenged *S. epidermidis* data indicating that capsule expression is not affected by D-sphingosine.

3.4.5 Oxidative stress

The carotenoid pigment provides integrity of the pathogen's cell membrane (Mishra *et al.*, 2011). Staphyloxanthin is found to assist in bacterial survival under stress and during infections (Giachino *et al.*, 2001; Kahlon *et al.*, 2010). The pigment has an antioxidant action that enhances bacterial resistance to reactive oxygen species (ROS) generated by host immune system (Clauditz *et al.*, 2006). Thus, decrease in staphyloxanthin production would result in increased bacterial susceptibility to oxidative stress as well as membrane disruption. Although the biosynthesis pathway for the carotenoid staphyloxanthin was downregulated in response to D-sphingosine challenge in *S. aureus*, further investigation of the *crt* operon (Chapter 4) indicated that its expression was

upregulated after prolonged incubation (24h) with D-sphingosine, suggesting that in contrast adaptation and continued growth includes increased staphyloxanthin expression.

Exprssion of *msrA* encoding methionine sulfoxide reductase was increased after D-sphingosine challenge of *S. aureus* but not *S. epidermidis*, which shows differences in protein repair due to damage, which is an upregulated function category in the COGs analysis. MsrA increases resistance to oxidative stress by reducing methionine sulfoxide residues in proteins to methionine and therefore restore protein function (Brot and Weissbach, 2000; Moskovitz *et al.*, 1995). A study by Singh and Wilkinson (2001) indicated that a *msrA* mutant is more susceptible to hydrogen peroxide. MsrA is strongly induced by cell wall active antimicrobials, and it was proposed by the authors that exposure to cell wall active antimicrobials causes oxidative damage to proteins that must be repaired (Singh and Wilkinson, 2001; Singh *et al.*, 2001; Utaida *et al.*, 2003).

S. epidermidis does not produce staphyloxanthin, so resistance against membrane fluidity changes and destabilisation/disorder must be achieved through other methods. A major mechanism to alter membrane fluidity is via adjusting branched chain fatty acid and saturated fatty acid content in the membrane, where branched chain fatty acids increase membrane fluidity while saturated fatty acids increase rigidity of the membrane (Singh *et al.*, 2008; Schujman and de Mendoza, 2005). The *lpd* gene, which controls synthesis of branched chain fatty acids in staphylococci, (Singh *et al.*, 2008) was not differentially expressed in either *S. epidermidis* or *S. aureus* meaning the control mechanisms differentiating these species remain unresolved.

3.4.6 General stress response of both *S. aureus* and *S. epidermidis*

The CtsR regulon is upregulated in protein damaging conditions, such as heat shock (Derre *et al.*, 1999; Elsholz *et al.*, 2010). The D-sphingosine challenge induces a general stress response that includes upregulation of *ctsR* (4.3 fold in *S. aureus*, 6.1 fold in *S. epidermidis*), and its regulon genes, *dnaJ* (increased 2.5

fold in *S. aureus* and 2.1 fold in *S. epidermidis*), *dnaK* (increased 2.8 fold in *S. aureus* and *S. epidermidis*). Further, protease and chaperone protein genes concerned with repair and recycling were upregulated in both species supporting the requirement for repair and recycling of proteins.

The mode of action of sphingosine is similar to that of sapienic acid and results in loss of low molecular weight solutes, amino acids and proteins (Alnaseri *et al*., 2015). In light of this, the notable upregulation of amino acid biosynthesis in both species could represents a general response to osmotic stress due to leakage caused by membrane disruption. The downregulation of pyrimidine metabolism together with the upregulation of amino acid biosynthesis and stress response genes is similar to the stringent response to nutrient starvation, where cellular energy is directed away from growth toward nutrient stocking (Durfee *et al.,* 2008).

Energy production in *S. epidermidis* was strongly upregulated while no significant regulation trend was observed in *S. aureus*. This may indicate that *S. epidermidis* has more efficient mechanisms for D-sphingosine resistance than *S. aureus*. Of note, energetically expensive resistance mechanisms of *S. aureus* such as capsule and staphyloxanthin biosynthesis were downregulated when challenged with D-sphingosine, possibly signifying a need for greater energy conservation and restoration.

Chapter 4: Characterisation of DE genes in the Transcriptome of *S. aureus* Challenged with D-Sphingosine

4.1 Introduction

4.1.1 Staphyloxanthin biosynthesis

Staphyloxanthin is a yellowish-orange carotenoid pigment that gives *S. aureus* its golden colour and is described to have a role in the oxidative resistance and membrane integrity of *S. aureus* (Liu & Nizet, 2009).

A series of *crt* enzymes are involved in staphyloxanthin biosynthesis (Figure 4.1): dehydrosqualene synthase (CrtM) enzyme catalyses formation of dehydrosqualene (4,4'-diapophytoene); CrtN dehydrogenates dehydrosqualene to form the intermediate 4,4'-diaponeurosporene (Raisig and Sandmann, 1999), which is a yellow pigment; CrtP oxidizes the terminal methyl group to generate 4,4'-diaponeurosporenic Acid; finally CrtQ and CrtO esterifies glucose to yield the final compound staphyloxanthin (Pelz *et al.,* 2005).

The carotenoid pigment contributes to the integrity of the pathogen's cell membrane (Mishra *et al.*, 2011). It was reported that more than 90% of *S. aureus* isolates from infected humans are pigmented (Lennette *et al.,* 1985) and staphyloxanthin assists survival under stress and during infections (Giachino *et al.*, 2001; Kahlon *et al.*, 2010). The pigment has an antioxidant action that enhances resistance of the bacteria to reactive oxygen species (ROS) generated by host immune system (Clauditz *et al.*, 2006).

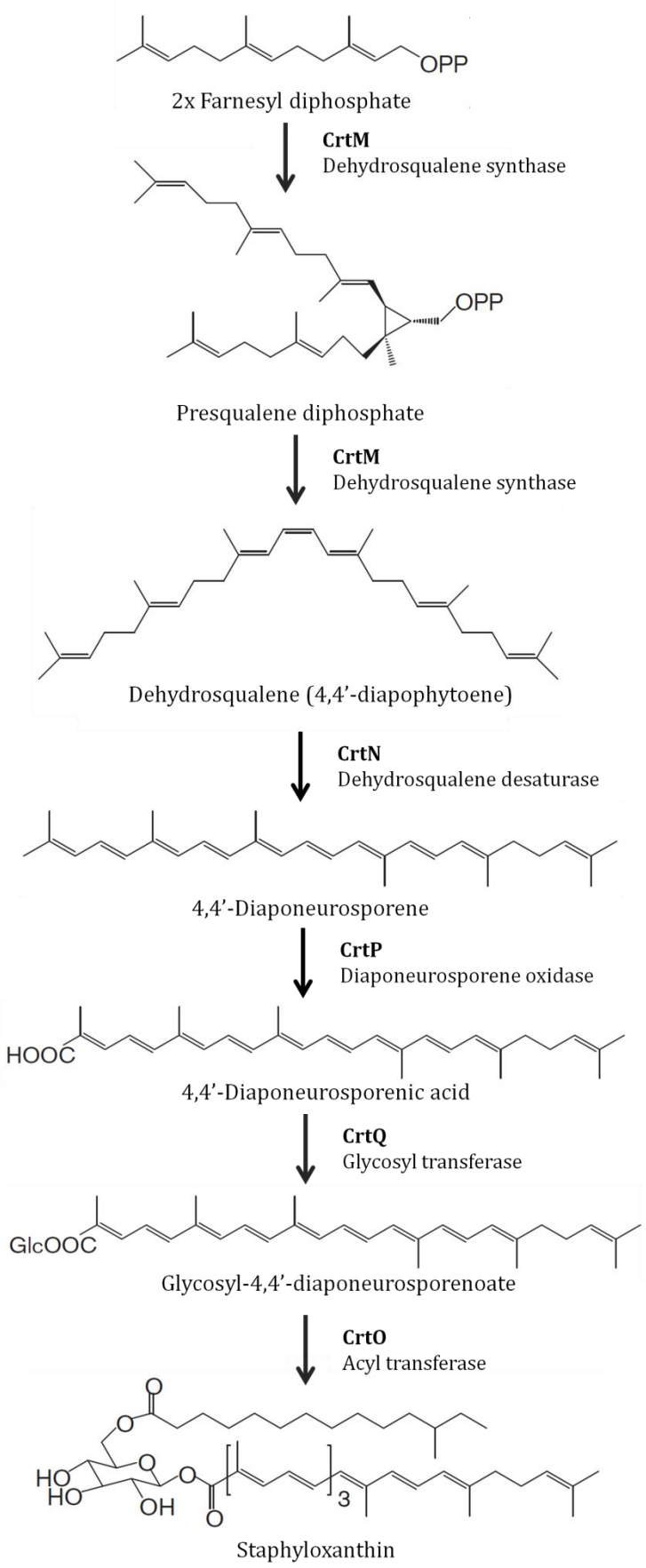

Figure 4.1 Staphyloxanthin biosynthesis pathway. (Leejae *et al*., 2013; Pelz et., al., 2015)

4.1.2 Phosphate-specific transport (Pst) system

The Pst (phosphate-specific transport) system is a high-affinity, low-velocity, free-Pi transporter that is structurally similar to ABC transporters (Ames, 1986) and is expressed by many species, including *E. coli, Bacillus subtilis,* and *S. aureus*. The proteins encoded by the *pst* operon comprise a binding protein PstS, two integral inner membrane proteins PstC and PstA, and an ATP binding protein PstB (Webb e*t al.*, 1994). In *S. aureus*, the organisation of the genes is such that *pstS* is monocistronic followed downstream by the *pstCABphoU* polycistronic operon.

The first four genes *pstS, pstC, pstA* and *pstB* in the *pst* operon of *E. coli* are required for phosphate transport when the concentration of Pi is low (Cox *et al.*, 1981). Mutation of any of these genes will abolish Pi uptake (Sprague *et al.,* 1975). Two phosphate transport systems are involved in Pi intake during phosphate-replete growth in *E. coli*: Pit is a low-affinity Pi transporter (Harris *et al.*, 2001) that is independent of Pi concentration; and PhoPR (Carter et al., 2004). In contrast, the *pst* operon encodes a PhoP-dependent high-affinity Pi transporter that is induced specifically in response to Pi starvation (Qi *et al.*, 1997). The *pst* operon is transcribed from a housekeeping sigma A-type promoter, which is located upstream of *pstS* (Qi *et al.*, 1997) and can be induced during alkali stress (Atalla and Schumann, 2003); it becomes the main transporter of phosphate when Pi concentration is lower than 0.1 mM. A reduction in Pi uptake (approximately 7 fold) was observed in *pst* mutants (Prágai *et al.*, 2001).

Both *E. coli* and *S. aureus* have a regulatory gene *phoU,* while *B. subtilis* does not. The ATP binding protein of *B. subtilis* consists of PstBA and PstBB subunits (similar to PstB for *E. coli* and *S. aureus*), and the *pstB2* gene is in the position of *phoU* in *E. coli* and *S. aureus* at the 3' end of the operon. PhoU is considered to be a switch in *E. coli* multidrug tolerance and impacts on widespread processes beyond inorganic phosphate (Pi) transport (Li and Zhang, 2007).

4.1.3 PhoRP alkaline phosphatase synthesis regulatory system

S. aureus, S. epidermidis and *S. xylosus* are phophatase producers (Varaldo and Satta, 1978). Phosphatase was found in approximately 90%, 70%, and 89% of the *S. aureus, S. epidermidis* and *S. xylosus* strains respectively (Soro *et al.,* 1990). PhoRP is a TCS for alkaline phosphatase biosynthesis and is well studied in *B. subtili*s and *E. coli* (Liu and Hulett, 1997; Seki et al., 1988; Seki et al., 1987). PhoP is a substrate for both the kinase and phosphatase activities of its cognate sensor kinase PhoR (Liu and Hulett, 1997). *B. subtilis* genes encode three secreted alkaline phosphatases (APases): *phoA* (APaseA); *phoB* (APaseB); and *phoD* (APaseD) (Hulett, 1993; Hulett, 1995; Hulett, 1996) and activation of *phoB* is controlled by PhoP (Liu and Hulett, 1997). The APases are expressed during phosphate starvation, generating inorganic phosphate that can be mobilised by the phosphate-specific transport system (Pst system) for translocation into the cell (Rao and Torriani, 1990; Willsky *et al.*, 1973)

4.1.4 Haem-sensor system (HssRS) and haem regulated transporter (HrtAB)

Haem-iron acquisition is vital to staphylococcal pathogenesis (Skaar et al., 2004; Torres *et al*., 2006). Iron is an essential cofactor for many biochemical processes and is required by all pathogenic bacteria for infection; its limitation is a significant barrier encountered when colonising verebrates (Bullen, 1999). Most vertebrate iron is in the form of the metalloporphyrin haem, which is the functional cofactor of haemoglobin for blood and myoglobin for muscle oxygen transport and storage (Deiss, 1983). *S. aureus* acquires haem as a nutrient source through expression of high efficiency uptake systems to transport host-derived haem into the staphylococcal cytoplasm (Mazmanian *et al*., 2003; Skaar *et al*., 2004; Torres *et al*., 2006; Vermeiren *et al*., 2006). This process is facilitated by hemolysin-mediated rupture of erythrocytes upon entry into the blood stream (Bernheimer *et al*., 1968; Skaar and Schneewind, 2004).

Whilst being an important nutrient source for invading pathogens, the intracellular accumulation of haem is toxic due to its reactivity (Torres *et al.*, 2007). An increasing inhibitory effect of hemin on growth of *S. aureus* was revealed with concentrations ranging from 5 - 10 μM in iron-replete medium (Torres *et al.*, 2007). Therefore, the value of haem as an iron source is balanced against its toxicity at high concentrations using adaptable mechanisms to prevent surplus haem accumulation and make use of exogenous haem to satisfy iron needs (Everse and Hsia *et al.*, 1997).

Torres *et al* (2007) reported that *S. aureus* senses haem and subsequently alters protein expression, using a haem-sensor system (HssRS) responding to haem to upregulate HrtAB haem transporter. HrtAB consists of an ATP-binding protein (HrtA) and a permease (HrtB), making up a canonical ABC-type transporter system. The HrtAB efflux pump plays an essential role in intracellular haem homeostasis of *S. aureus* (Torres *et al.*, 2007) with major upregulation (45 fold) observed in *S. aureus* challenged with exogenous hemin (the oxidised form of haem) (Friedman *et al*., 2006).

Inactivation of either *hssRS* or *hrtAB* resulted in increased expression and secretion of staphylococcal virulence factors (Torres *et al.*, 2007). The HssRS and HrtAB proteins are conserved across Gram-positive pathogens, including *S. epidermidis* and *Bacillus anthracis* that also show adaptation to hemin toxicity, and it was proposed that these important human pathogens sense their vertebrate hosts to modulate virulence and orthologous Hss and Hrt systems may act across genera to coordinate a response to excess hemin exposure (Torres *et al.*, 2007).

4.2 Chapter aims

In the previous chapter, an RNA-Seq directed approach was undertaken to document the transcriptomic response of *S. aureus* Newman and *S. epidermidis* Tü3298 to D-sphingosine challenge. The analysis defined a sphingosine stimulon across both species with which it is possible to test individual genetic contributions of loci to the survival of each species from sphingosine.

Given the relative ease of genetic manipulation of *S. aureus,* this chapter describes experiments of selected genes in the RNA-Seq data analysis to characterise D-sphingosine resistance of *S. aureus*. Primary focus was on two hierarchical regulators, the two component systems VraSR (*vraSR*) and SaeRS (*saeRS*), the Pst phosphate transport system (*pstS* and *pstCABphoU*) and a hypothetical gene *NWMN_0542*. These were selected because they were highly up or down regulated (>2 or <-2 Log2 FC) in both *S. aureus* and *S. epidermidis*.

4.3 Results

Target loci were selected from the transcriptomic study in the previous chapter based on common regulation by both *S. aureus* and *S. epidermidis* in their response to D-sphingosine. The chosen subset of genes was also proposed for further study based on their known roles or the extent of up/down regulation in the transcriptional responses (Table 4.1). To investigate the contribution of each of the selected genes in turn, primary studies were pursued with a determination of MICs of gene mutants.

Both species showed marked upregulation of VraSR (~5 fold increase for both *vraS* and *vraR* in *S. aureus* and ~6.5 fold increase for both in *S. epidermidis*) after challenge with D-sphingosine. VraSR is a TCS involved in the control of cell wall peptidoglycan biosynthesis (Cui *et al.*, 2009). Increased expression of *vraSR* together with its cognate cell wall stress stimulon (including *pbpB, murZ,* and *msrA1* described in chapter 3) supports that D-sphingosine causes cell wall damage or inhibits cell wall biosynthesis. To explore this potential, the role of *vraRS* in sphingosine resistance in *S. aureus* was investigated further. MIC assay of *vraR* and *vraS* allelic replacement mutant strains (SH1000 *vraR::tet* and SH1000 *vraS::tet*) was undertaken using the described methods. Both SH1000 *vraR::tet* and SH1000 *vraS::tet* showed a lower MIC (6.6 μM) than the wild type SH1000 strain (16.3 μM), which supports that VraSR TCS contributes to D-sphingosine resistance in *S. aureus*.

Table 4.1 Comparison of selected genes of the D-sphingosine responses from RNA-Seq analysis of *S. epidermidis* Tü3298 and *S. aureus* Newman. Differential expression of genes after D-sphingosine challenge is indicated with colour blocks shown in the colour key. Values indicate Log_2 fold change values. A white colour block represents no differential expression; A grey colour block and a cross 'X' indicates that the gene is absent in the species.

> 4.0
3.0 to3.9
2.0 to 2.9
1.0 to 1.9
0.5 to 0.9
-0.9 to -0.5
-1.9 to -1.0
-2.9 to -2.0
-3.9 to -3.0

***S. epidermidis* Tü3298**		***S. aureus* Newman**		**Alternative gene names**
Gene name	Log2 Fold Change		Gene name	
Global regulators				
vraR	2.7	2.3	*vraR*	
SETU_01443	2.7	2.3	*vraS*	
SETU_00326	-2.4	-3.0	*saeR*	
SETU_00325	-2.3	-3.0	*saeS*	
Phosphate uptake				
X		2.7	*phoU*	
SETU_00964	1.5	4.1	*pstS*	
SETU_00963	1.5	3.8	*NWMN_1299*	*pstC*
SETU_00962	1.6	3.5	*NWMN_1298*	*pstA*
SETU_00961	1.7	3.1	*pstB*	
SETU_01249		0.9	*phoR*	
SETU_01250		0.9	*phoP*	
SETU_02057		2.0	*phoB*	

Table 4.1 continued

***S. epidermidis* Tü3298**		***S. aureus* Newman**		**Alternative gene names**
Gene name	Log2 Fold Change		Gene name	
Iron uptake				
SETU_01817		1.6	*NWMN_2261*	*hrtA*
SETU_01818		1.6	*NWMN_2262*	*hrtB*
SETU_01819		0.9	*NWMN_2263*	*hssR*
SETU_01820		0.7	*NWMN_2264*	*hssS*
Staphyloxanthin biosynthesis				
X		-1.3	*crtM*	
X		-1.2	*crtN*	
X		-1.6	*NWMN_2463*	*crtQ*
X		-1.7	*crtP*	
X		-1.5	*NWMN_2465*	*crtO*
Predicted protein				
SETU_00201	5.6	6.1	*NWMN_0542*	*vraX*

4.3.1 Phosphate specific transport (*pst*) system

The *pstS* and *pstCABphoU* operons of *S. aureu*s were investigated further based upon each gene being highly upregulated over 8-fold, which could indicate a contributory role of Pst transport of phosphate in survival from D-sphingosine. The importance of phosphate for protection from or adaptation to D-sphingosine challenge was first examined by supplementation of culture medium with phosphate in an MIC assay (Figure 4.2).

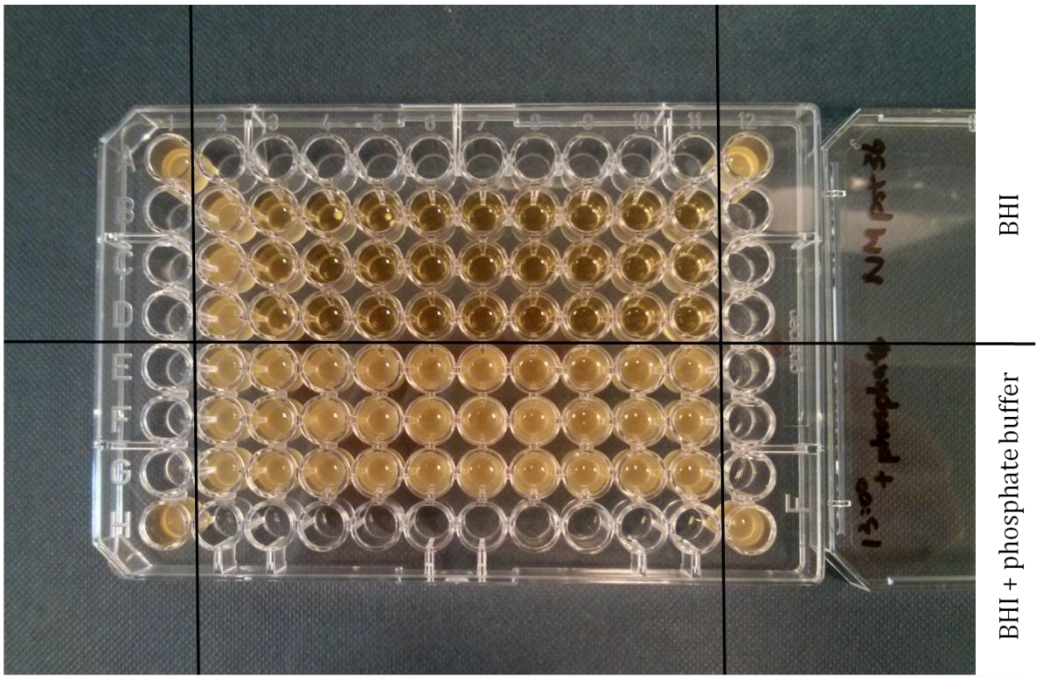

	1	2	3	4	5	6	7	8	9	10	11	12
A	control											control
B		16.5	33	49.5	66	82.5	99	115.5	132	148.5	165	
C		16.5	33	49.5	66	82.5	99	115.5	132	148.5	165	
D		16.5	33	49.5	66	82.5	99	115.5	132	148.5	165	
E		16.5	33	49.5	66	82.5	99	115.5	132	148.5	165	
F		16.5	33	49.5	66	82.5	99	115.5	132	148.5	165	
G		16.5	33	49.5	66	82.5	99	115.5	132	148.5	165	
H	control											control

Figure 4.2 D-sphingosine MIC assay of *S. aureus* Newman survival in the absence and presence of 0.1 M phosphate. Cells were assayed in BHI broth with a range of concentrations of D-sphingosine from 16.5 to 165 uM across wells 1-10 as indicated. Three technical repeats were set for each group and blank controls were prepared without any antibiotics. The two blank controls at the top corners were mixed with diluted culture and BHI broth only, and the bottom blank controls were mixed with diluted culture, BHI broth and additional Pi.

Minimum inhibitory concentration (MIC) was determined using 96 well plates to culture bacteria. Tested strains were grown for 24 h, diluted to OD_{600}=0.2 with BHI broth and 100 µl of diluted culture was then added to each well containing different concentrations of D-sphingosine; cells were incubated at 37°C for 24 h. MIC was performed in the absence and presence of 0.1 M phosphate buffer.

Addition of Pi dramatically increased resistance of wild type *S. aureus* Newman to D-sphingosine such that growth inhibition was not observed at even the highest concentrations (Figure 4.2). The same experiment was repeated on *S. aureus* strains SH1000 and Newman with various growth media (BHI, THB and chemical defined media incorporating different phosphate concentrations), and similar results were observed to confirm that this phenomenon was not strain and media dependent. Different phosphate concentrations were tested to detect the lowest additional Pi concentration that would produce a difference in D-sphingosine resistance. Fifty μM of added Pi was found to result in a consistent increased D-sphingosine resistance in both WT Newman and SH1000, which doubled the MIC value to 33 μM compared with 16.3 μM when cultured in BHI only.

4.3.2 Construction of a *pst* operon mutant

The Pst transporter of *E. coli* functions as a high affinity Pi transport system activated by phosphate limitation (Qi *et al*., 1997; Ames, 1986). To investigate the role of the *S. aureus* Pst system in sphingosine survival, a *pstSCAB* allelic replacement mutant was constructed using an antibiotic resistance cassette in place of the four genes. Flanking DNA consisting of upstream DNA plus *pstS'* (first part of *pstS*), and downstream flanking DNA plus *pstB'* (latter part of *pstB*) was ligated together with a tetracycline resistance cassette into the suicide plasmid vector pMUTIN4 (Vagner *et al*., 1998) (Figure 4.3). This vector was designed to remove most of the *pstS* and *pstCAB* operons and replace with the resistance cassette.

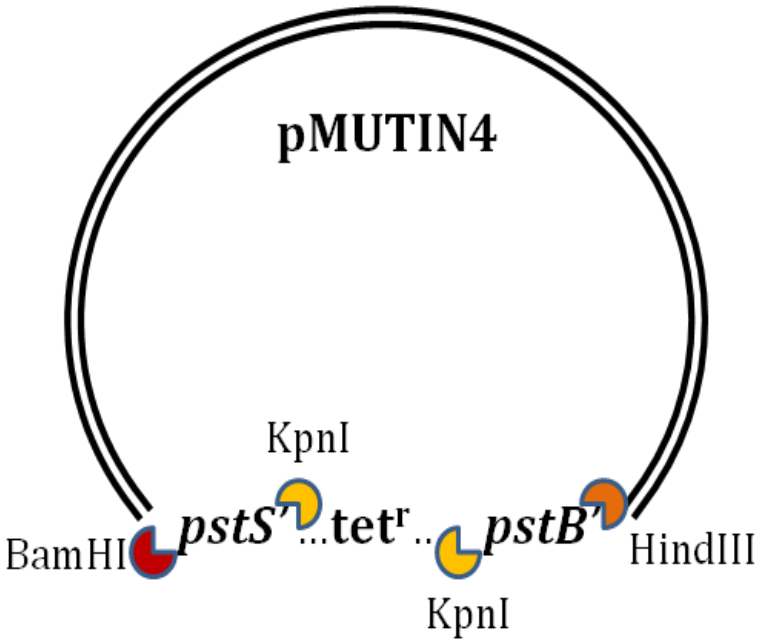

Figure 4.3 Cloning of *pstS-pstCAB* vector for allelic replacement. Plasmid pMutin4 was digested with BamHI and HindIII and co-ligated with the DNA fragments: *pstS'* DNA fragment digested with BamHI and KpnI; tetracycline cassette digested with KpnI; *pstB'* DNA fragment digested with KpnI and HindIII. DNA fragments were ligated using T4 DNA ligase.

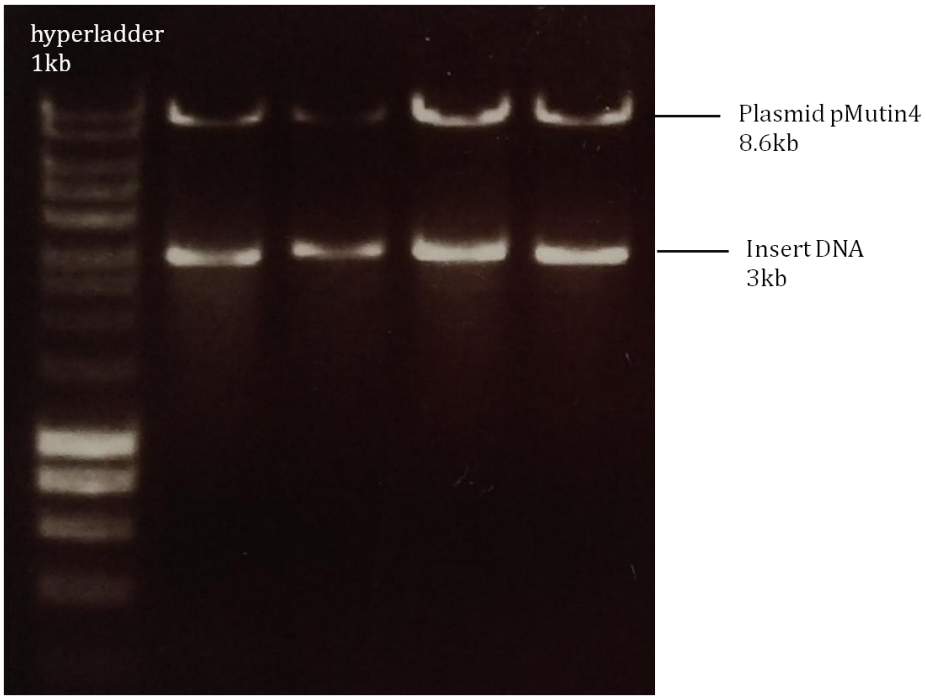

Figure 4.4 Restriction digest of plasmid from candidate clones. Plasmid was extracted from selected clones and was digested BamHI and HindIII. The expected sizes of DNA were observed indicating successful cloning: pMUTIN4 (~8.6kb); pstS'tetB' insert (~3kb).

Correct vector cloning was confirmed by restriction digest of purified plasmid from successfully transformed *E. coli* colonies (Figure 4.4). The purified plasmid was used for subsequent electro-transformation of *S. aureus* RN4220 and a lysate of this strain made with phage phi11 for transduction of strain Newman with selection for tetracycline resistance. Transductants were selected and confimed to have the designed *pstS* and *pstCAB* operons deleted in Newman. This allelic replacement mutant was used in a series of experiments to investigate if there was a role for the Pst transporter system in D-sphingosine resistance of *S. aureus*.

A chemically defined medium (CDM) was prepared according to the method described by Hussain *et al.* (1991) to control phosphate concentrations during cell culture (Chapter 2, section 2.2.2). Sufficient trace metals were added to assist bacterial growth and a range of phosphate concentrations were added to the culture to test the effect of differing amounts. The bacteria grew very slowly when phosphate concentrations were reduced, and the lowest concentration

that was found to be able to support *S. aureus* growth (overnight culture reach OD_{600}=1) was about 12 mM. A lower MIC of D-sphingosine is predicted for the *pst* operon mutant if D-sphingosine causes phosphate deficiency or a requirement to metabolise the lipid, on the basis that this phosphate transporter contributes to D-sphingosine resistance in *S. aureus*.

Results of MIC tests showed no difference between the constructed *pst* mutant and wild type Newman strain (tested with THB, BHI and CDM media containing 12-60 mM Pi). A possible explanation for the lack of a phenotype could be that depletion of this transporter triggers expression of other phosphate related transport systems, such as PhoRP, to maintain Pi uptake. Therefore, to examine this the transcription of a set of PhoRP related genes (include *phoP*, *phoR*, *phoB*) was assessed with the mutant strain using qPCR under the same culture and challenge conditions as RNA extraction for RNA-Seq. However, no altered regulation was detected for any of the tested genes.

4.3.3 Characterising transposon library mutants for survival phenotypes

A targeted approach was used to determine the involvement of genes that were DE in the RNA-Seq data and pathways that were of interest for D-sphingosine survival. The Nebraska Transposon Library of *S. aureus* JE2 (for information see section 2.3.8) is a research community resource that contains *bursa aurealis* transposon inactivation of over 1,900 genes. To further investigate the role of Pst phosphate transporters, *pstS* and *phoU* single gene mutant strains were obtained and the transposon insertions were selected in *S. aureus* Newman by phage transduction.

Consistent with pronounced upregulation of the *pst* operon, upregulated expression of *phoR* (1.9 fold change increase) also suggested an increased need for inorganic phosphate uptake by upregulation of alkaline phosphatase. PhoPR was investigated as it regulates synthesis of alkaline phosphatase, which is expressed during phosphate starvation and yields inorganic phosphate that can be ultimately targeted by the phosphate-specific transport system (Pst system), for translocation into the cell (Rao and Torriani, 1990; Willsky *et al.*, 1973).

Previous work in the Horsburgh group in Liverpool identified an efflux pump (encoded by *Sar2632*) that exports the AFA linoleic acid in *S. aureus* MRSA252. This efflux transporter was hypothesised to be induced by sphingosine since its mode of action was proposed to be similar to AFA lipids with membrane damage and leakage of solutes (Bibel *et al.*, 1993; Fischer *et al.*, 2013; Bergsson *et al.,* 2001). However, the homologous gene *NWMN_2442* in strain Newman was not differentially expressed by D-sphingosine challenge. It is likely that there is an alternative or more efficient way to export sphingosines. Therefore, other upregulated transporters were investigated. A *hrtB* mutant was created to investigate this upregulated transporter regulatory system (*hrtAB-hssRS*) in D-sphingosine resistance.

To verify the location of the transposon insertions and confirm successful transduction, primers were designed that were specific to the *bursa aurealis* transposon and these were used together with primers of the target genes to use PCR amplification for confirmation of correct gene insertion (indicated in

chapter 2, table 2.3). PCR amplification confirmed that each transposon/gene was amplified with correct size (Figure 4.5).

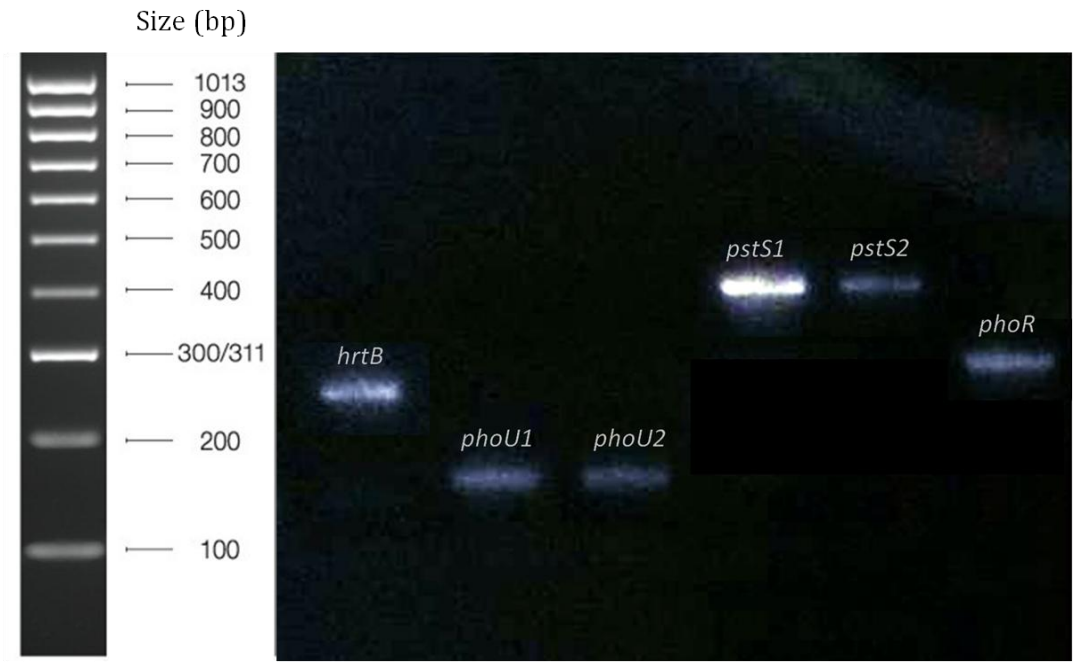

Figure 4.5 PCR amplification of transductants from JE2 to Newman. PCR primers and expected product sizes are listed in chapter 2, table 2.3. Corresponding gene names are shown in the figure, and the numbers represent for different replicates of the same gene (e.g. *phoU1* and *phoU2* indicate two successful *phoU* allelic replaced transductants confirmed by PCR).

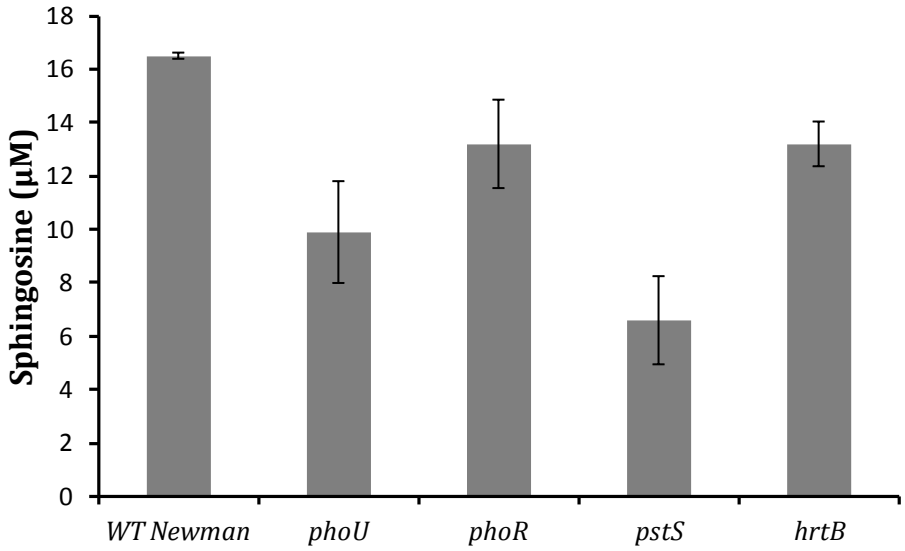

Figure 4.6 D-sphingosine MIC of *S. aureus* Newman *bursa aurealis* transposon mutants. Assays were performed in BHI broth. Error bars indicate standard deviation of three repeat experiments.

All of the mutant strains show lower MICs compared with wild type Newman strain as expected (Figure 4.6). *phoU, pstS* and *phoR* mutants (loss of function) show lower MICs than the wild type control, suggesting that the phosphate-specific transport Pst and the alkaline phosphatase synthesis regulatory system PhoPR play a role in D-sphingosine resistance in *S. aureus*, which furthermore indicated the role of phosphate in *S. aureus* survival from sphingosine. MIC results for the *hrtB* mutant suggest that haem transport and regulation plays a role in D-sphingosine resistance.

4.3.4 DE comparison of various *S. aureus* strains by qPCR

Transcriptomics analysis of the response to D-sphingosine was assessed using *S. aureus* strain Newman and *S. epidermidis* strain Tü3298. qPCR validation was done to support RNA-Seq data. In addition to qPCR validation with *S. aureus* Newman, other *S. aureus* stains, including wild type SH1000, MRSA252 and SF8300 (references see chapter2, table2.1) were included in qPCR quantitation to further compare host genetic background influences. (Table 4.2)

Table 4.2 Differential expression of selected genes in response to D-sphingosine challenge determined by qPCR. Coloured boxes represent the range of fold change. A grey box indicates no expression of the gene.

> 6.0
3.0 to 5.9
2.0 to 2.9
1.0 to 1.9
-0.9 to 0.9
< -2.9

strains	*pstB*	*saeR*	*NWMN_0542*	*vraA*
Newman				
SH1000				
MRSA252				
SF8300				
Tü3298				

Upregulation of *pstB* was seen in all tested strains, indicating a consistent change in expression of the Pst transporter in *S. aureus* by D-sphingosine challenge. Both species showed downregulation in expression of global regulator *saeRS* (8 and 8 fold decrease of *saeR* and *saeS* respectively in *S. aureus*; 5.3 and 4.9 fold decrease of *saeR* and *saeS* respectively in *S. epidermidis*).

Although *saeRS* was found to be down regulated 8-fold in Newman, all the other tested *S. aureus* strains (SH1000, MRSA252, SF8300) did not show differential expression by qPCR (Table 4.2). The strain Newman SaeS contains a L18P substitution ($SaeS^P$) in the first transmembrane helix due to SNP polymorphism of the gene, while strain SH1000, MRSA252 and SF8300 do not (Steinhuber *et al.*, 2003). This SNP results in the increased kinase activity of SaeS in Newman, which may be responsible for the difference in *saeR* differential expression found in these qPCR examined *S. aureus* strains.

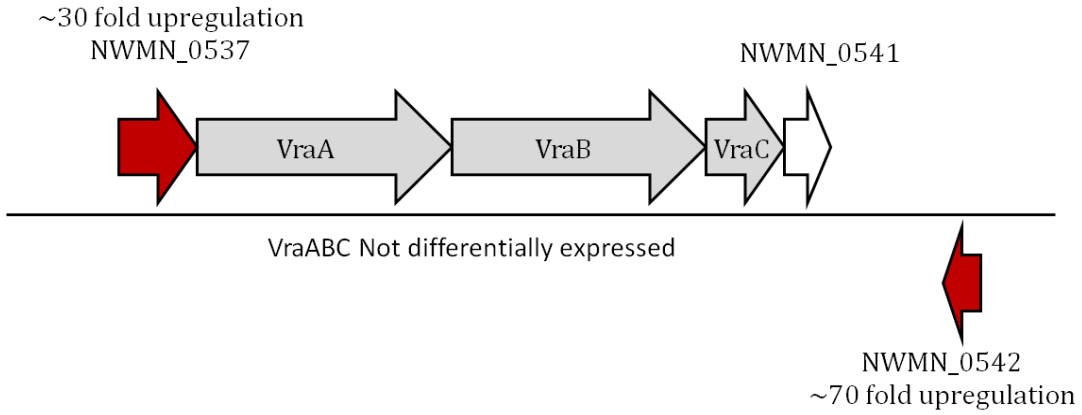

Figure 4.7 Gene clusters of *NWMN_0537, NWMN_0542,* and *vraABC* operon. VraA is a long chain fatty acid CoA ligase; VraB is an acetyl-CoA C-acetyltransferase; VraC is a conserved hypothetical protein with 2 predicted transmembrane domains; NWMN_0537, NWMN_0541 and NWMN_0542 are conserved hypothetical proteins.

The most upregulated genes in the transcriptome analysis data of *S. aureus* Newman were *NWMN_0537* (4.9 $\log_2$FC, 30 fold increase) and *NWMN_0542* (6.1 $\log_2$FC, 70 fold increase), both of which are hypothetical proteins with unknown function. *NWMN_0542* was named *vraX* and was suggested without experimentation to play a role in glycopeptides resistance of *S. aureus* (Scherl *et al.*, 2006). More recently, it was reported to have a role in innate immune evasion by binding C1q to inhibit the formation of C1-complex of the classical complement pathway (Yan *et al.*, 2017).

Both RNA-Seq and qPCR results show that expression of other genes of the *vraABC* operon were not coregulated with *NWMN_0542* or *NWMN_0537*, thus suggesting *NWMN_0542* and *NWMN_0537* are part of the sphingosine stimulon independently regulated compared with the glycopeptide stimulon that sees coregulation of the *vraABC* operon and *NWMN_0542* , *NWMN_0537* (Scherl *et al.*, 2006).

4.3.5 Sphingosine-induced changes in pigment gene expression and H_2O_2 survival

Expression of each gene in the operon encoding enzymes for staphyloxanthin biosynthesis was downregulated by D-sphingosine challenge: *crtM, crtN, crtQ, crtP, crtO*; 2.5, 2.3, 3.2, 3.0, 2.8-fold, respectively in the RNA-Seq data (Chapter 3, Table 3.7). Therefore, a lower level of pigmentation was predicted in bacteria treated with D-sphingosine. To test this hypothesis, *S. aureus* culture was incubated with 5 μM D-sphingosine, with a 0.03% ethanol solvent control for 24 h, followed by pigment extraction. A photometric absorbance spectrum assay was performed on the methanol extract.

The lab strains *S. aureus* Newman and SH1000 were tested in the absorbance assay using three biological and three technical replicates to calculate mean values. The results indicated that sphingosine treatment caused increased staphyloxanthin production compared with the ethanol control (Figure 4.8), which was opposite to RNA-Seq data. However, it is not possible to measure pigment very easily during early exponential growth phase, so the cells for assay were harvested after 24 h incubation with sphingosine. The transcriptome study saw RNA harvested 20 min after challenge with D-sphingosine. Thus, the *crt* genes expression immediately after challenge reveals their downregulation, while long-term exposure generates a different response that might reflect adaptation during subsequent growth phases and D-sphingosine might induce either an oxidative or general stress response upon prolonged exposure.

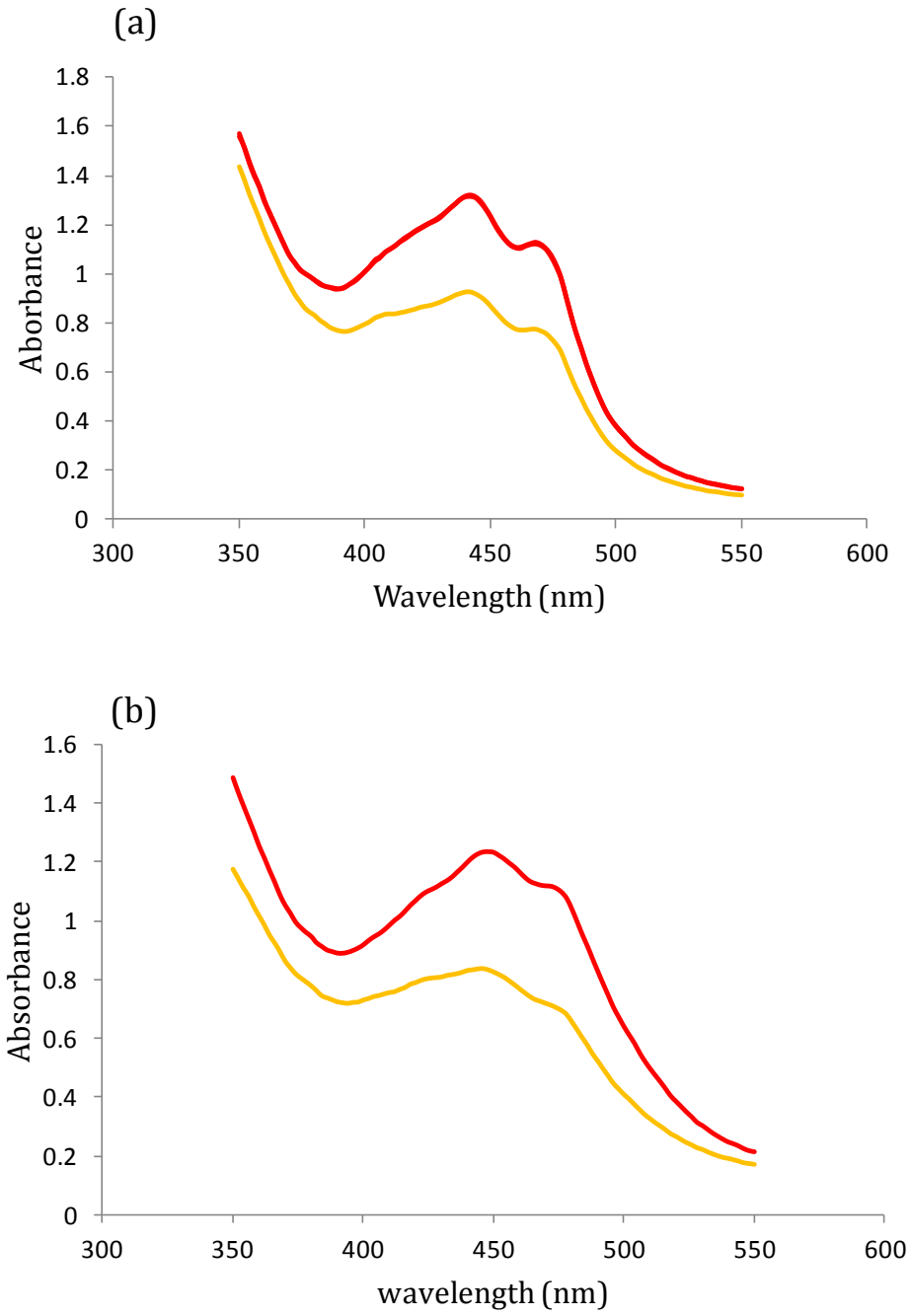

Figure 4.8 Absorbance spectrum assay of methanol-extracted staphyloxanthin. Cells of *S. aureus* Newman(a) and SH1000 (b) were tested by methanol extraction after exposure to 5 μM D-sphingosine (red) or ethanol control (yellow). The x-axis corresponds to the light wavelength and the y-axis is the absorbance value for the corresponding wavelength.

To explore the detected increase in pigmentation after long-term exposure to D-sphingosine, survival from peroxide was tested. Cells of both *S. aureus* and *S. epidermidis* strains were challenged with 7.5 mM hydrogen peroxide after culture in the absence and presence of D-sphingosine, as described in section 2.2.4. Pre-treatment of cells was achieved by 24 h incubation with 5 μM D-sphingosine with 0.03% (v/v) ethanol serving as a solvent control. Cells were harvested by centrifugation, and washed with PBS. To generate a similar killing dynamic, 3.2 mM H_2O_2 was used with *S. epidermidis* Tü3298 because its susceptibility to H_2O_2 was much higher than that of *S. aureus*.

Both *S. aureus* Newman and SH1000 cultures with sphingosine showed greater survival in the presence of the peroxide over the first 60 min of the assay compared with the control, untreated cells (Figure 4.9b, 4.9c). This outcome is consistent with the increased pigmentation described above for cells treated with D-sphingosine and consistent with the reported effect of staphyloxanthin in the protection of the bacteria from peroxide. For *S. epidermidis* Tü3298 D-sphingosine treated cells, there was no obvious difference (Figure 4.9a) in survival from H_2O_2 and this is consistent with the absence of pigment in this species. Higher peroxide concentrations only increased the rate of bacterial killing, with no observable difference for D-sphingosine pre-treated groups and the control cells.

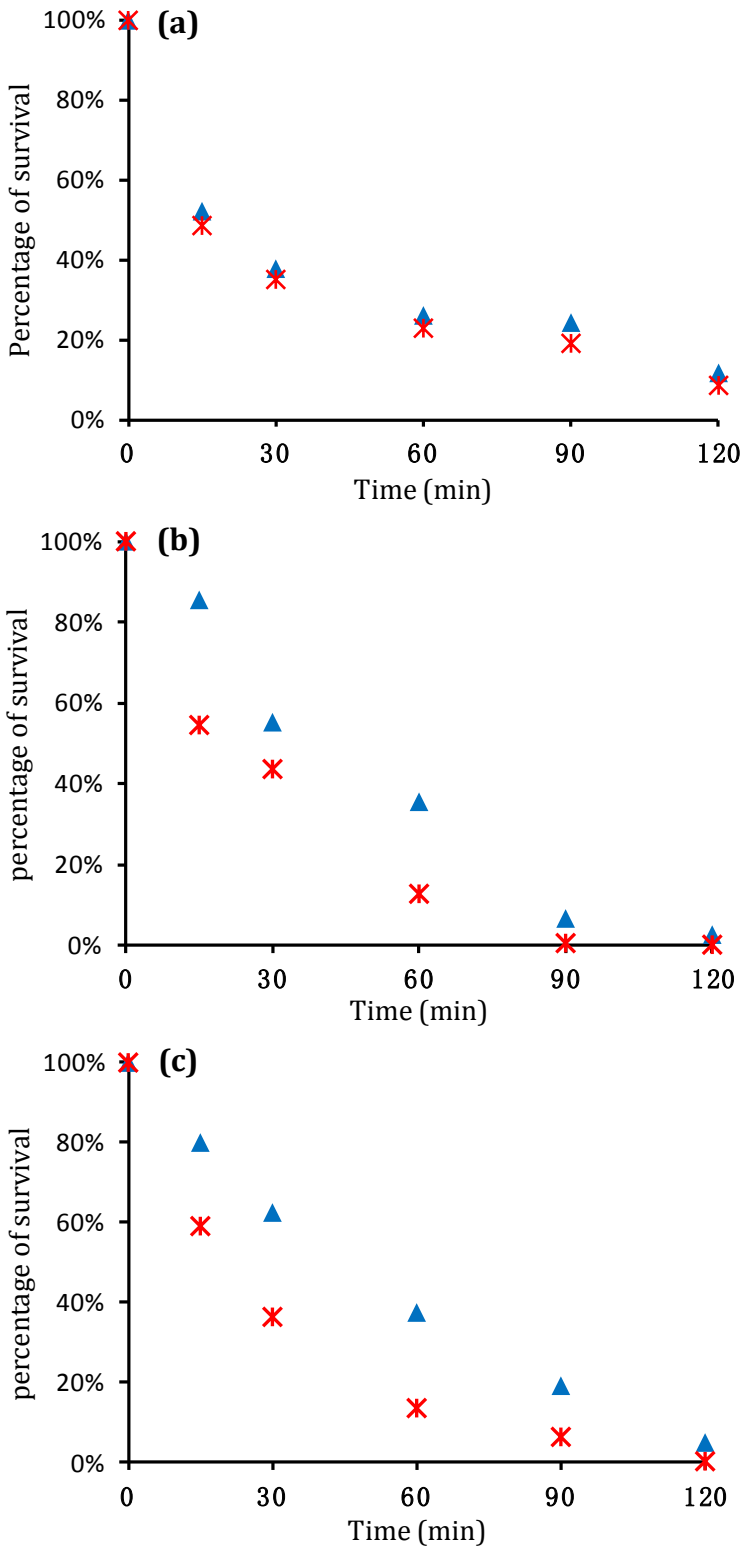

Figure 4.9 Survival of peroxide challenged *S. aureus* and *S. epidermidis* with or without 5 µM D-sphingosine pre-treatment. Cells of *S. epidermidis* Tü3298 (a), *S. aureus* Newman (b) or *S. aureus* SH1000 (c) were challenged with hydrogen peroxide (7.5 mM H_2O_2 *S. aureus*; 3.2 mM H_2O_2 *S. epidermidis*). Blue triangle represents D-sphingosine treated cells and red star represents ethanol control cells. Experiments were repeated three times.

4.4 Discussion

The experiments in this chapter confirmed that the increased expression of the VraSR global regulator of cell wall synthesis has a role in D-sphingosine resistance of *S. aureus*. As proposed in chapter 3, sphingosine might be a cell wall targetting antimicrobial that inhibits cell wall biosynthesis or lead to cell wall damage. Upregulation of VraSR could be a response for damage repair, or may alter regulation of cell wall biosynthesis to produce a thicker or more rigid cell wall layers to prevent penetration of D-sphingosine.

HrtAB is a haem regulated transporter that is controlled by the haem-sensor system HssRS. Both HrtAB and HssRS were upregulated in response to D-sphingosine challenge (3 fold for *hrtA*, 3 fold for *hrtB*, 1.9 fold for *hssR*, 1.6 fold for *hssS*). To compare, the Haem-sensor system (HssRS) and haem regulated transporter (HrtAB) were not differentially expressed in *S. epidermidis* after challenge with D-sphingosine. Although the MIC results for the *hrtB* mutant suggest that haem transport and regulation could play a role in D-sphingosine resistance, only an increase in expression of *hrt* and *hss* must be sufficient to indicate haem/iron-starvation since none of the many genes (such as *isd* operon, *sir, sfa,* and *sbn*) involved in iron acquisition were differentially expressed. Other than iron acquisition, HrtAB system may be activated by sphingosine, or it might export D-sphingosine or a derivative made by metabolism.

The downregulation of the *crt* operon for staphyloxanthin biosynthesis evident in the transcriptomic data makes it tempting to suggest a lower pigmentation level with alteration in membrane lipid synthesis could result from D-sphingosine interaction. The downregulation of pigment production does results in decreased resistance to oxidative stress. However, further experiments in this chapter revealed that the pigmentation level of *S. aureus* was increased after sphingosine addition for 24 h, suggesting bacteria respond differently during growth in its continuous presence. The hydrogen peroxide killing test supports this increased staphyloxanthin production due to D-sphingosine since the sphingosine challenged cells had higher resistance to hydrogen peroxide compared with ethanol controls.

4.4.1 Inorganic phosphate (Pi) and *S. aureus* survival to D-sphingosine

Inorganic phosphate (Pi) is an essential nutrient to living organisms. Cellular metabolism depends on the maintenance of appropriate concentrations of intracellular Pi (Watanabe *et al.*, 2008; Wongwisansri and Laybourn, 2005; Konberg *et al.*, 1999; Ghillebert *et al.*, 2010). Pi is not only required for biosynthesis of cellular components such as ATP, nucleic acids, phospholipids and proteins, it is also central to many metabolic pathways including protein activation, energy production, and carbon and amino acid metabolic processes (Wu *et al.*, 2003). Pi starvation-responsive genes are linked with multiple metabolic pathways, implying a complex Pi regulation system in microorganisms and plants (Yang and Finnegan, 2010; Luan,2003; Hunter, 1995).

In this study, upregulation of the high affinity inorganic phosphate transporter Pst, and the alkaline phosphatase PhoB plus its synthesis regulatory system PhoRP, suggests a requirement for Pi acquisition in *S. aureus* challenged with D-sphingosine. No difference was observed between the D-sphingosine survival of a *pstS-pstCAB* depletion mutant strain compared with the wild type Newman strain (described in section 4.3.2). Similar regulation of these genes was observed in a study of methicillin-resistant *S. aureus* where strong upregulation of the *pstS* and *pstCABphoU* operons was induced by antimicrobial peptide ranalexin (Overton *et al.,* 2011). Similarly, in their further investigation, genetic disruption of the *pstC* transmembrane component of the Pi transporter did not have any effect on ranalexin sensitivity. It was suggested that MRSA adopts a PhoU-mediated persister phenotype to acquire antimicrobial tolerance, but upregulation of the Pi transporter is not a major component of this response (Overton *et al.,* 2011). These genes could be part of a cell wall or cell membrane stress response that is not directly involved or essential in protection from these antimicrobial stimuli.

In contrast, the *pstS::Tn* mutant in this study showed different results from the above data. This *pstS* mutant cells were more sensitive to D-sphingosine compared with wild-type cells, which supports the hypothesis that the *pst*

transporter increases sphingosine survival in *S. aureus*. Altogether, these results might indicate that Pst plays a role in D-sphingosine resistance in *S. aureus*, and deletion of the phosphate-binding protein PstS was essential for disruption of the phosphate ABC transporter Pst. Given that a single allelic replacement variant *pstS* has a different phenotype from the combined operon depletion mutant *pstS-pstCAB*, PstS might also have a role separate from Pst transporter. Deletion of the *pstS* and *pstCAB* genes may alter expression of other genes, such as its repressor regulator *phoU* that increases bacterial resistance to D-sphingosine. Additionally, *phoU* was proposed to suppress the *pst S* and *pstCAB* operons (Overton *et al.,* 2011), but both *phoU* and *pstSCAB* were found upregulated, suggesting a secondary regulatory mechanism for either or both of these genes.

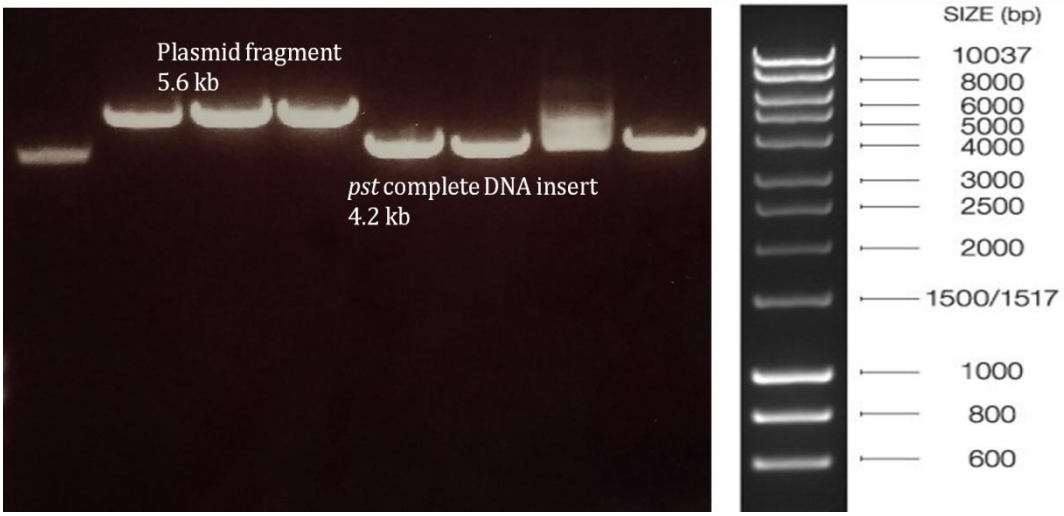

Figure 4.10 Double digestion of *pst* complement after *E. coli* transformation. Plasmids extracted from the transformed *E. coli* colonies were double digested with restriction enzymes BamHI and HindIII. Two clear bands in the same column of the gel image was expected for successfully transformation (one 5.6 kb sized for plasmid psk5632, one 4.2 kb sized for *pst* complete DNA insert). However, no successful transformants were detected.

Complementation of the gene mutants can be achieved by introducing a shuttle vector, such as pSK5632, into *S. aureus* with the relevant operon cloned using sufficient upstream and downstream DNA to include leader and any terminator sequences. A higher expression level of the target gene can be achieved when using high copy number plasmids and the plasmid pSK5632 is low copy in *S. aureus* (Grkovic *et al.*, 2003). Whether the *pst* operon plays a role in staphylococcal resistance to sphingosine could also be determined if higher expression of the *pst* operon increases bacterial resistance. Yet, the creation of complementation strains was unsuccessful, as the plasmid extracted from the transformants were modified in *E. coli* (figure 4.10). The gel image for digested plasmid indicated a range of plasmid sizes but there was no identification of correctly-sized plasmid and insert, supporting rearrangements in *E. coli*. This phenomenon is well known for *S. aureus* membrane proteins and has been described (Horsburgh et al., 2004; Kenny et al., 2013). It is likely that there is toxicity associated with the insertion and mistargeting of the newly synthesised

protein, which can lead to destabilisation of the membrane upon aggregation of expressed proteins. This membrane disruption may trigger proton leak and loss of energy homeostasis (Wanger *et al.*, 2007; Hattab *et al.*, 2014). The presence of near consensus transcription and translation sequences for *E. coli* that are present in *S. aureus* operons compounds the problem, and the toxicity of overexpression of membrane proteins in *E. coli* may explain the problem of no successful transformants detected.

To bypass the toxicity in *E. coli*, previous solutions include direct transformation of ligation reactions into *S. aureus* RN4220 and this was also conducted for the *pst* plasmid construct in several attempts at electroporation, but no successful transformation occurred.

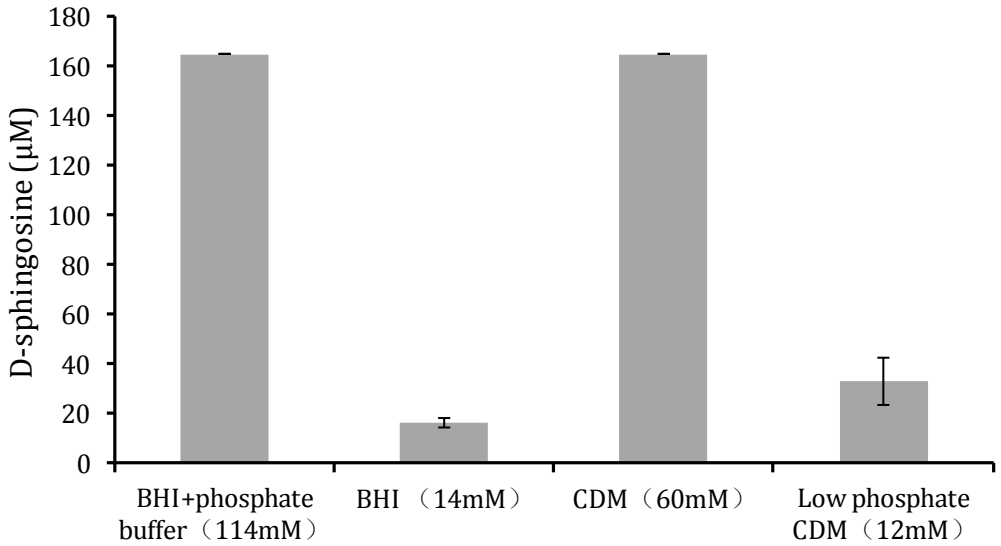

Figure 4.11 Different media based MIC tests of Newman *pstSCAB::tet* strain. Wild type *S. aureus* Newman was tested using BHI and CDM media, with or without additional Pi. Final phosphate concentrations (mM) in the media are indicated in the brackets. The highest D-sphingosine concentration used in this test was 165 μM, the exact MIC that the bacteria can tolerate in the media with additional phosphate could be higher. Error bars indicate standard deviation of three biological repeats.

Having established that addition of Pi dramatically increased MIC of *S. aureus* to D-sphingosine (Figure 4.2), it was investigated if this effect was broth-dependent, since it is possible that the components of growth media may interact with additional inorganic phosphate and D-sphingosine to collectively produce this phenomenon. Therefore, the growth experiment was performed using standard and low phosphate CDM, and BHI with or without additional Pi (Figure 4.11). The results exhibited a similar pattern as that in the original THB experiment, suggesting the nature of the growth medium is not relevant to the effect.

Sphingosine can be phosphorylated *in vivo* via sphingosine kinase to form sphingosine-1-phosphate (S1P), which is a bioactive sphingolipid metabolite involved in mammalian cell growth regulation (Zhang *et al.*, 1991; Spiegel and Milstien, 2000). S1P was found to be a second messenger in cellular proliferation and survival (Olivera and Spiegel, 1993; Cuvillier *et al.*, 1996). It was also suggested that S1P protects cells from ceramide-mediated apoptosis (Cuvillier *et al.*, 1996). Fischer *et al* (2013) predicted sphingosine uptake by *S. aureus*. However, whether sphingosine can be phosphorylated via bacterial enzyme activity, or phosphorylated sphingosine has similar signalling activity in bacteria is not known. From these transcriptome data there is no obvious candidate for an extracellular kinase activity, though the cell could import S1P and might dephosphorylate S1P using its alkaline phosphatases. Specific experiments were not performed to investigate this further.

To summarise, while Pi is required as a component of energy metabolism and kinase/phosphatase signalling processes, whether treatment of D-sphingosine leads to phosphate starvation in staphylococci thereby inducing the *pst* transporter genes, or whether Pst possesses other functions facilitating staphylococcal sphingosine resistance remains to be resolved.

Chapter 5: The individual contributions of *farE/R* genes and SNPs that increase *S. aureus* survival to D-sphingosine

5.1 Introduction

5.1.1 Mechanism of action of sphingosines and AFAs

Human skin possesses two discrete sets of lipids associated with its superficial layers of keratinocytes: the uppermost outward facing surface is coated with sebaceous lipids; and beneath these topmost layers the stratum corneum lipids form a structured supportive network. These two lipid fractions differ markedly in their composition, with the sebaceous lipids being dominated by squalene, wax esters and triacyclglycerols, whereas the epidermal lipids comprise a stoichiometric 1:1:1 ratio of ceramide, fatty acids and cholesterol. Both of these sets contain antimicrobial lipids. The epidermal lipids contain antimicrobial sphingosines, generated from the hydrolysis of ceramide. Antimicrobial lipids of the skin include sphingoid bases (sphingosines) and fatty acids.

Sphingosines are widely active against bacteria and fungi (Drake *et al*., 2008; Desbois and Smith, 2010). Approximately 270 μM of sphingosine can be observed on healthy skin, whilst only 140-160 μM is present on atopic dermatitis skin that becomes typically heavily colonised by *S. aureus* (Arikawa *et al.*, 2002), suggesting an association between sphingosine and *S. aureus* colonisation on skin. D-sphingosine was described to have a similar mode of action as AFAs through membrane leakage and loss of low molecular weight components of *S. aureus* (Parsons *et al.,* 2012). However, the carboxyl group was believed to be essential for toxicity of AFAs (Zheng *et al*., 2005), while sphingosines do not have carboxyl groups. Moreover, sphingosines cause profound morphological changes, including rugged membrane surface, decrease in cell size and loss of cell wall (Fischer *et al.,* 2013), while AFA treated *S. aureus* cells have no significant change in morphology (Parsons *et al.,* 2012).

Sphingosines are evidently more efficient than AFAs at causing membrane disruption as they lead to visible effects and cell lysis (Fischer *et al.,* 2013).

While sphingosines and AFAs do not have an identical action mode, similar mechanisms are found with each targeting the cell membrane. Previous studies have focused on responses to AFAs only, with the effects of sphingosine on cell transcriptional and translational outcomes remaining unstudied. By investigating the effects of sphingosine on survival and transcriptional responses of staphylococci it will be possible to determine the extent to which there are overlapping resistance mechanisms that protect *S. aureus* against different skin lipids, including sphingosines.

5.1.2 FarRE fatty acid resistance regulator and effector system

Previous research in the Horsburgh group identified an MmpL efflux pump (encoded by *sar2632*) in *S. aureus* MRSA252 that contributed to survival from the AFA, linoleic acid (Kenny et al., 2009). Transcripts of the *sar2632* gene were 2-fold upregulated after linoleic acid challenge and an allelic replacement mutant had three-fold reduced survival on linoleic acid containing agar plates. Subsequent studies by others characterised the *sar2632* gene homolog in *S. aureus* USA300 encoding the MmpL efflux pump and ascribed the 'fatty acid resistance' gene as *farE*. The *farR and farE* genes are a divergon that encode a TetR-like regulator and a membrane transporter effector in *S. aureus* and FarR regulation was shown to be induced by arachidonic acid, in addition to the previously assigned linoleic acid (Alnaseri *et al.*, 2015; Kenny et al., 2009). Expression of the FarE efflux pump of *S. aureus* is controlled by the regulator FarR and contributes to resistance to linoleic and arachidonic acids (Alnaseri *et al.,* 2015), and was found to support resistance to sapienic acid of *S. aureus* (Moran, 2015).

5.2 Chapter Aims

Previous research conducted in the Horsburgh group at Liverpool, sought to investigate the determinants that contribute to survival of *S. aureus* and *S. epidermidis* from the amino alcohol sphingosine, using D-sphingosine as a readily available representative of these skin lipids. An experimental evolution approach was used in the previous study, where *in vitro* selection of both species was performed for clones with increased MIC to sphingosine (Moran, 2015). Genome re-sequencing and mapping of genetic variance revealed multiple single nucleotide polymorphisms (SNPs), and several SNPs mapped to the previously identified *mmpL* lipid efflux locus (Moran, 2015), and those genes subsequently named *farRE* (Alnaseri *et al.*, 2015*)*.

Taking into consideration the potentially contributing roles of those identified SNPs, together with the described roles of FarR and FarE in *S. aureus* lipid resistance, the aim of this chapter is to dissect the SNPs and identify the individual contributions of the *farR* and *farE* genes and the mapped SNPs to resistance of *S. aureus* to sphingosine. This investigation will be achieved using allelic replacement mutants and generation of allelic variants with defined SNPs, to determinate the contribution of this genetic locus in resistance of *S. aureus* to D-sphingosine.

5.3 Results

5.3.1 Construction of allelic variants of *farE* and *farR* genes

Previous work in the Horsburgh lab group revealed that *in vitro* selection of *S. aureus* for increased growth yield at high concentrations of sphingosine resulted in multiple genetic changes, which included SNPs in the divergon *farE-farR* (Moran, 2015). Three evolved strains: 9A, 9B, 15C, were identified and characterised by Moran (2015) (Table 5.1) and these strains had various combinations of three non-synonymous SNPs in the *farR* gene (FarR A40S, D94Y and E151K). The study determined that the selected clones bearing these SNPs (amongst other SNPs) had increased sphingosine MIC. To provide confirmatory evidence for the role of the individual SNPs in the *farR* genes contributing to increased MIC, attempts were made to generate mutants bearing the annotated nucleotide changes (see chapter 2, section 2.3).

Table 5.1 Genetic polymorphisms identified in the *farR* locus in a previous study. (Data from Moran, 2015)

Gene	Evolved isolate	Position of change	Gene SNP position	Base change	Amino acid substitution
farR	9A	2641724	451/549 bp	G/A	E151K
farR	9B	2641391	118/549 bp	G/T	A40S
		2641553	280/549 bp	G/T	D94Y
farR	15C	2641553	280/549 bp	G/T	D94Y
		2641724	451/549 bp	G/A	E151K

Table 5.2 PCR primers for *farR* gene cloning. Primers were designed with addition of restriction enzyme recognition sequences (underlined) AAGCT and GGATCC for *Hin*dIII and *Bam*HI, respectively.

Primer name	Sequence 5'-3'	product size
FarR_Forward	ACTAAGCTACGATGAAAGAGACTGA	572bp
FarR_Reverse	ACTGGATCCACGCTATTTAATCTTAAT	

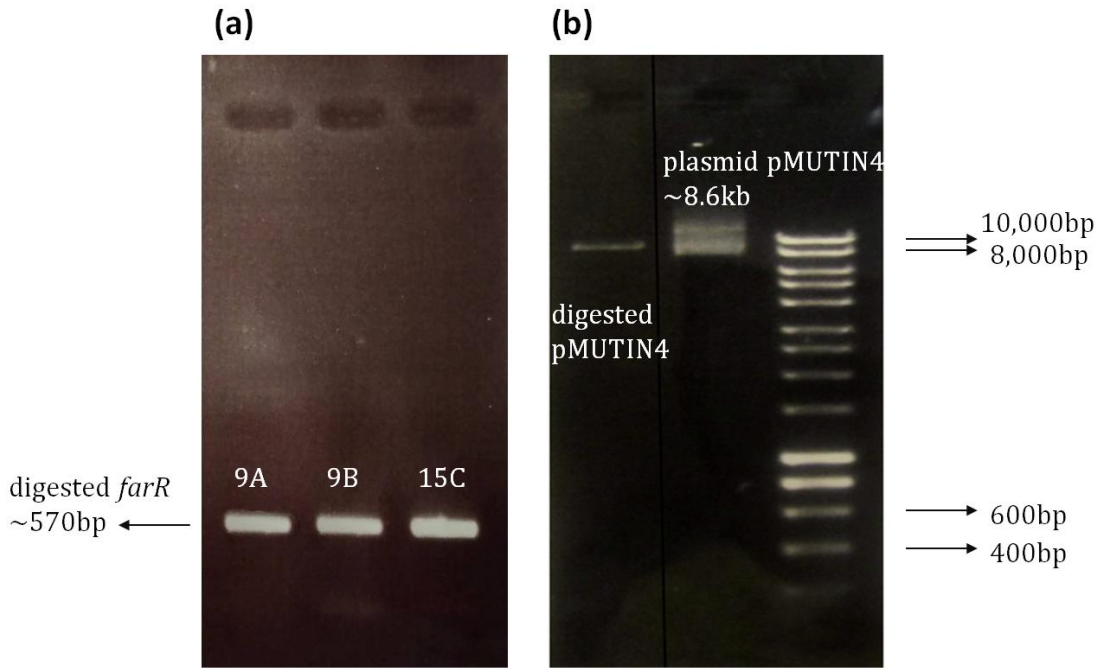

Figure 5.1Cloning of farR alleles into pMUTIN4. (a) Digested *farR* DNA fragments. The *farR* alleles were PCR amplified from DNA of strains 9A, 9B and 9C, respectively, followed by digestion with restriction enzymes *Bam*HI and *Hind*III. (b) Uncut and digested plasmid pMUTIN4. Plasmid pMUTIN4 was extracted and digested with *Bam*HI and *Hind*III; plasmid pMUTIN4 before (right lane) and after (left lane) double digestion.

Primers for PCR amplification of *farR* were designed with the addition of restriction enzyme recognition sequences AAGCT and GGATCC for *Hind*III and *Bam*HI, respectively (Table 5.2). Insert DNA fragments for cloning into the vector pMUTIN4 in *E. coli* were amplified from evolved strains 9A, 9B and 9C, with different combinations of the target SNPs A40S, D94Y and E151K (Table 5.1). The PCR products were purified and digested with *Bam*HI and *Hind*III (Figure 5.1a) with different restriction enzymes used to limit self-ligation between the DNA fragments.

Plasmid pMUTIN4 used in this experiment is a high copy number vector (Vagner *et al.*, 1998) when it replicates in *E. coli* and acts as a suicide vector in *S. aureus*. The plasmid was digested with the same combination of restriction

enzymes *Bam*HI and *Hind*III as the insert DNA fragments, again to minimise self-ligation. The single band of linear plasmid DNA of correct size confirmed digestion (Figure 5.1b). The double digested plasmid and insert DNA fragments were ligated using T4 ligase and *E. coli* Top10 was transformed followed by selection and screening for correct clones.

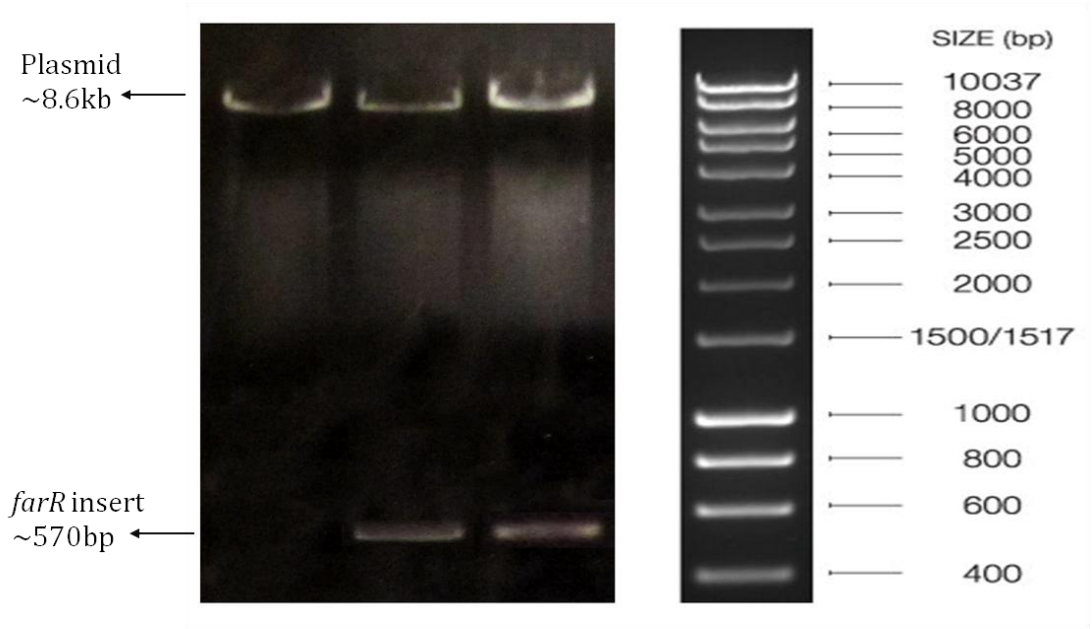

Figure 5.2. Double digestion of *far*R plasmids purified from *E. coli*. Plasmids were extracted form the *E. coli* transformants and double digested with restriction enzymes *Bam*HI and *Hind*III to release the cloned DNA with the sizes of fragments shown. DNA markers from an adjacent section of gel are shown alongside.

E. coli transformant clones were screened for those that contained plasmids with a *farR* insert. Purified plasmids were double digested with *Bam*HI and *Hin*dIII to identify the desired plasmids, i.e. correctly sized *farR* insert DNA band and plasmid pMUTIN4 band (Figure 5.2). Correctly cloned plasmids were then purified and used to transform *S. aureus* RN4220 via electroporation, using the method described by Schenk and Ladagga (1992). *S. aureus* RN4220 can accept

foreign DNA since it a restriction gene mutation means incoming DNA is modified with addition of methyl groups but degraded at a reduced rate. The plasmid pMUTIN4 cannot replicate in *S. aureus* but recombination with the genome can be selected if cloned homologous regions are present. A combination of 5 μg ml^{-1} erythromycin and 25 μg ml^{-1} lincomycin was used to select for recombination of the suicide vector and to minimise selection of spontaneous erythromycin resistance. A chosen clone was then lysed with phage φ11 to propagate generalised transducing phage bearing the allele for transduction of the integrated plasmid to *S. aureus* SH1000.

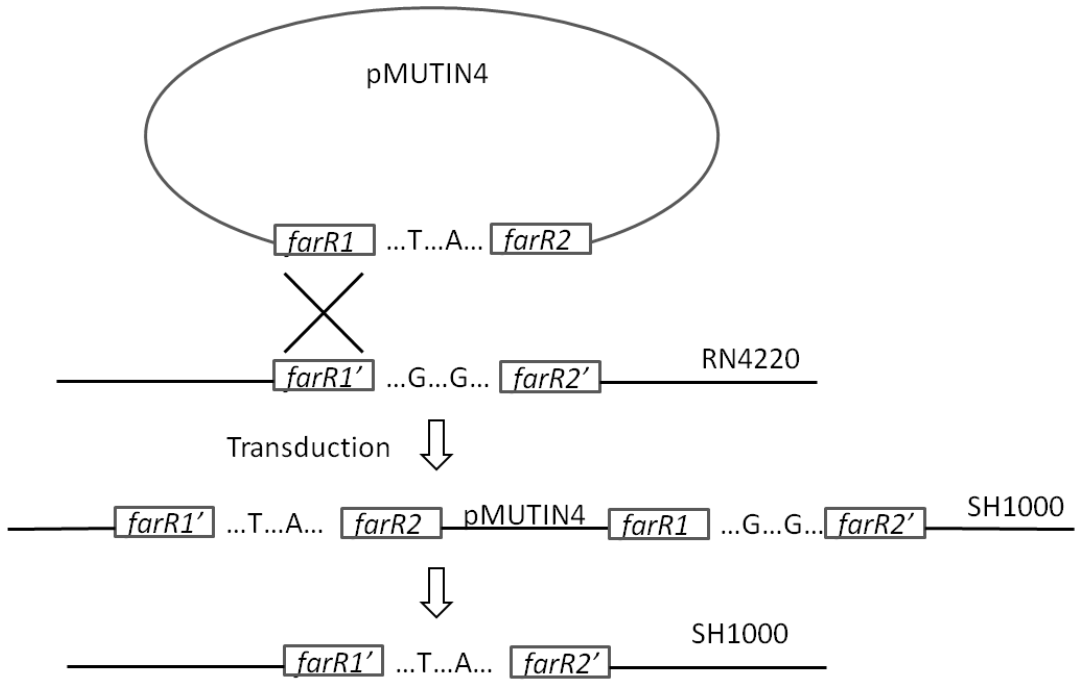

Figure 5.3 Schematic of integration and resolution of SNP alleles using pMUTIN4. SNP containing *farR* DNA fragment shares near identical sequnce with the gene of the recipient RN4220 stain. The insert-vector plasmid construct was integrated into the RN4220 genome via single Campbell integration event. Plasmid lost occurs after recombination of *farR* and *farR'* (SNP containing *farR* gene) during growth in the absence of antibiotic selection.

S. aureus SH1000 was used as recipient strain to generate the *farR* SNPs found in clones 9A, 9B and 15C in the same strain used for evolution with D-sphingosine. After selection, transductants were grown in BHI without antibiotic for 48 h to permit recombination that will generate a single locus and potentially replace wild-type *farR* by the constructed *farR* SNP allele. During this recombination, the plasmid is deleted (Figure 5.3), with loss of erythromycin resistance encoded by pMUTIN4, and this change of phenotype was used to identify clones where recombination had occurred.

Table 5.3 PCR primers for SNP screening. Forward primers for *farR* SNPs A40S, D94Y and E151K. PCR reactions were prepared with these SNP screening forward primers and the FarR_Reverse primer (Table 5.2) respectively for detection of each SNP.

Primer name	Sequence 5'-3'	product size
SNP screening_A40S	TTTGCGACAACT (12)	454 bp
SNP screening_D94Y	GCGATTTCTCTCAAATA (17)	298 bp
SNP screening_E151K	CGACTCGTTGATTA (14)	124 bp

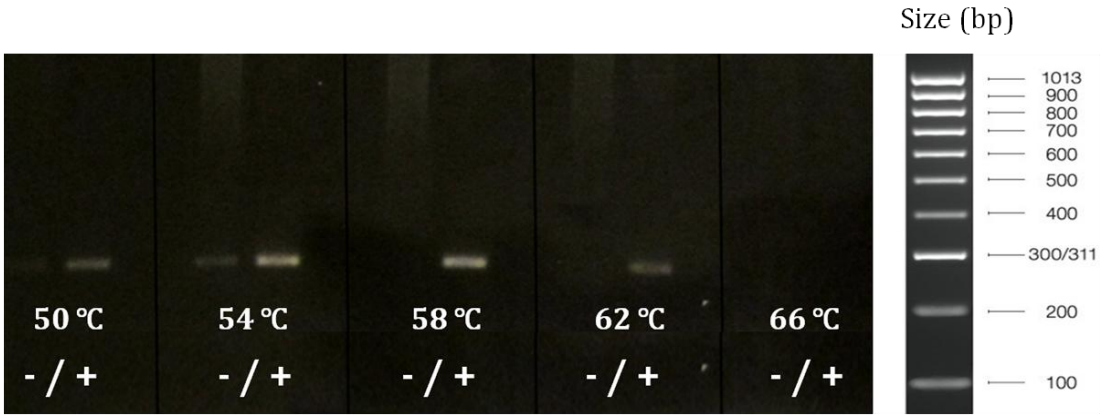

Figure 5.4 PCR optimisation of SNP screening primer D94Y. DNA of *S. aureus* SH1000 was used as template for negative controls (-), DNA of 15C evolved clone was used as template for positive controls (+). Both positive and negative templates were amplified with 50-54°C annealing temperature; only positive controls were amplified with 58-62°C annealing temperature; neither positive nor negative templates were amplified at 66°C annealing temperature.

To identify those clones having undergone recombination that have maintained the SNP containing allele, primers for screening to identify the presence of the SNP were designed with the desired nucleotide mismatch at the 3' end (Table 5.3). The location of the mismatch at this position prevents amplification of the wild-type DNA amplicon at high annealing temperatures; short lengths (12-17 nt) and high annealing temperature increase primer specificity to SNP containing template rather than wild type. The optimum annealing temperature of each SNP screening primer was determined with PCR reactions at various annealing temperatures, using DNA of strain SH1000 as negative template and strains 9A, 9B or 15C as positive (SNP) template. For SNP D94Y, the screening primer only amplified the positive template with 58-62°C annealing temperature, with greater amplification yield at 58°C than 62°C (Figure 5.4); 58°C was considered to be the optimum annealing temperature for SNP screening primer D94Y. Utilising the same method, the determined optimum annealing temperature for SNP screening primers A40S and E151K were 58°C and 50°C, respectively.

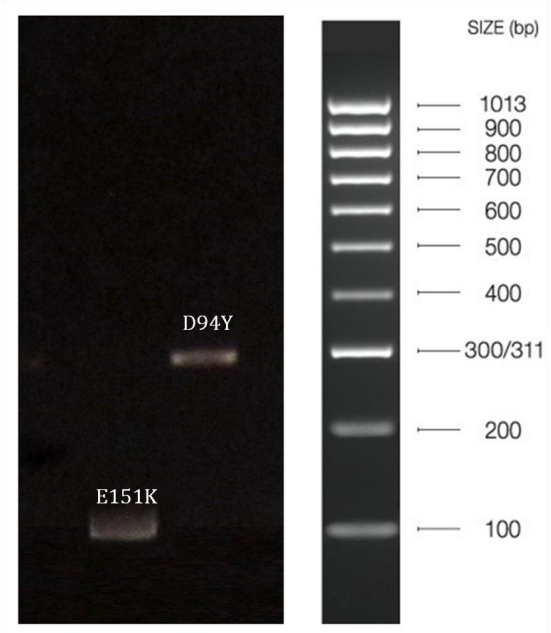

Figure 5.5. PCR screening of SNPs in a selected *farR* clone after recombination. Single colonies were tested with SNP screening primers (Table 5.3) to detect potential correct SNP-bearing clones. A variant with both SNPs D94Y and E151K was found.

Using this PCR screen method, colonies that were positive for the target SNPs were selected. The *farR* gene fragments were then PCR amplified and sent for sequencing using the Sanger method for confirmation (GATC, UK). The DNA sequences were compared with wild type using NCBI nucleotide BLAST (Basic Local Alignment Search Tool) algorithm (NCBI). Although a range of desired *farR* allelic variants were sought (table 5.1), only one *farR* SNP variant strain was constructed and confirmed by Sanger sequencing: FarR.D94Y.E151K, contains two SNPs: *Saouhsc-02867*-(E151K; G2641724A) and *Saouhsc*-02867-(D94Y; G2641553T).

5.3.2 D-sphingosine survival test of *farE and farR* allelic replacement mutants and *farR* SNP variant

To assess the role of the *S. aureus farE* and *farR* genes in sphingosine survival, the minimum inhibitory concentration (MIC) of D-sphingosine was determined for the *farE and farR* allelic replacement mutants (unpublished lab strain SH1000 *farE::tet* and SH1000 *farR::tet* from Horsburgh Lab) and the *farR* SNP variant (SH1000 FarR.D94Y.E151K). MIC values were compared with wild type SH1000. Bacteria were cultured in BHI broth, then 96 well plates were used for MIC tests. A range of concentrations of D-sphingosine were prepared with BHI broth and 100 µl was added to each well of the 96 well plate. Test strains were grown for 24 h, diluted to OD_{600}=0.2 with BHI broth, then 100 µl was added to each well and incubated at 37°C for 24 h. Each experiment comprised at least 3 technical repeats and 5 biological repeats.

The SNP variant SH1000 FarR.D94Y.E151K was capable of growth at high concentrations of D-sphingosine (165 µM), although the MIC was not as high as the original evolved isolate 15C (485 µM) (Figure 5.6b) that contained further SNPs not studied here. Other non-synonymous SNPs present in coding regions of 15C include genes encoding: ATP synthase (*saouhsc_02341*); hypothetical CAAX protease (*saouhsc_02587*); extracellular matrix binding protein homolog (*ebh*); methicillin resistance determinant (*fmhA*); sorbitol dehydrogenase (*saouhsc_00217*); and upstream substitution of sigmaB regulator (*rsbU*); transglycosylase (*Saouhsc_01840*), hypothetical proteins (*saouhsc_00235, saouhsc_01130, saouhsc_01584, saouhsc_01918, saouhsc_02189*) (Moran, 2015).

In support of the genes contributing to sphingosine resistance, both *farE* and *farR* allelic replacement mutants had reduced MIC for sphingosine (9.9 and 11.75 µM respectively), compared with 16.3 µM in the wild type (Figure 5.6a). Altogether, the MIC tests support the hypothesis that the FarRE regulator-transport system contributes to resistance of *S. aureus* to the antimicrobial lipid D-sphingosine (Figure 5.6).

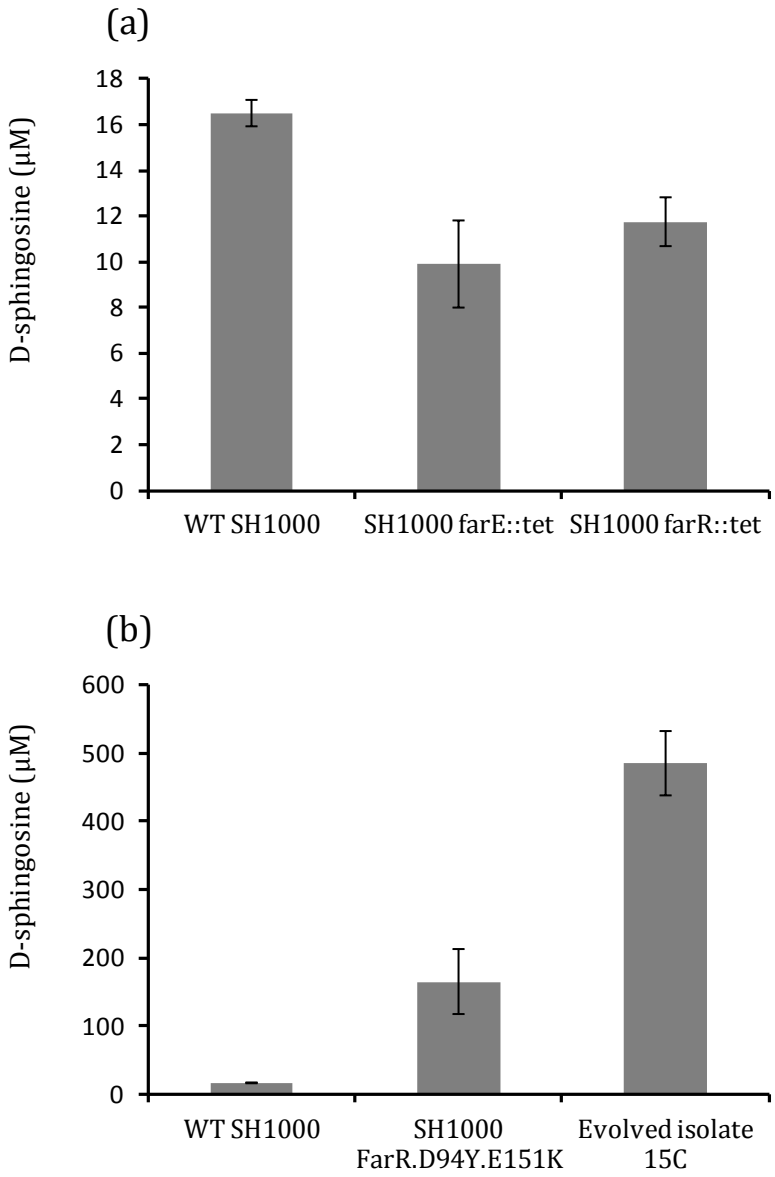

Figure 5.6 D-sphingosine MIC assay of *farE* and *farR* mutant strains. D-sphingosine MIC results of (a) *farE* and *farR* allelic replacement mutants and (b) SH1000 FarR.D94Y.E151K compared with wild-type SH1000. The strains SH1000 *farE::tet*, SH1000 *farR::tet*, original evolved isolate 15C and the *farR* SNP variant SH1000 FarR.D94Y.E151K were assayed in BHI medium and compared with wild type SH1000. Error bars indicate standard deviation of three repeated experiments.

As a further assay of D-sphingosine survival, wild type *S. aureus* SH1000 and isogenic mutant strains *farE::tet, farR::tet* were cultured with a sub-lethal concentration of D-sphingosine (5 μM). Control groups were cultured with solvent only (0.03% v/v ethanol). Bacteria were grown for 24 h prior to survival assay with sphingosine. It was hypothesised that bacteria pre-treated with a sub-lethal concentration of D-sphingosine would have greater resistance to D-sphingosine. Harvested cells were challenged with 5 μM, 10 μM, 15 μM, or 20 μM D-sphingosine. This range of D-sphingosine concentrations was used to find an appropriate lethal concentration to differentiate killing over time due to D-sphingosine and for comparing pre-treated groups and controls.

Both *farE* and far*R* allelic replacement mutants were 100% killed by 15 μM D-sphingosine rapidly within 15 min (Figure 5.7bc), while wild type SH1000 was 60% killed in 30 min (Figure 5.7a). Ten μM D-sphingosine was not lethal to wild type SH1000 (Figure 5.7d), but killed 95% SH1000 *farE::tet* in 30 min (Figure 5.7e) and killed 80% SH1000 *farR::tet* in 90 min (Figure 5.7f). These data support the conclusion of the MIC tests that *farE* and *farR* depletion results in decreased tolerance of *S. aureus* to D-sphingosine. Moreover, the results also indicated that pre-treatment of a sub-lethal concentration of D-sphingosine increased the resistance to a previously lethal concentration in all three strains (death rate of the pre-treated bacteria was slower, and less bacteria were killed than control), and was more pronounced in *farE* and *farR* allelic replacement mutants. These data support inducible resistance mechanisms of *S. aureus* to D-sphingosine.

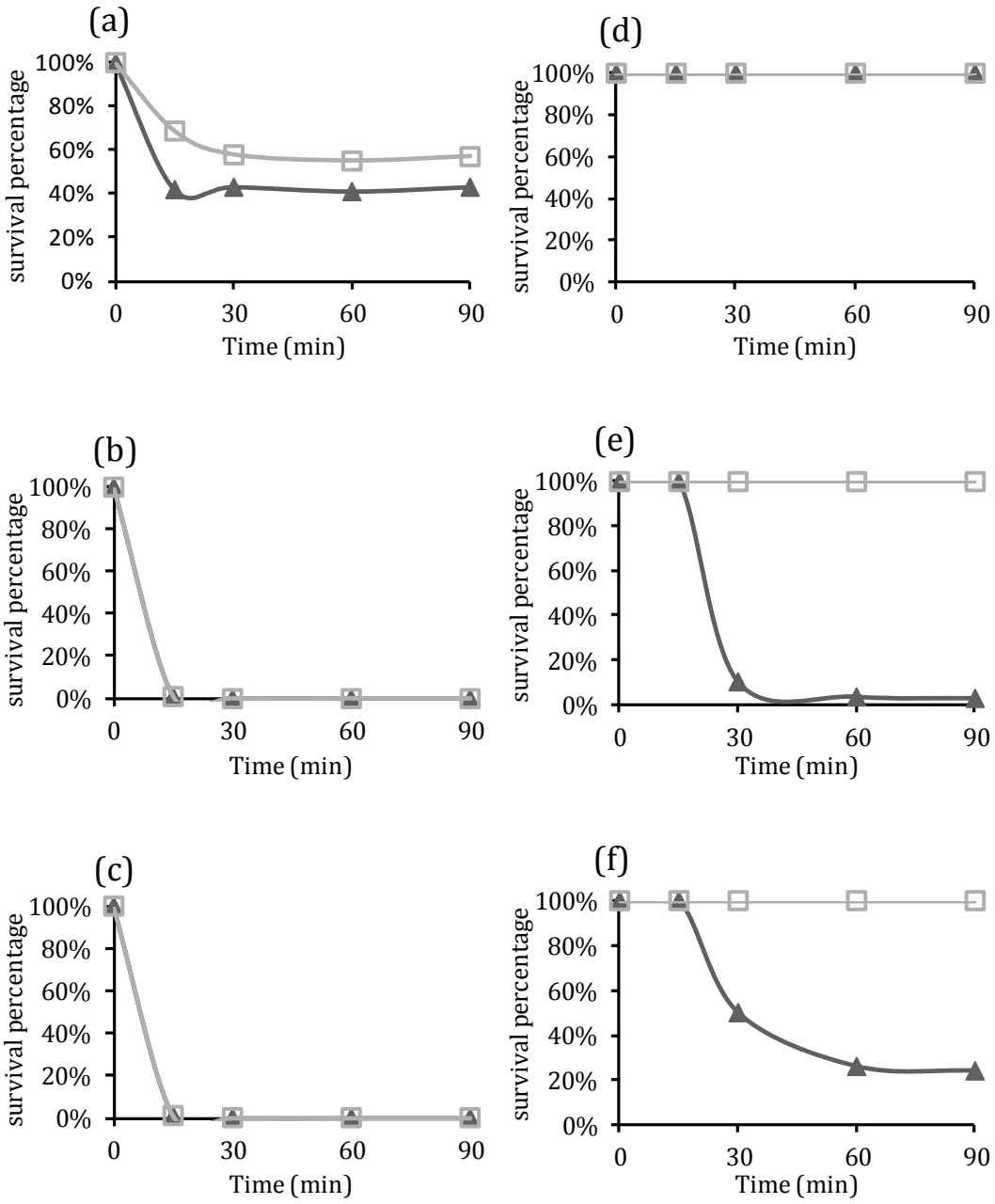

Figure 5.7 D-sphingosine survival of *S. aureus* strains cultured in the absence and presence of D-sphingosine. Cells were cultured in the absence (ethanol solvent control; triangle) or presence of 5 uM D-sphingosine (open square). WT SH1000 challenged with 15 μM (a) or 10 μM (d) D-sphingosine. SH1000 *farE::tet* strain challenged with 15 μM (b) or 10 μM (e) D-sphingosine. SH1000 *farR::tet* strain challenged with 15 μM (c) or 10 μM (f). Data is representative of 2 experiments showing similar results.

5.4 Discussion

Whilst one aim of this part of the research study was to generate a range of SNP variants of the *farR* gene encoding a lipid efflux transporter, this had only limited success. Of the three SNPs previously identified in *farR* and targetted for construction as single isogenic variants in *S. aureus*, just SH1000 variant encoding protein FarR.D94Y.E151K variant was created successfully. No mutants with either single or double SNPs could be found from those colonies screened. However, the single variant generated SH1000 FarR.D94Y.E151K had increased resistance to D-sphingosine, compared with its isogenic parent. This strongly supports a potential role for the FarR-FarE gene locus in resistance to the lipid D-sphingosine.

In addition to this experiment, analysis of *farE* and *farR* allelic replacement mutants was performed with D-sphingosine MIC assays and challenge survival assays. These studies revealed that SH1000 *farE::tet* and SH1000 *farR::tet* both had markedly reduced resistance to D-sphingosine. The contrast with the *farR*-SNP variant is important since the reduced resistance supports that the *farR* SNPs might be more regulatory rather than mutations affecting specificity for D-sphingosine. However, such declarations require further study with more elegant experiments looking at transport and gel retardation of the *farE* promoter/leader DNA. Nonetheless the data supports that the FarR-FarE proteins play a role in facilitating D-sphingosine resistance in *S. aureus*. Given these findings it might be expected that upregulation of *farR-farE* would be seen in the RNA-seq data (Chapter 3). Yet, no differential expression of either *farE* or *farR* was observed in the D-sphingosine challenge *S. aureus* transcriptome. Therefore, it is credible that the ability of FarR to sense sphingosine is absent, while FarE is capable of sphingosine export. A combination of biochemical and structural studies would resolve this knowledge gap.

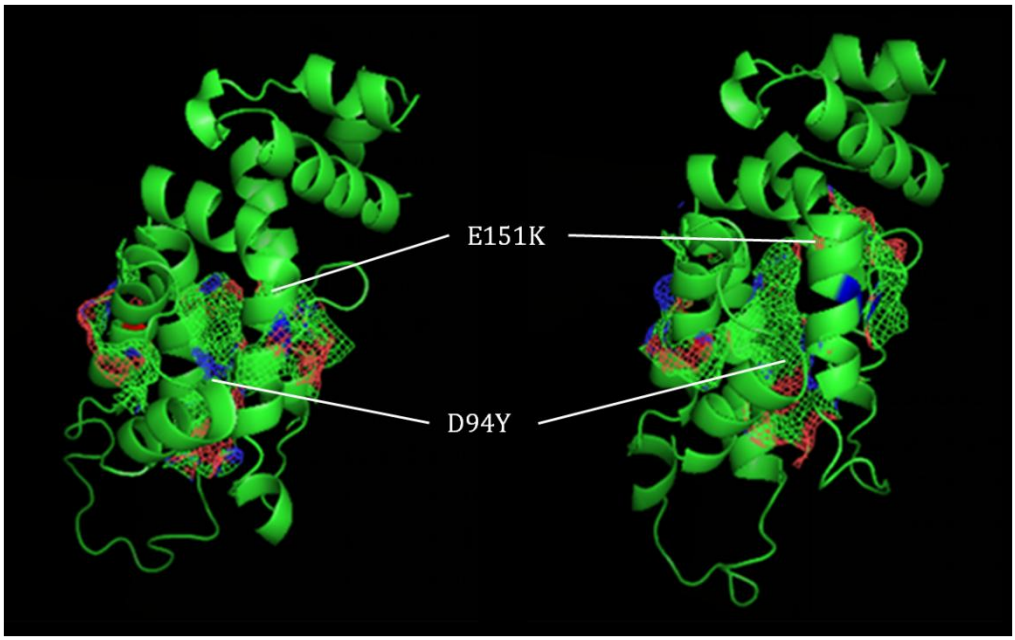

Figure 5.8 Protein model of *S. aureus* FarR protein showing sites of amino acid replacements. The FarR protein encoded by strain SH1000 (left) and the variant SH1000 FarR.D94Y.E151K (right) are highlighted with the relevant amino acid positions of the SNP. Protein models were constructed using modeller (version 9.17), then visualised with Pymol. The mesh like pattern shows surface charge of the protein, where red shows positive charge, blue shows negative charge, and green is neutral.

The FarR protein belongs to the TetR family with known structures forming homodimers, with the N-terminal domain containing a DNA binding helix-turn-helix motif, and the C-terminal domain acting as the substrate binding domain (Ramos *et al.*, 2005). TetR proteins have a pocket structure in the substrate-binding domain. The protein is in relaxed state when not binding with the substrates, and this relaxed state is capable of DNA binding. TetR protein shifts to a tensed state when binding its substrates, so that binding of DNA is inhibited. This enables transcription from TetR-regulated promoters (Ramos *et al.*, 2005). Previous work in the laboratory proposed that FarR could be a transcriptional regulator of the FarE efflux transporter (Moran, 2015), which transports fatty acids and this was later confirmed to be the case for linoleic acid and arachidonic acids (Alnaseri *et al.*, 2015). It was hypothesised that FarR functions

as repressor of *farE* in the absence of inducer, but may act to promote expression of a positive-acting transcription factor that is needed to activate *farE* in presence of exogenous fatty acids (Alnaseri *et al.*, 2015).

In this study, protein models were constructed using modeller (version 9.17), then visualised with Pymol (Figure 5.8). In the variant protein SH1000 FarR.D94Y.E151K, the amino acid changes cause tyrosine substitution for aspartic acid and lysine substitution for glutamic acid. The substitution of negatively-charged aspartic acid with the neutral amino acid tyrosine which has a bulky hydrophobic side chain, and the substitution of negatively-charged glutamic acid with the positively-charged lysine appear to alter surface charge of the protein (Figure 5.8, blue indicates negative charged, red means positive charged, and green stays neutral). It is possible that these amino acid changes affect how this repressor interacts with its substrate, or alternatively changes the protein to a tensed state, independent of substrate binding (always tensed causing constitutive expression of FarE).

While the FarR SNP mutant strain exhibited higher resistance to D-sphingosine compared with the wild type strain, the lack of differential expression of either *farE* or *farR* in the transcriptomics response of *S. aureus* to D-sphingosine may suggests that D-sphingosine is not a natural substrate for FarR, and does not induce expression of either FarE (or FarR). The experimental evolution that resulted in the protein variants after D-sphingosine selection reveals potential plasticity in this transporter system. The changes in structure and surface charge may contribute to recognition of D-sphingosine as a substrate, and thus activate transcription factor for expression of FarE. Future studies could use qPCR to test the hypothesis that expression of FarE in the variant SH1000 FarR.D94Y.E151K is independent of the presence of of D-sphingosine.

Chapter 6: General Discussion

This study investigated the effects of skin antimicrobial lipid D-sphingosine upon *S. aureus*, with a focus upon discovering determinants that affect antimicrobial lipid resistance of *S. aureus*. These responses and determinants were expected to inform on the mechanism of action of D-sphingosine and evolved mechanisms of *S. aureus*. To complete these aims, RNA-Seq and qPCR were used to dissect the transcriptional responses of *S. aureus* Newman and *S. epidermidis* Tü3298 after challenge with D-sphingosine. Combined with experimental evolution data, individual contributions of genes and SNPs that increase *S. aureus* survival to sphingosine from transcriptomics data and from previous work of the Horsburgh group were further investigated.

Antimicrobial lipid sphingosine is less well studied than AFAs, where their mode of action was proposed to be similar with membrane damage and leakage of solutes (Bibel *et al*., 1993; Fischer *et al*., 2013; Bergsson *et al.,* 2001). Although the detailed antimicrobial mechanisms of sphingosine on bacteria is not well established, several possibilities exist: sphingosine may act on *S. aureus* by penetrating and disrupting the cell wall or altering changes in cytoplasmic membrane; it may penetrate the cell walls and the cytoplasmic membranes of bacteria, then enter and disrupt the cytoplasm similar to the mechanism described by Bergsson *et al.* (2001) for *S. aureus*. The RNA-Seq data analysis (Chapter 3) showed: increased expression of the cell wall stress stimulon (including VraSR, Pbp2, MurZ and MsrA1); overlap with the transcriptomic response to antibiotics that target cell wall (vancomycin, bacitracin, fosfomycin and oxacillin) and membrane (such as ovispirin and temporin); increased expression of genes for peptidoglycan and membrane lipid biosynthesis. Collectively, these *S. aureus* transcriptomic responses support D-sphingosine as having both cell wall stress and membrane disrupting actions.

Whilst colonising skin, there is a further way, distinct from cell wall or membrane disruption, whereby sphingosine could affect *S. aureus*. Epidermal sphingosine can be phosphorylated by host sphingosine kinase to form sphingosine-1-phosphate (S1P) that is sensed for regulation of cellular

proliferation and survival of mammalian cells (Zhang *et al.*, 1991; Spiegel and Milstien, 2000). S1P is a major regulator of the vascular system, where it regulates angiogenesis, vascular stability, and permeability. S1P is also recognized as a regulator of T- and B- cells in the immune system (Sharma *et al.*, 2013). In addition, Fischer *et al* (2013) predicted sphingosine uptake by *S. aureus*. Moreover, transcriptomic data analysis (Chapter 4) has revealed phosphate acquisition in response to D-sphingosine. However, whether sphingosine can be phosphorylated via bacterial enzyme activity, or if phosphorylated sphingosine has similar signalling activity in bacteria is not known. *S. aureus* alkaline phosphatase activity may also permit manipulation of environmental S1P to influence the skin regulatory pathways and should be investigated in future studies.

The transcriptomic analysis of D-sphingosine challenged *S. aureus* that was undertaken in this study identified upregulation of the high affinity phosphate specific transporter (Pst) and the PhoRP alkaline phosphatase synthesis regulatory system, both of which control import of inorganic phosphate (Pi) into the cell cytoplasm. The reason for this induction was not determined in the study and several possibilities exist as to why the lipid drives this expression change. It is likely that sphingosine induce lipid synthesis due to damage, or sphingosines might be directed into lipid biosynthesis pathways that require phosphate. Alternatively, D-sphingosine might cause effects such as phosphate starvation through an undefined action or induction of phospholipid synthesis that requires increased phosphate. Inductively coupled plasma mass spectrometry (ICP-MS) could be utilised in future work to quantitatively determine variation of phosphate concentration in cells of untreated and D-sphingosine-treated *S. aureus*. ICP-MS combines a high temperature ICP (Inductively Coupled Plasma) source with a mass spectrometer. The ICP source atomises and ionises the sample. These ions are then brought into the mass spectrometer and are separated and detected by the mass spectrometer via their specific mass-to-charge (M/Z) ratio. The most commonly used type of mass spectrometer is the quadrupole mass filter (Ruth, 2005). ICP-MS is able to analyse phosphorus levels via quadrupole detection of the natural isotope of

phosphorus, ^{31}P at *m/z*=31 and the PO^+ moiety at *m/z*=47 (Zhang *et al.*, 2010; Profrock and Prange, 2012).

Further investigation of the phosphate transporter (Chapter 4) indicated that increased environmental Pi concentration assisted D-sphingosine resistance of *S. aureus* strains, and both *pstS* and *phoR* mutants are more susceptible to D-sphingosine than wild type control. These experiments provide the possibility of phosphorylation of sphingosine within *S. aureus* cells that reduces toxicity by directing the lipid towards metabolism. Alternatively, phosphorylated sphingosine may serve as a messenger that induce bacterial growth and survival to antimicrobial lipids. Ericson *et al.*, (2017) reported that fatty acids (FAs) negatively regulate SaeRS signalling, and FA kinase activates production of SaeRS-dependent virulence factor in *S. aureus* by lowering inhibitory FA levels. SaeRS-mediated transcription was found to be restored in FA kinase-negative strains when the intracellular FA pool is reduced (Ericson *et al.*, 2017). Given the similar action mode between sphingosine and AFAs, together with the downregulation of SaeRS in both *S. aureus* and *S. epidermidis* by D-sphingosine treatment, sphingosine might also affect the FA pool and FA kinase activity to induce similar effects on cellular lipid homeostasis regulation.

Isotope labelling techniques can help with investigation of sphingosine and phosphate metabolism in the bacteria. Biological studies based on isotope labelling have been widely established. This technique is particularly powerful in biochemical pathway analysis allowing scientists to trace the conversion of one chemical to another following incorporation of heavy atoms from precursor substrates into different metabolic products (Chokkathukalam *et al*., 2014; Fan *et al*., 2012). Usage of radioactive isotopes is a common method in isotope labelling research due to its high sensitivity. The amount of radioactive isotope used in the study must be strictly controlled within the limits of what an experimental organism can support, since excess radiation will induce mutations and alter outcomes, and instead stable isotopes remove mutagenic effects for ease of study. Stable isotopes have the same number of protons as the common elements, and consequently share the same physicochemical properties, but differ in mass due to a difference in the number of neutrons,

which enables mass spectrum based analytical tools to easily separate isotopically labelled compounds based on mass differences (Chokkathukalam *et al*., 2014).

By treatment of staphylococci with a customised isotope-labelled D-sphingosine and then tracking its flux in bacterial metabolic pathways, it could be determined whether sphingosine enters the cell membrane; whether bacteria consume sphingosine as a carbon source, and if so, which metabolic pathways sphingosine passes through. To facilitate our understanding of the potential reaction between inorganic phosphate and D-sphingosine, *S. aureus* cells pre-cultured in chemical defined medium (CDM) with ^{31}Pi and then transferred into a new CDM medium with radioactively labelled ^{32}Pi, could be followed by challenge with ^{14}C labelled D-sphingosine. ^{14}C and ^{32}P emit β rays (i.e. electrons), which cause flashes of light and can then be detected in a photomultiplier tube (Rennie, 1999). The energy spectra of ^{14}C and ^{32}P are different, with ^{32}P having a higher average energy. Thus, the detector can separate isotope counts by frequency distribution of kinetic energy consumption and emitted β particle number, which enables dual-labelling techniques (Rennie, 1999). Through the radioactively labelled isotope method, it could be predicted whether D-sphingosine reacts with inorganic phosphate by comparing the tracing signals of ^{14}C and ^{32}P. Furthermore, isotope tracing may also indicate the location for phosphorylation of D-sphingosine (for example, in the medium, on the cell surface, or the cytoplasm) if D-sphingosine can be phosphorylated by *S. aureus*.

To further identify determinants that may affect antimicrobial lipid resistance of *S. aureus*, the transcriptional response of *S. epidermidis* after D-sphingosine treatment was investigated and compared (Chapter 3). These data revealed there were more described resistance responses in *S. aureus* than *S. epidermidis*. Some of these determinants are not common to both species, and no obvious functionally analogous alternatives to these resistance mechanisms were reported in *S. epidermidis*.

Both *S. aureus* and *S. epidermidis* downregulated expression of global regulator SaeRS. Since the strain Newman contains a L18P substitution mutation ($SaeS^P$) in the first transmembrane helix, other *S. aureus* strains (SH1000, MRSA252 and SF8300) were examined by qPCR to inspect whether the differential expression of *saeRS* by D-sphingosine challenge is strain-dependent (Chapter 4). It was found that although *saeRS* was strongly down regulated 8-fold in Newman, while all the other tested *S. aureus* strains did not show differential expression. In contrast, *S. epidermidis* Tü3298 also downregulated *saeRS* despite the conclusion that differential expression of *saeRS* was strain dependent in *S. aureus*. As discussed in chapter 3, SaeRS mainly regulates expression of extracellular toxins and cellular adherence factors genes in *S. aureus* (Liang *et al*., 2006; Rogasch *et al.*, 2006); it regulates expression of biosynthesis genes, including pyruvate metabolism and amino acid synthesis and metabolism genes in *S. epidermidis* (Handke *et al.*, 2007). Whether SaeRS is a functional determinant for D-sphingosine resistance is unclear. For future studies, the *saeS* restored Newman HG strain (Mainiero *et al.*, 2010) can be assessed, including D-sphingosine survival tests and its transcriptional response.

In response to D-sphingosine, both *S. aureus* and *S. epidermidis* upregulated expression of the VraSR two component regulatory system. MIC assay using *vraR* and *vraS* allelic replacement mutant strains (SH1000 *vraR::tet* and SH1000 *vraS::tet*) supported the hypothesis that VraSR TCS contributes to D-sphingosine resistance in *S. aureus* (Chapter 4). To determine whether the contribution of VraSR is a common feature of staphylococcal responses, *vraR* and *vraS* mutants in *S. epidermidis* could be generated for further investigation. Gene mutation is less straightforward for *S. epidermidis*, but the equivalent transposon mutant library generated with *bursa aurealis* has been made similar to the Nebraska library for *S. aureus* and this would enable a facile approach to study gene contributions (Yajjala *et al.*, 2016). VraSR controls cell wall peptidoglycan biosynthesis, and its upregulation might indicate that the bacteria produce a thicker cell wall to protect from the antimicrobial lipid sphingosine, or the lipid might cause loss of cell wall material that must be replaced. Electron microscopy can be used to visualise and measure cell wall

thickness of wild type and allelic replacement strains with or without D-sphingosine treatment.

Aside from staphyloxanthin gene expression, no major transcriptional changes were observed with genes regulating membrane fluidity in the transcriptomic response to D-sphingosine challenge. There could still be changes in membrane fluidity, since several studies of Gram-positive bacteria have shown that alterations in membrane fluidity are not controlled at the transcriptional or translational level (Pesakhov et al., 2007; Fozo and Quivey, 2004; Schujman and de Mendoza, 2005). Membrane fluidity is commonly assessed using various fluorogenic membrane probes and fluorescence polarization (FP) measurements (Kaneko *et al.*, 2007; Fox and Delohery, 1987). Alterations in lipid phase transitions change the mobility of a membrane bound fluorophore, which can be excited by polarised light and measured (Kushnareva and Dell, 2009; Finegold, 1976). Samples can be taken at different growth phases (mid-exponential phase, late-exponential phase, early stationary phase and mid-stationary phase) for comparison. Decreases in membrane integrity and increases in membrane fluidity are expected in the sample taken at the early stage after exposure to D-sphingosine due to the ability of D-sphingosine to permeabilise the cell membrane. The membrane may become rigid to prevent penetration of D-sphingosine during later growth.

These analyses could be supported by lipidomic analyses. The lipidome is defined as the complete lipid profile within a cell, tissue, organism, or ecosystem. Study of the lipidome can provide insight investigation of pathways and networks of cellulr lipids in biological systems (Wenk, 2005; Watson, 2006). Lipidomics can help to examine the structures, functions, interactions, and dynamics of cellular lipids and the changes that occur during perturbation of the system (Han and Gross, 2003). Lipidomics research can identify and quantify the thousands of cellular lipid species and their interactions with other metabolites. This advance is based on recent advances in technologies such as mass spectrometry (MS), nuclear magnetic resonance (NMR) spectroscopy, fluorescence spectroscopy, dual polarisation interferometry and computational methods. The momentum is due to recognition of the role of lipids in many

metabolic diseases such as obesity, atherosclerosis, stroke, hypertension and diabetes (Han, 2007).

The staphyloxanthin biosynthesis genes in *S. aureus* were downregulated after 20 min of D-sphingosine treatment (Chapter 3), while production of staphyloxanthin was upregulated following 24 h incubation with the lipid (Chapter 4). To broaden the RNA-Seq data, which reports the immediate transcriptomic response, further RNA-Seq studies of later growth stages could be investigated. Further, determining the differential transcription when there is constant exposure to D-sphingosine would produce data on adaptation. Additionally, these data could be supported with a quantitative proteomics application in future research. The focus of this method is study of the proteome, which is dynamic and defined as the set of proteins expressed in a specific cell under a particular condition (Aebersold and Mann, 2003). To prepare samples for proteomics, *S. aureus* and *S. epidermidis* can be grown and challenged with D-sphingosine with the same conditions as the RNA-Seq experiments, harvesting samples at equivalent growth stages. Study of the proteome of staphylococci after D-sphingosine exposure, together with the transcriptome analysis, would help to establish a more comprehensive understanding about the bacterial response to this antimicrobial lipid.

Previous *in vitro* experimental evolution experiments with *S. aureus* with selection for growth with D-sphingosine above MIC conducted in the Horsburgh group detected multiple single nucleotide polymorphisms (SNPs) in an identified lipid efflux locus (Moran, 2015), later named *farRE* (Alnaseri *et al.*, 2015). Allelic variants with defined SNPs and inactivation mutations were generated to determine the contribution of this genetic locus. MIC and survival assays supported that the *farRE* contributes to D-sphingosine resistance in *S. aureus* (Chapter 5). Alnaseri *et al.* (2015) hypothesised that FarR functions as repressor of *farE* in the absence of inducer, but acts to promote expression of *farE* in the presence of exogenous fatty acids. Upregulation of *farRE* was not found in the RNA-seq data, indicating that D-sphingosine is not a natural substrate for FarR to activate expression of FarE. However, changes in structure and surface charge in SH1000 FarR.D94Y.E151K may contribute to recognition

of D-sphingosine as a substrate, thus activating the transcription factor for expression of FarE. The evolved FarR with D-sphingosine challenge reveals potential plasticity in the transporter system under selection. Curiously, both the *farR* and *farE* mutants had increased sensitivity to sphingosine as judged by their reduced MIC values. This could be explained if the lipid pools were examined to identify the transitional lipid that is formed during detoxification and presumed incorporation into lipid pools. Should the converted lipid not enter metabolism, then the intermediary lipid would need to be exported from the cell and it could be this form that is recognized by the FarE exporter. Further experiments, including lipidomics to identify the cellular/membrane associated lipids would add value to the study to resolve the fate of sphingosine intracellularly in *S. aureus*, which has not yet been determined.

During construction of the SNP allelic variant, the most time-consuming procedure was to screen and select for correct SNP-containing clones. Since the SH1000 FarR.D94Y.E151K variant has 10-fold increased MIC, compared with wild type SH1000, a high concentration of D-sphingosine (for example, 2-3 fold of the MIC of wild type) could be applied as preliminary selection for potentially SNP-bearing variants. The anticipation would be that this would not select for secondary mutations, however clones could be tested after identification by whole genome sequencing for confirmation of the single SNP variant only. When creating the FarR.D94Y.E151K variant, genomic DNA was extracted from single colonies and PCR screened for SNPs, with only one desired variant in 200-300 tested colonies. To save time, pools of genomes from 10-20 colonies could be made to serve as the PCR template for SNP screening. After a pool was identified as positive, single colonies in the pools can be further assessed using the screening method. If a more simple and faster method for SNP variants creation can be established, study of the contribution of single SNP to sphingosine resistance will become more effective. The position of the SNP in the cloned segment of DNA will also be important for outcross to ensure that the WT copy is lost together with the suicide plasmid by recombination. Further experiments to identify the most efficient positioning and length of insert would also facilitate this process.

Once the remaining *farR* SNP variants are regenerated, qPCR could be utilised to determine differential expression of *farE* in the SNP variant treated with D-sphingosine. Increased expression is expected if the variant FarR can recognize sphingosine as its substrate and induce expression of *farE*.

The collective contribution of lipids to antimicrobial activity is poorly understood. Both the epidermal and sebaceous lipids are combinations of several antimicrobial activities together with lipids of various forms and concentrations, some of which have no demonstrated antimicrobial activity. The individual roles of lipids can be studied in research, such as the study presented here, however the actions of the lipids can be studied in future with analysis of sebum. This is not entirely straightforward since sebum is likely to vary from one individual to another, as well the level of production on skin. However, future experimental evolution experiments could be conducted with sebum or with a combination of D-sphingosine and other skin antimicrobial lipid such as linoleic acid, oleic acid, and sapienic acid. MIC assays can be applied prior to evolution passaging. Combinatorial lipid studies will also help to show synergistic antimicrobial effects on bacteria, where lipid combinations may share similar modes of action; the combinations that increase bacteria resistance may indicate shared determinants for bacterial resistance to these antimicrobial lipids.

Over the process of this investigation, one concern that could limit the validity and impact of these data is: how do results gained *in vitro* differ from the *in vivo* scenario. For example, approximately 270 μM of sphingosine can be observed on healthy skin, whilst only 140-160 μM is present on atopic dermatitis skin that becomes typically heavily colonised by *S. aureus* (Arikawa *et al.*, 2002). However, 10-15 μM of D-sphingosine was found to kill *S. aureus* rapidly in *in vitro* experiments by Parsons *et al.* (2012). The D-sphingosine concentrations used in this study were 5 μM, even lower than their study and much below that reported on the human skin. The effects of other lipids may act to buffer some of the toxicity of individual lipids given the higher availabilities of cholesterol and

its esters, squalene and waxes. Moreover, the skin is a much more complex environment, with the stress of water supply, pH gradient, antimicrobial effects from a series of peptides from the host and other bacteria, as well as competition for resources.

To overcome the perceived and known divergence between *in vitro* and *in vivo* scenarios, animal models were established. A useful animal model system must be clinically relevant, experimentally robust, ethically acceptable, convenient to perform and provide both reliable and reproducible results (Kugelberg *et al*., 2005). Rodent Epidermal skin models were used for studies of *S. aureus* (Onunkwo *et al*., 2010). However, the results from studies using rodent skin models have shown a lack of consistency over extended periods of time, which complicates interpretation of data with respect to bacterial localisation and replication in the skin (Kanzaki *et al*., 1996; Abe *et al*., 1993; Kugelberg *et al*., 2005). Besides, human skin and rodent skin have considerable differences in both histology and immunology and the amount of sphingosine. Moreover, the majority of existing *S. aureus* animal skin models require severe mechanical disruption of the skin to compromise the initial barrier function which facilitates bacterial growth (Nippe *et al*., 2010; Cho *et al*., 2011; Inoshima *et al*., 2011).

Due to the need for a physiologically relevant model system to dissect the interactions of *S. aureus* with intact human skin, 3-D organotypic human skin tissue models were established to examine the processes of staphylococcal skin colonisation and infection (Ridky *et al*., 2010; Kretz *et al*., 2013). These models fall into two main categories: the *ex vivo* human skin explant cultures and regenerated 3-D organotypic models derived from primary cells and/or human cell lines.

The *ex vivo* human skin explants are typically acquired from neonatal foreskin, surgical or cadaveric tissues, which can be maintained in cell culture media or on supports in an air-liquid interface and remain viable in culture for up to two weeks (Popov *et al*., 2014). The advantage of skin explants is that they contain all components of the skin tissue, including all resident cell types of the

epidermis and dermis as well as skin appendages. However, there are also limitations originating from genetic variations between each individual, and the relatively restricted availability of human skin (Popov *et al*., 2014).

The 3-D human skin culture models are an informative and tractable experimental system for future investigations to dispel the above concern (Ridky *et al*., 2010; Groeber *et al*., 2011; Song *et al*., 2012; Kretz *et al*, 2013, Hogk *et al*., 2013). Organotropic 3-D skin models are generally comprises primary or immortalised human keratinocytes, grown at an air-liquid interface on a supporting matrix, which can be seeded with fibroblasts (Lebonvallet *et al.*, 2010, Gangatirkar *et al*., 2007; Stark *et al*., 2004). The matrix can be seeded with fibroblasts and other relevant cells including melanocytes, endothelial cells and nervous cells (Auxenfans *et al*., 2009). Moreover, the entire human skin proteins, cells and other components including the skin-derived antimicrobials can all be involved in the 3-D human organotropic model, to establish a very similar thickness and cellular architecture with the human epidermis (Popov *et al*., 2014).

With help of skin models and their further development to be more representative, future research studies will be able to provide a deeper understanding of the relationship between staphylococci and the epidermal lipid sphingosine, together with other skin lipids. Such studies will help to unravel the survival mechanisms and species differences between the different staphylococci that successfully colonise our largest organ.

Chapter 7: References

ABE, Y., AKIYAMA, H. & ARATA, J. 1993. Furuncle-like lesions in mouse experimental skin infections with *Staphylococcus aureus*. *J Dermatol,* 20**,** 198-202.

ADHIKARI, R. P. & NOVICK, R. P. 2008. Regulatory organization of the staphylococcal sae locus. *Microbiology,* 154**,** 949-59.

AEBERSOLD, R. & MANN, M. 2003. Mass spectrometry-based proteomics. *Nature,* 422**,** 198-207.

ALLAKER, R. P. & KAPAS, S. 2003. Adrenomedullin and mucosal defence: interaction between host and microorganism. *Regul Pept,* 112**,** 147-52.

ALLAKER, R. P., ZIHNI, C. & KAPAS, S. 1999. An investigation into the antimicrobial effects of adrenomedullin on members of the skin, oral, respiratory tract and gut microflora. *FEMS Immunol Med Microbiol,* 23**,** 289-93.

ALLGAIER, H., JUNG, G., WERNER, R. G., SCHNEIDER, U. & ZÄHNER, H. 1986. Epidermin: sequencing of a heterodet tetracyclic 21-peptide amide antibiotic. *European Journal of Biochemistry,* 160**,** 9-22.

ALLIGNET, J., AUBERT, S., DYKE, K. G. H. & EL SOLH, N. 2001. *Staphylococcus caprae* Strains Carry Determinants Known To Be Involved in Pathogenicity: a Gene Encoding an Autolysin-Binding Fibronectin and the ica Operon Involved in Biofilm Formation. *Infection and Immunity,* 69**,** 712-18.

ALNASERI, H., ARSIC, B., SCHNEIDER, J. E., KAISER, J. C., SCINOCCA, Z. C., HEINRICHS, D. E. & MCGAVIN, M. J. 2015. Inducible Expression of a Resistance-Nodulation-Division-Type Efflux Pump in *Staphylococcus aureus* Provides Resistance to Linoleic and Arachidonic Acids. *J Bacteriol,* 197**,** 1893-905.

AMES, G. F. 1986. Bacterial periplasmic transport systems: structure, mechanism, and evolution. *Annu Rev Biochem,* 55**,** 397-425.

ANDERSON, K. L., ROBERTS, C., DISZ, T., VONSTEIN, V., HWANG, K., OVERBEEK, R., OLSON, P. D., PROJAN, S. J. & DUNMAN, P. M. 2006. Characterization of the

Staphylococcus aureus heat shock, cold shock, stringent, and SOS responses and their effects on log-phase mRNA turnover. *J Bacteriol,* 188**,** 6739-56.

ARIKAWA, J., ISHIBASHI, M., KAWASHIMA, M., TAKAGI, Y., ICHIKAWA, Y. & IMOKAWA, G. 2002. Decreased levels of sphingosine, a natural antimicrobial agent, may be associated with vulnerability of the stratum corneum from patients with atopic dermatitis to colonization by *Staphylococcus aureus*. *J Invest Dermatol,* 119**,** 433-9.

ARRECUBIETA, C., LEE, M. H., MACEY, A., FOSTER, T. J. & LOWY, F. D. 2007. SdrF, a *Staphylococcus epidermidis* surface protein, binds type I collagen. *J Biol Chem,* 282**,** 18767-76.

ASWANI, V., TREMBLAY, D. M., MOINEAU, S. & SHUKLA, S. K. 2011. *Staphylococcus epidermidis* bacteriophages from the anterior nares of humans. *Appl Environ Microbiol,* 77**,** 7853-5.

AUXENFANS, C., FRADETTE, J., LEQUEUX, C., GERMAIN, L., KINIKOGLU, B., BECHETOILLE, N., BRAYE, F., AUGER, F. A. & DAMOUR, O. 2009. Evolution of three dimensional skin equivalent models reconstructed in vitro by tissue engineering. *Eur J Dermatol,* 19**,** 107-13.

BAE, T., GLASS, E. M., SCHNEEWIND, O. & MISSIAKAS, D. 2008. Generating a collection of insertion mutations in the *Staphylococcus aureus* genome using bursa aurealis. *Methods Mol Biol,* 416**,** 103-16.

BAE, T. & SCHNEEWIND, O. 2006. Allelic replacement in *Staphylococcus aureus* with inducible counter-selection. *Plasmid,* 55**,** 58-63.

BAYLES, K. W. 2007. The biological role of death and lysis in biofilm development. *Nat Rev Microbiol,* 5**,** 721-6.

BELCHEVA, A. & GOLEMI-KOTRA, D. 2008. A close-up view of the VraSR two-component system. A mediator of *Staphylococcus aureus* response to cell wall damage. *J Biol Chem,* 283**,** 12354-64.

BELCHEVA, A., VERMA, V. & GOLEMI-KOTRA, D. 2009. DNA-binding activity of the vancomycin resistance associated regulator protein VraR and the role of phosphorylation in transcriptional regulation of the vraSR operon. *Biochemistry,* 48**,** 5592-601.

BEN ZAKOUR, N. L., GUINANE, C. M. & FITZGERALD, J. R. 2008. Pathogenomics of the staphylococci: insights into niche adaptation and the emergence of new virulent strains. *FEMS Microbiol Lett,* 289**,** 1-12.

BERA, A., BISWAS, R., HERBERT, S. & GOTZ, F. 2006. The presence of peptidoglycan O-acetyltransferase in various staphylococcal species correlates with lysozyme resistance and pathogenicity. *Infect Immun,* 74**,** 4598-604.

BERGSSON, G., ARNFINNSSON, J., STEINGRIMSSON, O. & THORMAR, H. 2001. Killing of Gram-positive cocci by fatty acids and monoglycerides. *Apmis,* 109**,** 670-8.

BERNHEIMER, A. W., AVIGAD, L. S. & GRUSHOFF, P. 1968. Lytic effects of staphylococcal alpha-toxin and delta-hemolysin. *J Bacteriol,* 96**,** 487-91.

BESTEBROER, J., POPPELIER, M. J., ULFMAN, L. H., LENTING, P. J., DENIS, C. V., VAN KESSEL, K. P., VAN STRIJP, J. A. & DE HAAS, C. J. 2007. Staphylococcal superantigen-like 5 binds PSGL-1 and inhibits P-selectin-mediated neutrophil rolling. *Blood,* 109**,** 2936-43.

BIBEL, D. J., ALY, R., SHAH, S. & SHINEFIELD, H. R. 1993. Sphingosines: antimicrobial barriers of the skin. *Acta Derm Venereol,* 73**,** 407-11.

BIBEL, D. J., ALY, R. & SHINEFIELD, H. R. 1992a. Antimicrobial activity of sphingosines. *J Invest Dermatol,* 98**,** 269-73.

BIBEL, D. J., ALY, R. & SHINEFIELD, H. R. 1992b. Inhibition of microbial adherence by sphinganine. *Can J Microbiol,* 38**,** 983-5.

BIBEL, D. J., ALY, R. & SHINEFIELD, H. R. 1995. Topical sphingolipids in antisepsis and antifungal therapy. *Clin Exp Dermatol,* 20**,** 395-400.

BIEBER, T. 2008. Atopic dermatitis. *N Engl J Med,* 358**,** 1483-94.

BLACK, M. B., PARKS, B. B., PLUTA, L., CHU, T. M., ALLEN, B. C., WOLFINGER, R. D. & THOMAS, R. S. 2014. Comparison of microarrays and RNA-seq for gene expression analyses of dose-response experiments. *Toxicol Sci,* 137**,** 385-403.

BLAKE, K. L., O'NEILL, A. J., MENGIN-LECREULX, D., HENDERSON, P. J., BOSTOCK, J. M., DUNSMORE, C. J., SIMMONS, K. J., FISHWICK, C. W., LEEDS, J. A. & CHOPRA, I. 2009. The nature of *Staphylococcus aureus* MurA and MurZ and approaches for detection of peptidoglycan biosynthesis inhibitors. *Mol Microbiol,* 72**,** 335-43.

BLANPAIN, C. & FUCHS, E. 2009. Epidermal homeostasis: a balancing act of stem cells in the skin. *Nat Rev Mol Cell Biol,* 10**,** 207-17.

BOLLMANN, R. 1987. J. J. Bullen and E. Griffiths (Editors), Iron and Infection — Molecular, Physiological and Clinical Aspects. IX + 325 S., 70 Abb., 30 Tab. Chichester-New York-Brisbane-Toronto-Singapore 1987. John Wiley and Sons. *Journal of Basic Microbiology,* 27**,** 448.

BORE, E., LANGSRUD, S., LANGSRUD, O., RODE, T. M. & HOLCK, A. 2007. Acid-shock responses in *Staphylococcus aureus* investigated by global gene expression analysis. *Microbiology,* 153**,** 2289-303.

BOWDEN, M. G., VISAI, L., LONGSHAW, C. M., HOLLAND, K. T., SPEZIALE, P. & HOOK, M. 2002. Is the GehD lipase from *Staphylococcus epidermidis* a collagen binding adhesin? *J Biol Chem,* 277**,** 43017-23.

BOYLE-VAVRA, S., YIN, S., CHALLAPALLI, M. & DAUM, R. S. 2003. Transcriptional induction of the penicillin-binding protein 2 gene in *Staphylococcus aureus* by cell wall-active antibiotics oxacillin and vancomycin. *Antimicrob Agents Chemother,* 47**,** 1028-36.

BOYLE-VAVRA, S., YIN, S. & DAUM, R. S. 2006. The VraS/VraR two-component regulatory system required for oxacillin resistance in community-acquired methicillin-resistant *Staphylococcus aureus*. *FEMS Microbiol Lett,* 262**,** 163-71.

BRATT, C., DAWSON, D., DRAKE, D., BROGDEN, K. & WERTZ, P. 2010. Oral Mucosal Lipids: Antibacterial Activity and Induction of Ultrastructural Damage.

BREUER, K., S, H. A., KAPP, A. & WERFEL, T. 2002. *Staphylococcus aureus:* colonizing features and influence of an antibacterial treatment in adults with atopic dermatitis. *Br J Dermatol,* 147**,** 55-61.

BREUKINK, E., VAN KRAAIJ, C., DEMEL, R. A., SIEZEN, R. J., KUIPERS, O. P. & DE KRUIJFF, B. 1997. The C-terminal region of nisin is responsible for the initial interaction of nisin with the target membrane. *Biochemistry,* 36**,** 6968-76.

BROGDEN, N. K., MEHALICK, L., FISCHER, C. L., WERTZ, P. W. & BROGDEN, K. A. 2012. The emerging role of peptides and lipids as antimicrobial epidermal barriers and modulators of local inflammation. *Skin pharmacology and physiology,* 25**,** 167-181.

BROOKER, B. E. & FULLER, R. 1984. The adhesion of coagulase negative staphylococci to human skin and its relevance to the bacterial flora of milk. *J Appl Bacteriol,* 57**,** 325-32.

BROT, N. & WEISSBACH, H. 2000. Peptide methionine sulfoxide reductase: biochemistry and physiological role. *Biopolymers,* 55**,** 288-96.

BU, S., YAMANAKA, M., PEI, H., BIELAWSKA, A., BIELAWSKI, J., HANNUN, Y. A., OBEID, L. & TROJANOWSKA, M. 2006. Dihydrosphingosine 1-phosphate stimulates MMP1 gene expression via activation of ERK1/2-Ets1 pathway in human fibroblasts. *Faseb J,* 20**,** 184-6.

BURIAN, M., RAUTENBERG, M., KOHLER, T., FRITZ, M., KRISMER, B., UNGER, C., HOFFMANN, W. H., PESCHEL, A., WOLZ, C. & GOERKE, C. 2010a. Temporal expression of adhesion factors and activity of global regulators during establishment of *Staphylococcus aureus* nasal colonization. *J Infect Dis,* 201**,** 1414-21.

BURIAN, M., WOLZ, C. & GOERKE, C. 2010b. Regulatory adaptation of *Staphylococcus aureus* during nasal colonization of humans. *PLoS One,* 5**,** e10040.

BURKE, F. M., MCCORMACK, N., RINDI, S., SPEZIALE, P. & FOSTER, T. J. 2010. Fibronectin-binding protein B variation in *Staphylococcus aureus*. *BMC Microbiol,* 10**,** 160.

CAMPBELL, J., SINGH, A. K., SWOBODA, J. G., GILMORE, M. S., WILKINSON, B. J. & WALKER, S. 2012. An antibiotic that inhibits a late step in wall teichoic acid biosynthesis induces the cell wall stress stimulon in *Staphylococcus aureus. Antimicrob Agents Chemother,* 56**,** 1810-20.

CANDI, E., SCHMIDT, R. & MELINO, G. 2005. The cornified envelope: a model of cell death in the skin. *Nat Rev Mol Cell Biol,* 6**,** 328-40.

CARTRON, M. L., ENGLAND, S. R., CHIRIAC, A. I., JOSTEN, M., TURNER, R., RAUTER, Y., HURD, A., SAHL, H.-G., JONES, S. & FOSTER, S. J. 2014. Bactericidal Activity of the Human Skin Fatty Acid cis-6-Hexadecanoic Acid on *Staphylococcus aureus. Antimicrobial Agents and Chemotherapy,* 58**,** 3599-3609.

CHAMBERLAIN, N. R. & BRUEGGEMANN, S. A. 1997. Characterisation and expression of fatty acid modifying enzyme produced by *Staphylococcus epidermidis*. *J Med Microbiol,* 46**,** 693-7.

CHAMBERLAIN, N. R., MEHRTENS, B. G., XIONG, Z., KAPRAL, F. A., BOARDMAN, J. L. & REARICK, J. I. 1991. Correlation of carotenoid production, decreased membrane fluidity, and resistance to oleic acid killing in *Staphylococcus aureus* 18Z. *Infect Immun,* 59**,** 4332-7.

CHILLER, K., SELKIN, B. A. & MURAKAWA, G. J. 2001. Skin microflora and bacterial infections of the skin. *J Investig Dermatol Symp Proc,* 6**,** 170-4.

CHIPMAN, D. M. & SHARON, N. 1969. Mechanism of lysozyme action. *Science,* 165**,** 454-65.

CHO, J. S., XUAN, C. & MILLER, L. S. 2010. Lucky number seven: RNase 7 can prevent *Staphylococcus aureus* skin colonization. *J Invest Dermatol,* 130**,** 2703-6.

CHO, J. S., ZUSSMAN, J., DONEGAN, N. P., RAMOS, R. I., GARCIA, N. C., USLAN, D. Z., IWAKURA, Y., SIMON, S. I., CHEUNG, A. L., MODLIN, R. L., KIM, J. & MILLER, L. S. 2011. Noninvasive in vivo imaging to evaluate immune responses and antimicrobial therapy against *Staphylococcus aureus* and USA300 MRSA skin infections. *J Invest Dermatol,* 131**,** 907-15.

CHO, S. H., STRICKLAND, I., BOGUNIEWICZ, M. & LEUNG, D. Y. 2001. Fibronectin and fibrinogen contribute to the enhanced binding of *Staphylococcus aureus* to atopic skin. *J Allergy Clin Immunol,* 108**,** 269-74.

CHOKKATHUKALAM, A., KIM, D. H., BARRETT, M. P., BREITLING, R. & CREEK, D. J. 2014. Stable isotope-labeling studies in metabolomics: new insights into structure and dynamics of metabolic networks. *Bioanalysis,* 6**,** 511-24.

CHUNG, M. C., WINES, B. D., BAKER, H., LANGLEY, R. J., BAKER, E. N. & FRASER, J. D. 2007. The crystal structure of staphylococcal superantigen-like protein 11 in complex with sialyl Lewis X reveals the mechanism for cell binding and immune inhibition. *Mol Microbiol,* 66**,** 1342-55.

CLARKE, S. R., ANDRE, G., WALSH, E. J., DUFRENE, Y. F., FOSTER, T. J. & FOSTER, S. J. 2009. Iron-regulated surface determinant protein A mediates adhesion of *Staphylococcus aureus* to human corneocyte envelope proteins. *Infect Immun,* 77**,** 2408-16.

CLARKE, S. R., MOHAMED, R., BIAN, L., ROUTH, A. F., KOKAI-KUN, J. F., MOND, J. J., TARKOWSKI, A. & FOSTER, S. J. 2007. The *Staphylococcus aureus* surface protein IsdA mediates resistance to innate defenses of human skin. *Cell Host Microbe,* 1**,** 199-212.

CLARKE, S. R., WILTSHIRE, M. D. & FOSTER, S. J. 2004. IsdA of *Staphylococcus aureus* is a broad spectrum, iron-regulated adhesin. *Mol Microbiol,* 51**,** 1509-19.

CLAUDITZ, A., RESCH, A., WIELAND, K. P., PESCHEL, A. & GOTZ, F. 2006. Staphyloxanthin plays a role in the fitness of *Staphylococcus aureus* and its ability to cope with oxidative stress. *Infect Immun,* 74**,** 4950-3.

COATES, R., MORAN, J. & HORSBURGH, M. J. 2014. Staphylococci: colonizers and pathogens of human skin. *Future Microbiol,* 9**,** 75-91.

COGEN, A. L., NIZET, V. & GALLO, R. L. 2008. Skin microbiota: a source of disease or defence? *Br J Dermatol,* 158**,** 442-55.

COGEN, A. L., YAMASAKI, K., MUTO, J., SANCHEZ, K. M., CROTTY ALEXANDER, L., TANIOS, J., LAI, Y., KIM, J. E., NIZET, V. & GALLO, R. L. 2010a. *Staphylococcus epidermidis* antimicrobial delta-toxin (phenol-soluble modulin-gamma) cooperates with host antimicrobial peptides to kill group A Streptococcus. *PLoS One,* 5**,** e8557.

COGEN, A. L., YAMASAKI, K., SANCHEZ, K. M., DORSCHNER, R. A., LAI, Y., MACLEOD, D. T., TORPEY, J. W., OTTO, M., NIZET, V., KIM, J. E. & GALLO, R. L. 2010b. Selective antimicrobial action is provided by phenol-soluble modulins derived from *Staphylococcus epidermidis*, a normal resident of the skin. *J Invest Dermatol,* 130**,** 192-200.

CORRIGAN, R. M., MIAJLOVIC, H. & FOSTER, T. J. 2009. Surface proteins that promote adherence of *Staphylococcus aureus* to human desquamated nasal epithelial cells. *BMC Microbiology,* 9**,** 22-22.

CORRIGAN, R. M., RIGBY, D., HANDLEY, P. & FOSTER, T. J. 2007. The role of *Staphylococcus aureus* surface protein SasG in adherence and biofilm formation. *Microbiology,* 153**,** 2435-46.

COSTELLO, E. K., LAUBER, C. L., HAMADY, M., FIERER, N., GORDON, J. I. & KNIGHT, R. 2009. Bacterial community variation in human body habitats across space and time. *Science,* 326**,** 1694-7.

COTTER, P. D. & HILL, C. 2003. Surviving the Acid Test: Responses of Gram-Positive Bacteria to Low pH. *Microbiology and Molecular Biology Reviews,* 67**,** 429-453.

COX, G. B., ROSENBERG, H., DOWNIE, J. A. & SILVER, S. 1981. Genetic analysis of mutants affected in the Pst inorganic phosphate transport system. *J Bacteriol,* 148**,** 1-9.

CUVILLIER, O., PIRIANOV, G., KLEUSER, B., VANEK, P. G., COSO, O. A., GUTKIND, S. & SPIEGEL, S. 1996. Suppression of ceramide-mediated programmed cell death by sphingosine-1-phosphate. *Nature,* 381**,** 800-3.

DARGES, J. W., ROBINSON, S. P. & ADAMS, L. M. 1997. Inhibition of leukotriene B4 (LTB4) in human neutrophils by L-threo-dihydrosphingosine. *Adv Exp Med Biol,* 400a**,** 387-92.

DE GOFFAU, M. C., VAN DIJL, J. M. & HARMSEN, H. J. 2011. Microbial growth on the edge of desiccation. *Environ Microbiol,* 13**,** 2328-35.

DE GOFFAU, M. C., YANG, X., VAN DIJL, J. M. & HARMSEN, H. J. 2009. Bacterial pleomorphism and competition in a relative humidity gradient. *Environ Microbiol,* 11**,** 809-22.

DEISS, A. 1983. Iron metabolism in reticuloendothelial cells. *Semin Hematol,* 20**,** 81-90.

DERRE, I., RAPOPORT, G. & MSADEK, T. 1999. CtsR, a novel regulator of stress and heat shock response, controls clp and molecular chaperone gene expression in gram-positive bacteria. *Mol Microbiol,* 31**,** 117-31.

DESBOIS, A. P. & SMITH, V. J. 2010. Antibacterial free fatty acids: activities, mechanisms of action and biotechnological potential. *Appl Microbiol Biotechnol,* 85**,** 1629-42.

DICK, C. F., DOS-SANTOS, A., #233, ARA, L., #250, JO, MEYER-FERNANDES, J., #233 & ROBERTO 2011. Inorganic Phosphate as an Important Regulator of Phosphatases. *Enzyme Research,* 2011**,** 7.

DIEP, B. A., GILL, S. R., CHANG, R. F., PHAN, T. H., CHEN, J. H., DAVIDSON, M. G., LIN, F., LIN, J., CARLETON, H. A., MONGODIN, E. F., SENSABAUGH, G. F. & PERDREAU-REMINGTON, F. 2006. Complete genome sequence of USA300, an epidemic clone of community-acquired meticillin-resistant *Staphylococcus aureus*. *Lancet,* 367**,** 731-9.

DING, Y., ONODERA, Y., LEE, J. C. & HOOPER, D. C. 2008. NorB, an efflux pump in *Staphylococcus aureus* strain MW2, contributes to bacterial fitness in abscesses. *J Bacteriol,* 190**,** 7123-9.

DONG, H., NILSSON, L. & KURLAND, C. G. 1995. Gratuitous overexpression of genes in Escherichia coli leads to growth inhibition and ribosome destruction. *J Bacteriol,* 177**,** 1497-504.

DRAKE, D. R., BROGDEN, K. A., DAWSON, D. V. & WERTZ, P. W. 2008. Thematic review series: skin lipids. Antimicrobial lipids at the skin surface. *J Lipid Res,* 49**,** 4-11.

DURFEE, T., HANSEN, A. M., ZHI, H., BLATTNER, F. R. & JIN, D. J. 2008. Transcription profiling of the stringent response in Escherichia coli. *J Bacteriol,* 190**,** 1084-96.

DUTHIE, E. S. & LORENZ, L. L. 1952. Staphylococcal coagulase; mode of action and antigenicity. *J Gen Microbiol,* 6**,** 95-107.

ELEK, S. D. 1956. Experimental staphylococcal infections in the skin of man. *Ann N Y Acad Sci,* 65**,** 85-90.

ELIAS, P. M. 2007. The skin barrier as an innate immune element. *Semin Immunopathol,* 29**,** 3-14.

ELSHOLZ, A. K., MICHALIK, S., ZUHLKE, D., HECKER, M. & GERTH, U. 2010. CtsR, the Gram-positive master regulator of protein quality control, feels the heat. *Embo J,* 29**,** 3621-9.

ERICSON, M. E., SUBRAMANIAN, C., FRANK, M. W. & ROCK, C. O. 2017. Role of Fatty Acid Kinase in Cellular Lipid Homeostasis and SaeRS-Dependent Virulence Factor Expression in *Staphylococcus aureus*. *MBio,* 8.

ERNST, C. M. & PESCHEL, A. 2011. Broad-spectrum antimicrobial peptide resistance by MprF-mediated aminoacylation and flipping of phospholipids. *Mol Microbiol,* 80**,** 290-9.

EVERSE, J. & HSIA, N. 1997. The toxicities of native and modified hemoglobins. *Free Radic Biol Med,* 22**,** 1075-99.

FALORD, M., KARIMOVA, G., HIRON, A. & MSADEK, T. 2012. GraXSR proteins interact with the VraFG ABC transporter to form a five-component system

required for cationic antimicrobial peptide sensing and resistance in *Staphylococcus aureus*. *Antimicrob Agents Chemother,* 56**,** 1047-58.

FAN, T. W., LORKIEWICZ, P. K., SELLERS, K., MOSELEY, H. N., HIGASHI, R. M. & LANE, A. N. 2012. Stable isotope-resolved metabolomics and applications for drug development. *Pharmacol Ther,* 133**,** 366-91.

FAN, X., LIU, Y., SMITH, D., KONERMANN, L., SIU, K. W. & GOLEMI-KOTRA, D. 2007. Diversity of penicillin-binding proteins. Resistance factor FmtA of *Staphylococcus aureus*. *J Biol Chem,* 282**,** 35143-52.

FAURSCHOU, M. & BORREGAARD, N. 2003. Neutrophil granules and secretory vesicles in inflammation. *Microbes Infect,* 5**,** 1317-27.

FIERER, N., HAMADY, M., LAUBER, C. L. & KNIGHT, R. 2008. The influence of sex, handedness, and washing on the diversity of hand surface bacteria. *Proc Natl Acad Sci U S A,* 105**,** 17994-9.

FINEGOLD, L. 1976. Cell membrane fluidity: molecular modeling of particle aggregations seen in electron microscopy. *Biochim Biophys Acta,* 448**,** 393-8.

FISCHER, C. L., DRAKE, D. R., DAWSON, D. V., BLANCHETTE, D. R., BROGDEN, K. A. & WERTZ, P. W. 2012. Antibacterial Activity of Sphingoid Bases and Fatty Acids against Gram-Positive and Gram-Negative Bacteria. *Antimicrobial Agents and Chemotherapy,* 56**,** 1157-61.

FISCHER, C. L., WALTERS, K. S., DRAKE, D. R., BLANCHETTE, D. R., DAWSON, D. V., BROGDEN, K. A. & WERTZ, P. W. 2013. Sphingoid bases are taken up by Escherichia coli and *Staphylococcus aureus* and induce ultrastructural damage. *Skin Pharmacology and Physiology,* 26**,** 36-44.

FLOCK, J. I., FRöMAN, G., JöNSSON, K., GUSS, B., SIGNäS, C., NILSSON, B., RAUCCI, G., HööK, M., WADSTRöM, T. & LINDBERG, M. 1987. Cloning and expression of the gene for a fibronectin-binding protein from *Staphylococcus aureus*. *Embo J,* 6**,** 2351-7.

FLUHR, J. W., KAO, J., JAIN, M., AHN, S. K., FEINGOLD, K. R. & ELIAS, P. M. 2001. Generation of free fatty acids from phospholipids regulates stratum corneum acidification and integrity. *J Invest Dermatol,* 117**,** 44-51.

FOSTER, T. 1996. Staphylococcus. *In:* BARON, S. (ed.) *Medical Microbiology.* 4th ed. Galveston (TX).

FOSTER, T. J. 2009. Colonization and infection of the human host by staphylococci: adhesion, survival and immune evasion. *Vet Dermatol,* 20**,** 456-70.

FOSTER, T. J. & MCDEVITT, D. 1994. Surface-associated proteins of *Staphylococcus aureus*: their possible roles in virulence. *FEMS Microbiol Lett,* 118**,** 199-205.

FOX, M. H. & DELOHERY, T. M. 1987. Membrane fluidity measured by fluorescence polarization using an EPICS V cell sorter. *Cytometry,* 8**,** 20-5.

FOZO, E. M. & QUIVEY, R. G., JR. 2004. The fabM gene product of Streptococcus mutans is responsible for the synthesis of monounsaturated fatty acids and is necessary for survival at low pH. *J Bacteriol,* 186**,** 4152-8.

FRANK, D. N., FEAZEL, L. M., BESSESEN, M. T., PRICE, C. S., JANOFF, E. N. & PACE, N. R. 2010. The Human Nasal Microbiota and *Staphylococcus aureus* Carriage. *PLoS ONE,* 5**,** e10598.

FREDRICKS, D. N. 2001. Microbial ecology of human skin in health and disease. *J Investig Dermatol Symp Proc,* 6**,** 167-9.

FRIEDMAN, D. B., STAUFF, D. L., PISHCHANY, G., WHITWELL, C. W., TORRES, V. J. & SKAAR, E. P. 2006. *Staphylococcus aureus* redirects central metabolism to increase iron availability. *PLoS Pathog,* 2**,** e87.

GANGATIRKAR, P., PAQUET-FIFIELD, S., LI, A., ROSSI, R. & KAUR, P. 2007. Establishment of 3D organotypic cultures using human neonatal epidermal cells. *Nat Protoc,* 2**,** 178-86.

GAO, Z., TSENG, C. H., PEI, Z. & BLASER, M. J. 2007. Molecular analysis of human forearm superficial skin bacterial biota. *Proc Natl Acad Sci U S A,* 104**,** 2927-32.

GARDETE, S., WU, S. W., GILL, S. & TOMASZ, A. 2006. Role of VraSR in antibiotic resistance and antibiotic-induced stress response in *Staphylococcus aureus*. *Antimicrob Agents Chemother,* 50**,** 3424-34.

GARZONI, C. & KELLEY, W. L. 2009. *Staphylococcus aureus*: new evidence for intracellular persistence. *Trends Microbiol,* 17**,** 59-65.

GHILLEBERT, R., SWINNEN, E., DE SNIJDER, P., SMETS, B. & WINDERICKX, J. 2011. Differential roles for the low-affinity phosphate transporters Pho87 and Pho90 in Saccharomyces cerevisiae. *Biochem J,* 434**,** 243-51.

GIACHINO, P., ENGELMANN, S. & BISCHOFF, M. 2001. Sigma(B) activity depends on RsbU in *Staphylococcus aureus*. *J Bacteriol,* 183**,** 1843-52.

GIACOMONI, P. U., MAMMONE, T. & TERI, M. 2009. Gender-linked differences in human skin. *J Dermatol Sci,* 55**,** 144-9.

GIARDINE, B., RIEMER, C., HARDISON, R. C., BURHANS, R., ELNITSKI, L., SHAH, P., ZHANG, Y., BLANKENBERG, D., ALBERT, I., TAYLOR, J., MILLER, W., KENT, W. J. & NEKRUTENKO, A. 2005. Galaxy: a platform for interactive large-scale genome analysis. *Genome Res,* 15**,** 1451-5.

GIRAUDO, A. T., CALZOLARI, A., CATALDI, A. A., BOGNI, C. & NAGEL, R. 1999. The sae locus of *Staphylococcus aureus* encodes a two-component regulatory system. *FEMS Microbiol Lett,* 177**,** 15-22.

GIULIANI, A., PIRRI, G., BOZZI, A., DI GIULIO, A., ASCHI, M. & RINALDI, A. C. 2008. Antimicrobial peptides: natural templates for synthetic membrane-active compounds. *Cell Mol Life Sci,* 65**,** 2450-60.

GOECKS, J., NEKRUTENKO, A. & TAYLOR, J. 2010. Galaxy: a comprehensive approach for supporting accessible, reproducible, and transparent computational research in the life sciences. *Genome Biol,* 11**,** R86.

GREENWAY, D. L. & DYKE, K. G. 1979. Mechanism of the inhibitory action of linoleic acid on the growth of *Staphylococcus aureus*. *J Gen Microbiol,* 115**,** 233-45.

GRICE, E. A., KONG, H. H., CONLAN, S., DEMING, C. B., DAVIS, J., YOUNG, A. C., BOUFFARD, G. G., BLAKESLEY, R. W., MURRAY, P. R., GREEN, E. D., TURNER, M. L. & SEGRE, J. A. 2009. Topographical and temporal diversity of the human skin microbiome. *Science,* 324**,** 1190-2.

GRICE, E. A., KONG, H. H., CONLAN, S., DEMING, C. B., DAVIS, J., YOUNG, A. C., PROGRAM, N. C. S., BOUFFARD, G. G., BLAKESLEY, R. W., MURRAY, P. R., GREEN, E. D., TURNER, M. L. & SEGRE, J. A. 2009. Topographical and Temporal Diversity of the Human Skin Microbiome. *Science (New York, N.Y.),* 324**,** 1190-1192.

GRICE, E. A. & SEGRE, J. A. 2011. The skin microbiome. *Nat Rev Micro,* 9**,** 244-253.

GRKOVIC, S., BROWN, M. H., HARDIE, K. M., FIRTH, N. & SKURRAY, R. A. 2003. Stable low-copy-number *Staphylococcus aureus* shuttle vectors. *Microbiology,* 149**,** 785-94.

GROICHER, K. H., FIREK, B. A., FUJIMOTO, D. F. & BAYLES, K. W. 2000. The *Staphylococcus aureus* lrgAB operon modulates murein hydrolase activity and penicillin tolerance. *J Bacteriol,* 182**,** 1794-801.

GUEROUT-FLEURY, A. M., SHAZAND, K., FRANDSEN, N. & STRAGIER, P. 1995. Antibiotic-resistance cassettes for Bacillus subtilis. *Gene,* 167**,** 335-6.

GUO, H., HALL, J. W., YANG, J. & JI, Y. 2017. The SaeRS Two-Component System Controls Survival of *Staphylococcus aureus* in Human Blood through Regulation of Coagulase. *Front Cell Infect Microbiol,* 7**,** 204.

HACHEM, J. P., CRUMRINE, D., FLUHR, J., BROWN, B. E., FEINGOLD, K. R. & ELIAS, P. M. 2003. pH directly regulates epidermal permeability barrier homeostasis, and stratum corneum integrity/cohesion. *J Invest Dermatol,* 121**,** 345-53.

HAN, X. 2007. Neurolipidomics: challenges and developments. *Front Biosci,* 12**,** 2601-15.

HAN, X. & GROSS, R. W. 2003. Global analyses of cellular lipidomes directly from crude extracts of biological samples by ESI mass spectrometry: a bridge to lipidomics. *J Lipid Res,* 44**,** 1071-9.

HANDKE, L. D., ROGERS, K. L., OLSON, M. E., SOMERVILLE, G. A., JERRELLS, T. J., RUPP, M. E., DUNMAN, P. M. & FEY, P. D. 2008. *Staphylococcus epidermidis* saeR is an effector of anaerobic growth and a mediator of acute inflammation. *Infect Immun,* 76**,** 141-52.

HANSEN, U., HUSSAIN, M., VILLONE, D., HERRMANN, M., ROBENEK, H., PETERS, G., SINHA, B. & BRUCKNER, P. 2006. The anchorless adhesin Eap (extracellular adherence protein) from *Staphylococcus aureus* selectively recognizes extracellular matrix aggregates but binds promiscuously to monomeric matrix macromolecules. *Matrix Biol,* 25**,** 252-60.

HARA, J., HIGUCHI, K., OKAMOTO, R., KAWASHIMA, M. & IMOKAWA, G. 2000. High-expression of sphingomyelin deacylase is an important determinant of ceramide deficiency leading to barrier disruption in atopic dermatitis. *J Invest Dermatol,* 115**,** 406-13.

HARTFORD, O., O'BRIEN, L., SCHOFIELD, K., WELLS, J. & FOSTER, T. J. 2001. The Fbe (SdrG) protein of *Staphylococcus epidermidis* HB promotes bacterial adherence to fibrinogen. *Microbiology,* 147**,** 2545-52.

HATTAB, G., SUISSE, A. Y. T., ILIOAIA, O., CASIRAGHI, M., DEZI, M., WARNET, X. L., WARSCHAWSKI, D. E., MONCOQ, K., ZOONENS, M. & MIROUX, B. 2014. Membrane Protein Production in Escherichia coli: Overview and Protocols. *In:* MUS-VETEAU, I. (ed.) *Membrane Proteins Production for Structural Analysis.* New York, NY: Springer New York.

HEILMANN, C. 2011. Adhesion mechanisms of staphylococci. *Adv Exp Med Biol,* 715**,** 105-23.

HEILMANN, C., HARTLEIB, J., HUSSAIN, M. S. & PETERS, G. 2005. The multifunctional *Staphylococcus aureus* autolysin aaa mediates adherence to immobilized fibrinogen and fibronectin. *Infect Immun,* 73**,** 4793-802.

HEILMANN, C., THUMM, G., CHHATWAL, G. S., HARTLEIB, J., UEKOTTER, A. & PETERS, G. 2003. Identification and characterization of a novel autolysin (Aae)

with adhesive properties from *Staphylococcus epidermidis*. *Microbiology,* 149**,** 2769-78.

HELL, W., MEYER, H. G. & GATERMANN, S. G. 1998. Cloning of aas, a gene encoding a Staphylococcus saprophyticus surface protein with adhesive and autolytic properties. *Mol Microbiol,* 29**,** 871-81.

HELLER, M. J. 2002. DNA microarray technology: devices, systems, and applications. *Annu Rev Biomed Eng,* 4**,** 129-53.

HERBERT, S., BERA, A., NERZ, C., KRAUS, D., PESCHEL, A., GOERKE, C., MEEHL, M., CHEUNG, A. & GöTZ, F. 2007. Molecular Basis of Resistance to Muramidase and Cationic Antimicrobial Peptide Activity of Lysozyme in Staphylococci. *PLoS Pathogens,* 3**,** e102.

HERBERT, S., NEWELL, S. W., LEE, C., WIELAND, K.-P., DASSY, B., FOURNIER, J.-M., WOLZ, C. & DöRING, G. 2001. Regulation of *Staphylococcus aureus* Type 5 and Type 8 Capsular Polysaccharides by CO(2). *Journal of Bacteriology,* 183**,** 4609-4613.

HIGAKI, S., MOROHASHI, M., YAMAGISHI, T. & HASEGAWA, Y. 1999. Comparative study of staphylococci from the skin of atopic dermatitis patients and from healthy subjects. *Int J Dermatol,* 38**,** 265-9.

HIGGINS, D. L., CHANG, R., DEBABOV, D. V., LEUNG, J., WU, T., KRAUSE, K. M., SANDVIK, E., HUBBARD, J. M., KANIGA, K., SCHMIDT, D. E., JR., GAO, Q., CASS, R. T., KARR, D. E., BENTON, B. M. & HUMPHREY, P. P. 2005. Telavancin, a multifunctional lipoglycopeptide, disrupts both cell wall synthesis and cell membrane integrity in methicillin-resistant *Staphylococcus aureus*. *Antimicrob Agents Chemother,* 49**,** 1127-34.

HIRSCHHAUSEN, N., SCHLESIER, T., SCHMIDT, M. A., GOTZ, F., PETERS, G. & HEILMANN, C. 2010. A novel staphylococcal internalization mechanism involves the major autolysin Atl and heat shock cognate protein Hsc70 as host cell receptor. *Cell Microbiol,* 12**,** 1746-64.

HOGK, I., RUPP, S. & BURGER-KENTISCHER, A. 2013. 3D-tissue model for herpes simplex virus-1 infections. *Methods Mol Biol*, 1064, 239-51.

HORSBURGH, M. J., AISH, J. L., WHITE, I. J., SHAW, L., LITHGOW, J. K. & FOSTER, S. J. 2002. sigmaB modulates virulence determinant expression and stress resistance: characterization of a functional rsbU strain derived from *Staphylococcus aureus* 8325-4. *J Bacteriol,* 184**,** 5457-67.

HOWARD, B.J. & KLOOS, W.E. 1987. *Staphylococci.* Clinical and Pathogenic Microbiology. Mosby, Washington DC. 231-44.

HUANG, W. C., TSAI, T. H., CHUANG, L. T., LI, Y. Y., ZOUBOULIS, C. C. & TSAI, P. J. 2014. Anti-bacterial and anti-inflammatory properties of capric acid against Propionibacterium acnes: a comparative study with lauric acid. *J Dermatol Sci,* 73**,** 232-40.

HUESCA, M., PERALTA, R., SAUDER, D. N., SIMOR, A. E. & MCGAVIN, M. J. 2002. Adhesion and virulence properties of epidemic Canadian methicillin-resistant *Staphylococcus aureus* strain 1: identification of novel adhesion functions associated with plasmin-sensitive surface protein. *J Infect Dis,* 185**,** 1285-96.

HULETT, F. M. 1993. Regulation of Phosphorus Metabolism. *Bacillus subtilis and Other Gram-Positive Bacteria.* American Society of Microbiology.

HULETT, F. M. 1995. Complex Phosphate Regulation by Sequential Switches in Bacillus subtilis. *Two-Component Signal Transduction.* American Society of Microbiology.

HULETT, F. M. 1996. The signal-transduction network for Pho regulation in Bacillus subtilis. *Mol Microbiol,* 19**,** 933-9.

HUNTER, T. 1995. Protein kinases and phosphatases: the yin and yang of protein phosphorylation and signaling. *Cell,* 80**,** 225-36.

HUSSAIN, M., BECKER, K., VON EIFF, C., SCHRENZEL, J., PETERS, G. & HERRMANN, M. 2001. Identification and Characterization of a Novel 38.5-Kilodalton Cell Surface Protein of *Staphylococcus aureus* with Extended-

Spectrum Binding Activity for Extracellular Matrix and Plasma Proteins. *Journal of Bacteriology,* 183**,** 6778-6786.

IMOKAWA, G., ABE, A., JIN, K., HIGAKI, Y., KAWASHIMA, M. & HIDANO, A. 1991. Decreased level of ceramides in stratum corneum of atopic dermatitis: an etiologic factor in atopic dry skin? *J Invest Dermatol,* 96**,** 523-6.

INOSHIMA, I., INOSHIMA, N., WILKE, G. A., POWERS, M. E., FRANK, K. M., WANG, Y. & BUBECK WARDENBURG, J. 2011. A *Staphylococcus aureus* pore-forming toxin subverts the activity of ADAM10 to cause lethal infection in mice. *Nat Med,* 17**,** 1310-4.

ISHIKAWA, J., NARITA, H., KONDO, N., HOTTA, M., TAKAGI, Y., MASUKAWA, Y., KITAHARA, T., TAKEMA, Y., KOYANO, S., YAMAZAKI, S. & HATAMOCHI, A. 2010. Changes in the ceramide profile of atopic dermatitis patients. *J Invest Dermatol,* 130**,** 2511-4.

IWAI, I., HAN, H., DEN HOLLANDER, L., SVENSSON, S., OFVERSTEDT, L. G., ANWAR, J., BREWER, J., BLOKSGAARD, M., LALOEUF, A., NOSEK, D., MASICH, S., BAGATOLLI, L. A., SKOGLUND, U. & NORLEN, L. 2012. The human skin barrier is organized as stacked bilayers of fully extended ceramides with cholesterol molecules associated with the ceramide sphingoid moiety. *J Invest Dermatol,* 132**,** 2215-25.

IWASE, T., UEHARA, Y., SHINJI, H., TAJIMA, A., SEO, H., TAKADA, K., AGATA, T. & MIZUNOE, Y. 2010. *Staphylococcus epidermidis* Esp inhibits *Staphylococcus aureus* biofilm formation and nasal colonization. *Nature,* 465**,** 346-9.

JEONG, D. W., CHO, H., LEE, H., LI, C., GARZA, J., FRIED, M. & BAE, T. 2011. Identification of the P3 promoter and distinct roles of the two promoters of the SaeRS two-component system in *Staphylococcus aureus*. *J Bacteriol,* 193**,** 4672-84.

JEZEK, P., ENGSTOVA, H., ZACKOVA, M., VERCESI, A. E., COSTA, A. D., ARRUDA, P. & GARLID, K. D. 1998. Fatty acid cycling mechanism and mitochondrial uncoupling proteins. *Biochim Biophys Acta,* 1365**,** 319-27.

JIN, K., HIGAKI, Y., TAKAGI, Y., HIGUCHI, K., YADA, Y., KAWASHIMA, M. & IMOKAWA, G. 1994. Analysis of beta-glucocerebrosidase and ceramidase activities in atopic and aged dry skin. *Acta Derm Venereol,* 74**,** 337-40.

JONCA, N., LECLERC, E. A., CAUBET, C., SIMON, M., GUERRIN, M. & SERRE, G. 2011. Corneodesmosomes and corneodesmosin: from the stratum corneum cohesion to the pathophysiology of genodermatoses. *Eur J Dermatol,* 21 Suppl 2**,** 35-42.

JONSSON, K., SIGNAS, C., MULLER, H. P. & LINDBERG, M. 1991. Two different genes encode fibronectin binding proteins in *Staphylococcus aureus*. The complete nucleotide sequence and characterization of the second gene. *Eur J Biochem,* 202**,** 1041-8.

JUNGERSTED, J. M., HELLGREN, L. I., JEMEC, G. B. & AGNER, T. 2008. Lipids and skin barrier function--a clinical perspective. *Contact Dermatitis,* 58**,** 255-62.

KAHLON, A. K., ROY, S. & SHARMA, A. 2010. Molecular docking studies to map the binding site of squalene synthase inhibitors on dehydrosqualene synthase of *Staphylococcus aureus*. *J Biomol Struct Dyn,* 28**,** 201-10.

KANEHISA, M. 1997. A database for post-genome analysis. *Trends Genet,* 13**,** 375-6.

KANEHISA, M. & GOTO, S. 2000. KEGG: kyoto encyclopedia of genes and genomes. *Nucleic Acids Res,* 28**,** 27-30.

KANEHISA, M., GOTO, S., SATO, Y., KAWASHIMA, M., FURUMICHI, M. & TANABE, M. 2014. Data, information, knowledge and principle: back to metabolism in KEGG. *Nucleic Acids Research,* 42**,** D199-D205.

KANEKO, T., MATSUI, H., SHIMOKAWA, O., NAKAHARA, A. & HYODO, I. 2007. Cellular membrane fluidity measurement by fluorescence polarization in indomethacin-induced gastric cellular injury in vitro. *J Gastroenterol,* 42**,** 939-46.

KANZAKI, H., MORISHITA, Y., AKIYAMA, H. & ARATA, J. 1996. Adhesion of *Staphylococcus aureus* to horny layer: role of fibrinogen. *J Dermatol Sci,* 12**,** 132-9.

KAPRAL, F. A., SMITH, S. & LAL, D. 1992. The esterification of fatty acids by *Staphylococcus aureus* fatty acid modifying enzyme (FAME) and its inhibition by glycerides. *J Med Microbiol,* 37**,** 235-7.

KENNEDY, A. D., OTTO, M., BRAUGHTON, K. R., WHITNEY, A. R., CHEN, L., MATHEMA, B., MEDIAVILLA, J. R., BYRNE, K. A., PARKINS, L. D., TENOVER, F. C., KREISWIRTH, B. N., MUSSER, J. M. & DELEO, F. R. 2008. Epidemic community-associated methicillin-resistant *Staphylococcus aureus*: recent clonal expansion and diversification. *Proc Natl Acad Sci U S A,* 105**,** 1327-32.

KENNY, J. G., WARD, D., JOSEFSSON, E., JONSSON, I. M., HINDS, J., REES, H. H., LINDSAY, J. A., TARKOWSKI, A. & HORSBURGH, M. J. 2009. The *Staphylococcus aureus* response to unsaturated long chain free fatty acids: survival mechanisms and virulence implications. *PLoS One,* 4**,** e4344.

KIM, B. E., BIN, L., YE, Y. M., RAMAMOORTHY, P. & LEUNG, D. Y. M. 2013. IL-25 enhances HSV-1 replication by inhibiting filaggrin expression, and acts synergistically with Th2 cytokines to enhance HSV-1 replication. *J Invest Dermatol,* 133**,** 2678-2685.

KIM, S., HONG, I., HWANG, J. S., CHOI, J. K., RHO, H. S., KIM, D. H., CHANG, I., LEE, S. H., LEE, M. O. & HWANG, J. S. 2006. Phytosphingosine stimulates the differentiation of human keratinocytes and inhibits TPA-induced inflammatory epidermal hyperplasia in hairless mouse skin. *Mol Med,* 12**,** 17-24.

KING, N. P., BEATSON, S. A., TOTSIKA, M., ULETT, G. C., ALM, R. A., MANNING, P. A. & SCHEMBRI, M. A. 2011. UafB is a serine-rich repeat adhesin of Staphylococcus saprophyticus that mediates binding to fibronectin, fibrinogen and human uroepithelial cells. *Microbiology,* 157**,** 1161-75.

KING, N. P., SAKINC, T., BEN ZAKOUR, N. L., TOTSIKA, M., HERAS, B., SIMERSKA, P., SHEPHERD, M., GATERMANN, S. G., BEATSON, S. A. & SCHEMBRI, M. A. 2012.

Characterisation of a cell wall-anchored protein of *Staphylococcus saprophyticus* associated with linoleic acid resistance. *BMC Microbiol,* 12**,** 8.

KISHIDA, H., UNZAI, S., ROPER, D. I., LLOYD, A., PARK, S. Y. & TAME, J. R. 2006. Crystal structure of penicillin binding protein 4 (dacB) from Escherichia coli, both in the native form and covalently linked to various antibiotics. *Biochemistry,* 45**,** 783-92.

KLOOS, W. E. & MUSSELWHITE, M. S. 1975. Distribution and persistence of Staphylococcus and Micrococcus species and other aerobic bacteria on human skin. *Appl Microbiol,* 30**,** 381-5.

KLOOS, W. E. & SCHLEIFER, K. H. 1975. Isolation and Characterization of Staphylococci from Human Skin II. Descriptions of Four New Species: *Staphylococcus warneri, Staphylococcus capitis, Staphylococcus hominis*, and *Staphylococcus simulans1*. *International Journal of Systematic and Evolutionary Microbiology,* 25**,** 62-79.

KLUYTMANS, J. A. & WERTHEIM, H. F. 2005. Nasal carriage of *Staphylococcus aureus* and prevention of nosocomial infections. *Infection,* 33**,** 3-8.

KNOX, K. W. & WICKEN, A. J. 1973. Immunological properties of teichoic acids. *Bacteriological Reviews,* 37**,** 215-257.

KOCIANOVA, S., VUONG, C., YAO, Y., VOYICH, J. M., FISCHER, E. R., DELEO, F. R. & OTTO, M. 2005. Key role of poly-γ-dl-glutamic acid in immune evasion and virulence of *Staphylococcus epidermidis*. *Journal of Clinical Investigation,* 115**,** 688-94.

KOHLER, T., WEIDENMAIER, C. & PESCHEL, A. 2009. Wall Teichoic Acid Protects *Staphylococcus aureus* against Antimicrobial Fatty Acids from Human Skin. *Journal of Bacteriology,* 191**,** 4482-4.

KONG, H. H., OH, J., DEMING, C., CONLAN, S., GRICE, E. A., BEATSON, M. A., NOMICOS, E., POLLEY, E. C., KOMAROW, H. D., MURRAY, P. R., TURNER, M. L. & SEGRE, J. A. 2012. Temporal shifts in the skin microbiome associated with

disease flares and treatment in children with atopic dermatitis. *Genome Res,* 22**,** 850-9.

KOPRIVNJAK, T., MLAKAR, V., SWANSON, L., FOURNIER, B., PESCHEL, A. & WEISS, J. P. 2006. Cation-induced transcriptional regulation of the dlt operon of *Staphylococcus aureus*. *J Bacteriol,* 188**,** 3622-30.

KORNBERG, A., RAO, N. N. & AULT-RICHE, D. 1999. Inorganic polyphosphate: a molecule of many functions. *Annu Rev Biochem,* 68**,** 89-125.

KRAUS, D., HERBERT, S., KRISTIAN, S. A., KHOSRAVI, A., NIZET, V., GOTZ, F. & PESCHEL, A. 2008. The GraRS regulatory system controls *Staphylococcus aureus* susceptibility to antimicrobial host defenses. *BMC Microbiol,* 8**,** 85.

KRETZ, M., SIPRASHVILI, Z., CHU, C., WEBSTER, D. E., ZEHNDER, A., QU, K., LEE, C. S., FLOCKHART, R. J., GROFF, A. F., CHOW, J., JOHNSTON, D., KIM, G. E., SPITALE, R. C., FLYNN, R. A., ZHENG, G. X., AIYER, S., RAJ, A., RINN, J. L., CHANG, H. Y. & KHAVARI, P. A. 2013. Control of somatic tissue differentiation by the long non-coding RNA TINCR. *Nature,* 493**,** 231-5.

KUBICA, M., GUZIK, K., KOZIEL, J., ZAREBSKI, M., RICHTER, W., GAJKOWSKA, B., GOLDA, A., MACIAG-GUDOWSKA, A., BRIX, K., SHAW, L., FOSTER, T. & POTEMPA, J. 2008. A potential new pathway for *Staphylococcus aureus* dissemination: the silent survival of S. aureus phagocytosed by human monocyte-derived macrophages. *PLoS One,* 3**,** e1409.

KUGELBERG, E., NORSTROM, T., PETERSEN, T. K., DUVOLD, T., ANDERSSON, D. I. & HUGHES, D. 2005. Establishment of a superficial skin infection model in mice by using *Staphylococcus aureus* and Streptococcus pyogenes. *Antimicrob Agents Chemother,* 49**,** 3435-41.

KURODA, M., KURODA, H., OSHIMA, T., TAKEUCHI, F., MORI, H. & HIRAMATSU, K. 2003. Two-component system VraSR positively modulates the regulation of cell-wall biosynthesis pathway in *Staphylococcus aureus*. *Mol Microbiol,* 49**,** 807-21.

KURODA, M., OHTA, T., UCHIYAMA, I., BABA, T., YUZAWA, H., KOBAYASHI, I., CUI, L., OGUCHI, A., AOKI, K., NAGAI, Y., LIAN, J., ITO, T., KANAMORI, M., MATSUMARU,

H., MARUYAMA, A., MURAKAMI, H., HOSOYAMA, A., MIZUTANI-UI, Y., TAKAHASHI, N. K., SAWANO, T., INOUE, R., KAITO, C., SEKIMIZU, K., HIRAKAWA, H., KUHARA, S., GOTO, S., YABUZAKI, J., KANEHISA, M., YAMASHITA, A., OSHIMA, K., FURUYA, K., YOSHINO, C., SHIBA, T., HATTORI, M., OGASAWARA, N., HAYASHI, H. & HIRAMATSU, K. 2001. Whole genome sequencing of meticillin-resistant *Staphylococcus aureus*. *Lancet,* 357**,** 1225-40.

KURODA, M., TANAKA, Y., AOKI, R., SHU, D., TSUMOTO, K. & OHTA, T. 2008. *Staphylococcus aureus* giant protein Ebh is involved in tolerance to transient hyperosmotic pressure. *Biochem Biophys Res Commun,* 374**,** 237-41.

KUSHNAREVA, Y. D., E.J. 2009. Membrane fluidity measurements using UV fluorescence polarization. *In:* BMG LABTECH

LAARMAN, A. J., RUYKEN, M., MALONE, C. L., VAN STRIJP, J. A., HORSWILL, A. R. & ROOIJAKKERS, S. H. 2011. *Staphylococcus aureus* metalloprotease aureolysin cleaves complement C3 to mediate immune evasion. *J Immunol,* 186**,** 6445-53.

LAI, Y., COGEN, A. L., RADEK, K. A., PARK, H. J., MACLEOD, D. T., LEICHTLE, A., RYAN, A. F., DI NARDO, A. & GALLO, R. L. 2010. Activation of TLR2 by a small molecule produced by *Staphylococcus epidermidis* increases antimicrobial defense against bacterial skin infections. *J Invest Dermatol,* 130**,** 2211-21.

LAI, Y., DI NARDO, A., NAKATSUJI, T., LEICHTLE, A., YANG, Y., COGEN, A. L., WU, Z.-R., HOOPER, L. V., VON AULOCK, S., RADEK, K. A., HUANG, C.-M., RYAN, A. F. & GALLO, R. L. 2009. Commensal bacteria regulate TLR3-dependent inflammation following skin injury. *Nature medicine,* 15**,** 1377-1382.

LAI, Y., VILLARUZ, A. E., LI, M., CHA, D. J., STURDEVANT, D. E. & OTTO, M. 2007. The human anionic antimicrobial peptide dermcidin induces proteolytic defence mechanisms in staphylococci. *Mol Microbiol,* 63**,** 497-506.

LAMPE, M. A., BURLINGAME, A. L., WHITNEY, J., WILLIAMS, M. L., BROWN, B. E., ROITMAN, E. & ELIAS, P. M. 1983. Human stratum corneum lipids: characterization and regional variations. *J Lipid Res,* 24**,** 120-30.

LANGMEAD, B., TRAPNELL, C., POP, M. & SALZBERG, S. L. 2009. Ultrafast and memory-efficient alignment of short DNA sequences to the human genome. *Genome Biol,* 10**,** R25.

LAURSEN, N. S., GORDON, N., HERMANS, S., LORENZ, N., JACKSON, N., WINES, B., SPILLNER, E., CHRISTENSEN, J. B., JENSEN, M., FREDSLUND, F., BJERRE, M., SOTTRUP-JENSEN, L., FRASER, J. D. & ANDERSEN, G. R. 2010. Structural basis for inhibition of complement C5 by the SSL7 protein from *Staphylococcus aureus*. *Proc Natl Acad Sci U S A,* 107**,** 3681-6.

LEADBETTER, M. R., ADAMS, S. M., BAZZINI, B., FATHEREE, P. R., KARR, D. E., KRAUSE, K. M., LAM, B. M., LINSELL, M. S., NODWELL, M. B., PACE, J. L., QUAST, K., SHAW, J. P., SORIANO, E., TRAPP, S. G., VILLENA, J. D., WU, T. X., CHRISTENSEN, B. G. & JUDICE, J. K. 2004. Hydrophobic vancomycin derivatives with improved ADME properties: discovery of telavancin (TD-6424). *J Antibiot (Tokyo),* 57**,** 326-36.

LEBONVALLET, N., JEANMAIRE, C., DANOUX, L., SIBILLE, P., PAULY, G. & MISERY, L. 2010. The evolution and use of skin explants: potential and limitations for dermatological research. *Eur J Dermatol,* 20**,** 671-84.

LEEJAE, S., HASAP, L. & VORAVUTHIKUNCHAI, S. P. 2013. Inhibition of staphyloxanthin biosynthesis in *Staphylococcus aureus* by rhodomyrtone, a novel antibiotic candidate. *J Med Microbiol,* 62**,** 421-8.

LEHMAN, M. K., BOSE, J. L., SHARMA-KUINKEL, B. K., MOORMEIER, D. E., ENDRES, J. L., SADYKOV, M. R., BISWAS, I. & BAYLES, K. W. 2015. Identification of the amino acids essential for LytSR-mediated signal transduction in *Staphylococcus aureus* and their roles in biofilm-specific gene expression. *Mol Microbiol,* 95**,** 723-37.

LENNETTE, E.H., BALOWS, A., HAUSLER, W.J.J. & SHADOMY, H.J. (Eds) 1985. *Manual of Clinical Microbiology*, 4th ed. Washington, DC: American Society for Microbiology.

LEUNG, D. Y. 2013. New insights into atopic dermatitis: role of skin barrier and immune dysregulation. *Allergol Int,* 62**,** 151-61.

LEYDEN, J. J., MARPLES, R. R. & KLIGMAN, A. M. 1974. *Staphylococcus aureus* in the lesions of atopic dermatitis. *Br J Dermatol,* 90**,** 525-30.

LEYDEN, J. J., MCGINLEY, K. J., MILLS, O. H. & KLIGMAN, A. M. 1975. Age-related changes in the resident bacterial flora of the human face. *J Invest Dermatol,* 65**,** 379-81.

LI, M., CHA, D. J., LAI, Y., VILLARUZ, A. E., STURDEVANT, D. E. & OTTO, M. 2007. The antimicrobial peptide-sensing system aps of *Staphylococcus aureus*. *Mol Microbiol,* 66**,** 1136-47.

LI, M., LAI, Y., VILLARUZ, A. E., CHA, D. J., STURDEVANT, D. E. & OTTO, M. 2007. Gram-positive three-component antimicrobial peptide-sensing system. *Proceedings of the National Academy of Sciences of the United States of America,* 104**,** 9469-74.

LIANG, X., YU, C., SUN, J., LIU, H., LANDWEHR, C., HOLMES, D. & JI, Y. 2006. Inactivation of a two-component signal transduction system, SaeRS, eliminates adherence and attenuates virulence of *Staphylococcus aureus*. *Infect Immun,* 74**,** 4655-65.

LIBBERTON, B., COATES, R. E., BROCKHURST, M. A. & HORSBURGH, M. J. 2014. Evidence that intraspecific trait variation among nasal bacteria shapes the distribution of *Staphylococcus aureus*. *Infect Immun,* 82**,** 3811-5.

LIU, G. Y. & NIZET, V. 2009. Color me bad: microbial pigments as virulence factors. *Trends Microbiol,* 17**,** 406-13.

LIU, Q., YEO, W.-S. & BAE, T. 2016. The SaeRS Two-Component System of *Staphylococcus aureus*. *Genes,* 7**,** 81.

LIU, W. & HULETT, F. M. 1997. Bacillus subtilis PhoP binds to the phoB tandem promoter exclusively within the phosphate starvation-inducible promoter. *J Bacteriol,* 179**,** 6302-10.

LUAN, S. 2003. Protein phosphatases in plants. *Annu Rev Plant Biol,* 54**,** 63-92.

MACINTOSH, R. L., BRITTAN, J. L., BHATTACHARYA, R., JENKINSON, H. F., DERRICK, J., UPTON, M. & HANDLEY, P. S. 2009. The terminal A domain of the fibrillar accumulation-associated protein (Aap) of *Staphylococcus epidermidis* mediates adhesion to human corneocytes. *J Bacteriol,* 191**,** 7007-16.

MADISON, K. C. 2003. Barrier function of the skin: "la raison d'etre" of the epidermis. *J Invest Dermatol,* 121**,** 231-41.

MAINIERO, M., GOERKE, C., GEIGER, T., GONSER, C., HERBERT, S. & WOLZ, C. 2010. Differential target gene activation by the *Staphylococcus aureus* two-component system saeRS. *J Bacteriol,* 192**,** 613-23.

MANTIONE, K. J., KREAM, R. M., KUZELOVA, H., PTACEK, R., RABOCH, J., SAMUEL, J. M. & STEFANO, G. B. 2014. Comparing bioinformatic gene expression profiling methods: microarray and RNA-Seq. *Med Sci Monit Basic Res,* 20**,** 138-42.

MARPLES, R. R. 1982. Sex, constancy, and skin bacteria. *Arch Dermatol Res,* 272**,** 317-20.

MARRAFFINI, L. A. & SONTHEIMER, E. J. 2008. CRISPR interference limits horizontal gene transfer in staphylococci by targeting DNA. *Science,* 322**,** 1843-5.

MASCHER, T., HELMANN, J. D. & UNDEN, G. 2006. Stimulus perception in bacterial signal-transducing histidine kinases. *Microbiol Mol Biol Rev,* 70**,** 910-38.

MATOUSEK, J. L. & CAMPBELL, K. L. 2002. A comparative review of cutaneous pH. *Vet Dermatol,* 13**,** 293-300.

MATSUO, M., OOGAI, Y., KATO, F., SUGAI, M. & KOMATSUZAWA, H. 2011. Growth-phase dependence of susceptibility to antimicrobial peptides in *Staphylococcus aureus*. *Microbiology,* 157**,** 1786-97.

MAZMANIAN, S. K., SKAAR, E. P., GASPAR, A. H., HUMAYUN, M., GORNICKI, P., JELENSKA, J., JOACHMIAK, A., MISSIAKAS, D. M. & SCHNEEWIND, O. 2003. Passage of heme-iron across the envelope of *Staphylococcus aureus*. *Science,* 299**,** 906-9.

MCALEESE, F., WU, S. W., SIERADZKI, K., DUNMAN, P., MURPHY, E., PROJAN, S. & TOMASZ, A. 2006. Overexpression of genes of the cell wall stimulon in clinical isolates of *Staphylococcus aureus* exhibiting vancomycin-intermediate- S. aureus-type resistance to vancomycin. *J Bacteriol,* 188**,** 1120-33.

MCCALLUM, N., MEIER, P. S., HEUSSER, R. & BERGER-BACHI, B. 2011. Mutational analyses of open reading frames within the vraSR operon and their roles in the cell wall stress response of *Staphylococcus aureus*. *Antimicrob Agents Chemother,* 55**,** 1391-402.

MCCALLUM, N., SPEHAR, G., BISCHOFF, M. & BERGER-BACHI, B. 2006. Strain dependence of the cell wall-damage induced stimulon in *Staphylococcus aureus*. *Biochim Biophys Acta,* 1760**,** 1475-81.

MCDEVITT, D., FRANCOIS, P., VAUDAUX, P. & FOSTER, T. J. 1994. Molecular characterization of the clumping factor (fibrinogen receptor) of *Staphylococcus aureus*. *Mol Microbiol,* 11**,** 237-48.

MCEWAN, N. A., MELLOR, D. & KALNA, G. 2006. Adherence by Staphylococcus intermedius to canine corneocytes: a preliminary study comparing noninflamed and inflamed atopic canine skin. *Vet Dermatol,* 17**,** 151-4.

MCGETTIGAN, P. A. 2013. Transcriptomics in the RNA-seq era. *Curr Opin Chem Biol,* 17**,** 4-11.

MCKENNEY, D., HüBNER, J., MULLER, E., WANG, Y., GOLDMANN, D. A. & PIER, G. B. 1998. The ica Locus of *Staphylococcus epidermidis* Encodes Production of the Capsular Polysaccharide/Adhesin. *Infection and Immunity,* 66**,** 4711-4720.

MEEHL, M., HERBERT, S., GöTZ, F. & CHEUNG, A. 2007. Interaction of the GraRS Two-Component System with the VraFG ABC Transporter To Support Vancomycin-Intermediate Resistance in *Staphylococcus aureus*. *Antimicrobial Agents and Chemotherapy,* 51**,** 2679-89.

MEIER, S., GOERKE, C., WOLZ, C., SEIDL, K., HOMEROVA, D., SCHULTHESS, B., KORMANEC, J., BERGER-BäCHI, B. & BISCHOFF, M. 2007. σ(B) and the σ(B)-

Dependent arlRS and yabJ-spoVG Loci Affect Capsule Formation in *Staphylococcus aureus*. *Infection and Immunity,* 75**,** 4562-71.

MELNIK, B. 2006. [Disturbances of antimicrobial lipids in atopic dermatitis]. *J Dtsch Dermatol Ges,* 4**,** 114-23.

MEMPEL, M., SCHMIDT, T., WEIDINGER, S., SCHNOPP, C., FOSTER, T., RING, J. & ABECK, D. 1998. Role of *Staphylococcus aureus* surface-associated proteins in the attachment to cultured HaCaT keratinocytes in a new adhesion assay. *J Invest Dermatol,* 111**,** 452-6.

MISHRA, N. N., LIU, G. Y., YEAMAN, M. R., NAST, C. C., PROCTOR, R. A., MCKINNELL, J. & BAYER, A. S. 2011. Carotenoid-related alteration of cell membrane fluidity impacts *Staphylococcus aureus* susceptibility to host defense peptides. *Antimicrob Agents Chemother,* 55**,** 526-31.

MOSKOVITZ, J., RAHMAN, M. A., STRASSMAN, J., YANCEY, S. O., KUSHNER, S. R., BROT, N. & WEISSBACH, H. 1995. Escherichia coli peptide methionine sulfoxide reductase gene: regulation of expression and role in protecting against oxidative damage. *J Bacteriol,* 177**,** 502-7.

MOSS, B., SQUIRE, J. R. & ET AL. 1948. Nose and skin carriage of *Staphylococcus aureus* in patients receiving penicillin. *Lancet,* 1**,** 320-5.

MULCAHY, M. E., GEOGHEGAN, J. A., MONK, I. R., O'KEEFFE, K. M., WALSH, E. J., FOSTER, T. J. & MCLOUGHLIN, R. M. 2012. Nasal colonisation by *Staphylococcus aureus* depends upon clumping factor B binding to the squamous epithelial cell envelope protein loricrin. *PLoS Pathog,* 8**,** e1003092.

MURATA, Y., OGATA, J., HIGAKI, Y., KAWASHIMA, M., YADA, Y., HIGUCHI, K., TSUCHIYA, T., KAWAINAMI, S. & IMOKAWA, G. 1996. Abnormal expression of sphingomyelin acylase in atopic dermatitis: an etiologic factor for ceramide deficiency? *J Invest Dermatol,* 106**,** 1242-9.

MUTHAIYAN, A., SILVERMAN, J. A., JAYASWAL, R. K. & WILKINSON, B. J. 2008. Transcriptional Profiling Reveals that Daptomycin Induces the *Staphylococcus*

aureus Cell Wall Stress Stimulon and Genes Responsive to Membrane Depolarization. *Antimicrobial Agents and Chemotherapy,* 52**,** 980-990.

NAGAMACHI, E., HIRAI, Y., TOMOCHIKA, K. & KANEMASA, Y. 1992. Studies on osmotic stability of liposomes prepared with bacterial membrane lipids by carboxyfluorescein release. *Microbiol Immunol,* 36**,** 231-4.

NAGARAJAN, V. & ELASRI, M. O. 2007. SAMMD: *Staphylococcus aureus* Microarray Meta-Database. *BMC Genomics,* 8**,** 351-351.

NAGASE, N., SASAKI, A., YAMASHITA, K., SHIMIZU, A., WAKITA, Y., KITAI, S. & KAWANO, J. 2002. Isolation and species distribution of staphylococci from animal and human skin. *J Vet Med Sci,* 64**,** 245-50.

NAIR, D., MEMMI, G., HERNANDEZ, D., BARD, J., BEAUME, M., GILL, S., FRANCOIS, P. & CHEUNG, A. L. 2011. Whole-genome sequencing of *Staphylococcus aureus* strain RN4220, a key laboratory strain used in virulence research, identifies mutations that affect not only virulence factors but also the fitness of the strain. *J Bacteriol,* 193**,** 2332-5.

NEU, H. C., DREYFUS, J., 3RD & CANFIELD, R. E. 1968. Effect of human lysozyme on gram-positive and gram-negative bacteria. *Antimicrob Agents Chemother (Bethesda),* 8**,** 442-4.

NI EIDHIN, D., PERKINS, S., FRANCOIS, P., VAUDAUX, P., HOOK, M. & FOSTER, T. J. 1998. Clumping factor B (ClfB), a new surface-located fibrinogen-binding adhesin of *Staphylococcus aureus*. *Mol Microbiol,* 30**,** 245-57.

NILSSON, M., BJERKETORP, J., GUSS, B. & FRYKBERG, L. 2004. A fibrinogen-binding protein of Staphylococcus lugdunensis. *FEMS Microbiol Lett,* 241**,** 87-93.

NILSSON, M., FRYKBERG, L., FLOCK, J. I., PEI, L., LINDBERG, M. & GUSS, B. 1998. A fibrinogen-binding protein of *Staphylococcus epidermidis*. *Infect Immun,* 66**,** 2666-73.

NIPPE, N., VARGA, G., HOLZINGER, D., LOFFLER, B., MEDINA, E., BECKER, K., ROTH, J., EHRCHEN, J. M. & SUNDERKOTTER, C. 2011. Subcutaneous infection

with S. aureus in mice reveals association of resistance with influx of neutrophils and Th2 response. *J Invest Dermatol,* 131**,** 125-32.

NOBLE, W. C., VALKENBURG, H. A. & WOLTERS, C. H. 1967. Carriage of *Staphylococcus aureus* in random samples of a normal population. *The Journal of Hygiene,* 65**,** 567-573.

NOVICK, R. P. & JIANG, D. 2003. The staphylococcal saeRS system coordinates environmental signals with agr quorum sensing. *Microbiology,* 149**,** 2709-17.

NYGAARD, T. K., PALLISTER, K. B., RUZEVICH, P., GRIFFITH, S., VUONG, C. & VOYICH, J. M. 2010. SaeR Binds a Consensus Sequence within Virulence Gene Promoters to Advance USA300 Pathogenesis. *The Journal of Infectious Diseases,* 201**,** 241-254.

O'BRIEN, L. M., WALSH, E. J., MASSEY, R. C., PEACOCK, S. J. & FOSTER, T. J. 2002. *Staphylococcus aureus* clumping factor B (ClfB) promotes adherence to human type I cytokeratin 10: implications for nasal colonization. *Cell Microbiol,* 4**,** 759-70.

OHNIWA, R. L., KITABAYASHI, K. & MORIKAWA, K. 2013. Alternative cardiolipin synthase Cls1 compensates for stalled Cls2 function in *Staphylococcus aureus* under conditions of acute acid stress. *FEMS Microbiol Lett,* 338**,** 141-6.

OLIVERA, A. & SPIEGEL, S. 1993. Sphingosine-1-phosphate as second messenger in cell proliferation induced by PDGF and FCS mitogens. *Nature,* 365**,** 557-60.

OLSON, M. E., NYGAARD, T. K., ACKERMANN, L., WATKINS, R. L., ZUREK, O. W., PALLISTER, K. B., GRIFFITH, S., KIEDROWSKI, M. R., FLACK, C. E., KAVANAUGH, J. S., KREISWIRTH, B. N., HORSWILL, A. R. & VOYICH, J. M. 2013. *Staphylococcus aureus* nuclease is an SaeRS-dependent virulence factor. *Infect Immun,* 81**,** 1316-24.

O'NEILL, A. J., LINDSAY, J. A., GOULD, K., HINDS, J. & CHOPRA, I. 2009. Transcriptional Signature following Inhibition of Early-Stage Cell Wall Biosynthesis in *Staphylococcus aureus*. *Antimicrobial Agents and Chemotherapy,* 53**,** 1701-4.

ONUNKWO, C. C., HAHN, B. L. & SOHNLE, P. G. 2010. Clearance of experimental cutaneous *Staphylococcus aureus* infections in mice. *Arch Dermatol Res,* 302**,** 375-82.

O'RIORDAN, K. & LEE, J. C. 2004. *Staphylococcus aureus* Capsular Polysaccharides. *Clinical Microbiology Reviews,* 17**,** 218-234.

OTTO, M. 2010. Staphylococcus colonization of the skin and antimicrobial peptides. *Expert Review of Dermatology,* 5**,** 183-195.

PARK, B., IWASE, T. & LIU, G. Y. 2011. Intranasal application of S. epidermidis prevents colonization by methicillin-resistant *Staphylococcus aureus* in mice. *PLoS One,* 6**,** e25880.

PARSONS, J. B., YAO, J., FRANK, M. W., JACKSON, P. & ROCK, C. O. 2012. Membrane Disruption by Antimicrobial Fatty Acids Releases Low-Molecular-Weight Proteins from *Staphylococcus aureus*. *Journal of Bacteriology,* 194**,** 5294-304.

PATEL, K. & GOLEMI-KOTRA, D. 2015. Signaling mechanism by the *Staphylococcus aureus* two-component system LytSR: role of acetyl phosphate in bypassing the cell membrane electrical potential sensor LytS. *F1000Res,* 4**,** 79.

PATTON, T. G., YANG, S. J. & BAYLES, K. W. 2006. The role of proton motive force in expression of the *Staphylococcus aureus* cid and lrg operons. *Mol Microbiol,* 59**,** 1395-404.

PAULMANN, M., ARNOLD, T., LINKE, D., OZDIREKCAN, S., KOPP, A., GUTSMANN, T., KALBACHER, H., WANKE, I., SCHUENEMANN, V. J., HABECK, M., BURCK, J., ULRICH, A. S. & SCHITTEK, B. 2012. Structure-activity analysis of the dermcidin-derived peptide DCD-1L, an anionic antimicrobial peptide present in human sweat. *J Biol Chem,* 287**,** 8434-43.

PAVICIC, T., WOLLENWEBER, U., FARWICK, M. & KORTING, H. C. 2007. Anti-microbial and -inflammatory activity and efficacy of phytosphingosine: an in vitro and in vivo study addressing acne vulgaris. *Int J Cosmet Sci,* 29**,** 181-90.

PECHOUS, R., LEDALA, N., WILKINSON, B. J. & JAYASWAL, R. K. 2004. Regulation of the Expression of Cell Wall Stress Stimulon Member Gene msrA1 in Methicillin-Susceptible or -Resistant *Staphylococcus aureus*. *Antimicrobial Agents and Chemotherapy,* 48**,** 3057-63.

PELZ, A., WIELAND, K. P., PUTZBACH, K., HENTSCHEL, P., ALBERT, K. & GOTZ, F. 2005. Structure and biosynthesis of staphyloxanthin from *Staphylococcus aureus*. *J Biol Chem,* 280**,** 32493-8.

PERCY, M. G. & GRUNDLING, A. 2014. Lipoteichoic acid synthesis and function in gram-positive bacteria. *Annu Rev Microbiol,* 68**,** 81-100.

PERIASAMY, S., CHATTERJEE, S. S., CHEUNG, G. Y. C. & OTTO, M. 2012. Phenol-soluble modulins in staphylococci: What are they originally for? *Communicative & Integrative Biology,* 5**,** 275-7.

PESAKHOV, S., BENISTY, R., SIKRON, N., COHEN, Z., GOMELSKY, P., KHOZIN-GOLDBERG, I., DAGAN, R. & PORAT, N. 2007. Effect of hydrogen peroxide production and the Fenton reaction on membrane composition of Streptococcus pneumoniae. *Biochim Biophys Acta,* 1768**,** 590-7.

PESCHEL, A., JACK, R. W., OTTO, M., COLLINS, L. V., STAUBITZ, P., NICHOLSON, G., KALBACHER, H., NIEUWENHUIZEN, W. F., JUNG, G., TARKOWSKI, A., VAN KESSEL, K. P. M. & VAN STRIJP, J. A. G. 2001. *Staphylococcus aureus* Resistance to Human Defensins and Evasion of Neutrophil Killing via the Novel Virulence Factor Mprf Is Based on Modification of Membrane Lipids with l-Lysine. *The Journal of Experimental Medicine,* 193**,** 1067-76.

PESCHEL, A., OTTO, M., JACK, R. W., KALBACHER, H., JUNG, G. & GOTZ, F. 1999. Inactivation of the dlt operon in *Staphylococcus aureus* confers sensitivity to defensins, protegrins, and other antimicrobial peptides. *J Biol Chem,* 274**,** 8405-10.

PIETIAINEN, M., FRANCOIS, P., HYYRYLAINEN, H. L., TANGOMO, M., SASS, V., SAHL, H. G., SCHRENZEL, J. & KONTINEN, V. P. 2009. Transcriptome analysis of the responses of *Staphylococcus aureus* to antimicrobial peptides and

characterization of the roles of vraDE and vraSR in antimicrobial resistance. *BMC Genomics,* 10**,** 429.

PINHO, M. G., DE LENCASTRE, H. & TOMASZ, A. 2001. An acquired and a native penicillin-binding protein cooperate in building the cell wall of drug-resistant staphylococci. *Proc Natl Acad Sci U S A,* 98**,** 10886-91.

POPOV, L., KOVALSKI, J., GRANDI, G., BAGNOLI, F. & AMIEVA, M. R. 2014. Three-Dimensional Human Skin Models to Understand *Staphylococcus aureus* Skin Colonization and Infection. *Front Immunol,* 5**,** 41.

POTTS, M. 1994. Desiccation tolerance of prokaryotes. *Microbiol Rev,* 58**,** 755-805.

PROFROCK, D. & PRANGE, A. 2012. Inductively coupled plasma-mass spectrometry (ICP-MS) for quantitative analysis in environmental and life sciences: a review of challenges, solutions, and trends. *Appl Spectrosc,* 66**,** 843-68.

PROJAN, S.J. & NOVICK, R.P. 1997. *The molecular basis of pathogenicity*. Churchill Livingston, London. 55-81

PROKSCH, E., BRANDNER, J. M. & JENSEN, J. M. 2008. The skin: an indispensable barrier. *Exp Dermatol,* 17**,** 1063-72.

PRUETT, S. T., BUSHNEV, A., HAGEDORN, K., ADIGA, M., HAYNES, C. A., SULLARDS, M. C., LIOTTA, D. C. & MERRILL, A. H. 2008. Thematic Review Series: Sphingolipids. Biodiversity of sphingoid bases ("sphingosines") and related amino alcohols. *Journal of Lipid Research,* 49**,** 1621-39.

QI, Y., KOBAYASHI, Y. & HULETT, F. M. 1997. The pst operon of Bacillus subtilis has a phosphate-regulated promoter and is involved in phosphate transport but not in regulation of the pho regulon. *J Bacteriol,* 179**,** 2534-9.

RAISIG, A. & SANDMANN, G. 1999. 4,4'-diapophytoene desaturase: catalytic properties of an enzyme from the C(30) carotenoid pathway of *Staphylococcus aureus*. *J Bacteriol,* 181**,** 6184-7.

RAMIA, N. F., TANG, L., COCOZAKI, A. I. & LI, H. 2014. *Staphylococcus epidermidis* Csm1 is a 3′–5′ exonuclease. *Nucleic Acids Research,* 42**,** 1129-1138.

RAMOS, J. L., MARTINEZ-BUENO, M., MOLINA-HENARES, A. J., TERAN, W., WATANABE, K., ZHANG, X., GALLEGOS, M. T., BRENNAN, R. & TOBES, R. 2005. The TetR family of transcriptional repressors. *Microbiol Mol Biol Rev,* 69**,** 326-56.

RAMSLAND, P. A., WILLOUGHBY, N., TRIST, H. M., FARRUGIA, W., HOGARTH, P. M., FRASER, J. D. & WINES, B. D. 2007. Structural basis for evasion of IgA immunity by *Staphylococcus aureus* revealed in the complex of SSL7 with Fc of human IgA1. *Proceedings of the National Academy of Sciences of the United States of America,* 104**,** 15051-6.

RAMUNDO, M. S., BELTRAME, C. O., BOTELHO, A. M., COELHO, L. R., SILVA-CARVALHO, M. C., FERREIRA-CARVALHO, B. T., NICOLAS, M. F., GUEDES, I. A., DARDENNE, L. E., O'GARA, J. & FIGUEIREDO, A. M. 2016. A unique SaeS allele overrides cell-density dependent expression of saeR and lukSF-PV in the ST30-SCCmecIV lineage of CA-MRSA. *Int J Med Microbiol,* 306**,** 367-80.

RAO, N. N. & TORRIANI, A. 1990. Molecular aspects of phosphate transport in Escherichia coli. *Mol Microbiol,* 4**,** 1083-90.

RENNIE, M. J. 1999. An introduction to the use of tracers in nutrition and metabolism. *Proc Nutr Soc,* 58**,** 935-44.

RENZONI, A., BARRAS, C., FRANCOIS, P., CHARBONNIER, Y., HUGGLER, E., GARZONI, C., KELLEY, W. L., MAJCHERCZYK, P., SCHRENZEL, J., LEW, D. P. & VAUDAUX, P. 2006. Transcriptomic and functional analysis of an autolysis-deficient, teicoplanin-resistant derivative of methicillin-resistant *Staphylococcus aureus*. *Antimicrob Agents Chemother,* 50**,** 3048-61.

RICE, K. C. & BAYLES, K. W. 2008. Molecular control of bacterial death and lysis. *Microbiol Mol Biol Rev,* 72**,** 85-109.

RICE, K. C., FIREK, B. A., NELSON, J. B., YANG, S. J., PATTON, T. G. & BAYLES, K. W. 2003. The *Staphylococcus aureus* cidAB operon: evaluation of its role in

regulation of murein hydrolase activity and penicillin tolerance. *J Bacteriol,* 185**,** 2635-43.

RICE, K. C., MANN, E. E., ENDRES, J. L., WEISS, E. C., CASSAT, J. E., SMELTZER, M. S. & BAYLES, K. W. 2007. The cidA murein hydrolase regulator contributes to DNA release and biofilm development in *Staphylococcus aureus*. *Proc Natl Acad Sci U S A,* 104**,** 8113-8.

RICE, K. C., NELSON, J. B., PATTON, T. G., YANG, S. J. & BAYLES, K. W. 2005. Acetic acid induces expression of the *Staphylococcus aureus* cidABC and lrgAB murein hydrolase regulator operons. *J Bacteriol,* 187**,** 813-21.

RICE, R. H. & GREEN, H. 1977. The cornified envelope of terminally differentiated human epidermal keratinocytes consists of cross-linked protein. *Cell,* 11**,** 417-22.

RICHARDS, A. M., NICHOLLS, M. G., LEWIS, L. & LAINCHBURY, J. G. 1996. Adrenomedullin. *Clin Sci (Lond),* 91**,** 3-16.

RIDKY, T. W., CHOW, J. M., WONG, D. J. & KHAVARI, P. A. 2010. Invasive three-dimensional organotypic neoplasia from multiple normal human epithelia. *Nat Med,* 16**,** 1450-5.

RIEG, S., GARBE, C., SAUER, B., KALBACHER, H. & SCHITTEK, B. 2004. Dermcidin is constitutively produced by eccrine sweat glands and is not induced in epidermal cells under inflammatory skin conditions. *Br J Dermatol,* 151**,** 534-9.

RIPPKE, F., SCHREINER, V. & SCHWANITZ, H. J. 2002. The acidic milieu of the horny layer: new findings on the physiology and pathophysiology of skin pH. *Am J Clin Dermatol,* 3**,** 261-72.

ROBERSON, E. B. & FIRESTONE, M. K. 1992. Relationship between Desiccation and Exopolysaccharide Production in a Soil Pseudomonas sp. *Applied and Environmental Microbiology,* 58**,** 1284-91.

ROBINSON, M. D., MCCARTHY, D. J. & SMYTH, G. K. 2010. edgeR: a Bioconductor package for differential expression analysis of digital gene expression data. *Bioinformatics,* 26**,** 139-40.

ROBINSON, M. D. & OSHLACK, A. 2010. A scaling normalization method for differential expression analysis of RNA-seq data. *Genome Biol,* 11**,** R25.

ROCHE, F. M., MEEHAN, M. & FOSTER, T. J. 2003. The *Staphylococcus aureus* surface protein SasG and its homologues promote bacterial adherence to human desquamated nasal epithelial cells. *Microbiology,* 149**,** 2759-67.

ROGASCH, K., RUHMLING, V., PANE-FARRE, J., HOPER, D., WEINBERG, C., FUCHS, S., SCHMUDDE, M., BROKER, B. M., WOLZ, C., HECKER, M. & ENGELMANN, S. 2006. Influence of the two-component system SaeRS on global gene expression in two different *Staphylococcus aureus* strains. *J Bacteriol,* 188**,** 7742-58.

ROMANTSOV, T., GUAN, Z. & WOOD, J. M. 2009. Cardiolipin and the osmotic stress responses of bacteria. *Biochim Biophys Acta,* 1788**,** 2092-100.

ROTH, R. R. & JAMES, W. D. 1988. Microbial ecology of the skin. *Annu Rev Microbiol,* 42**,** 441-64.

RYAN, K.J. & Ray, C.G. (Eds) 2004. Sherris medical microbiology. 4th ed. McGraw Hill. 551-2.

SABA, J. D. & HLA, T. 2004. Point-counterpoint of sphingosine 1-phosphate metabolism. *Circ Res,* 94**,** 724-34.

SAKINC, T., KLEINE, B. & GATERMANN, S. G. 2006. SdrI, a serine-aspartate repeat protein identified in Staphylococcus saprophyticus strain 7108, is a collagen-binding protein. *Infect Immun,* 74**,** 4615-23.

SAKINC, T., KLEINE, B., MICHALSKI, N., KAASE, M. & GATERMANN, S. G. 2009. SdrI of *Staphylococcus saprophyticus* is a multifunctional protein: localization of the fibronectin-binding site. *FEMS Microbiol Lett,* 301**,** 28-34.

SASS, P., JANSEN, A., SZEKAT, C., SASS, V., SAHL, H.-G. & BIERBAUM, G. 2008. The lantibiotic mersacidin is a strong inducer of the cell wall stress response of *Staphylococcus aureus*. *BMC Microbiology,* 8**,** 186-186.

SASS, V., PAG, U., TOSSI, A., BIERBAUM, G. & SAHL, H. G. 2008. Mode of action of human beta-defensin 3 against *Staphylococcus aureus* and transcriptional analysis of responses to defensin challenge. *Int J Med Microbiol,* 298**,** 619-33.

SCHAFER, D., LAM, T. T., GEIGER, T., MAINIERO, M., ENGELMANN, S., HUSSAIN, M., BOSSERHOFF, A., FROSCH, M., BISCHOFF, M., WOLZ, C., REIDL, J. & SINHA, B. 2009. A point mutation in the sensor histidine kinase SaeS of *Staphylococcus aureus* strain Newman alters the response to biocide exposure. *J Bacteriol,* 191**,** 7306-14.

SCHAFER, L. & KRAGBALLE, K. 1991. Abnormalities in epidermal lipid metabolism in patients with atopic dermatitis. *J Invest Dermatol,* 96**,** 10-5.

SCHERL, A., FRANCOIS, P., CHARBONNIER, Y., DESHUSSES, J. M., KOESSLER, T., HUYGHE, A., BENTO, M., STAHL-ZENG, J., FISCHER, A., MASSELOT, A., VAEZZADEH, A., GALLE, F., RENZONI, A., VAUDAUX, P., LEW, D., ZIMMERMANN-IVOL, C. G., BINZ, P. A., SANCHEZ, J. C., HOCHSTRASSER, D. F. & SCHRENZEL, J. 2006. Exploring glycopeptide-resistance in *Staphylococcus aureus*: a combined proteomics and transcriptomics approach for the identification of resistance-related markers. *BMC Genomics,* 7**,** 296.

SCHITTEK, B., HIPFEL, R., SAUER, B., BAUER, J., KALBACHER, H., STEVANOVIC, S., SCHIRLE, M., SCHROEDER, K., BLIN, N., MEIER, F., RASSNER, G. & GARBE, C. 2001. Dermcidin: a novel human antibiotic peptide secreted by sweat glands. *Nat Immunol,* 2**,** 1133-7.

SCHMID-WENDTNER, M. H. & KORTING, H. C. 2006. The pH of the skin surface and its impact on the barrier function. *Skin Pharmacol Physiol,* 19**,** 296-302.

SCHOMMER, N. N. & GALLO, R. L. 2013. Structure and function of the human skin microbiome. *Trends in microbiology,* 21**,** 660-8.

SCHRODER, J. M. & HARDER, J. 2006. Antimicrobial skin peptides and proteins. *Cell Mol Life Sci,* 63**,** 469-86.

SCHUJMAN, G. E. & DE MENDOZA, D. 2005. Transcriptional control of membrane lipid synthesis in bacteria. *Curr Opin Microbiol,* 8**,** 149-53.

SEGRE, J. A. 2006. Epidermal barrier formation and recovery in skin disorders. *J Clin Invest,* 116**,** 1150-8.

SEGRE, J. A. 2006. Epidermal differentiation complex yields a secret: mutations in the cornification protein filaggrin underlie ichthyosis vulgaris. *J Invest Dermatol,* 126**,** 1202-4.

SEKI, T., YOSHIKAWA, H., TAKAHASHI, H. & SAITO, H. 1987. Cloning and nucleotide sequence of phoP, the regulatory gene for alkaline phosphatase and phosphodiesterase in Bacillus subtilis. *J Bacteriol,* 169**,** 2913-6.

SEKI, T., YOSHIKAWA, H., TAKAHASHI, H. & SAITO, H. 1988. Nucleotide sequence of the Bacillus subtilis phoR gene. *J Bacteriol,* 170**,** 5935-8.

SENYUREK, I., PAULMANN, M., SINNBERG, T., KALBACHER, H., DEEG, M., GUTSMANN, T., HERMES, M., KOHLER, T., GOTZ, F., WOLZ, C., PESCHEL, A. & SCHITTEK, B. 2009. Dermcidin-derived peptides show a different mode of action than the cathelicidin LL-37 against *Staphylococcus aureus*. *Antimicrob Agents Chemother,* 53**,** 2499-509.

SEVERIN, A., WU, S. W., TABEI, K. & TOMASZ, A. 2004. Penicillin-binding protein 2 is essential for expression of high-level vancomycin resistance and cell wall synthesis in vancomycin-resistant *Staphylococcus aureus* carrying the enterococcal vanA gene complex. *Antimicrob Agents Chemother,* 48**,** 4566-73.

SHARMA, N., AKHADE, A. S. & QADRI, A. 2013. Sphingosine-1-phosphate suppresses TLR-induced CXCL8 secretion from human T cells. *J Leukoc Biol,* 93**,** 521-8.

SHARMA-KUINKEL, B. K., MANN, E. E., AHN, J.-S., KUECHENMEISTER, L. J., DUNMAN, P. M. & BAYLES, K. W. 2009. The *Staphylococcus aureus* LytSR Two-

Component Regulatory System Affects Biofilm Formation. *Journal of Bacteriology,* 191**,** 4767-4775.

SHULMAN, J.A. & NAHMIAS, A.J. 1972. *taphylococcal infections: clinical aspects*. Wiley, New York. 457-82.

SHI, L., BIELAWSKI, J., MU, J., DONG, H., TENG, C., ZHANG, J., YANG, X., TOMISHIGE, N., HANADA, K., HANNUN, Y. A. & ZUO, J. 2007. Involvement of sphingoid bases in mediating reactive oxygen intermediate production and programmed cell death in Arabidopsis. *Cell Res,* 17**,** 1030-40.

SHIRAKURA, Y., KIKUCHI, K., MATSUMURA, K., MUKAI, K., MITSUTAKE, S. & IGARASHI, Y. 2012. 4,8-Sphingadienine and 4-hydroxy-8-sphingenine activate ceramide production in the skin. *Lipids Health Dis,* 11**,** 108.

SHOCKMAN, G. D. & BARRETT, J. F. 1983. Structure, function, and assembly of cell walls of gram-positive bacteria. *Annu Rev Microbiol,* 37**,** 501-27.

SINGH, V. K., HATTANGADY, D. S., GIOTIS, E. S., SINGH, A. K., CHAMBERLAIN, N. R., STUART, M. K. & WILKINSON, B. J. 2008. Insertional inactivation of branched-chain alpha-keto acid dehydrogenase in *Staphylococcus aureus* leads to decreased branched-chain membrane fatty acid content and increased susceptibility to certain stresses. *Appl Environ Microbiol,* 74**,** 5882-90.

SINGH, V. K., JAYASWAL, R. K. & WILKINSON, B. J. 2001. Cell wall-active antibiotic induced proteins of *Staphylococcus aureus* identified using a proteomic approach. *FEMS Microbiol Lett,* 199**,** 79-84.

SINGH, V. K., MOSKOVITZ, J., WILKINSON, B. J. & JAYASWAL, R. K. 2001. Molecular characterization of a chromosomal locus in *Staphylococcus aureus* that contributes to oxidative defence and is highly induced by the cell-wall-active antibiotic oxacillin. *Microbiology,* 147**,** 3037-45.

SKAAR, E. P., HUMAYUN, M., BAE, T., DEBORD, K. L. & SCHNEEWIND, O. 2004. Iron-source preference of *Staphylococcus aureus* infections. *Science,* 305**,** 1626-8.

SLANETZ, L. W. & JAWETZ, E. 1941. Isolation and Characteristics of Bacteriophages for Staphylococci of Bovine Mastitis. *Journal of Bacteriology,* 41**,** 447-55.

SNODGRASS, J. L., MOHAMED, N., ROSS, J. M., SAU, S., LEE, C. Y. & SMELTZER, M. S. 1999. Functional Analysis of the *Staphylococcus aureus* Collagen Adhesin B Domain. *Infection and Immunity,* 67**,** 3952-3959.

SOBRAL, R. G., JONES, A. E., DES ETAGES, S. G., DOUGHERTY, T. J., PEITZSCH, R. M., GAASTERLAND, T., LUDOVICE, A. M., DE LENCASTRE, H. & TOMASZ, A. 2007. Extensive and genome-wide changes in the transcription profile of *Staphylococcus aureus* induced by modulating the transcription of the cell wall synthesis gene murF. *J Bacteriol,* 189**,** 2376-91.

SOLLID, J. U., FURBERG, A. S., HANSSEN, A. M. & JOHANNESSEN, M. 2014. *Staphylococcus aureus*: determinants of human carriage. *Infect Genet Evol,* 21**,** 531-41.

SOMERVILLE, D. A. 1969. The normal flora of the skin in different age groups. *Br J Dermatol,* 81**,** 248-58.

SONG, C., WEICHBRODT, C., SALNIKOV, E. S., DYNOWSKI, M., FORSBERG, B. O., BECHINGER, B., STEINEM, C., DE GROOT, B. L., ZACHARIAE, U. & ZETH, K. 2013. Crystal structure and functional mechanism of a human antimicrobial membrane channel. *Proceedings of the National Academy of Sciences of the United States of America,* 110**,** 4586-91.

SONG, Y., LUNDE, C. S., BENTON, B. M. & WILKINSON, B. J. 2012. Further insights into the mode of action of the lipoglycopeptide telavancin through global gene expression studies. *Antimicrob Agents Chemother,* 56**,** 3157-64.

SPIEGEL, S. & MILSTIEN, S. 2000. Sphingosine-1-phosphate: signaling inside and out. *FEBS Lett,* 476**,** 55-7.

SPIEGEL, S. & MILSTIEN, S. 2003. Sphingosine-1-phosphate: an enigmatic signalling lipid. *Nat Rev Mol Cell Biol,* 4**,** 397-407.

SPIEGEL, S. & MILSTIEN, S. 2011. The outs and the ins of sphingosine-1-phosphate in immunity. *Nat Rev Immunol,* 11**,** 403-15.

SPRAGUE, G. F., JR., BELL, R. M. & CRONAN, J. E., JR. 1975. A mutant of Escherichia coli auxotrophic for organic phosphates: evidence for two defects in inorganic phosphate transport. *Mol Gen Genet,* 143**,** 71-7.

STARK, H.-J., SZABOWSKI, A., FUSENIG, N. E. & MAAS-SZABOWSKI, N. 2004. Organotypic cocultures as skin equivalents: A complex and sophisticated in vitro system. *Biological Procedures Online,* 6**,** 55-60.

STEED, P. M. & WANNER, B. L. 1993. Use of the rep technique for allele replacement to construct mutants with deletions of the pstSCAB-phoU operon: evidence of a new role for the PhoU protein in the phosphate regulon. *J Bacteriol,* 175**,** 6797-809.

STEINHUBER, A., GOERKE, C., BAYER, M. G., DORING, G. & WOLZ, C. 2003. Molecular architecture of the regulatory Locus sae of *Staphylococcus aureus* and its impact on expression of virulence factors. *J Bacteriol,* 185**,** 6278-86.

STOCK, A. M., ROBINSON, V. L. & GOUDREAU, P. N. 2000. Two-component signal transduction. *Annu Rev Biochem,* 69**,** 183-215.

SUN, F., LI, C., JEONG, D., SOHN, C., HE, C. & BAE, T. 2010. In the *Staphylococcus aureus* two-component system sae, the response regulator SaeR binds to a direct repeat sequence and DNA binding requires phosphorylation by the sensor kinase SaeS. *J Bacteriol,* 192**,** 2111-27.

TAKIGAWA, H., NAKAGAWA, H., KUZUKAWA, M., MORI, H. & IMOKAWA, G. 2005. Deficient production of hexadecenoic acid in the skin is associated in part with the vulnerability of atopic dermatitis patients to colonization by *Staphylococcus aureus*. *Dermatology,* 211**,** 240-8.

TATUSOV, R. L., KOONIN, E. V. & LIPMAN, D. J. 1997. A genomic perspective on protein families. *Science,* 278**,** 631-7.

TAYLOR, D., DAULBY, A., GRIMSHAW, S., JAMES, G., MERCER, J. & VAZIRI, S. 2003. Characterization of the microflora of the human axilla. *Int J Cosmet Sci,* 25**,** 137-45.

THAKKER, M., PARK, J. S., CAREY, V. & LEE, J. C. 1998. *Staphylococcus aureus* serotype 5 capsular polysaccharide is antiphagocytic and enhances bacterial virulence in a murine bacteremia model. *Infect Immun,* 66**,** 5183-9.

THURLOW, L. R., JOSHI, G. S., CLARK, J. R., SPONTAK, J. S., NEELY, C. J., MAILE, R. & RICHARDSON, A. R. 2013. Functional modularity of the arginine catabolic mobile element contributes to the success of USA300 methicillin-resistant *Staphylococcus aureus*. *Cell Host Microbe,* 13**,** 100-7.

TORRES, V. J., PISHCHANY, G., HUMAYUN, M., SCHNEEWIND, O. & SKAAR, E. P. 2006. *Staphylococcus aureus* IsdB is a hemoglobin receptor required for heme iron utilization. *J Bacteriol,* 188**,** 8421-9.

TORRES, V. J., STAUFF, D. L., PISHCHANY, G., BEZBRADICA, J. S., GORDY, L. E., ITURREGUI, J., ANDERSON, K. L., DUNMAN, P. M., JOYCE, S. & SKAAR, E. P. 2007. A *Staphylococcus aureus* regulatory system that responds to host heme and modulates virulence. *Cell host & microbe,* 1**,** 109-119.

TRUONG-BOLDUC, Q. C., VILLET, R. A., ESTABROOKS, Z. A. & HOOPER, D. C. 2014. Native efflux pumps contribute resistance to antimicrobials of skin and the ability of *Staphylococcus aureus* to colonize skin. *J Infect Dis,* 209**,** 1485-93.

TSAI, M., OHNIWA, R. L., KATO, Y., TAKESHITA, S. L., OHTA, T., SAITO, S., HAYASHI, H. & MORIKAWA, K. 2011. *Staphylococcus aureus* requires cardiolipin for survival under conditions of high salinity. *BMC Microbiol,* 11**,** 13.

UCKAY, I., PITTET, D., VAUDAUX, P., SAX, H., LEW, D. & WALDVOGEL, F. 2009. Foreign body infections due to *Staphylococcus epidermidis*. *Ann Med,* 41**,** 109-19.

UEHARA, Y., NAKAMA, H., AGEMATSU, K., UCHIDA, M., KAWAKAMI, Y., ABDUL FATTAH, A. S. & MARUCHI, N. 2000. Bacterial interference among nasal inhabitants: eradication of *Staphylococcus aureus* from nasal cavities by artificial implantation of Corynebacterium sp. *J Hosp Infect,* 44**,** 127-33.

UTAIDA, S., DUNMAN, P. M., MACAPAGAL, D., MURPHY, E., PROJAN, S. J., SINGH, V. K., JAYASWAL, R. K. & WILKINSON, B. J. 2003. Genome-wide transcriptional profiling of the response of *Staphylococcus aureus* to cell-wall-active antibiotics reveals a cell-wall-stress stimulon. *Microbiology,* 149**,** 2719-32.

VAGNER, V., DERVYN, E. & EHRLICH, S. D. 1998. A vector for systematic gene inactivation in Bacillus subtilis. *Microbiology,* 144**,** 3097-104.

VALE, P. F. & LITTLE, T. J. 2010. CRISPR-mediated phage resistance and the ghost of coevolution past. *Proc Biol Sci,* 277**,** 2097-103.

VALENZUELA, M., CERDA, O. & TOLEDO, H. 2003. Overview on chemotaxis and acid resistance in Helicobacter pylori. *Biol Res,* 36**,** 429-36.

VAN DER OOST, J., JORE, M. M., WESTRA, E. R., LUNDGREN, M. & BROUNS, S. J. 2009. CRISPR-based adaptive and heritable immunity in prokaryotes. *Trends Biochem Sci,* 34**,** 401-7.

VARALDO, P. E. & SATTA, G. 1978. Grouping of Staphylococci on the Basis of Their Bacteriolytic-Activity Patterns: A New Approach to the Taxonomy of the Micrococcaceae. *International Journal of Systematic and Evolutionary Microbiology,* 28**,** 148-153.

VERMEIREN, C. L., PLUYM, M., MACK, J., HEINRICHS, D. E. & STILLMAN, M. J. 2006. Characterization of the heme binding properties of *Staphylococcus aureus* IsdA. *Biochemistry,* 45**,** 12867-75.

VILLARI, P., SARNATARO, C. & IACUZIO, L. 2000. Molecular Epidemiology of *Staphylococcus epidermidis* in a Neonatal Intensive Care Unit over a Three-Year Period. *Journal of Clinical Microbiology,* 38**,** 1740-6.

VOLKOV, A., LIAVONCHANKA, A., KAMNEVA, O., FIEDLER, T., GOEBEL, C., KREIKEMEYER, B. & FEUSSNER, I. 2010. Myosin cross-reactive antigen of Streptococcus pyogenes M49 encodes a fatty acid double bond hydratase that plays a role in oleic acid detoxification and bacterial virulence. *J Biol Chem,* 285**,** 10353-61.

WAGNER, S., BAARS, L., YTTERBERG, A. J., KLUSSMEIER, A., WAGNER, C. S., NORD, O., NYGREN, P. A., VAN WIJK, K. J. & DE GIER, J. W. 2007. Consequences of membrane protein overexpression in Escherichia coli. *Mol Cell Proteomics,* 6**,** 1527-50.

WANG, Q. M., PEERY, R. B., JOHNSON, R. B., ALBORN, W. E., YEH, W. K. & SKATRUD, P. L. 2001. Identification and characterization of a monofunctional glycosyltransferase from *Staphylococcus aureus*. *J Bacteriol,* 183**,** 4779-85.

WANG, Z., GERSTEIN, M. & SNYDER, M. 2009. RNA-Seq: a revolutionary tool for transcriptomics. *Nat Rev Genet,* 10**,** 57-63.

WALDVOGEL, F.A. 1990. *Staphylococcus aureus*. Principles and Practice of Infectious Disease. Churchill Livingston, London. 1489-510.

WANN, E. R., GURUSIDDAPPA, S. & HOOK, M. 2000. The fibronectin-binding MSCRAMM FnbpA of *Staphylococcus aureus* is a bifunctional protein that also binds to fibrinogen. *J Biol Chem,* 275**,** 13863-71.

WATANABE, T., OZAKI, N., IWASHITA, K., FUJII, T. & IEFUJI, H. 2008. Breeding of wastewater treatment yeasts that accumulate high concentrations of phosphorus. *Applied Microbiology and Biotechnology,* 80**,** 331-338.

WATSON, A. D. 2006. Thematic review series: systems biology approaches to metabolic and cardiovascular disorders. Lipidomics: a global approach to lipid analysis in biological systems. *J Lipid Res,* 47**,** 2101-11.

WATT, F. M. & FUJIWARA, H. 2011. Cell-extracellular matrix interactions in normal and diseased skin. *Cold Spring Harb Perspect Biol,* 3.

WEBB, D. C., ROSENBERG, H. & COX, G. B. 1992. Mutational analysis of the Escherichia coli phosphate-specific transport system, a member of the traffic ATPase (or ABC) family of membrane transporters. A role for proline residues in transmembrane helices. *J Biol Chem,* 267**,** 24661-8.

WEIDENMAIER, C., KOKAI-KUN, J. F., KRISTIAN, S. A., CHANTURIYA, T., KALBACHER, H., GROSS, M., NICHOLSON, G., NEUMEISTER, B., MOND, J. J. &

PESCHEL, A. 2004. Role of teichoic acids in *Staphylococcus aureus* nasal colonization, a major risk factor in nosocomial infections. *Nat Med,* 10**,** 243-5.

WEIDENMAIER, C., KOKAI-KUN, J. F., KULAUZOVIC, E., KOHLER, T., THUMM, G., STOLL, H., GOTZ, F. & PESCHEL, A. 2008. Differential roles of sortase-anchored surface proteins and wall teichoic acid in *Staphylococcus aureus* nasal colonization. *Int J Med Microbiol,* 298**,** 505-13.

WENK, M. R. 2005. The emerging field of lipidomics. *Nat Rev Drug Discov,* 4**,** 594-610.

WERTHEIM, H. F., VERVEER, J., BOELENS, H. A., VAN BELKUM, A., VERBRUGH, H. A. & VOS, M. C. 2005. Effect of mupirocin treatment on nasal, pharyngeal, and perineal carriage of *Staphylococcus aureus* in healthy adults. *Antimicrob Agents Chemother,* 49**,** 1465-7.

WIEDEMANN, I., BREUKINK, E., VAN KRAAIJ, C., KUIPERS, O. P., BIERBAUM, G., DE KRUIJFF, B. & SAHL, H. G. 2001. Specific binding of nisin to the peptidoglycan precursor lipid II combines pore formation and inhibition of cell wall biosynthesis for potent antibiotic activity. *J Biol Chem,* 276**,** 1772-9.

WILKINSON, B.J. 1997. *Biology.* The Staphylococci in human Diseases. Church-ill Livingston, London. 1-38

WILLIAMS, R. E. 1963. Healthy carriage of *Staphylococcus aureus*: its prevalence and importance. *Bacteriol Rev,* 27**,** 56-71.

WILLIAMS, R. J., HENDERSON, B., SHARP, L. J. & NAIR, S. P. 2002. Identification of a Fibronectin-Binding Protein from *Staphylococcus epidermidis*. *Infection and Immunity,* 70**,** 6805-10.

WILLIAMS, S. E., BROWN, T. I., ROGHANIAN, A. & SALLENAVE, J. M. 2006. SLPI and elafin: one glove, many fingers. *Clin Sci (Lond),* 110**,** 21-35.

WILLSKY, G. R., BENNETT, R. L. & MALAMY, M. H. 1973. Inorganic Phosphate Transport in Escherichia coli: Involvement of Two Genes Which Play a Role in Alkaline Phosphatase Regulation. *Journal of Bacteriology,* 113**,** 529-539.

Wolf R.E. 2005. Available at: https://crustal.usgs.gov/laboratories/icpms/intro.html [Accessed September 2017].

WONGWISANSRI, S. & LAYBOURN, P. J. 2005. Disruption of Histone Deacetylase Gene RPD3 Accelerates PHO5 Activation Kinetics through Inappropriate Pho84p Recycling. *Eukaryotic Cell,* 4**,** 1387-1395.

WOS-OXLEY, M. L., PLUMEIER, I., VON EIFF, C., TAUDIEN, S., PLATZER, M., VILCHEZ-VARGAS, R., BECKER, K. & PIEPER, D. H. 2010. A poke into the diversity and associations within human anterior nare microbial communities. *Isme j,* 4**,** 839-51.

WU, P., MA, L., HOU, X., WANG, M., WU, Y., LIU, F. & DENG, X. W. 2003. Phosphate starvation triggers distinct alterations of genome expression in Arabidopsis roots and leaves. *Plant Physiol,* 132**,** 1260-71.

WU, S., ZHU, Z., FU, L., NIU, B. & LI, W. 2011. WebMGA: a customizable web server for fast metagenomic sequence analysis. *BMC Genomics,* 12**,** 444.

YAJJALA, V. K., WIDHELM, T. J., ENDRES, J. L., FEY, P. D. & BAYLES, K. W. 2016. Generation of a Transposon Mutant Library in *Staphylococcus aureus* and *Staphylococcus epidermidis* Using bursa aurealis. *Methods Mol Biol,* 1373**,** 103-10.

YAN, J., HAN, D., LIU, C., GAO, Y., LI, D., LIU, Y. & YANG, G. 2017. *Staphylococcus aureus* VraX specifically inhibits the classical pathway of complement by binding to C1q. *Mol Immunol,* 88**,** 38-44.

YANG, S. J., BAYER, A. S., MISHRA, N. N., MEEHL, M., LEDALA, N., YEAMAN, M. R., XIONG, Y. Q. & CHEUNG, A. L. 2012. The *Staphylococcus aureus* two-component regulatory system, GraRS, senses and confers resistance to selected cationic antimicrobial peptides. *Infect Immun,* 80**,** 74-81.

YANG, S. J., XIONG, Y. Q., YEAMAN, M. R., BAYLES, K. W., ABDELHADY, W. & BAYER, A. S. 2013. Role of the LytSR two-component regulatory system in adaptation to cationic antimicrobial peptides in *Staphylococcus aureus*. *Antimicrob Agents Chemother,* 57**,** 3875-82.

YANG, S.-J., XIONG, Y. Q., YEAMAN, M. R., BAYLES, K. W., ABDELHADY, W. & BAYER, A. S. 2013. Role of the LytSR Two-Component Regulatory System in Adaptation to Cationic Antimicrobial Peptides in *Staphylococcus aureus*. *Antimicrobial Agents and Chemotherapy,* 57**,** 3875-82.

YANG, X. J. & FINNEGAN, P. M. 2010. Regulation of phosphate starvation responses in higher plants. *Ann Bot,* 105**,** 513-26.

YE, J., COULOURIS, G., ZARETSKAYA, I., CUTCUTACHE, I., ROZEN, S. & MADDEN, T. L. 2012. Primer-BLAST: a tool to design target-specific primers for polymerase chain reaction. *BMC Bioinformatics,* 13**,** 134.

YIN, S., DAUM, R. S. & BOYLE-VAVRA, S. 2006. VraSR two-component regulatory system and its role in induction of pbp2 and vraSR expression by cell wall antimicrobials in *Staphylococcus aureus*. *Antimicrob Agents Chemother,* 50**,** 336-43.

ZEEUWEN, P. L., BOEKHORST, J., VAN DEN BOGAARD, E. H., DE KONING, H. D., VAN DE KERKHOF, P. M., SAULNIER, D. M., VAN, S., II, VAN HIJUM, S. A., KLEEREBEZEM, M., SCHALKWIJK, J. & TIMMERMAN, H. M. 2012. Microbiome dynamics of human epidermis following skin barrier disruption. *Genome Biol,* 13**,** R101.

ZHANG, H., DESAI, N. N., OLIVERA, A., SEKI, T., BROOKER, G. & SPIEGEL, S. 1991. Sphingosine-1-phosphate, a novel lipid, involved in cellular proliferation. *J Cell Biol,* 114**,** 155-67.

ZHANG, H., ZHANG, L., PENG, L. J., DONG, X. W., WU, D., WU, V. C. & FENG, F. Q. 2012. Quantitative structure-activity relationships of antimicrobial fatty acids and derivatives against *Staphylococcus aureus*. *J Zhejiang Univ Sci B,* 13**,** 83-93.

ZHANG, J., DYER, K. D. & ROSENBERG, H. F. 2003. Human RNase 7: a new cationic ribonuclease of the RNase A superfamily. *Nucleic Acids Research,* 31**,** 602-607.

ZHANG, Y., KUBACHKA, K. M. & CARUSO, J. A. 2010. Enhancing determination of organophosphate species in high inorganic phosphate matrices: application to nerve agent degradation products. *Analytical Methods,* 2**,** 1243-1248.

ZHENG, C. J., YOO, J. S., LEE, T. G., CHO, H. Y., KIM, Y. H. & KIM, W. G. 2005. Fatty acid synthesis is a target for antibacterial activity of unsaturated fatty acids. *FEBS Lett,* 579**,** 5157-62.

ZHU, T., LOU, Q., WU, Y., HU, J., YU, F. & QU, D. 2010. Impact of the *Staphylococcus epidermidis* LytSR two-component regulatory system on murein hydrolase activity, pyruvate utilization and global transcriptional profile. *BMC Microbiology,* 10**,** 287-287.

Appendix I: Selected SAMMD datasets

Acid shock

Regulator : Acid-shock (20min)

Growth phase : expression of wild type strain (50583) at exponential phase (OD 1.0 at 600nm) is compared to the corresponding acid-shocked (450-500 µl of 6.5 M HCl for 20min) expression of 50583.

Stabilising agent used : RNA Protect

Fold change cut off :

Replicates : Triplicate

Strain used : 50583

Array type : TIGR-PFGRC S. aureus DNA Microarray

Raw data : GEO:GSE7273

Software : GeneSpring

Reference: BORE, E., LANGSRUD, S., LANGSRUD, O., RODE, T. M. & HOLCK, A. 2007. Acid-shock responses in *Staphylococcus aureus* investigated by global gene expression analysis. *Microbiology,* 153**,** 2289-303.

Bacitracin

Regulator : Bacitracin

Growth phase : early exponential (OD 0.3 at 600nm) phase wild type (8325-4) expression is compared to the Bacitracin treated (6.7 units/ml for 60min) 8325-4 expression.

Stabilising agent used : NONE

Fold change cut off : 2

Replicates : Duplicate

Strain used : 8325-4

Array type : *S. aureus* Affymetrix GeneChip

Raw data : NOT AVAILABLE

Software : GeneSpring

Reference: UTAIDA, S., DUNMAN, P. M., MACAPAGAL, D., MURPHY, E., PROJAN, S. J., SINGH, V. K., JAYASWAL, R. K. & WILKINSON, B. J. 2003. Genome-wide transcriptional profiling of the response of *Staphylococcus aureus* to cell-wall-active antibiotics reveals a cell-wall-stress stimulon. *Microbiology,* 149**,** 2719-32.

Dermaseptin

Regulator : Antimicrobial peptide (Dermaseptin)

Growth phase : expression of early exponential phase (OD 0.6) S. aureus cells incubated in the presence of 3 micromolar Dermaseptin for 10min is compared to the untreated cells expression.

Stabilising agent used : NOT AVAILABLE

Fold change cut off : 2

Replicates : Triplicate

Strain used : Newman

Array type : Agilent Chip

Raw data : GEO:GSE15800

Software : GeneSpring 7.3

Reference: PIETIAINEN, M., FRANCOIS, P., HYYRYLAINEN, H. L., TANGOMO, M., SASS, V., SAHL, H. G., SCHRENZEL, J. & KONTINEN, V. P. 2009. Transcriptome analysis of the responses of *Staphylococcus aureus* to antimicrobial peptides and characterization of the roles of vraDE and vraSR in antimicrobial resistance. *BMC Genomics,* 10**,** 429.

Enduracidin

Regulator : Enduracidin (60min)

Growth phase : expression of mid-exponential phase S. aureus cells, added with one microgram/ml of enduracidin and incubated for 60min was compared to that of the corresponding control cells expression.

Stabilising agent used : RNAProtect

Fold change cut off : 2

Replicates : Triplicate

Strain used : ATCC29213

Array type : PFGRC Array Version 6

Raw data : GEO:GSE37272

Software : SAM

Reference: SONG, Y., LUNDE, C. S., BENTON, B. M. & WILKINSON, B. J. 2012. Further insights into the mode of action of the lipoglycopeptide telavancin through global gene expression studies. *Antimicrob Agents Chemother,* 56**,** 3157-64.

Fosfomycin/murB/murE

Regulator: Fosfomycin/murB/murE

Growth phase: expression of murB temperature sensitive mutant grown to OD 0.25 (600nm) is compared to that of the corresponding wild type cells expression.

Stabilising agent used : RNAProtect

Fold change cut off : 2

Replicates : Triplicate

Strain used : RN4220

Array type : Custom array

Raw data : ArrayExpress:E-BUGS-71

Software : GeneSpring 7.3.1

Reference: O'NEILL, A. J., LINDSAY, J. A., GOULD, K., HINDS, J. & CHOPRA, I. 2009. Transcriptional Signature following Inhibition of Early-Stage Cell Wall Biosynthesis in *Staphylococcus aureus*. *Antimicrobial Agents and Chemotherapy,* 53**,** 1701-1704.

Heat shock

Regulator : Heat shock

Growth phase : mid exponential phase (OD 0.25 at 600nm) wild type (UAMS-1) expression is compared to the corresponding cold shocked (42 Degree C for 30min with aeration) UAMS-1 expression.

Stabilising agent used : NONE

Fold change cut off : 2

Replicates : Duplicate

Strain used : UAMS-1

Array type : S. aureus Affymetrix GeneChip

Raw data : NOT AVAILABLE

Software : GeneSpring

Reference: ANDERSON, K. L., ROBERTS, C., DISZ, T., VONSTEIN, V., HWANG, K., OVERBEEK, R., OLSON, P. D., PROJAN, S. J. & DUNMAN, P. M. 2006. Characterization of the *Staphylococcus aureus* heat shock, cold shock, stringent, and SOS responses and their effects on log-phase mRNA turnover. *J Bacteriol,* 188**,** 6739-56.

Human beta-defensin 3

Regulator : Human beta-defensin 3 (STE)

Growth phase : expression of S. aureus cells grown to an OD of 0.8, added with 2 micro molar human beta-defensin 3 (short-term exposure) and further incubated for 20 min is compared with that of corresponding untreated cells expression.

Stabilising agent used : RNAProtect

Fold change cut off : 2

Replicates : Duplicate

Strain used : SG511

Array type : sciTRACER Custom array

Raw data : NOT AVAILABLE

Software : SAM

Reference: SASS, V., PAG, U., TOSSI, A., BIERBAUM, G. & SAHL, H. G. 2008. Mode of action of human beta-defensin 3 against *Staphylococcus aureus* and transcriptional analysis of responses to defensin challenge. *Int J Med Microbiol,* 298**,** 619-33.

Linoleic acid

Regulator : Linoleic acid (0.1 mM)

Growth phase : expression of late-exponential phase (OD 3.0, 600nm) S. aureus cells, added with 0.1 mM of linoleic acid and then grown for 20 min, is compared to that of the corresponding untreated cells expression.

Stabilising agent used : RNAProtect

Fold change cut off : 2

Replicates : Triplicate

Strain used : MRSA252

Array type : BuG@S

Raw data : ArrayExpress:E-BUGS-68

Software : GeneSpring 7.3.1

Reference: KENNY, J. G., WARD, D., JOSEFSSON, E., JONSSON, I. M., HINDS, J., REES, H. H., LINDSAY, J. A., TARKOWSKI, A. & HORSBURGH, M. J. 2009. The *Staphylococcus aureus* response to unsaturated long chain free fatty acids: survival mechanisms and virulence implications. *PLoS One,* 4**,** e4344.

Nisin

Regulator : Nisin

Growth phase : expression of ATCC 29213 grown to OD 0.4 (600nm) and induced with 20 µg/ml nisin for 15min was compared to the expression of the untreated ATCC 29213.

Stabilising agent used : RNA Protect, Trizon

Fold change cut off : 2

Replicates : Duplicate

Strain used : ATCC29213

Array type : TIGR-PFGRC S. aureus DNA Microarrays Version 2

Raw data : GEO:GSE9494

Software : TIGR-MIDAS, SAM

Reference: MUTHAIYAN, A., SILVERMAN, J. A., JAYASWAL, R. K. & WILKINSON, B. J. 2008. Transcriptional Profiling Reveals that Daptomycin Induces the *Staphylococcus aureus* Cell Wall Stress Stimulon and Genes Responsive to Membrane Depolarization. *Antimicrobial Agents and Chemotherapy,* 52**,** 980-990.

Ovispirin

Regulator : Antimicrobial peptide (Ovispirin)

Growth phase : expression of early exponential phase (OD 0.6) S. aureus cells incubated in the presence of 4 micromolar Ovispirin for 10min is compared to the untreated cells expression.

Stabilising agent used : NOT AVAILABLE

Fold change cut off : 2

Replicates : Triplicate

Strain used : Newman

Array type : Agilent Chip

Raw data : GEO:GSE15800

Software : GeneSpring 7.3

Reference: PIETIAINEN, M., FRANCOIS, P., HYYRYLAINEN, H. L., TANGOMO, M., SASS, V., SAHL, H. G., SCHRENZEL, J. & KONTINEN, V. P. 2009. Transcriptome analysis of the responses of *Staphylococcus aureus* to antimicrobial peptides and characterization of the roles of vraDE and vraSR in antimicrobial resistance. *BMC Genomics,* 10**,** 429.

Oxacillin

Regulator : Oxacillin

Growth phase : expression of SH1000 grown to OD 0.4 (600nm) and induced with 1.2 μg/ml oxacillin for 15min was compared to the expression of the untreated SH1000.

Stabilising agent used : RNA Protect, Trizon

Fold change cut off : 2

Replicates : Duplicate

Strain used : SH1000

Array type : TIGR-PFGRC S. aureus DNA Microarrays Version 2

Raw data : GEO:GSE9494

Software : TIGR-MIDAS, SAM

Reference : MUTHAIYAN, A., SILVERMAN, J. A., JAYASWAL, R. K. & WILKINSON, B. J. 2008. Transcriptional Profiling Reveals that Daptomycin Induces the *Staphylococcus aureus* Cell Wall Stress Stimulon and Genes Responsive to Membrane Depolarization. *Antimicrobial Agents and Chemotherapy,* 52**,** 980-990.

Teicoplanin

Regulator : Teicoplanin

Growth phase : late exponential phase (grown at 37C for 5hrs without shaking) expression of the teicoplanin-susceptible strain MRGR3 is compared to the expression of teicoplanin-resistant strain 14-4 expression.

Stabilising agent used : Ice-Cold Ethanol-Acetate

Fold change cut off : 1.5

Replicates : Triplicate

Strain used : MRGR3

Array type : StaphChip oligoarray from Agilent

Raw data : ArrayExpress:E-MEXP-738

Software : NOT AVAILABLE

Reference: RENZONI, A., BARRAS, C., FRANCOIS, P., CHARBONNIER, Y., HUGGLER, E., GARZONI, C., KELLEY, W. L., MAJCHERCZYK, P., SCHRENZEL, J., LEW, D. P. & VAUDAUX, P. 2006. Transcriptomic and functional analysis of an autolysis-deficient, teicoplanin-resistant derivative of methicillin-resistant *Staphylococcus aureus*. *Antimicrob Agents Chemother,* 50**,** 3048-61.

Telavancin

Regulator : Telavancin (15min)

Growth phase : expression of mid-exponential phase S. aureus cells, added with 8 microgram/ml of telavancin and incubated for 15min was compared to that of the corresponding control cells expression.

Stabilising agent used : RNAProtect

Fold change cut off : 2

Replicates : Triplicate

Strain used : ATCC29213

Array type : PFGRC Array Version 6

Raw data : GEO:GSE37272

Software : SAM

Reference: SONG, Y., LUNDE, C. S., BENTON, B. M. & WILKINSON, B. J. 2012. Further insights into the mode of action of the lipoglycopeptide telavancin through global gene expression studies. *Antimicrob Agents Chemother,* 56**,** 3157-64.

Temporin

Regulator : Antimicrobial peptide (Temporin)

Growth phase : expression of early exponential phase (OD 0.6) S. aureus cells incubated in the presence of 3 micromolar Temporin for 10min is compared to the untreated cells expression.

Stabilising agent used : NOT AVAILABLE

Fold change cut off : 2

Replicates : Triplicate

Strain used : Newman

Array type : Agilent Chip

Raw data : GEO:GSE15800

Software : GeneSpring 7.3

Reference: PIETIAINEN, M., FRANCOIS, P., HYYRYLAINEN, H. L., TANGOMO, M., SASS, V., SAHL, H. G., SCHRENZEL, J. & KONTINEN, V. P. 2009. Transcriptome analysis of the responses of *Staphylococcus aureus* to antimicrobial peptides and characterization of the roles of vraDE and vraSR in antimicrobial resistance. *BMC Genomics,* 10**,** 429.

Vancomycin

Regulator : Vancomycin

Growth phase : expression of wild type strain (Newman) (grown to OD 2.0 at 600nm) is compared to the expression of vancomycin treated (10 μg/ml for 5min at OD 2.0) Newman.

Stabilising agent used : NONE

Fold change cut off : 3

Replicates : Duplicate

Strain used : Newman

Array type : S. aureus Affymetrix GeneChip

Raw data : NOT AVAILABLE

Software: NOT AVAILABLE

Reference: MCCALLUM, N., SPEHAR, G., BISCHOFF, M. & BERGER-BACHI, B. 2006. Strain dependence of the cell wall-damage induced stimulon in *Staphylococcus aureus*. *Biochim Biophys Acta,* 1760**,** 1475-81.

Appendix II: COG scripts

Script1: counting_cogs

```
use strict;

my $all_genes = $ARGV[0];#web mga
my $list = $ARGV[1];#label cogs output
my $out = $ARGV[2];#name for output

open (all_genes, "$all_genes");

my $count = 0;
my @A = ();
my @B = ();
my @C = ();
my @D = ();
my @E = ();
my @F = ();
my @G = ();
my @H = ();
my @I = ();
my @J = ();
my @K = ();
my @L = ();
my @M = ();
my @N = ();
my @O = ();
my @P = ();
my @Q = ();
my @R = ();
my @S = ();
my @T = ();
my @U = ();
my @V = ();
my @W = ();
my @Y = ();
my @Z = ();

while (my $line = <all_genes>){
   if ($count != 0){
      my @temp = split (/\t/,$line);
      if ($temp[4] =~ m/A/){
         push (@A, $temp[4]);
      }
      if ($temp[4] =~ m/B/){
         push (@B, $temp[4]);
      }
      if ($temp[4] =~ m/C/){
         push (@C, $temp[4]);
      }
      if ($temp[4] =~ m/D/){
```

```
    push (@D, $temp[4]);
}
if ($temp[4] =~ m/E/){
    push (@E, $temp[4]);
}
if ($temp[4] =~ m/F/){
    push (@F, $temp[4]);
}
if ($temp[4] =~ m/G/){
    push (@G, $temp[4]);
}
if ($temp[4] =~ m/H/){
    push (@H, $temp[4]);
}
if ($temp[4] =~ m/I/){
    push (@I, $temp[4]);
}
if ($temp[4] =~ m/J/){
    push (@J, $temp[4]);
}
if ($temp[4] =~ m/K/){
    push (@K, $temp[4]);
}
if ($temp[4] =~ m/L/){
    push (@L, $temp[4]);
}
if ($temp[4] =~ m/M/){
    push (@M, $temp[4]);
}
if ($temp[4] =~ m/N/){
    push (@N, $temp[4]);
}
if ($temp[4] =~ m/O/){
    push (@O, $temp[4]);
}
if ($temp[4] =~ m/P/){
    push (@P, $temp[4]);
}
if ($temp[4] =~ m/Q/){
    push (@Q, $temp[4]);
}
if ($temp[4] =~ m/R/){
    push (@R, $temp[4]);
}
if ($temp[4] =~ m/S/){
    push (@S, $temp[4]);
}
if ($temp[4] =~ m/T/){
    push (@T, $temp[4]);
}
if ($temp[4] =~ m/U/){
    push (@U, $temp[4]);
}
```

```
      if ($temp[4] =~ m/V/){
         push (@V, $temp[4]);
      }
      if ($temp[4] =~ m/W/){
         push (@W, $temp[4]);
      }
      if ($temp[4] =~ m/Y/){
         push (@Y, $temp[4]);
      }
      if ($temp[4] =~ m/Z/){
         push (@Z, $temp[4]);
      }

   }
   $count++;
}

close all_genes;

my $tot_cogs =
@A+@B+@C+@D+@E+@F+@G+@H+@I+@J+@K+@L+@M+@N+@O+@P+@Q+@R+
@S+@T+@U+@V+@W+@Y+@Z;
my $pcent_A = (@A/$tot_cogs)*100;
my $pcent_B = (@B/$tot_cogs)*100;
my $pcent_C = (@C/$tot_cogs)*100;
my $pcent_D = (@D/$tot_cogs)*100;
my $pcent_E = (@E/$tot_cogs)*100;
my $pcent_F = (@F/$tot_cogs)*100;
my $pcent_G = (@G/$tot_cogs)*100;
my $pcent_H = (@H/$tot_cogs)*100;
my $pcent_I = (@I/$tot_cogs)*100;
my $pcent_J = (@J/$tot_cogs)*100;
my $pcent_K = (@K/$tot_cogs)*100;
my $pcent_L = (@L/$tot_cogs)*100;
my $pcent_M = (@M/$tot_cogs)*100;
my $pcent_N = (@N/$tot_cogs)*100;
my $pcent_O = (@O/$tot_cogs)*100;
my $pcent_P = (@P/$tot_cogs)*100;
my $pcent_Q = (@Q/$tot_cogs)*100;
my $pcent_R = (@R/$tot_cogs)*100;
my $pcent_S = (@S/$tot_cogs)*100;
my $pcent_T = (@T/$tot_cogs)*100;
my $pcent_U = (@U/$tot_cogs)*100;
my $pcent_V = (@V/$tot_cogs)*100;
my $pcent_W = (@W/$tot_cogs)*100;
my $pcent_Y = (@Y/$tot_cogs)*100;
my $pcent_Z = (@Z/$tot_cogs)*100;

open (list, "$list");

my $counter = 0;
my @A_up = ();
my @B_up = ();
```

```
my @C_up = ();
my @D_up = ();
my @E_up = ();
my @F_up = ();
my @G_up = ();
my @H_up = ();
my @I_up = ();
my @J_up = ();
my @K_up = ();
my @L_up = ();
my @M_up = ();
my @N_up = ();
my @O_up = ();
my @P_up = ();
my @Q_up = ();
my @R_up = ();
my @S_up = ();
my @T_up = ();
my @U_up = ();
my @V_up = ();
my @W_up = ();
my @Y_up = ();
my @Z_up = ();
my @A_down = ();
my @B_down = ();
my @C_down = ();
my @D_down = ();
my @E_down = ();
my @F_down = ();
my @G_down = ();
my @H_down = ();
my @I_down = ();
my @J_down = ();
my @K_down = ();
my @L_down = ();
my @M_down = ();
my @N_down = ();
my @O_down = ();
my @P_down = ();
my @Q_down = ();
my @R_down = ();
my @S_down = ();
my @T_down = ();
my @U_down = ();
my @V_down = ();
my @W_down = ();
my @Y_down = ();
my @Z_down = ();

while (my $line = <list>){
   if ($counter != 0){
      my @temp = split(/\t/, $line);
      if ($temp[1] <0){
```

```
if ($temp[5] =~ m/A/){
   push (@A_down, $temp[5]);
}
if ($temp[5] =~ m/B/){
   push (@B_down, $temp[5]);
}
if ($temp[5] =~ m/C/){
   push (@C_down, $temp[5]);
}
if ($temp[5] =~ m/D/){
   push (@D_down, $temp[5]);
}
if ($temp[5] =~ m/E/){
   push (@E_down, $temp[5]);
}
if ($temp[5] =~ m/F/){
   push (@F_down, $temp[5]);
}
if ($temp[5] =~ m/G/){
   push (@G_down, $temp[5]);
}
if ($temp[5] =~ m/H/){
   push (@H_down, $temp[5]);
}
if ($temp[5] =~ m/I/){
   push (@I_down, $temp[5]);
}
if ($temp[5] =~ m/J/){
   push (@J_down, $temp[5]);
}
if ($temp[5] =~ m/K/){
   push (@K_down, $temp[5]);
}
if ($temp[5] =~ m/L/){
   push (@L_down, $temp[5]);
}
if ($temp[5] =~ m/M/){
   push (@M_down, $temp[5]);
}
if ($temp[5] =~ m/N/){
   push (@N_down, $temp[5]);
}
if ($temp[5] =~ m/O/){
   push (@O_down, $temp[5]);
}
if ($temp[5] =~ m/P/){
   push (@P_down, $temp[5]);
}
if ($temp[5] =~ m/Q/){
   push (@Q_down, $temp[5]);
}
if ($temp[5] =~ m/R/){
   push (@R_down, $temp[5]);
```

```
    }
    if ($temp[5] =~ m/S/){
       push (@S_down, $temp[5]);
    }
    if ($temp[5] =~ m/T/){
       push (@T_down, $temp[5]);
    }
    if ($temp[5] =~ m/U/){
       push (@U_down, $temp[5]);
    }
    if ($temp[5] =~ m/V/){
       push (@V_down, $temp[5]);
    }
    if ($temp[5] =~ m/W/){
       push (@W_down, $temp[5]);
    }
    if ($temp[5] =~ m/Y/){
       push (@Y_down, $temp[5]);
    }
    if ($temp[5] =~ m/Z/){
       push (@Z_down, $temp[5]);
    }

}
elsif ($temp[1] >0){
    if ($temp[5] =~ m/A/){
       push (@A_up, $temp[5]);
    }
    if ($temp[5] =~ m/B/){
       push (@B_up, $temp[5]);
    }
    if ($temp[5] =~ m/C/){
       push (@C_up, $temp[5]);
    }
    if ($temp[5] =~ m/D/){
       push (@D_up, $temp[5]);
    }
    if ($temp[5] =~ m/E/){
       push (@E_up, $temp[5]);
    }
    if ($temp[5] =~ m/F/){
       push (@F_up, $temp[5]);
    }
    if ($temp[5] =~ m/G/){
       push (@G_up, $temp[5]);
    }
    if ($temp[5] =~ m/H/){
       push (@H_up, $temp[5]);
    }
    if ($temp[5] =~ m/I/){
       push (@I_up, $temp[5]);
    }
    if ($temp[5] =~ m/J/){
```

```
            push (@J_up, $temp[5]);
        }
        if ($temp[5] =~ m/K/){
            push (@K_up, $temp[5]);
        }
        if ($temp[5] =~ m/L/){
            push (@L_up, $temp[5]);
        }
        if ($temp[5] =~ m/M/){
            push (@M_up, $temp[5]);
        }
        if ($temp[5] =~ m/N/){
            push (@N_up, $temp[5]);
        }
        if ($temp[5] =~ m/O/){
            push (@O_up, $temp[5]);
        }
        if ($temp[5] =~ m/P/){
            push (@P_up, $temp[5]);
        }
        if ($temp[5] =~ m/Q/){
            push (@Q_up, $temp[5]);
        }
        if ($temp[5] =~ m/R/){
            push (@R_up, $temp[5]);
        }
        if ($temp[5] =~ m/S/){
            push (@S_up, $temp[5]);
        }
        if ($temp[5] =~ m/T/){
            push (@T_up, $temp[5]);
        }
        if ($temp[5] =~ m/U/){
            push (@U_up, $temp[5]);
        }
        if ($temp[5] =~ m/V/){
            push (@V_up, $temp[5]);
        }
        if ($temp[5] =~ m/W/){
            push (@W_up, $temp[5]);
        }
        if ($temp[5] =~ m/Y/){
            push (@Y_up, $temp[5]);
        }
        if ($temp[5] =~ m/Z/){
            push (@Z_up, $temp[5]);
        }

    }
  }
  $counter++;
}
```

```
close list;

my $tot_list_cogs =
@A_up+@B_up+@C_up+@D_up+@E_up+@F_up+@G_up+@H_up+@I_up+@J_up+@K_u
p+@L_up+@M_up+@N_up+@O_up+@P_up+@Q_up+@R_up+@S_up+@T_up+@U_up+
@V_up+@W_up+@Y_up+@Z_up+@A_down+@B_down+@C_down+@D_down+@E_do
wn+@F_down+@G_down+@H_down+@I_down+@J_down+@K_down+@L_down+@M_
down+@N_down+@O_down+@P_down+@Q_down+@R_down+@S_down+@T_down+
@U_down+@V_down+@W_down+@Y_down+@Z_down;

my $pcent_A_tot =((@A_up+@A_down)/$tot_list_cogs)*100;
my $pcent_B_tot =((@B_up+@B_down)/$tot_list_cogs)*100;
my $pcent_C_tot =((@C_up+@C_down)/$tot_list_cogs)*100;
my $pcent_D_tot =((@D_up+@D_down)/$tot_list_cogs)*100;
my $pcent_E_tot =((@E_up+@E_down)/$tot_list_cogs)*100;
my $pcent_F_tot =((@F_up+@F_down)/$tot_list_cogs)*100;
my $pcent_G_tot =((@G_up+@G_down)/$tot_list_cogs)*100;
my $pcent_H_tot =((@H_up+@H_down)/$tot_list_cogs)*100;
my $pcent_I_tot =((@I_up+@I_down)/$tot_list_cogs)*100;
my $pcent_J_tot =((@J_up+@J_down)/$tot_list_cogs)*100;
my $pcent_K_tot =((@K_up+@K_down)/$tot_list_cogs)*100;
my $pcent_L_tot =((@L_up+@L_down)/$tot_list_cogs)*100;
my $pcent_M_tot =((@M_up+@M_down)/$tot_list_cogs)*100;
my $pcent_N_tot =((@N_up+@N_down)/$tot_list_cogs)*100;
my $pcent_O_tot =((@O_up+@O_down)/$tot_list_cogs)*100;
my $pcent_P_tot =((@P_up+@P_down)/$tot_list_cogs)*100;
my $pcent_Q_tot =((@Q_up+@Q_down)/$tot_list_cogs)*100;
my $pcent_R_tot =((@R_up+@R_down)/$tot_list_cogs)*100;
my $pcent_S_tot =((@S_up+@S_down)/$tot_list_cogs)*100;
my $pcent_T_tot =((@T_up+@T_down)/$tot_list_cogs)*100;
my $pcent_U_tot =((@U_up+@U_down)/$tot_list_cogs)*100;
my $pcent_V_tot =((@V_up+@V_down)/$tot_list_cogs)*100;
my $pcent_W_tot =((@W_up+@W_down)/$tot_list_cogs)*100;
my $pcent_Y_tot =((@Y_up+@Y_down)/$tot_list_cogs)*100;
my $pcent_Z_tot =((@Z_up+@Z_down)/$tot_list_cogs)*100;

my $pcent_A_up =(@A_up/$tot_list_cogs)*100;
my $pcent_B_up =(@B_up/$tot_list_cogs)*100;
my $pcent_C_up =(@C_up/$tot_list_cogs)*100;
my $pcent_D_up =(@D_up/$tot_list_cogs)*100;
my $pcent_E_up =(@E_up/$tot_list_cogs)*100;
my $pcent_F_up =(@F_up/$tot_list_cogs)*100;
my $pcent_G_up =(@G_up/$tot_list_cogs)*100;
my $pcent_H_up =(@H_up/$tot_list_cogs)*100;
my $pcent_I_up =(@I_up/$tot_list_cogs)*100;
my $pcent_J_up =(@J_up/$tot_list_cogs)*100;
my $pcent_K_up =(@K_up/$tot_list_cogs)*100;
my $pcent_L_up =(@L_up/$tot_list_cogs)*100;
my $pcent_M_up =(@M_up/$tot_list_cogs)*100;
my $pcent_N_up =(@N_up/$tot_list_cogs)*100;
my $pcent_O_up =(@O_up/$tot_list_cogs)*100;
my $pcent_P_up =(@P_up/$tot_list_cogs)*100;
my $pcent_Q_up =(@Q_up/$tot_list_cogs)*100;
```

```
my $pcent_R_up =(@R_up/$tot_list_cogs)*100;
my $pcent_S_up =(@S_up/$tot_list_cogs)*100;
my $pcent_T_up =(@T_up/$tot_list_cogs)*100;
my $pcent_U_up =(@U_up/$tot_list_cogs)*100;
my $pcent_V_up =(@V_up/$tot_list_cogs)*100;
my $pcent_W_up =(@W_up/$tot_list_cogs)*100;
my $pcent_Y_up =(@Y_up/$tot_list_cogs)*100;
my $pcent_Z_up =(@Z_up/$tot_list_cogs)*100;

my $pcent_A_down =(@A_down/$tot_list_cogs)*100;
my $pcent_B_down =(@B_down/$tot_list_cogs)*100;
my $pcent_C_down =(@C_down/$tot_list_cogs)*100;
my $pcent_D_down =(@D_down/$tot_list_cogs)*100;
my $pcent_E_down =(@E_down/$tot_list_cogs)*100;
my $pcent_F_down =(@F_down/$tot_list_cogs)*100;
my $pcent_G_down =(@G_down/$tot_list_cogs)*100;
my $pcent_H_down =(@H_down/$tot_list_cogs)*100;
my $pcent_I_down =(@I_down/$tot_list_cogs)*100;
my $pcent_J_down =(@J_down/$tot_list_cogs)*100;
my $pcent_K_down =(@K_down/$tot_list_cogs)*100;
my $pcent_L_down =(@L_down/$tot_list_cogs)*100;
my $pcent_M_down =(@M_down/$tot_list_cogs)*100;
my $pcent_N_down =(@N_down/$tot_list_cogs)*100;
my $pcent_O_down =(@O_down/$tot_list_cogs)*100;
my $pcent_P_down =(@P_down/$tot_list_cogs)*100;
my $pcent_Q_down =(@Q_down/$tot_list_cogs)*100;
my $pcent_R_down =(@R_down/$tot_list_cogs)*100;
my $pcent_S_down =(@S_down/$tot_list_cogs)*100;
my $pcent_T_down =(@T_down/$tot_list_cogs)*100;
my $pcent_U_down =(@U_down/$tot_list_cogs)*100;
my $pcent_V_down =(@V_down/$tot_list_cogs)*100;
my $pcent_W_down =(@W_down/$tot_list_cogs)*100;
my $pcent_Y_down =(@Y_down/$tot_list_cogs)*100;
my $pcent_Z_down =(@Z_down/$tot_list_cogs)*100;

my $count_A = @A_up+@A_down ;
my $count_B = @B_up+@B_down ;
my $count_C = @C_up+@C_down ;
my $count_D = @D_up+@D_down ;
my $count_E = @E_up+@E_down ;
my $count_F = @F_up+@F_down ;
my $count_G = @G_up+@G_down ;
my $count_H = @H_up+@H_down ;
my $count_I = @I_up+@I_down ;
my $count_J = @J_up+@J_down ;
my $count_K = @K_up+@K_down ;
my $count_L = @L_up+@L_down ;
my $count_M = @M_up+@M_down ;
my $count_N = @N_up+@N_down ;
my $count_O = @O_up+@O_down ;
my $count_P = @P_up+@P_down ;
my $count_Q = @Q_up+@Q_down ;
my $count_R = @R_up+@R_down ;
```

```
my $count_S = @S_up+@S_down ;
my $count_T = @T_up+@T_down ;
my $count_U = @U_up+@U_down ;
my $count_V = @V_up+@V_down ;
my $count_W = @W_up+@W_down ;
my $count_Y = @Y_up+@Y_down ;
my $count_Z = @Z_up+@Z_down ;

my $count_A_up = @A_up ;
my $count_B_up = @B_up ;
my $count_C_up = @C_up ;
my $count_D_up = @D_up ;
my $count_E_up = @E_up ;
my $count_F_up = @F_up ;
my $count_G_up = @G_up ;
my $count_H_up = @H_up ;
my $count_I_up = @I_up ;
my $count_J_up = @J_up ;
my $count_K_up = @K_up ;
my $count_L_up = @L_up ;
my $count_M_up = @M_up ;
my $count_N_up = @N_up ;
my $count_O_up = @O_up ;
my $count_P_up = @P_up ;
my $count_Q_up = @Q_up ;
my $count_R_up = @R_up ;
my $count_S_up = @S_up ;
my $count_T_up = @T_up ;
my $count_U_up = @U_up ;
my $count_V_up = @V_up ;
my $count_W_up = @W_up ;
my $count_Y_up = @Y_up ;
my $count_Z_up = @Z_up ;

my $count_A_down = @A_down ;
my $count_B_down = @B_down ;
my $count_C_down = @C_down ;
my $count_D_down = @D_down ;
my $count_E_down = @E_down ;
my $count_F_down = @F_down ;
my $count_G_down = @G_down ;
my $count_H_down = @H_down ;
my $count_I_down = @I_down ;
my $count_J_down = @J_down ;
my $count_K_down = @K_down ;
my $count_L_down = @L_down ;
my $count_M_down = @M_down ;
my $count_N_down = @N_down ;
my $count_O_down = @O_down ;
my $count_P_down = @P_down ;
my $count_Q_down = @Q_down ;
my $count_R_down = @R_down ;
my $count_S_down = @S_down ;
```

```
my $count_T_down = @T_down ;
my $count_U_down = @U_down ;
my $count_V_down = @V_down ;
my $count_W_down = @W_down ;
my $count_Y_down = @Y_down ;
my $count_Z_down = @Z_down ;


open (out, ">$out");



print out
"COG_class\tPercent_of_genome\tPercent_of_gene_list\tpercent_up_of_gene_list\tPerce
nt_down_of_gene_list\ttotal_count\tup_count\tdown_count\nA\t$pcent_A\t$pcent_A_t
ot\t$pcent_A_up\t$pcent_A_down\t$count_A\t$count_A_up\t$count_A_down\nB\t$pc
ent_B\t$pcent_B_tot\t$pcent_B_up\t$pcent_B_down\t$count_B\t$count_B_up\t$count
_B_down\nC\t$pcent_C\t$pcent_C_tot\t$pcent_C_up\t$pcent_C_down\t$count_C\t$co
unt_C_up\t$count_C_down\nD\t$pcent_D\t$pcent_D_tot\t$pcent_D_up\t$pcent_D_dow
n\t$count_D\t$count_D_up\t$count_D_down\nE\t$pcent_E\t$pcent_E_tot\t$pcent_E_u
p\t$pcent_E_down\t$count_E\t$count_E_up\t$count_E_down\nF\t$pcent_F\t$pcent_F
_tot\t$pcent_F_up\t$pcent_F_down\t$count_F\t$count_F_up\t$count_F_down\nG\t$pc
ent_G\t$pcent_G_tot\t$pcent_G_up\t$pcent_G_down\t$count_G\t$count_G_up\t$count
_G_down\nH\t$pcent_H\t$pcent_H_tot\t$pcent_H_up\t$pcent_H_down\t$count_H\t$c
ount_H_up\t$count_H_down\nI\t$pcent_I\t$pcent_I_tot\t$pcent_I_up\t$pcent_I_down
\t$count_I\t$count_I_up\t$count_I_down\nJ\t$pcent_J\t$pcent_J_tot\t$pcent_J_up\t$p
cent_J_down\t$count_J\t$count_J_up\t$count_J_down\nK\t$pcent_K\t$pcent_K_tot\t$
pcent_K_up\t$pcent_K_down\t$count_K\t$count_K_up\t$count_K_down\nL\t$pcent_L
\t$pcent_L_tot\t$pcent_L_up\t$pcent_L_down\t$count_L\t$count_L_up\t$count_L_do
wn\nM\t$pcent_M\t$pcent_M_tot\t$pcent_M_up\t$pcent_M_down\t$count_M\t$count
_M_up\t$count_M_down\nN\t$pcent_N\t$pcent_N_tot\t$pcent_N_up\t$pcent_N_down
\t$count_N\t$count_N_up\t$count_N_down\nO\t$pcent_O\t$pcent_O_tot\t$pcent_O_u
p\t$pcent_O_down\t$count_O\t$count_O_up\t$count_O_down\nP\t$pcent_P\t$pcent_
P_tot\t$pcent_P_up\t$pcent_P_down\t$count_P\t$count_P_up\t$count_P_down\nQ\t$
pcent_Q\t$pcent_Q_tot\t$pcent_Q_up\t$pcent_Q_down\t$count_Q\t$count_Q_up\t$co
unt_Q_down\nR\t$pcent_R\t$pcent_R_tot\t$pcent_R_up\t$pcent_R_down\t$count_R\t
$count_R_up\t$count_R_down\nS\t$pcent_S\t$pcent_S_tot\t$pcent_S_up\t$pcent_S_do
wn\t$count_S\t$count_S_up\t$count_S_down\nT\t$pcent_T\t$pcent_T_tot\t$pcent_T_
up\t$pcent_T_down\t$count_T\t$count_T_up\t$count_T_down\nU\t$pcent_U\t$pcent
_U_tot\t$pcent_U_up\t$pcent_U_down\t$count_U\t$count_U_up\t$count_U_down\nV\
t$pcent_V\t$pcent_V_tot\t$pcent_V_up\t$pcent_V_down\t$count_V\t$count_V_up\t$co
unt_V_down\nW\t$pcent_W\t$pcent_W_tot\t$pcent_W_up\t$pcent_W_down\t$count_
W\t$count_W_up\t$count_W_down\nY\t$pcent_Y\t$pcent_Y_tot\t$pcent_Y_up\t$pcen
t_Y_down\t$count_Y\t$count_Y_up\t$count_Y_down\nZ\t$pcent_Z\t$pcent_Z_tot\t$pc
ent_Z_up\t$pcent_Z_down\t$count_Z\t$count_Z_up\t$count_Z_down\n"
```

Script2: label_cogs

```
#usage: gene list, web mga output 2, name
use strict;

my $gene_list = $ARGV[0];#file 1st collumn ordered gene list 2nd collumn whatever (eg
Fold change) tab or space delimited
my $cog_data = $ARGV[1];#output 2 from web MGA cog analysis

open(gene_list, "$gene_list");

my %list;

my $counter = 0;

while (my $line = <gene_list>){
       if ($counter != 0){
     $line =~ s/\n//;#substitute newline character with nothing
     $line =~ s/\r//;#substirute return character with nothing
     my @temp = split(/\t/,$line);
      $list{$temp[0]} = $temp[1];
   }
   $counter++;
}

open (cog, "$cog_data");
open (out, ">$ARGV[2]");

print out "official_gene_name\tfold_change\tcog_hit\tE-
value\tcog_description\tcog_class\tcog_class_description\n";

while (my $line = <cog>){
   $line =~ s/\n//;#substitute newline character with nothing
   $line =~ s/\r//;#substirute return character with nothing
    if ($counter != 0){
      my @temp = split (/\t/, $line);
      my $value = $list{$temp[0]};
      if ($value =~ m/\w/){
          print out
"$temp[0]\t$list{$temp[0]}\t$temp[1]\t$temp[2]\t$temp[5]\t$temp[6]\t$temp[7]\n";
      }
   }
   $counter++
}

close cog;
close out;
```

Appendix III: RNA-Seq data

Appendix Table 1 DE genes of *S. aureus* Newman in response to 5μM D-sphingosine challenge. The level of fold change **(logFC)** is based on log2, DE genes shown in this table all have more than 2 fold changes. All DE genes have **FDR** (false discovery rate) ≤ 0.05.

Gene	Gene Description	logFC	FDR
NWMN_0006	ADP-dependent (S)-NAD(P)H-hydrate dehydratase	-1.959735517	6.32E-30
serS	seryl-tRNA synthetase	-0.994123363	1.30E-07
NWMN_0022	hypothetical protein	-1.554251435	7.40E-14
NWMN_0030	hypothetical protein	-1.204553476	9.01E-13
NWMN_0049	hypothetical protein	1.246338474	7.53E-13
sarH1	accessory regulator A-like protein	-1.62570734	3.98E-23
sirC	siderophore compound ABC transporter permease SirC	-1.115350198	4.58E-08
NWMN_0093	truncated IS200 transposase family protein	-1.020927239	1.88E-06
capA	capsular polysaccharide synthesis enzyme CapA	-1.021923017	0.001399474
capB	capsular polysaccharide synthesis enzyme CapB	-1.144390389	0.000277759
NWMN_0122	hypothetical protein	1.029174053	1.57E-08
ipdC	indole-3-pyruvate decarboxylase	1.034397132	2.50E-08
glcA	glucose-specific PTS transporter protein IIABC component	-1.677084752	2.67E-19
NWMN_0149	azoreductase	-1.23143586	3.91E-12
NWMN_0150	hypothetical protein	2.135076524	2.79E-11
NWMN_0157	hypothetical protein	-3.266011727	8.22E-86
pflB	Formate acetyltransferase	-2.177329331	1.66E-10
NWMN_0163	hypothetical protein	-2.09794827	4.01E-09
NWMN_0165	hypothetical protein	-1.880158903	4.84E-19
coa	staphylocoagulase	-5.429586438	8.31E-95
fadE	acyl-CoA synthetase FadE-like protein	1.042241634	2.07E-05

NWMN_0171	acetyl-CoA 2Facetoacetyl-CoA transferase	1.722902685	9.84E-17
ldh1	L-lactate dehydrogenase	-1.012596466	0.000947057
NWMN_0177	similar to PTS transport system 2C IIBC component	1.046168631	9.31E-10
lytS	autolysin sensor histidine kinase	-1.097318156	1.37E-09
lytR	two-component response regulator	-1.021490425	2.78E-07
lrgA	Antiholin-like protein LrgA	-2.273579371	6.46E-08
lrgB	Antiholin-like protein LrgB	-1.918354962	0.000175949
NWMN_0199	PTS system, IIA component	1.960211134	1.55E-22
bglA	6-phospho-beta-glucosidase	1.752869764	8.35E-24
lytM	peptidoglycan hydrolase	1.204757975	6.62E-09
NWMN_0249	nucleotidase lipoprotein family protein	-1.212881346	3.53E-09
NWMN_0250	ABC transporter permease	-1.05147355	1.79E-08
NWMN_0262	Truncated triacylglycerol lipase precursor(lipid management)	-2.634011837	5.39E-36
NWMN_0297	hypothetical protein	-1.01125955	0.031320192
NWMN_0298	hypothetical protein	-1.054032148	0.037392445
NWMN_0299	hypothetical protein	-1.089734692	0.022583101
NWMN_0300	hypothetical protein	-1.018940659	0.027380805
NWMN_0301	hypothetical protein	-1.039637718	0.011603068
metE	5-methyltetrahydropteroyltriglutamate--homocysteine S-methyltransferase	1.317212346	4.65E-13
metH	bifunctional homocysteine S-methyltransferase-methylenetetrahydrofolate reductase	1.361349637	8.56E-14
rpsF	30S ribosomal protein S6	-1.193878896	1.07E-11
NWMN_0358	single-strand DNA-binding family protein	-1.234740397	1.23E-12
rpsR	30S ribosomal protein S18	-1.278742184	5.87E-13
NWMN_0362	hypothetical protein	-3.127615252	2.45E-78
NWMN_0363	hypothetical protein	-1.756174719	2.58E-21
NWMN_0364	hypothetical protein	-1.293022751	7.08E-09
NWMN_0366	hypothetical protein	-1.569105998	2.81E-11
ahpC	alkyl hydroperoxide reductase subunit C	-0.99595264	6.66E-12
set1nm	Staphylococcal enterotoxin-like toxin	-2.297534733	3.27E-26

set2nm	Staphylococcal enterotoxin-like toxin	-2.017747072	3.14E-14
set3nm	superantigen-like protein	-1.305993877	8.05E-09
set4nm	Staphylococcal enterotoxin-like toxin	-2.220637761	1.39E-18
set5nm	superantigen-like protein	-1.078733561	1.59E-07
set6nm	superantigen-like protein	-1.374610935	1.41E-09
set7nm	superantigen-like protein Staphylococcal enterotoxin-like toxin	-4.76024477	1.14E-53
set8nm	Staphylococcal enterotoxin-like toxin	-2.29813069	1.21E-16
set9nm	superantigen-like protein	-1.502138734	3.84E-08
set10nm	superantigen-like protein	-1.569221754	1.63E-13
set11nm	superantigen-like protein Staphylococcal enterotoxin-like toxin	-4.600549793	5.51E-76
NWMN_0401	hypothetical protein	-4.642923689	2.45E-78
NWMN_0402	hypothetical protein	-2.129075577	2.08E-21
lpl4nm	tandem lipoprotein	1.190038277	5.32E-06
lpl5nm	tandem lipoprotein	1.042567321	6.87E-06
ndhF	NADH dehydrogenase subunit 5	1.148805408	2.03E-10
NWMN_0419	hypothetical protein	1.113583438	3.34E-09
NWMN_0433	hypothetical protein	1.379971109	6.75E-11
gltC	Transcription activator of glutamate synthase operon	1.979457907	7.80E-25
NWMN_0460	similar to translation initiation inhibitor	-1.003180303	6.36E-07
spoVG	regulatory protein SpoVG	-1.255908423	1.03E-12
NWMN_0480	GntR family regulatory protein	1.88388838	2.94E-19
NWMN_0482	glutamine amidotransferase subunit PdxT	-1.024313458	1.05E-08
nupC	pyrimidine nucleoside transport protein	-1.057583082	3.21E-10
ctsR	Transcriptional regulator CtsR	2.057606015	3.62E-20
NWMN_0485	UvrB/UvrC motif domain protein	2.155624124	1.87E-21
NWMN_0486	Protein-arginine kinase	2.265540933	9.00E-25
clpC	ATP-dependent Clp protease, ATP-binding subunit ClpC	2.306479027	1.15E-23
rplA	50S ribosomal protein L1	-1.098010133	1.86E-11
rplJ	50S ribosomal protein L10	-1.142245061	4.29E-10

rplL	50S ribosomal protein L7%2FL12	-1.211537488	5.82E-14
NWMN_0506	putative ribosomal protein L7Ae-like	-1.260954425	3.00E-11
rpsL	30S ribosomal protein S12	-1.218933169	5.43E-10
rpsG	30S ribosomal protein S7	-1.284511359	3.52E-12
fus	elongation factor G	-1.13461012	1.67E-07
NWMN_0517	haloacid dehalogenase-like hydrolase	1.035553359	6.54E-10
NWMN_0532	glucosamine-6-phosphate isomerase	1.144687047	2.44E-12
NWMN_0537	hypothetical protein	4.875464164	2.90E-58
NWMN_0542	hypothetical protein	6.140607571	1.80E-155
NWMN_0547	hypothetical protein	-1.520115296	1.50E-12
adh1	similar to zinc-dependent eukaryotic ADH enzymes and distinct from fermentative ADHs	-2.342061937	2.43E-15
NWMN_0587	similar to esterase lipase	-1.412253714	3.16E-08
NWMN_0592	site-specific recombinase	-1.579599768	8.21E-09
mnhA	putative monovalent cation antiporter subunit A	-1.232160259	1.48E-07
mnhB	putative monovalent cation antiporter subunit B	-1.147862434	6.46E-06
mnhC	putative monovalent cation antiporter subunit C	-1.313858301	8.68E-08
mnhD	putative monovalent cation antiporter subunit D	-1.125509576	3.60E-07
mnhE	putative monovalent cation antiporter subunit E	-1.067191092	9.15E-07
mnhF	putative monovalent cation antiporter subunit F	-1.033456405	2.69E-06
mnhG	putative monovalent cation antiporter subunit G	-1.084455508	2.52E-08
NWMN_0605	hypothetical protein	2.477199925	3.80E-17
NWMN_0622	hypothetical protein	1.545048211	3.33E-25
NWMN_0626	similar to acetyltransferase GNAT family protein	1.098523326	1.54E-09
NWMN_0653	ABC transporter ATP-binding MsbA family protein	1.023075108	4.21E-10
NWMN_0654	ABC transporter ATP-binding MsbA family protein	1.112083839	8.13E-12
NWMN_0667	fructose operon transcriptional regulator	-1.197555188	6.68E-07
fruB	fructose 1-phosphate kinase	-1.435861494	4.21E-10
fruA	fructose specific permease	-1.211811879	4.58E-08
nagA	N-acetylglucosamine-6-phosphate deacetylase	1.05614507	2.25E-09

NWMN_0672	aldo-keto reductase family protein	1.613788206	4.39E-19
NWMN_0673	similar to glycosyl transferase group 2 family protein	1.46986363	6.30E-21
saeS	Histidine protein kinase SaeS	-2.957105913	1.03E-43
saeR	DNA-binding response regulator SaeR	-3.038304556	7.67E-53
NWMN_0676	hypothetical protein	-3.562638455	4.25E-55
NWMN_0677	hypothetical protein	-3.189158434	2.07E-34
clpP	ATP-dependent Clp protease proteolytic subunit	2.138092999	2.78E-22
NWMN_0757	secreted von Willebrand factor-binding protein precursor	-5.693549252	2.90E-209
ssp	Extracellular matrix protein-binding protein emp	-3.011508267	9.75E-21
NWMN_0759	hypothetical protein	-4.553436148	1.30E-101
NWMN_0760	Thermonuclease	-2.452045639	7.62E-27
cspC	cold-shock protein CSD family protein	-1.259020411	1.82E-14
NWMN_0774	similar to thioredoxin	1.014250988	4.75E-08
NWMN_0783	CsbD-like superfamily protein	-1.331348053	7.72E-13
NWMN_0791	hypothetical protein	1.121371392	7.11E-10
NWMN_0792	similar to oxidoreductase 2-nitropropane dioxygenase family	1.088059219	4.56E-08
NWMN_0810	hypothetical protein	1.212439408	7.62E-10
NWMN_0826	NADH-dependent flavin oxidoreductase	1.633485863	1.66E-13
glpQ	glycerophosphoryl diester phosphodiesterase	1.296975305	1.33E-12
argH	argininosuccinate lyase	1.810650639	6.20E-27
argG	argininosuccinate synthase	1.133195068	3.36E-11
NWMN_0839	fumarylacetoacetate hydrolase family protein	1.055412058	5.71E-10
clpB	Chaperone protein ClpB	2.110851446	4.79E-14
NWMN_0875	hypothetical protein	1.34884086	2.43E-14
NWMN_0876	GTP pyrophosphokinase	1.164831667	2.03E-12
ppnK	inorganic polyphosphate ATP-NAD kinase	1.018022319	8.23E-10
NWMN_0897	lipoate-protein ligase A	1.390696922	3.64E-13
NWMN_0900	hypothetical protein	1.145682382	1.59E-07
NWMN_0920	hypothetical protein	1.375997156	1.44E-09

NWMN_0926	autolysis and methicillin resistant-related protein FmtA	1.358601137	1.59E-07
NWMN_0931	hypothetical protein	1.198111782	1.05E-08
NWMN_0970	hypothetical protein	1.660139203	1.62E-14
NWMN_0972	hypothetical protein	1.268860585	4.08E-11
NWMN_1018	hypothetical protein	-1.004805973	0.000302247
NWMN_1021	hypothetical protein	-1.028007424	0.034406639
NWMN_1066	similar to fibrinogen-binding protein	-3.279842274	6.78E-53
NWMN_1067	formyl peptide receptor-like 1 inhibitory protein FPRL1 inhibitory protein	-4.173111334	6.56E-52
NWMN_1068	hypothetical protein	-1.734610178	5.15E-26
NWMN_1069	hypothetical protein Fibrinogen-binding protein	-4.107813329	1.52E-80
NWMN_1070	similar to fibrinogen-binding protein	-4.244328874	1.50E-72
NWMN_1075	hypothetical protein	-2.224229685	1.83E-11
NWMN_1076	hypothetical protein	-2.204473039	1.22E-09
NWMN_1077	hypothetical protein	-2.226084687	2.54E-08
NWMN_1106	putative transposase;protein	1.461275419	0.038591686
NWMN_1109	bifunctional pyrimidine regulatory protein PyrR uracil phosphoribosyltransferase;	-1.138913692	4.68E-10
NWMN_1110	uracil permease	-1.829815715	7.47E-18
NWMN_1111	aspartate carbamoyltransferase catalytic subunit	-1.871193982	2.94E-19
NWMN_1112	dihydroorotase	-1.604832669	1.49E-16
NWMN_1113	carbamoyl phosphate synthase small subunit	-1.420033809	1.30E-13
NWMN_1114	carbamoyl phosphate synthase large subunit	-1.286268046	6.52E-14
NWMN_1115	orotidine 5-phosphate decarboxylase	-1.31231274	5.29E-14
NWMN_1116	orotate phosphoribosyltransferase	-1.112818267	9.27E-11
NWMN_1149	16S rRNA-processing protein RimM	-1.224776078	2.79E-09
NWMN_1150	tRNA guanine methyltransferase	-1.167056782	3.54E-09
NWMN_1151	50S ribosomal protein L19	-1.060698763	7.96E-13
NWMN_1196	hypothetical protein	1.416965362	2.97E-08
NWMN_1209	aerobic glycerol-3-phosphate dehydrogenase	1.63003247	1.12E-25
NWMN_1213	glutathione peroxidase	1.278092794	9.77E-14

NWMN_1229	hypothetical protein	1.418662343	0.001776487
NWMN_1239	Aspartokinase	2.56787952	5.95E-44
NWMN_1240	Homoserine dehydrogenase	2.465369772	9.82E-55
NWMN_1241	Threonine synthase	2.380276566	1.64E-47
NWMN_1242	Homoserine kinase	2.572809134	8.43E-51
NWMN_1277	prephenate dehydrogenase	1.100969238	5.53E-12
NWMN_1294	hypothetical protein	1.180369195	3.08E-08
NWMN_1296	Phosphate-specific transport system accessory protein PhoU	2.716499199	3.19E-30
NWMN_1297	Phosphate import ATP-binding protein PstB	3.112777021	7.52E-36
NWMN_1298	Phosphate ABC transporter, permease protein	3.467284479	6.94E-38
NWMN_1299	phosphate ABC transporter permease	3.752487737	5.70E-45
NWMN_1300	Phosphate ABC transporter, phosphate-binding protein PstS	4.146614468	6.00E-43
NWMN_1303	ABC transporter ATP-binding protein	-1.372272011	4.76E-18
NWMN_1304	aspartate kinase	1.295524597	4.99E-10
NWMN_1305	aspartate semialdehyde dehydrogenase;protein	1.295437181	7.75E-12
NWMN_1306	dihydrodipicolinate synthase	1.549922577	1.82E-16
NWMN_1307	dihydrodipicolinate reductase	1.571086702	1.19E-16
NWMN_1308	tetrahydrodipicolinate acetyltransferase	1.691782184	4.01E-20
NWMN_1309	hippurate hydrolase	1.86885007	2.24E-20
alr2	alanine racemase 2	1.679261757	2.43E-16
lysA	diaminopimelate decarboxylase	1.345835367	4.36E-15
NWMN_1315	acylphosphatase	1.092605988	2.53E-10
NWMN_1318	putative transposase for IS1272	1.65856771	0.034406639
ctpA	carboxyl-terminal protease	1.205880059	1.77E-07
NWMN_1333	phosphotransferase system glucose-specific IIA component	1.689672005	1.67E-20
msrB	methionine sulfoxide reductase B	1.787095291	1.48E-20
msrA	methionine sulfoxide reductase A	1.762971686	7.20E-19
NWMN_1343	hypothetical protein	1.317783667	6.13E-12

NWMN_1346	hypothetical protein Quinolone resistance protein NorB	-3.716617079	1.70E-33
NWMN_1347	Amino acid permease	-4.60366978	4.28E-50
NWMN_1348	Threonine dehydratase II	-4.862602194	1.74E-60
NWMN_1349	Alanine dehydrogenase	-5.052442908	3.03E-66
NWMN_1352	hypothetical protein	-1.387515314	1.66E-10
NWMN_1371	hypothetical protein	1.016327243	1.72E-08
rpsA	30S ribosomal protein S1	1.318567697	3.91E-15
ebpS	elastin binding protein	1.156742096	2.76E-12
glyS	glycyl-tRNA synthetase	1.290077747	2.26E-16
prmA	ribosomal protein L11 methyltransferase	1.13002155	5.82E-12
dnaJ	chaperone protein DnaJ	1.267775971	4.65E-13
dnaK	molecular chaperone DnaK	1.464177138	1.91E-11
grpE	heat shock protein GrpE	1.436016688	1.23E-12
hrcA	heat-inducible transcription repressor	1.464535772	1.52E-12
NWMN_1503	enterotoxin family protein	1.133471169	8.96E-08
NWMN_1505	hypothetical protein	1.095810918	1.86E-07
NWMN_1525	luciferase family protein	1.058806542	9.40E-06
NWMN_1526	hypothetical protein	-1.269804003	3.43E-07
NWMN_1527	hypothetical protein	-1.117633382	6.68E-07
NWMN_1552	hypothetical protein	2.627725836	6.91E-27
NWMN_1553	hypothetical protein	2.921500847	1.18E-12
NWMN_1572	50S ribosomal protein L20	-1.185468435	5.62E-13
NWMN_1573	50S ribosomal protein L35	-1.170006865	5.05E-13
NWMN_1602	proline dipeptidase-like protein	1.543263116	2.17E-21
NWMN_1604	universal stress protein family protein	1.027847187	1.32E-10
NWMN_1612	hypothetical protein	1.116116969	3.73E-10
rpsD	30S ribosomal protein S4	-1.016945245	1.43E-09
NWMN_1615	osmotic stress-related protein	1.492257381	9.26E-15
NWMN_1616	aminotransferase class V	1.338631756	8.01E-17

NWMN_1617	D-3-phosphoglycerate dehydrogenase	1.482780252	1.35E-18
NWMN_1618	hypothetical protein	1.31804478	4.48E-15
NWMN_1621	hypothetical protein	2.37434327	8.78E-27
acuA	acetoin utilization	1.040788418	1.64E-06
acuC	acetoin utilization protein AcuC	1.038763722	3.08E-08
NWMN_1644	dipeptidase PepV	1.016702138	3.33E-12
NWMN_1655	accessory regulator Rot	-1.54475804	5.22E-22
NWMN_1672	putative translaldolase	1.032054643	1.52E-07
NWMN_1733	Foldase protein PrsA	2.222675429	1.35E-26
NWMN_1749	glutamine transport ATP-binding protein	1.015378211	1.75E-06
NWMN_1766	glycosyltransferase	1.836304776	1.07E-15
NWMN_1796	hypothetical protein	-1.170909748	0.012717705
NWMN_1821	ribonuclease	-1.185211626	8.89E-06
NWMN_1822	DNA-binding response regulator VraR	2.292267608	2.29E-23
NWMN_1823	Sensor protein VraS	2.30043501	1.55E-25
NWMN_1824	hypothetical protein	2.0841714	4.68E-19
NWMN_1825	hypothetical protein	1.651046352	5.23E-12
NWMN_1834	hypothetical protein	2.059095789	3.62E-12
NWMN_1872	65 kDa membrane protein	-2.984648365	1.73E-17
NWMN_1873	Truncated beta-hemolysin	-2.273099583	1.57E-20
NWMN_1876	complement inhibitor SCIN Staphylococcal complement inhibitor	-4.318333346	2.05E-94
NWMN_1877	Chemotaxis inhibitory protein	-5.386736207	6.79E-146
NWMN_1927	Leukocidin/hemolysin toxin family F subunit	-3.048172309	4.04E-71
NWMN_1928	Leukocidin/hemolysin toxin family S subunit	-3.188339582	1.98E-70
NWMN_1937	60 kDa chaperonin	2.11046038	4.62E-26
NWMN_1938	10 kDa chaperonin	2.069816466	7.11E-25
ilvC	ketol-acid reductoisomerase	1.101061667	1.05E-09
leuA	2-isopropylmalate synthase	1.191773245	3.01E-10

leuB	3-isopropylmalate dehydrogenase	1.125825129	2.72E-10
leuC	isopropylmalate isomerase large subunit	1.230933208	1.33E-12
leuD	isopropylmalate isomerase small subunit	1.141723039	3.86E-09
ilvA	threonine dehydratase	1.079366752	9.18E-09
NWMN_1985	ATP-dependent RNA helicase DEAD box family protein	-1.002420768	1.94E-06
NWMN_2022	peptide chain release factor 1	-0.99650741	5.43E-10
murZ	UDP-N-acetylglucosamine 1-carboxyvinyltransferase	1.073235626	3.06E-08
NWMN_2036	hypothetical protein	1.147341758	3.48E-13
manA1	mannose-6-phosphate isomerase class I	-1.008029596	3.28E-09
NWMN_2050	cation efflux family protein	1.018631946	2.89E-06
mtlA	mannitol-specific IIA component	-1.054554954	5.62E-05
NWMN_2086	alkaline shock protein 23	-1.739371505	3.00E-12
NWMN_2087	hypothetical protein	-1.841586549	1.50E-11
NWMN_2088	hypothetical protein	-1.73526875	1.06E-10
alsD	alpha-acetolactate decarboxylase	1.706229482	2.60E-13
alsS	acetolactate synthase	1.752311904	3.76E-12
NWMN_2119	30S ribosomal protein S9	-1.134311223	6.43E-14
NWMN_2120	50S ribosomal protein L13	-1.049819429	4.66E-11
rplQ	50S ribosomal protein L17	-1.143545439	5.00E-11
rpoA	DNA-directed RNA polymerase subunit alpha	-1.107059355	9.79E-08
rpsK	30S ribosomal protein S11	-1.068119749	9.20E-09
rpsM	30S ribosomal protein S13	-1.10204374	1.40E-09
rpmJ	50S ribosomal protein L36	-1.049868208	9.20E-09
infA	translation initiation factor IF-1	-1.113733924	3.10E-08
adk	adenylate kinase	-1.095316744	4.21E-07
secY	preprotein translocase subunit SecY	-1.009486742	3.95E-06
rplO	50S ribosomal protein L15	-1.181508109	8.11E-09
rpmD	50S ribosomal protein L30	-1.357834476	3.84E-13
rpsE	30S ribosomal protein S5	-1.247978323	6.96E-10

rplR	50S ribosomal protein L18	-1.277414475	4.23E-10
rplF	50S ribosomal protein L6	-1.253036245	4.22E-10
rpsH	30S ribosomal protein S8	-1.336877812	2.33E-11
rpsN	30S ribosomal protein S14	-1.310708673	1.25E-11
rplE	50S ribosomal protein L5	-1.200276055	1.92E-08
rplX	50S ribosomal protein L24	-1.235568948	6.39E-10
rplN	50S ribosomal protein L14	-1.200219593	3.02E-09
rpsQ	30S ribosomal protein S17	-1.311074765	6.13E-12
rpmC	50S ribosomal protein L29	-1.36996599	1.86E-14
rplP	50S ribosomal protein L16	-1.20256782	2.41E-10
rpsC	30S ribosomal protein S3	-1.199523864	1.23E-10
rplV	50S ribosomal protein L22	-1.285426785	3.52E-13
rpsS	30S ribosomal protein S19	-1.212528793	5.07E-12
rplB	50S ribosomal protein L2	-1.117807376	2.19E-10
rplW	50S ribosomal protein L23	-1.185874157	1.51E-13
rplD	50S ribosomal protein L4	-1.173846005	6.29E-12
rplC	50S ribosomal protein L3	-1.174326276	2.71E-11
rpsJ	30S ribosomal protein S10	-1.205988948	8.40E-13
NWMN_2154	hypothetical protein	1.098558799	2.11E-09
NWMN_2185	iron compound ABC transporter iron compound-binding protein	-1.266226727	8.38E-15
ureA	urease subunit gamma	1.190355813	0.000111179
ureB	urease subunit beta	1.315930624	1.32E-10
ureC	urease subunit alpha	1.050994038	2.66E-09
sarY	hypothetical protein	-1.04458751	2.97E-09
NWMN_2198	transcriptional regulator AraC family protein	-1.312025809	2.20E-10
NWMN_2199	secretory antigen precursor SsaA	-1.00772592	2.68E-09
NWMN_2200	Na+/H+ antiporter NhaC	-2.297490383	3.02E-45
NWMN_2201	Dehydrogenase family protein	-2.610492379	2.46E-56
NWMN_2209	hypothetical protein	-1.005536816	1.19E-06

NWMN_2210	formate dehydrogenase-like protein	-1.049464945	2.13E-07
NWMN_2211	cell envelope-related transcriptional attenuator	1.197015331	9.53E-10
NWMN_2213	DeoR family regulatory protein	1.010096884	1.06E-08
NWMN_2223	hypothetical protein	1.820631329	1.07E-17
NWMN_2246	sodium glutamate symporter	-1.135844335	2.32E-12
NWMN_2258	HTH-type transcriptional regulator TcaR	-2.872159254	5.92E-77
NWMN_2261	ABC transporter ATP-binding protein	1.623274146	1.12E-08
NWMN_2262	hypothetical protein	1.626608109	1.46E-08
NWMN_2265	hypothetical protein	2.561818936	2.09E-34
NWMN_2266	hypothetical protein	2.58144146	4.70E-33
NWMN_2279	PTS system sucrose-specific IIBC component	-1.111842817	4.00E-07
NWMN_2288	Probable nitrate transporter NarT	-2.67261286	1.60E-28
NWMN_2297	Nitrate reductase, alpha subunit	-2.049841392	4.61E-12
nirB	assimilatory nitrite reductase large subunit	-1.361887152	1.81E-12
NWMN_2301	Nitrite reductase transcriptional regulator NirR	-2.198425223	3.27E-26
NWMN_2304	hypothetical protein	-1.212103278	0.000344938
NWMN_2306	Zn-binding lipoprotein adcA-like protein	-2.321088679	3.42E-21
NWMN_2317	immunoglobulin G-binding protein Sbi	-3.799191913	8.01E-70
NWMN_2318	Gamma-hemolysin component A	-2.213278172	1.18E-22
NWMN_2319	gamma-hemolysin component C	-1.831420259	1.03E-12
NWMN_2320	gamma hemolysin component B	-1.57392231	2.29E-12
NWMN_2331	glycerate kinase	1.724823745	9.96E-21
NWMN_2332	hypothetical protein	1.968987394	4.44E-28
opp1A	oligopeptide permease peptide-binding protein	-1.42179085	6.43E-15
NWMN_2365	hypothetical protein	-1.131850385	2.24E-09
NWMN_2366	hypothetical protein	-1.572910656	3.70E-13
NWMN_2367	hypothetical protein	-1.716943302	1.04E-19
NWMN_2368	hypothetical protein	-1.118549557	7.63E-06
NWMN_2369	short chain dehydrogenase	-1.01859753	7.26E-05

NWMN_2377	hypothetical protein	-2.436987013	2.11E-19
NWMN_2396	C-terminal part of fibronectin binding protein B	-1.614585231	3.68E-10
NWMN_2397	fibronectin binding protein B precursor	-1.657734574	3.96E-13
NWMN_2398	C-terminal part of fibronectin binding protein A	-3.285334963	5.69E-67
NWMN_2399	fibronectin binding protein A	-3.475875538	1.55E-66
NWMN_2405	hypothetical protein	1.081733235	4.57E-05
NWMN_2412	ABC transporter, ATP-binding protein	-2.735192865	4.44E-42
NWMN_2413	hypothetical protein	-2.647995265	5.51E-32
NWMN_2427	acetyltransferase GNAT family protein	-1.005816665	5.07E-08
NWMN_2432	hypothetical protein	2.174951327	2.85E-26
NWMN_2435	hypothetical protein	1.179182534	1.10E-09
NWMN_2436	hypothetical protein	1.022013415	2.60E-06
NWMN_2437	PTS system glucose-specific IIABC component	-1.492122527	4.49E-13
NWMN_2440	Holin-like protein CidA	2.008012308	1.54E-11
NWMN_2448	ATP-dependent Clp protease, ATP-binding subunit ClpC	-3.128756663	1.87E-21
NWMN_2456	hypothetical protein	2.74672761	1.28E-14
NWMN_2457	cation-transporting ATPase E1-E2 family protein	1.279479547	1.94E-14
crtN	squalene synthase	-1.153962727	1.80E-05
crtM	squalene desaturase	-1.322452314	1.25E-06
NWMN_2463	glycosyl transferase group 2 family protein	-1.571953608	3.13E-09
crtI	phytoene dehydrogenase	-1.742897474	5.04E-11
NWMN_2465	hypothetical protein	-1.530638256	3.01E-10
oatA	secretory antigen precursor SsaA-like protein	-1.122243452	2.02E-09
NWMN_2467	O-acetyltransferase OatA	-1.222191599	3.38E-16
NWMN_2468	acetyltransferase GNAT family protein	-1.068380394	8.18E-09
NWMN_2490	hypothetical protein	-1.039647757	5.92E-10
NWMN_2502	hypothetical protein	-1.252768586	2.24E-05
NWMN_2510	glycine betaine aldehyde dehydrogenase	1.204437707	9.51E-10
NWMN_2526	Alkaline phosphatase III	2.021360086	2.26E-18

clfB	clumping factor B precursor	-1.560401321	8.31E-13
NWMN_2557	hypothetical protein	-1.31060434	4.56E-07
icaD	intercellular adhesion protein IcaD	1.428958075	1.56E-05
icaB	intercellular adhesion protein B	1.573773696	6.46E-15
lip	bifunctional phosphoribosyl-AMP cyclohydrolase%2Fphosphoribosyl-ATP pyrophosphatase	-1.808216671	2.97E-05
hisF	imidazole glycerol phosphate synthase subunit HisF	1.190622588	5.43E-10
hisA	methylideneamino imidazole-4-carboxamide isomerase	1.394713689	2.72E-08
hisH	imidazole glycerol phosphate synthase subunit HisH	1.535563553	1.43E-06
hisB	imidazoleglycerol-phosphate dehydratase	1.371104273	2.50E-05
hisC	histidinol-phosphate aminotransferase	1.542184524	3.36E-07
hisD	histidinol dehydrogenase	1.240750366	5.63E-05
hisG	ATP phosphoribosyltransferase catalytic subunit	1.088651906	0.000139343
NWMN_2583	hypothetical protein	1.024945094	7.95E-08
NWMN_2585	hypothetical protein	-1.024637938	1.16E-08
drp35	Drp35	1.066329774	1.70E-09
NWMN_2591	hypothetical protein	-1.172907571	3.37E-06
NWMN_2594	hypothetical protein	-1.096421507	5.39E-05
NWMN_2596	N-acetyltransferase family protein	1.142029634	2.17E-07
cspB	cold shock protein CspB	-1.531322997	9.20E-14
NWMN_rRNA02	23S ribosomal RNA	-1.191931394	0.007998508
NWMN_rRNA06	23S ribosomal RNA	-0.99524501	0.007037498
NWMN_rRNA09	23S ribosomal RNA	-1.055679329	0.005943289
NWMN_rRNA10	16S ribosomal RNA	-1.062979861	0.015573742
NWMN_rRNA15	23S ribosomal RNA	-1.352823151	0.000482589
NWMN_tRNA31	tRNA-Thr	-1.048489916	0.038451718
NWMN_tRNA48	tRNA-Ile	1.203381512	0.024067815
NWMN_tRNA49	tRNA-Gly	1.272918022	0.00038476

Appendix Table 2 DE genes of *S. epidermidis* Tü3298 in response to 5µM D-sphingosine challenge. The level of fold change **(logFC)** is based on log2, DE genes shown in this table all have more than 2 fold changes. All DE genes have **FDR** (false discovery rate) ≤ 0.05.

Gene	Gene Description	logFC	FDR
SETU_00282	secretory antigen SsaA-like protein	-2.766344	9.52E-21
SETU_00070	autolysin (N-acetylmuramoyl-L-alanine amidase	-2.745374	1.92E-15
SETU_00328	lipoprotein	-2.700149	0.0014474
SETU_00327	DoxX family protein	-2.563634	0.000945
SETU_00770	uracil permease	-2.454206	5.63E-17
SETU_01975	secretory antigen SsaA	-2.42695	5.82E-15
SETU_00326	response regulator	-2.365861	0.0008135
SETU_00325	histidine protein kinase	-2.270405	0.0019363
isaA	immunodominant antigen A	-2.119102	9.83E-06
SETU_02228	Putative protein-S-isoprenylcysteine methyltransferase	-2.110793	1.93E-07
SETU_00646	N-acetylmuramoyl-L-alanine amidase	-2.017126	3.98E-06
SETU_01355	tRNA-Met	-1.958448	1.99E-08
SETU_01990	ssaA protein	-1.912753	0.0005422
SETU_00316	hypothetical protein	-1.725449	9.83E-06
SETU_00059	hypothetical protein	-1.671056	1.93E-07
SETU_02363	hypothetical protein	-1.636509	4.97E-05
SETU_01252	hypothetical protein	-1.576558	7.50E-05
SETU_02365	Bacitracin transport ATP-binding protein bcrA	-1.5743	9.87E-05
SETU_01757	secretory antigen SsaA	-1.485684	0.0269249
SETU_02085	zinc metalloproteinase aureolysin	-1.477159	0.0173582
SETU_02088	putative lipoprotein	-1.47197	0.0020868
pyrB	aspartate carbamoyltransferase	-1.463435	3.91E-07

SETU_01913	poly (glycerol-phosphate) alpha-glucosyltransferase	-1.450237	1.38E-05
SETU_02205	ABC-2 family transporter protein	-1.445553	0.0019363
SETU_01891	amino acid transporter	-1.442578	0.0041218
SETU_02364	lantibiotic ABC transporter permease	-1.422004	0.0007582
SETU_00024	1,4-beta-N-acetylmuramidase	-1.393849	2.76E-05
SETU_00769	bifunctional pyrimidine regulatory protein PyrR uracil phosphoribosyltransferase	-1.379989	8.77E-07
SETU_01548	tRNA-Leu	-1.338624	0.0189738
SETU_00200	major facilitator family transporter	-1.333518	0.0001229
SETU_02356	Lipid A export ATP-binding/permease MsbA	-1.327345	0.0001386
SETU_01758	SMR-type multidrug efflux transporter	-1.306716	0.0002002
SETU_00272	membrane protein , putative	-1.269019	0.0003958
dltX	D-Ala-teichoic acid biosynthesis protein	-1.240581	0.0004152
SETU_02328	hypothetical protein	-1.231758	9.28E-05
SETU_02126	chloramphenicol resistance protein YfhI	-1.198924	0.0007701
infC	translation initiation factor IF-3	-1.173646	0.0163621
SETU_00588	tRNA-Ser	-1.1596	0.0248624
SETU_02341	BsaG protein	-1.134193	0.0193139
SETU_01410	tRNA-Met	-1.123722	0.0054929
rpsD	30S ribosomal protein S4	-1.120808	0.0127396
SETU_00818	DNA processing Smf protein	-1.119019	0.0007701
rpmI	50S ribosomal protein L35	-1.11505	0.005143
SETU_00184	Ser-Asp rich fibrinogen-binding, bone sialoprotein-binding protein	-1.11254	0.0178877
SETU_00479	D-alanine--poly(phosphoribitol) ligase subunit 1	-1.097967	0.0277311
SETU_00029	Transglycosylase associated protein	-1.092515	0.0061164
SETU_01417	tRNA-Ala	-1.090776	0.0382581
SETU_02000	hypothetical protein	-1.090436	0.0014996
SETU_00208	cationic amino acid transporter	-1.082609	0.0038271
SETU_00484	YuzD-like protein	-1.076474	0.0146863

SETU_02125	chloramphenicol resistance protein YfhI	-1.07263	0.0020864
SETU_00065	cysteine synthase	-1.069987	0.0006181
SETU_01759	SMR-type multidrug efflux transporter	-1.069949	0.0059512
SETU_00180	deoxypurine kinase	-1.060803	0.0002456
SETU_00925	Large-conductance mechanosensitive channel	-1.051639	0.0005432
SETU_00066	cystathionine gamma-synthase	-1.046057	0.0007701
SETU_01562	ATP-dependent RNA helicase	-1.040834	0.0275823
SETU_01796	DNA-3-methyladenine glycosidase	-1.031015	0.0016685
SETU_00949	ThiJ/PfpI family protein	-1.029363	0.0013731
SETU_01182	caffeoyl-CoA O-methyltransferase	-1.027307	0.0005918
SETU_00067	ABC transporter ATP-binding protein	-1.021485	0.0006318
SETU_02300	Yip1 domain protein	-1.00819	0.0039897
SETU_02264	rRNA large subunit methyltransferase	-1.006811	0.0193102
rplT	50S ribosomal protein L20	-1.002624	0.0100317
SETU_00424	pathogenicity island protein	1.000794	0.0019516
SETU_01812	transcriptional regulator	1.0042174	0.0376976
SETU_02171	dihydroxyacetone kinase subunit DhaK	1.0099166	0.0174084
SETU_01869	glycerate kinase	1.0152654	0.0112845
prmA	ribosomal protein L11 methyltransferase	1.0163692	0.0247033
SETU_02045	transcriptional regulator	1.0170919	0.0209625
SETU_02032	anaerobic ribonucleotide reductase activator protein	1.0180451	0.001756
SETU_02098	general stress protein 170	1.0195758	0.0106694
SETU_00528	oligopeptide transport system permease OppC	1.0262721	0.0072479
SETU_02277	homoserine-o-acetyltransferase	1.0288517	0.0173582
SETU_00905	homoserine dehydrogenase	1.0484057	0.023533
SETU_02313	hypothetical protein	1.0608674	0.0008068
SETU_02092	BigG family transcription antiterminator	1.0631818	0.0196826
SETU_01536	dihydroxy-acid dehydratase	1.076099	0.029984

SETU_01816	Integral membrane protein	1.0779834	0.0250961
SETU_01152	molecular chaperone DnaJ	1.0874792	0.025926
SETU_00256	lipoprotein	1.0977566	0.0002391
SETU_00919	hypothetical protein	1.1014148	0.0427906
SETU_01383	truncated transposase	1.1069847	0.0250961
SETU_02315	hypothetical protein	1.1138931	0.0003761
SETU_02083	arginine deiminase	1.1230474	0.0001039
SETU_01284	OsmC/Ohr family protein	1.1238116	0.0106694
SETU_01217	hypothetical protein	1.1265468	0.0209178
SETU_00491	ComA2 family protein	1.1305507	0.0042598
SETU_02082	ornithine carbamoyltransferase	1.1493931	6.46E-05
SETU_02143	hypothetical protein	1.1550498	0.0175604
SETU_00536	thimet oligopeptidase-like protein	1.1575587	0.0066944
SETU_00034	alkyl hydroperoxide reductase	1.1800357	0.0379135
SETU_00240	hypothetical protein	1.1818292	0.0022418
SETU_01841	NAD(P)H-flavin oxidoreductase	1.1956332	0.0009582
SETU_00960	negative regulator PhoU	1.1980143	0.0002269
SETU_02169	phosphotransferase mannnose-specific family component IIA	1.2077496	0.0023493
SETU_00530	oppF protein	1.2266035	0.0013016
SETU_00981	5-bromo-4-chloroindolyl phosphate hydrolysis protein XpaC	1.2362432	0.0002391
SETU_00035	alkyl hydroperoxide reductase	1.2478581	0.0112845
SETU_00490	Na+/H+ antiporter family protein	1.2523068	0.0011667
SETU_00982	tellurite resistance protein	1.2610599	0.000214
SETU_00529	oligopeptide transport ATP-binding protein subunit	1.2729135	0.0007701
SETU_02170	DAK2 domain-containing protein	1.2774838	0.0007701
SETU_01288	PTS system N-acetylglucosamine-specific transporter subunit IIBC	1.2811474	9.83E-06
SETU_01510	helix-turn-helix protein	1.2863653	0.0158079
SETU_02314	hypothetical protein	1.2879183	0.0105871

SETU_01765	truncated transposase	1.294459	0.0173582
SETU_01874	amino acid ABC transporter-like protein	1.2956636	7.26E-05
SETU_01987	mercuric ion-binding protein	1.3097681	0.0019363
SETU_00260	hypothetical protein	1.3112926	0.0045939
SETU_01768	DeoR family transcriptional regulator	1.3322159	7.26E-05
SETU_00058	hypothetical protein	1.3450016	1.95E-05
SETU_00958	hypothetical protein	1.3587182	0.0197906
SETU_00306	ABC transporter	1.3696359	0.0004788
SETU_00889	hypothetical protein	1.3984545	0.028688
SETU_01779	hypothetical protein	1.4044045	0.0146375
SETU_00305	ABC transporter ATP-binding protein	1.4110045	0.00036
SETU_01870	hypothetical protein	1.4198953	0.0005614
dnaK	molecular chaperone DnaK	1.4522594	0.0373415
SETU_01080	alpha-D-1,4-glucosidase	1.4531116	8.77E-07
SETU_01537	acetolactate synthase large subunit	1.4761263	0.0033671
SETU_00963	phosphate ABC transporter	1.476965	4.97E-05
SETU_01499	hypothetical protein	1.4946781	6.94E-06
SETU_01509	DNA binding domain, excisionase family	1.5171883	0.001168
SETU_00964	thioredoxine reductase	1.5402013	4.35E-05
SETU_01498	terminase, superantigen-encoding pathogenicity islands SaPI	1.5550301	3.91E-07
SETU_00962	phosphate ABC transporter	1.5573509	1.80E-06
SETU_00989	dihydrolipoamide succinyltransferase	1.5741056	3.82E-07
SETU_01544	threonine dehydratase	1.5820314	0.0035379
SETU_02028	glycine betaine aldehyde dehydrogenase gbsA	1.5868653	0.0026235
SETU_01917	gluconokinase	1.596315	3.45E-05
SETU_00313	hypothetical protein	1.6023287	0.03631
SETU_00229	alcohol dehydrogenase	1.6059174	0.0015641
SETU_00907	homoserine kinase	1.6172107	9.87E-05

argG	argininosuccinate synthase	1.6318571	0.0379135
sucA	2-oxoglutarate dehydrogenase E1	1.6332072	7.15E-07
SETU_00508	argininosuccinate lyase	1.6338	7.26E-05
clpP	ATP-dependent Clp protease proteolytic subunit	1.6345418	0.0032636
SETU_01513	molecular chaperone GroEL	1.648903	0.0014513
SETU_01507	pathogenicity island protein	1.6606976	0.0373415
SETU_01957	ribose transporter RbsU	1.6657941	0.022299
SETU_00682	cytochrome d ubiquinol oxidase subunit II-like protein	1.6678448	0.0004352
SETU_00961	phosphate transporter ATP-binding protein	1.6684012	1.02E-07
SETU_01154	heat shock protein GrpE	1.6923175	0.0010796
SETU_01955	ribokinase	1.6956079	0.0086072
SETU_02027	choline dehydrogenase	1.7035408	0.0006958
SETU_01332	truncated transposase	1.7233683	0.00455
SETU_01155	heat-inducible transcriptional repressor	1.7513007	0.0015641
groES	co-chaperonin GroES	1.7520444	8.47E-05
SETU_01340	phosphoenolpyruvate carboxykinase	1.7682791	0.000214
SETU_00903	hypothetical protein	1.7998051	2.25E-07
SETU_00673	myosin-cross-reactive antigen	1.8175857	5.64E-07
SETU_01500	pathogenicity island protein	1.8334579	1.02E-10
SETU_01542	isopropylmalate isomerase large subunit	1.8388232	0.0009552
SETU_01956	D-ribose pyranase	1.8475002	0.0158079
SETU_00681	cytochrome d ubiquinol oxidase subunit 1-like protein	1.8551069	1.20E-05
SETU_02128	triacylglycerol lipase	1.8974766	1.57E-05
SETU_00906	threonine synthase	1.9049743	1.35E-05
SETU_01367	protein export protein PrsA	1.9136543	0.0022179
SETU_00036	2-oxo-hepta-3-ene-1,7-dioate hydratase	1.9171705	0.0009479
SETU_02093	PTS system fructose-specific transporter subunit II	1.9371593	0.0214056
SETU_00230	hypothetical protein	1.9467513	4.63E-05

SETU_02090	acetoin reductase	1.9483192	0.0495542
lacG	6-phospho-beta-galactosidase	1.9697998	1.79E-12
SETU_00375	ribosomal subunit interface protein	1.9973614	3.61E-07
hisG	ATP phosphoribosyltransferase	2.0198135	0.0001726
hisZ	ATP phosphoribosyltransferase	2.058193	0.0007701
SETU_01538	acetolactate synthase 1 regulatory subunit	2.0591401	0.0086072
leuD	isopropylmalate isomerase small subunit	2.0828724	5.02E-05
SETU_01541	3-isopropylmalate dehydrogenase	2.1064437	0.0001229
SETU_01540	2-isopropylmalate synthase	2.1524792	8.47E-05
SETU_00057	putative transmembrane protein coupled to NADH-ubiquinone oxidoreductase chain 5	2.1574002	9.27E-09
isaB	immunodominant antigen B	2.1661333	3.12E-09
SETU_01671	galactose-6-phosphate isomerase subunit LacA	2.1670123	8.93E-13
SETU_01667	PTS system lactose-specific transporter subunit IIA	2.2158786	8.93E-13
SETU_00056	NADH dehydrogenase subunit 5	2.2424426	1.27E-12
lacE	PTS system lactose-specific transporter subunit IIBC	2.2521456	6.55E-15
SETU_00318	transcription repressor of fructose operon	2.291817	0.004395
SETU_01539	ketol-acid reductoisomerase	2.2982236	4.63E-05
SETU_01321	proline dehydrogenase	2.3786778	1.25E-15
SETU_00674	myosin-cross-reactive antigen	2.3993088	1.07E-18
SETU_01444	hypothetical protein	2.4299707	6.37E-05
SETU_01670	galactose-6-phosphate isomerase subunit LacB	2.4367947	6.16E-16
SETU_02150	branched-chain alpha-keto acid dehydrogenase subunit E2	2.4839392	7.22E-15
clpC	endopeptidase Clp ATP-binding subunit C	2.4970218	0.0005794
SETU_00142	ATP:guanido phosphotransferase	2.5729024	1.62E-05
SETU_00320	PTS system fructose-specific transporter subunit IIABC	2.5857933	0.000319
SETU_00140	CtsR family transcriptional regulator	2.5957483	1.39E-05
SETU_00319	fructose 1-phosphate kinase	2.5995257	0.000702
SETU_00141	UvrB/UvrC domain-containing protein	2.6018225	1.24E-05

SETU_01669	tagatose-6-phosphate kinase	2.6019058	6.83E-20
SETU_01646	hypothetical protein	2.6274864	1.52E-18
SETU_01443	transporter associated with VraSR	2.6802737	1.03E-05
SETU_01668	tagatose 1,6-diphosphate aldolase	2.7019562	6.01E-22
vraR	DNA-binding response regulator VraR	2.7195307	7.66E-06
SETU_01442	two-component sensor histidine kinase	2.7333151	6.94E-06
SETU_01983	1-pyrroline-5-carboxylate dehydrogenase	2.7343595	2.90E-22
SETU_00784	TM2 domain-containing protein	2.7418357	9.83E-06
SETU_01290	heat-shock protein htrA	2.9920056	4.69E-05
SETU_02151	branched-chain alpha-keto acid dehydrogenase E1	3.0080045	7.34E-18
SETU_00522	clpB protein	3.0795585	2.46E-06
SETU_02153	dihydrolipoamide dehydrogenase	3.2950081	1.22E-27
SETU_02152	branched-chain alpha-keto acid dehydrogenase E1	3.3326028	2.70E-21
SETU_01986	copper-transporting ATPase copA （also in Jo's sapi data）	3.6535435	1.17E-07
pfl	formate acetyltransferase	3.6927207	0.0106694
SETU_01218	hypothetical protein	3.7918843	4.87E-06
SETU_01985	hypothetical protein (ortholog to NWMN_2456 ?)	4.1056359	3.00E-06
pflA	pyruvate formate-lyase-activating enzyme	4.573273	0.0006202
SETU_00201	hypothetical protein	5.6249376	2.57E-09